# Lysozyme-Small Molecule Interactions

by

Abdul Wadood

A thesis submitted in partial fulfilment
for the degree of Ph.D.

Faculty of Science

Glasgow University


July 1998

Chemistry Department

To My Daughter Hamnah Wadood

Acknowledgements

I would like to express my deepest thanks to my supervisor Professor Alan Cooper for his help, advice, encouragement and all types of cooperation during whole of my research work. I am also thankful to Dr Kelvin Tyler for his cooperation and guidance. It is a pleasure to acknowledge my great indebtedness to Mrs. Margaret Nutley for providing technical support during experimental work. I am also grateful to Denise Currie (Chemistry Department librarian) for help in sorting scientific literature. I am also thankful to all of my past and present colleagues: Dr Steven Ford, Dr Stephen Robertson, Dr Michelle Lovatt, Dr Deborah McPhail, Lindsay McDermott, Sarah Baron and Andrew Heron for their cooperation. I am also grateful to other Glaswegians, especially Syed Tufail Hussain Shah (President UKIM), Dr Archie Roy (student advisor RNIB), Kate Sillars, Paddy Morton, Shafqat Salim Quazi, Sheikh Riaz, Mohammad Zulfiqar, Abdul Rahman Abid, Dr. Carolyn Converse, and Dr. Harold Hammer (registrar, Eye Infirmary) for their cooperation during my stay in Glasgow. I wish to extend my thanks to Professor Dr Mohammad Shafiq Khan, Vice Chancellor Islamia University Bahawalpur, for his help and support. I am also grateful to Ministry of Education, Government of Pakistan, for giving me grant to complete this research work. My thanks are reserved to my parents, wife, daughter, brothers and sisters for their patience, support and encouragement.

Abdul Wadood

Abbreviations:

| | |
|---|---|
| BLA | Bovine α-lactalbumin |
| DSC | Differential scanning calorimetry |
| EL | Equine lysozyme |
| HEWL | Hen egg white lysozyme |
| HSA | Human serum albumin |
| ITC | Isothermal Titration Calorimetry |
| MES | 2-(N-Morpholino)ethanesulfonic acid |
| MOPS | 3-(N-Morpholino)ethanesulfonic acid |
| NAG | N-acetyl-D-glucosamine |
| NAM | N-acetyl-muramic acid |
| PG | Penicillin-G |

# ABSTRACT

The interaction of hen egg white lysozyme with penicillin and a range of metal ions has been studied using microcalorimetry and related biophysical techniques. UV difference and fluorescence experiments on the binding of penicillin to lysozyme are ambiguous and reflect the variety of published observations, but there is no clear evidence that penicillin competes for example with N-acetylglucosamine (NAG) in the binding cleft. This is supported by ITC binding experiments which suggest that penicillin-G binds to a site on lysozyme remote from the active site. DSC studies are complicated by the thermal instability of penicillin-G in solution above 35°C. The effect is to reduce the apparent $T_m$ for unfolding of lysozyme in a manner that suggests that penicillin or its decomposition products bind preferentially to unfolded protein. This may explain some of the experimental uncertainties apparent in the published data. DSC measurements of the effect of metal ions (mono-, di-, and tri-valent) on the thermal unfolding stability of lysozyme show that, in general, their effect is to reduce the $T_m$ , sometimes with aggregation of the unfolded protein, consistent with metal ion binding to exposed groups on the unfolded polypeptide. The effect of $Al^{3+}$ ions has been explored in some detail. The interaction of lanthanide ions ($La^{3+}$ and $Eu^{3+}$) has also been studied by DSC, ITC and fluorescence methods. ITC in particular shows multiple binding sites for lanthanide ions on lysozyme, some of which compete with NAG binding. This is consistent with lanthanide ion binding to some of the carboxylate residues on the protein, including those in the active site.

CONTENTS

# 1 INTRODUCTION

Alexander Fleming discovered two important but unrelated antibacterial molecules - lysozyme and penicillin - which have had major impact upon our understanding of protein structure and antibiotic activity. Various researchers (e.g. Johnson, 1967) have suggested, despite their different origins, that penicillin might bind to lysozyme. The primary aim of this thesis is to examine the possible interactions of penicillin with lysozyme using calorimetric and other biophysical techniques. Complementary studies of metal ion binding are also included. This chapter reviews the general background necessary to set the scene for this work.

## 1.1 AIMS OF THESIS

The aims of this thesis are to investigate the thermodynamic basis of lysozyme interactions with penicillin-G and metal ions (especially lanthanide ions) in various buffer systems and also in the presence of NAG (N-acetyl glucosamine) as an inhibitor, in order to provide a greater understanding of the interactions involved in the recognition between proteins and small ligands.

Different techniques were used to study these interactions. UV/Vis spectroscopy was used initially to measure the activity of lysozyme with its substrate Micrococcus lysodeikticus in the presence of penicillin-G. Measurements of protein intrinsic fluorescence and fluorescence quenching enabled the binding to lysozyme of penicillin, NAG, and europium and lanthanum ions in various combinations. Similar competitive binding experiments were done using the calorimetric technique of ITC (isothermal titration calorimetry). Differential scanning calorimetry (DSC) was used to measure the stability of the protein metal complex and also to study the effect of different concentrations of a range of metal chlorides with lysozyme.

It is thought that the interaction of these small molecules and ions may represent an important functional role in some proteins, therefore it is of central importance to understand their basis of action, not only for an academic point of view, but also as a means of designing potential variants of enzymes and understanding their behaviour with metals and inhibitors.

## 1. 2 PROTEINS

Virtually every property that characterizes a living organisms is affected by proteins. Protein is derived from the Greek word Proteios, which means of the first rank. '' Proteins are naturally occuring polymers of high molecular mass, consisting of amino acids, linked by peptide bonds. This is illustrated by the condensation of two amino acids:

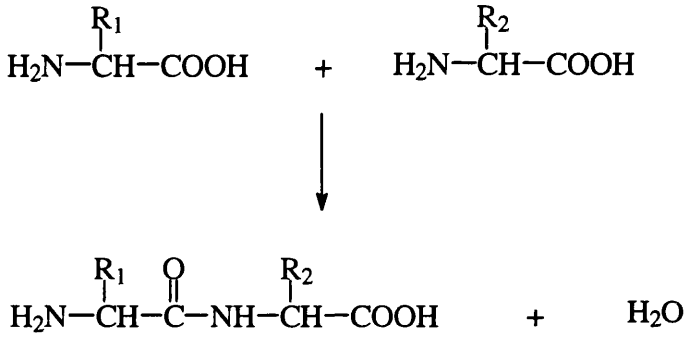

The commonly occuring amino acids are of 20 different kinds, 19 of which contain the same dipolar ion group $H_3N^+.C_1H(R).COO^-$ in the free amino acid form, differing only in the nature of the sidechain group (R). The 20th natural amino acid, proline, is similar, but its side chain is bonded to the nitrogen atom to give the cyclic imino acid:

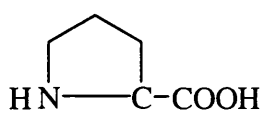

Proline

Except in glycine where the side chain is only a hydrogen atom, the central carbon atom is asymmetric and is always the L-isomer:-

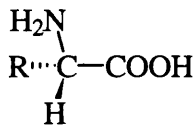

L-amino acid configuration

Protein constitutes more than 50% of the organic content of protoplasm, which is the major consituent of the dry material of living organisms, and they are the most important functional components of living cells. All naturally-occuring enzymes are proteins, and enzymes catalyze the many biochemical reactions that constitute the metabolism of the living cell. These reactions are controlled by appropriate enzymes or inhibitors. Some of the regulators and transmitters in these control processes are also proteins e.g. proteohormones. Similarly structural proteins contribute to the mechanical structure of organs and tissues (e.g. collagens), or they may constitute the bulk of a natural structure (e.g. the silk of insect). Ovalbumin (from egg white), casein (from milk) are the examples of the storage proteins. Othe examples of proteins are transport proteins (e.g. hemoglobin: transport of oxygen in vertebrate blood and serum albumin: transport of fatty acids and many other substances including hormones, drugs etc.), proteins involving in biochemical defense (e.g. antibodies), certain bacterial toxins (e.g. snake venoms). Proteins are also essential in milk coagulation, blood group specificity, memory processes and regulation of gene activity. The behaviour and properties of proteins are determined by their strucure, but theoretically there is no limit of polypeptide chain length and all permutations and combinations of amino acids are possible. Moreover possibilities of structural variation, attachment of non protein prosthetic groups, the quarternary structure offer almost unlimited functions

## 1:3 Classification of Proteins:

Proteins may be classified as follows (Brewer & Scott, 1983):-

1 Simple or unconjugated proteins

(i) Globular proteins: usually soluble in water or dilute salt solutions. Examples are albumins, globulins, protamines and histones (highly basic proteins associated with DNA in the cell nucleus), prolamines and glutelins (mainly plant proteins with a high proline and glutamic acid content).

(ii) Fibrous proteins: usually insoluble in water and salt solutions, greatly extended molecular structures with a very high degree of molecular asymmetry; structural proteins, very stable to acids, alkalis and proteolytic enzymes.

2 Conjugated proteins

These proteins contain the usually essential non protein moiety, prosthetic group, which is linked by covalent or non-covalent bond. Prosthetic groups include carbohydrates, lipids, nucleic acids, metals, heme groups and phosphate residues.

3 Proteins may be classified according to their origins, e.g. viral, bacterial, plant and animal proteins.

4 Different proteins, within one organism may be classified as blood, milk, cerebrospinal, secretory, muscle or structural proteins, etc.

5 Subcellular localization is also used for classification, e.g. ribosomal, microsomal, mitochondrial, lysosomal, nuclear, cytosol and membrane proteins.

## 1:4 The Structure of Proteins

Proteins consist of L-amino acid residues linked by peptide bonds. The sequence of amino acids in each polypeptide chain constitutes the primary structure of the protein. This can be determined by a systematic use of chemical procedures. Regular, repeating three-

dimensional features constitute the secondary structure. This is largely uninterrupted in fibrous, structural proteins but disrupted at many points in globular, functional proteins, including enzymes. The overall three-dimensional structure of each polypeptide chain is termed the tertiary structure. Proteins may consist of one or more polypeptide chains, the complete structure being called the quaternary structure.

## 1:5 ENZYMES

Living organisms possess complex networks of chemical reactions each of which is controlled by an enzyme. Enzymes are biological catalysts. They increase the rate of chemical reactions taking place within chemical living cells without themselves suffering any overall change. The reactants of enzyme-catalyzed reactions are called substrates and each enzyme has a unique property to react with a substrate or substrates to form product or products. They are able to affect almost every chemical reaction and also prevent unacceptable side reactions due to their extraordinary efficiency and specificity properties. But in many cases enzymes themselves are subject to complex control mechanisms. Many enzyme proteins lack catalytic activity without the presence of a non-protein component called a cofactor. In such cases the inactive part of an enzyme is termed the apoenzyme while the active part including the cofactor is called holoenzyme. The cofactor may be an organic molecule, coenzyme, or metal ion. Some enzymes bind cofactors more tightly than others. When a cofactor is bound so tightly that it is difficult to remove without damaging the enzyme it is sometimes called a prosthetic group.

Each substrate is bound to the enzyme at specific sites to form an enzyme-substrate complex in which reacting groups are held in close proximity to each other and to catalytic sites. That region of the enzyme's three-dimensional structure which contains the substrate binding sites and the catalytic sites is termed the active centre.

According to the Fischer lock-and-key hypothesis, the active site has rigid structural features which are complementary to those of each substrate. In contrast, the Koshland induced-fit-hypothesis suggests that at least some active sites are flexible, possessing a structure complementary to that of a substrate only when the latter is bound to the enzyme. These models can explain some aspects of enzyme specificity, but do not suggest any mechanism for the enzyme-catalyzed reaction.

## 1:6 INHIBITORS

An inhibitor is any substance that retards or decreases the rate of a chemical reaction; the opposite of a catalyst. For example antioxidants are well known inhibitors of oxidation reactions in food, rubber, and other organic materials. Protective coatings of various kinds inhibit the corrosion of metals. The most obvious example of the fatal effects which may be caused by the specific poisoning of a single enzyme is the toxicity of cyanide, which is primarily due to the inhibition of cytochrome oxidase, resulting in a cessation of the aerobic oxidation processes and death may occur in a very few minutes. In military point of view, the nerve gases, are essentially specific enzyme inhibitors.

An inhibitor may be irreversible or reversible. An irreversible inhibitor forms a stable compound often by the formation of a covalent bond with a particular amino acid residue in the enzyme which is essential for activity. The inhibitor can not be removed by gentle means. Reaction between the enzyme and inhibitor is progressive and takes place at a rate defined by rate constant.

The phenomenon of reversible inhibition is characterized by an equilibrium between enzyme and inhibitor defined by an equilibrium constant (K) which is a measure of the affinity of the enzyme for the inhibitor. Some of the possible examples of reversible inhibition is diagramatically shown in Figure 1.1.

COMPETITIVE INHIBITORS are the substances (usually structurally related to the substrate) that combine with an enzyme at the same site as the substrate. Inhibitor and substrate therefore compete for the same site forming [ES] or [EI] complexes; where E, S, and I represent enzyme, substrate and inhibitor respectively. For example indole, phenol and benzene bind in the binding pocket of chymotrypsin and inhibit the hydrolysis of derivatives of tryptophan, tyrosine and phenylalanine. The effect of a competitive inhibitor depends on the inhibitor concentration, the substrate concentration and the relative affinities of the substrate and the inhibitor for the enzyme. In general, at a particular inhibitor and enzyme concentration, if the substrate concentration is low then the inhibitor will compete favourably with the substrate for the binding sites on the enzyme and the degree of inhibition will be great. On the other hand if the substrate concentration is high

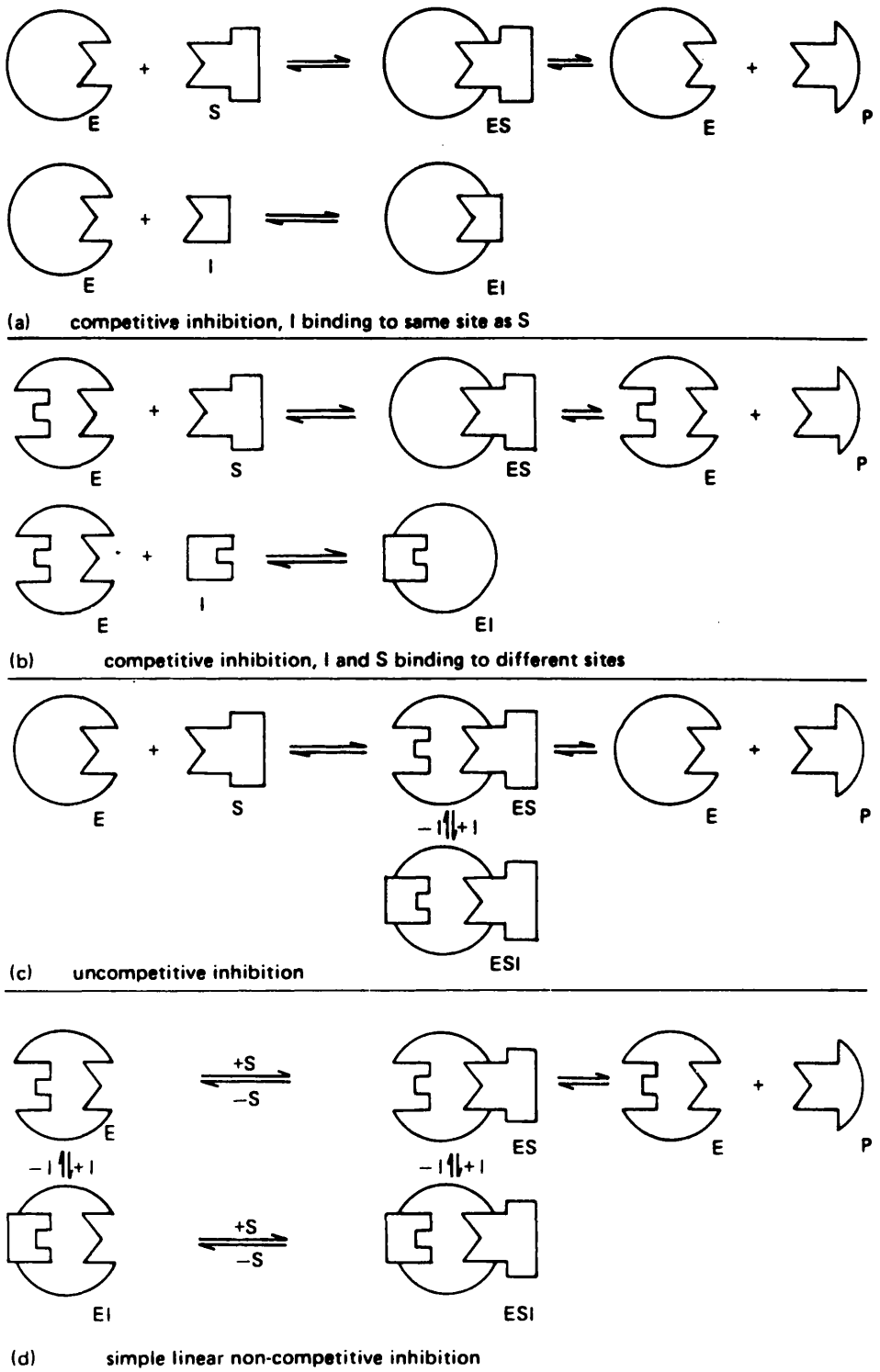


Figure 1.1: Diagrammatic representation of various examples of reversible enzyme inhibition (adapted from: T. Palmer (1995) "Understanding Enzymes" 4th.ed., Prentice Hall).

then the inhibitor will be much less successful in competing with the substrate for the available binding sites and the degree of inhibition will be less marked. At very high substrate concentration, molecules of substrate will predominate and the effect of inhibitor will be negligible.

STEADY-STATE KINETICS of a simple single-substrate single-binding-site single-intermediate enzyme-catalyzed reaction in the presence of a competitive inhibitor, I, may be represented by:

$$E + S \underset{k_{-1}}{\overset{k_1}{\rightleftharpoons}} ES \xrightarrow{k_2} E + P$$

$$E + I \rightleftharpoons EI$$

where E, S and ES are called enzyme, substrate, and enzyme-substrate complex respectively, and P is the final product. $k_1$, $k_2$ are the forward rate constants of reaction, and $k_{-1}$ is the reverse rate rate constant for the first step.

The dissociation constant for the reaction between E and I is $K_d$, where $K_d = \frac{[E][I]}{[EI]}$

and is also frequently called the inhibition constant $K_i$ . Equilibrium between enzyme and inhibitor will normally be established almost instantaneously on mixing.

NON-COMPETITIVE INHIBITORS are the substances that combine equally well with the enzyme or its enzyme-substrate complex. For example, inhibition of fructose 1,6 diphosphatase by AMP (adenosine-5'-monophosphate). This type of inhibition is very common with multi substrate enzymes. In this case three complexes are formed - ES, EI, and ESI- and of these only the ES complex breaks down to products. This type of inhibitor is not completely overcome by high substrate concentrations but reciprocal plots yield a Michaelis constant identical with that found in the absence of inhibitor. The situation for a simple single-substrate reaction will be as follows:

$$E + S \rightleftharpoons ES \rightarrow E + P$$

$$E + I \rightleftharpoons EI$$

$$ES + I \rightleftharpoons ESI$$

It has become established that inhibitors are classified according to the overall pattern observed. Therefore, non-competitive inhibition is only said to be present when the characteristics of simple linear non-competitive inhibition (i. e. linear Lineweaver-Burk plot, changed $V_{max}$, but unchanged $K_m$) are satisfied. Heavy-metal ions and organic molecules which bind to -SH groups of cysteine residues in the enzyme sometimes act as non-competitive inhibitors. Some groups such as cyanide which bind to the metal ions of metalloenzymes can destroy enzyme activity. However, in many cases such effects are irreversible; e.g., penicillin-G binds to hen egg-white lysozyme in the presence of NAG as a non competitive inhibitor (Mitsumori, et al., 1980; present work).

MIXED INHIBITORS obey the Michaelis-Menten kinetics but do not give patterns characteristic of competitive, uncompetitive or non-competitive inhibition. The other types of inhibitors are product inhibitors and substrate inhibitors. These types of inhibition are used in biochemical research and have applications in medicine and agriculture.

Allosteric inhibition, which results in more sigmoidal reaction characteristics, plays an important role in metabolic regulation in the living cell. All of these above forms are usually reversible, but irreversible forms also exist which have been used to identify amino acids in the active centres of enzymes. On purely academic grounds, specific enzyme inhibitors are frequently useful as tools, for instance many of the intermediates in glycolysis and yeast fermentation were discovered largely by the use of inhibitors blocking the various successive steps and allowing the corresponding intermediates to accumulate in sufficient quantities for isolation and identification. Similarly, the use of malonate, a competitive inhibitor of succinate dehydrogenase provided evidence for the existance of the citric cycle. (Palmer, 1995; Dixon & Webb, 1979).

## 1:7 Other LIGAND INTERACTION

A wide variety of physiological processes are the reflection of ligand interactions with macromolecules, especially with proteins. The most common are interactions between enzymes and their substrates (as described above) and with other molecules that influence activity. In addition there are interactions between hormones and hormone receptors, between small molecules and proteins involved in the active transport of small molecules, between ions and both nucleic acids and proteins and so on. Upon reflection, it is clear that virtually all biological phenomena depend on one or more ligand interactions. This is why a large number of biochemical and biophysical research depends on ligand interactions in depth. (Cantor, & Schimmel, 1980.)

## 1:8 PROTEIN FOLDING and STABILITY

The ability of polypeptides with appropriate sequence to fold into active native structures is essential for the expression of genetic information. Under suitable and appropriate physico-chemical conditions the folding of a protein is spontaneous and determined solely by its amino acid sequence. In principal, folding of the protein chain is entropically unfavourable. Restrictions of the inherently flexible polypeptide chain to a more limited region of a conformational space involves a reduction in conformational entropy (negative $\Delta S$, positive contribution to $\Delta G$) which must be offset by other more favourable free energy contributions if folding is to be stable. These additional contributions arrising from the multiplicity of interactions. This arises from the fact that the interactions between side chain and/or backbone groups, may be either enthalpic or entropic depending on the nature of the interaction, and will also contain major contributions from solvent (water) effects.

The stability of the folded and unfolded states of proteins are relative to each other. Therefore any factor which stabilizes the unfolded state reduces the magnitude of the free energy difference between them and consequently destabilizes the native (folded) state and *vice versa*. So all of the forces exerted in the folded state must be sufficient to counter the possible interactions in the unfolded state.

It is well known that various substances cause changes in the conformation of proteins when added to aqueous protein solutions. Investigations of these changes have provided useful information about the role of solvent in maintaining the native conformation of proteins, forces that contribute to the stability and mechanism of the folding-unfolding process. Thus, the small molecules act as effective probes of the solution conformation of proteins. The unique conformation of a protein that is essential for biological activity is denatured by heating, changing the pH or adding denaturants. The denaturation is highly cooperative and completely reversible under certain conditions. The reversible denaturation can be analysed on the basis of a two-state mechanism or a multi-state mechanism in which the protein is in equilibrium between the native and the unfolded states or an intermediate state (Sabulal & Kishore, 1996).

The native states of proteins are only marginally more stable than the unfolded state i.e., 5-15 kcal $mol^{-1}$. Usually the lifetimes of intermediates in folding are very short and their concentrations are very low. Thus, most single-domain proteins adhere to a two-state system: native(N) $\rightleftharpoons$ denatured(D) under equilibrium conditions, owing to the low population of the intermediate states. However, stable conformational states located between the native and unfolded states have also been found for several proteins (Kuwajima, 1989; Dobson, 1992; Palleros, et al., 1993; Kataoka, et al., 1995; Redfield et al., 1994). Hence it is important to obtain experimental information on the folding-unfolding behaviour of the proteins as a function of environmental factors including solvent, pH and temperature and the population of partially folded intermediate states to understand the mechanism of protein folding. Now most direct and complete thermodynamic parameters of the conformational states and transitions of globular proteins have been determined by calorimetry (Xie et al., 1991; Privalov, 1992; Ladbury et al., 1994; Sabulal & Kishore, 1995). Xie et al. (1991) showed that at increasing guanidine hydrochloride concentrations, the ratio of the van't Hoff to the calorimetric enthalpy increases monotonically to values greater than 1. They argued that the increase in this ratio occurs due to a decrease in the measured calorimetric enthalpy rather than an increase in van't Hoff enthalpy, arguing against protein oligomerization and suggesting that the addition of guanidine chloride shifts an increasing proportion of protein molecules to a state which does not undergo a cooperative or a significantly enthalpic unfolding transition.

In general, four types of non-covalent interactions are responsible for stabilizing the native state. These are hydrogen bonding, hydrophobic effect, electrostatic interactions, and van der Waals interactions. For details of many of these forces, the following reviews are useful (Kauzmann, 1959; Dill, 1990; Rose & Wolfenden, 1993).

## 1:8:1 HYDROGEN BONDING

Hydrogen bonding is very important in the case of biological systems. This arises when two electronegative atoms are linked together via a hydrogen atom, one of which is covalently bound to the hydrogen atom. The hydrogen bond is the strongest of the non-covalent interactions with a typical free energy in the gas phase of 25-80 kJ $mol^{-1}$ (Weiner et al.,1984; Meot-Nir & Sieck, 1986). Hydrogen bonds are asymmetric, since the proton is covalently bonded to one of the atom pairs and the distance between them is shorter than that of van der Waals contact distance. Hydrogen bonding can therefore be important in determining geometric constraints between enzyme and substrate and hence specificity. The overall binding energy of macromolecule-ligand depends on the hydrogen bond and its environments. The effective strength of the hydrogen bond is altered in aqueous solution due to competition with water hydrogen bonds. In aqueous solution, a macromolecule and ligand will participate in hydrogen bonding to surrounding water molecules and, therefore, there may be no net gain in the number of hydrogen bonds formed. When the two molecules associate, they usually have low enthalpy and free energy values due to the formation of hydrogen bonds between groups in water (Klotz & Franzen, 1962). There may be, however, an increase in entropy of the system due to the release of H-bonded water molecules to the bulk phase, which stabilizes the interaction.

The protein polar groups can form hydrogen bonds not only between themselves but also with water molecules. As for the interaction between charged groups, there are not very many in proteins. Therefore it is usually assumed that they play a minor role in stabilization of the protein structure (Hollecker & Creighton, 1982; Creighton, 1985), although they might be important in directing protein folding (Schoemaker et al., 1987).

By far the most important side chains, in terms of number of water molecules bound, are Asp and Glu whose $COO^-$ groups bind on average two water molecules each. These side chains also make a number of hydrogen bonds with protein atoms and show a strong tendency to have their hydrogen bonding potential fully satisfied. (Molyneux & Frank, 1961). Thus, those which have few or no hydrogen bonds with protein atoms are often highly hydrated.

In general, however hydrogen bonds may be more important in controlling specificity rather than stabilising the complexes themselves, α–helix and β–sheet structures depend largely on hydrogen bonding.

## 1:8:2 HYDROPHOBIC EFFECT

One way of describing the hydrophobic bond is the tendency of non-polar compound such as hydrocarbons to transfer from an aqueous solution to an organic phase. Therefore there is not much interaction between solvent and solute molecules as compared to normal hydrogen bonding. Water consists of a polar dynamic, loose network of hydrogen bonds. Therefore the presence of a non polar compound causes a local rearrangement in this network. The water molecules line up around the non polar molecule to preserve the hydrogen bonds (25 kJ/mol energy), so there is no large enthalpy change in the solvent but there is a decrease in entropy due to increase in the rearrangement of the network. A hydrophobic molecule is driven into the hydrophobic region of a protein by the regaining of entropy by water. The second factor favouring the self association of hydrocarbons is dispersion forces because dispersion forces are weaker in water due to low polarizability of oxygen and low atomic density as compared to hydrocarbons which have higher atomic density and polarizability.

In case of proteins they tend to fold in such a way that the non polar side chains form a hydrophobic core from where the water molecule is largely driven out. When hydrocarbon is introduced into polar solvent there is large positive change of heat capacity. Similarly this is also observed when protein molecules unfold.

## 1:8:3 ELECTROSTATIC INTERACTIONS

These are the interactions that occur between charged or dipolar atoms and molecules. As electrostatic interactions are the best understood type but their quantitative importance is difficult to assess because the interaction energies depend on the dielectric constant D of the medium. The problem of calculating dielectric effects in protein is especially difficult because of their heterogenity of structure. The dielectric constant is not uniform throughout the protein. The following types of electrostatic interactions energies exist:

(i) Between ions with net charge.
(ii) Between randomly oriented permanent dipoles.
(iii) Between an ion and a dipole induced by it.
(iv) Between a permanent dipole and a dipole induced by it.

As water has a high dielectric constant (around 80), the magnitude of the electrostatic force is increased in proteins when charged groups interact in the absence of water molecules. Therefore, during protein folding, few ion pairs are buried and only surface ion pairs take part in protein stability (Barlow & Thornton, 1983). This is probably due to the unfavourable energy which is associated with the buried charged groups in the hydrophobic region of the protein.

Electrostatic interactions between a macromolecule and ligand are also decreased by high salt concentrations. As salts attenuate the attraction between ion pairs by shielding the charge, whereas pH directly change the charge on acidic or basic groups. Therefore it has little effect on the stability of the protein which leads to the conclusion that ion pairs are not responsible for major effects in protein folding (Tanford, 1968).

### 1:8:4 VAN DER WAALS INTERACTIONS

Van der Waals repulsions occur when two atoms are so close to each other that there is interpenetration of their electronic clouds. Weak attractive interactions occur at slightly longer distances because of the attractive dispersion forces resulting from the mutual induction of electrostatic dipoles. Although a non polar molecule has no permanent dipole, there will be dipoles due to the local fluctuations of electron density. Because the energies depend on the induction of a dipole, therefore polarizability is an important factor in the strength of the interaction between any two atoms.

Although the attractive forces are weak and the van der Waals energies are low, they are additive and make significant contributions to binding when they are summed over a molecule. Thermodynamically, van der Waals interactions would normally be considered to contribute to the enthalpy of interactions but with no significant entropy term. For example it is found experimentally from heat of sublimation data that each methylene groups in a crystalline hydrocarbon has 8.4 kJ/mol of van der Waals energy, and that each CH group in benzene crystals has 6.7 kJ/mol. It has been calculated that van der Waals energy between the D subsite of lysozyme and the occupying glycopyranose ring is about –58. 5kJ/mol (–14 kcal/mol) (Warshel, & Levitt, 1976).

## 1:9 THERMODYNAMICS

Basic thermodynamic quantities like enthalpy, entropy and free energy are very important when we measure any conformational changes or other interaction in protein molecules. Therefore thermodynamic parameters are responsible for what happens when we change conditions like pressure, temperature, pH, ligand interactions of macromolecule, chemical denaturants, solvent changes, and so forth.

### 1:9:1 ENTHALPY

The thermal energy change at constant pressure, when there is no additional work, is called the enthalpy change. Therefore, $\Delta H = q_p$, where $q_p$ is the heat absorbed by the system at constant pressure. When temperature (T) increase enthalpy (H) also increases.

## 1:9:2 HEAT CAPACITY

The increase in total heat energy with respect to temperature is called the heat capacity and is represented by the symbol C. Therefore when temperature (T) increases at constant pressure the enthalpy (H) also increases. If heat capacity is measured at constant pressure it is called heat capacity at constant pressure and is designated by $C_p$. Similarly heat capacity at constant volume, involving change in internal energy (U), is represented by the symbol $C_v$.

Thus $C_p = \left(\frac{\partial H}{\partial T}\right)_P$ and $C_v = \left(\frac{\partial U}{\partial T}\right)_V$

For an infinitesimal changes of temperature

$dH = C_p\, dT$ (at constant pressure)

or $\Delta H = C_p \Delta T$ (at constant pressure)

as $q_p = C_p\, \Delta T$ (1st law of thermodynamics)

For ideal gases $C_p - C_v = nR$ where n is number of moles of gas involved and R is the gas constant. However, for most processes taking place in solution, and certainly for most biomolecular interactions which are normally studied at constant pressure, the difference between $C_p$ and $C_v$ is negligible.

Based on experimental observations of small molecules in water, the change in heat capacity ($\Delta C_p^0$) can give us some indication of hydrophobic interactions between the macromolecule (P) and ligand (L). A negative value of $\Delta C_p^0$ indicates that there is an increase in hydrophobic interactions whereas a positive value indicates a decrease in hydrophobic interactions.

## 1:9:3 ENTROPY

Simply entropy is a measure of degree of disorder or randomness of a system. For example the entropy of water is greater than that of ice at 273. 15 $K^0$ which means that the molecules of ice are more ordered as compared to water molecules. Similarly entropy of

water vapour is greater than water at 373. 15 $K^0$, again reflecting the greater freedom of motion (randomness of molecules in the gaseous phase). Thus some heat energy is required (i. e. latent heat of fusion or melting) for melting of ice at 273. 15 $K^0$ resulting an increse of entropy of the system. It follows that entropy and heat changes must be related in some way. Thus according to second law of thermodynamics the change in entropy of the system (dS) during some process (or reaction) is the heat absorbed by the system (dq) at a temperature (T).

Therefore, $dS \geq dq / T$ ---------- (1)

The inequality in the above equation refers to an irreversible process whereas the equality refers to a reversible process.

## 1:9:4 FREE ENERGY

According to second law of thermodynamics a reaction or a chemical process will proceed as long as $dq < TdS$. But most of the reactions take place at constant pressure and under such circumstances

$dq = dH$ ---------- (2)

i.e. the heat absorbed is equal to the change in enthalpy of the process

Substituting the value of dq, we have $dH < TdS$ or $dH - TdS < 0$. As far as this condition is satisfied, the reaction will proceed. The importance of the quantity (dH - TdS) as a measure of the extent to which a reaction will proceed is such that it is given a special symbol (dG).

i.e. $dG = dH - TdS$ ---------- (3)

Thus if a process occurs then $dG < 0$. The process will continue until an equilibrium is attained. At equilibrium, the second law states that

$dq = TdS$

Thus at constant pressure and at constant temperature condition

$dH = TdS$ ---------- (4)

Thus at equilibrium

$dG = dH - TdS = 0$

When larger changes are involved, then these equations become:

$\Delta G = \Delta H - T\Delta S$ ---------- (5)

The superscript 0 is used to indicate processes taking place under standard conditions. Thus when all components are present in their standard states

$$\Delta G^0 = \Delta H^0 - T\Delta S^0 \quad \text{---------- (6)}$$

From calorimeter, we measure directly $C_p$ and H. Thus at equilibrium, where $\Delta G = 0$, the $\Delta S = \Delta H/T$ (Price & Dwek, 1991).

The reaction will proceed if $\Delta G < 0$ and be at equilibrium if $\Delta G = 0$. Therefore $\Delta G$ is a measure of the work (or energy) that can be obtained from a reaction . At equilibrium no work can be obtained (since there is now no tendency for the reaction to proceed).
G is a state function like H and S. For most processes, $\Delta G$ is dominated by either the $\Delta H$ or $T\Delta S$ term, and the process is said to be enthalpy or entropy controlled. If $\Delta H$ for a reaction is large and negative, $\Delta G$ will be negative; therefore, highly exothermic reactions ($\Delta H$ negative) are favourable ($\Delta G$ negative) and $\Delta H$ dominated. In some cases $\Delta H$ is very small and the entropy term dominates. Examples of such processes are metal-ion complex formation with polydentate ligands and in some cases of protein denaturation. For example, at 313K and pH = 3, chymotrypsin can be denatured, $\Delta H$ is highly favourable, 62.7 kJ $mol^{-1}$ but $\Delta S$ is 1839 J $K^{-1}$ $mol^{-1}$ and so $\Delta G$ is –513 kJ $mol^{-1}$. As a result denaturation is highly favourable (Price & Dwek, 1991).

The denaturation of a protein involves the breaking of a large number of non covalent bonds (e.g. hydrogen bond) which are responsible for maintaining the highly ordered tertiary structure of the active form. Denaturation has thus increased the disorder of the system and so the denatured form is often referred to as the random coil form.

## 1:9:5 EQUILIBRIUM CONSTANT (K)

Biochemical systems are rarely at equilibrium because the matter is constantly entering and leaving the cells resulting in a steady state situation rather than a true equilibrium. However, these processes are governed by the laws of thermodynamics and can be understood in terms of equilibrium processes.

Consider a general reaction: $aA + bB \rightleftharpoons cC + dD$

The equilibrium constant K (which for binding processes is equivalent to the association constant or affinity constant $K_a$, and reciprocal of the dissociation constant, $1/K_a = K_d$) is given by

$$K = \frac{[C]^c[D]^d}{[A]^a[B]^b}$$

where the brackets [ ] indicate molar concentrations. Strictly speaking these should be thermodynamic activities, but in the case of dilute solutions, activity coefficient, $\gamma$, is unity and so activity and concentrations are almost same (i.e. $a = \gamma C$).

The typical units of binding constant is $M^{-1}$, $mM^{-1}$, is a measure of the strength of binding. Therefore large value of K means that the ligands are tightly bound to the macromolecule (more negative $\Delta G^0$).

When a ligand (L) molecule is bound to the protein (P) molecule according to the following equation

$$P + L \rightleftharpoons PL$$

where [P], [L] and [PL] are the equilibrium concentrations of protein, free ligand and the complex respectively, then

$$K = \frac{[PL]}{[P][L]}$$

The relationship between euilibrium constant and Gibbs free energy is as follows

$$\Delta G^0 = -RT\ln K \qquad \text{---------- (7)}$$

or $\Delta G^0 = -2.303\ RT \log K$

Combining equations 6 and 7 leads to

$$d/dT\ (\ln K) = \Delta H^0/RT^2 \qquad \text{---------- (8)}$$

This equation is called Van't Hoff isochore.

By integrating equation 8 between temperatures $T_1$ and $T_2$ we get

$$\int_{K1}^{K2} d(\ln K) = \int_{KT1}^{T2} \Delta H^0/RT^2 \, . \, dT$$

or $\ln K_2/K_1 = -\Delta H^0/R \, [\, 1/T_2 - 1/T_1 \,]$ ----------(9)

This is an equation of a straight line having slope $-\Delta H^0/R$, if we plot lnK vs 1/T. This equation can be used in two main ways:

(a) If we know the value of K at various temperatures, $\Delta H^\circ$ can be obtained from the slope of the graph, if we plot lnK vs 1/T

(b) If we know K and $\Delta H^0$ at one temperature we can calculate K at another temperature. (Price & Dwek, 1991)

The assumption that $\Delta H^0$ and $\Delta S^0$ are both independent of temperature are generally satisfactory, if the temperature range considered is very small. A significant exception occurs in the case of proteins. Thus for the denaturation of lysozyme by guanidinium hydrochloride, $\Delta H^0 = 90.3$ kJmol$^{-1}$ at T = 298 K and $\Delta C_p = 5.5$ kJK$^{-1}$mol$^{-1}$ ; also $\Delta H^0 =$ 62.7 kJmol$^{-1}$ at T = 293 K and $\Delta H^0 = 117.9$ kJmol$^{-1}$ at T = 303K (Pfeil & Privalov, 1976b). The large value of $\Delta C_p$ arises because of the break up of the three dimensional structure or denaturation, which involves the rupture of many non covalent bonds. For ideal solutions or ideal gases, $\Delta H$ is independent of pressure.

## 1:10 LYSOZYME

It has been reported that the early Romans used egg white in the treatment of eye infections, and some mothers are said to have used human milk for the same purpose, both media contain appreciable amounts of lysozyme. Later antibacterial properties of leukocytes, cow milk, *bacillus subtilis*, domestic hen egg-white and nasal secretions were described from 1880 to 1920 in different papers. However it was Fleming who first clearly showed that an enzyme substance present in a wide variety of secretions is capable of rapidly lysing (i.e. dissolving) certain bacteria, particularly a yellow, coccus, that he studied. He named the enzyme as lysozyme - lyso because of its capacity to lyse bacteria and zyme

because it was an enzyme. He also discovered a small round bacterium that was particularly susceptible to lysozyme; he named it *Micrococcus lysodeikticus* because it exhibited lysis (deiktikos means able to show in Greek). As lysozyme degrades highly purified chitin, it was proposed that lysozyme and related enzymes be called muramidases (Salton, 1964). Lysozymes are now defined as 1,4 β-N-acetylmuramidases cleaving the glycosidic linkage between the C-1 of N-acetylmuramic acid and the C-4 of N-acetylglucosamine in the bacterial peptidoglycan.

There are at least three different kinds of lysozyme and HEWL belongs to the c-type (chicken- or chick-type) lysozyme family which encompasses all the mammalian lysozymes, Hyalophora (moth) lysozymes and some birds (goose type or g-type) lysozymes. Plant, fungus, viral and bacterial lysozymes are also known. HEWL is 129 amino acids long and has a molecular weight of 14315 a.m.u. (Canfield, 1963).

Lysozyme is a protein which is widely distributed in nature and is easily available (Aramini et al., 1992; Lyster, 1992). A peculiarity of this enzyme is its lytic activity on the cell walls of the Gram-positive bacteria (Wang et al., 1990). In hen egg white lysozyme, basic amino acid residues (e.g. lysine or arginine) are present in high proportions and they give positive charges at neutral pH.

Lysozyme is a small monomeric protein with four α-helices which make up one, domain, encompassing the amino- and carboxy- terminal segments of the protein, and a triple-stranded antiparallel β-sheet that, with a long loop, makes up much of a second, domain. In addition, there are two $3_{10}$ helices, one in each domain, and a short region of double-stranded antiparallel β-sheet which links the two domains. The structure is stabilized by four disulphide bridges; these are maintained during the folding studies (Dobson, et al., 1994). Its primary sequence is shown below:

```
1                   10                  20
Lys-Val-Phe-Gly-Arg-Cys-Glu-Leu-Ala-Ala-Ala-Met-Lys-Arg-His-Gly-Leu-Asp-Asn-Tyr-Arg-Gly-
                    30                  40
Try-Ser-Leu-Gly-Asn-Trp-Val-Cys-Ala-Ala-Lys-Phe-Glu-Ser-Asn-Phe-Asn-Thr-Glu-Ala-Thr-Asn-
                    50                  60
```

Arg-Asn-Thr-Asp-Gly-Ser-Thr-Asp-Tyr-Gly-Ile-Leu-Glu-Ile-Asn-Ser-Arg-Trp-Trp-Cys-Asn-Asp-

70 80

Gly-Arg-Thr-Pro-Gly-Ser-Arg-Asn-Leu-Cys-Asn-Ile-Pro-Cys-Ser-Ala-Leu-Leu-Ser-Ser-Asp-Ile-Thr-

90 100 110

Ala-Ser-Val-Asn-Cys-Ala-Lys-Lys-Ile-Val-Ser-Asp-Gly-Asn-Gly-Met-Asn-Ala-Trp-Val-Ala-Trp-

120 129

Arg-Asn-Arg-Cys-Lys-Gly-Thr-Asp-Val-Glu-Ala-Trp-Ile-Arg-Gly-Cys-Arg-Leu

Lysozyme dissolves certain bacteria by cleaving the polysaccharide component of their cell walls. The function of the cell wall in bacteria is to confer mechanical support. A bacterial cell devoid of a cell wall usually bursts because of the high osmotic pressure inside the cell. The cell wall polysaccharide is made up of two kinds of sugars: N-acetylglucosamine (NAG) and N-acetylmuramate (NAM). In bacteria cell walls NAM and NAG are joined by glycosidic linkages C-1 of one sugar and C-4 of the other. The oxygen atom in a glycosidic bond can be located either above or below the plane of the sugar ring. The cell wall polysaccharide is an alternating polymer of NAM and NAG residues joined by $\beta(1\rightarrow4)$ glycosidic linkages. Polysaccharide chains have directionality. Different polysaccharide chains are cross-linked by short peptides that are attached to NAM residues. A schematic diagram of the cleavage is shown in Figure 1.2.

There are two proposed mechanisms by which HEWL hydrolyses saccharide oligomers (Figure 1.3). In both mechanisms glycosidic cleavage occurs between sugar residues at sites D and E of the enzyme cleft. The mechanism I scheme is based on X-ray data that was originally developed by Blake *et al.* between 1965 and 1972. This proposes that Glu-35 donates a hydrogen to the glycosidic oxygen with the resulting cation being stabilized by Asp-52, the addition of water finishes the process. The second scheme was suggested by Post and Karplus in 1986 to explain additional evidence that had been observed in the preceding 10 years. Scheme II does not require the distortion of sugar D and involves the cleavage of the endocyclic $C^1$ - $O^5$ bond. (See the recent review by Mckenzie and White, 1991).

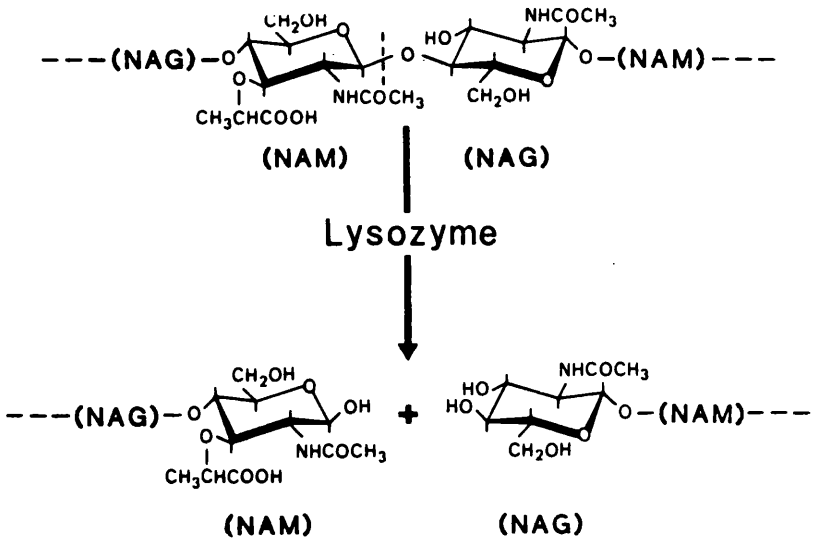


Figure 1.2: Overall reaction for cleavage by lysozyme of the glycosidic link between N-acetylmuramic acid (NAM) and N-acetylglucosamine (NAG) in the polysaccharide analogue of the bacerial cell wall (adapted from McKenzie & White, 1991).

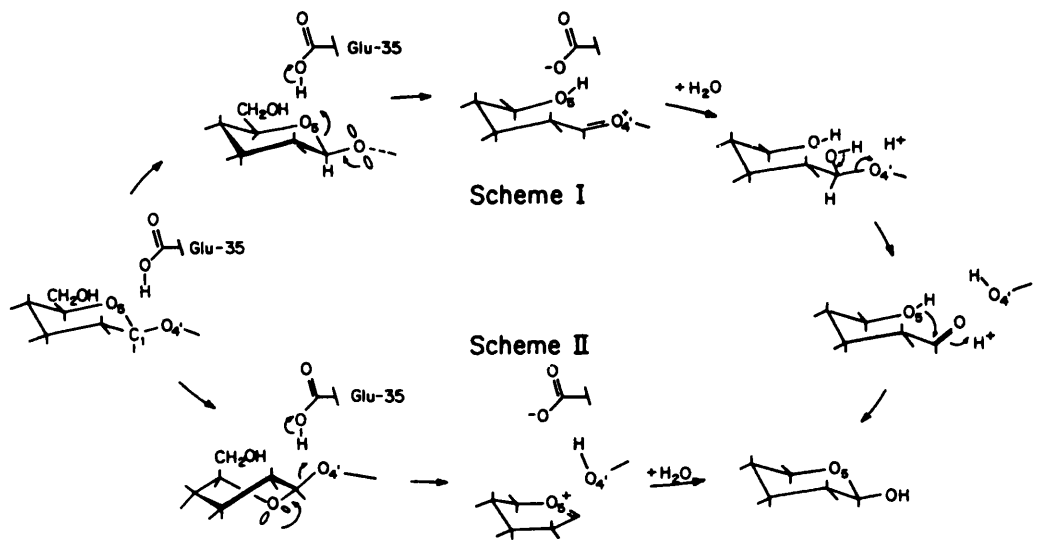


Figure 1.3: Alternative reaction mechanisms for lysozyme-catalysed cleavage of polysaccharide substrates (adapted from McKenzie & White, 1991).

The outline conformation of the molecule in solution has been suggested to be similar to the x-ray structure, because of the correlation between known chemical properties of the molecule and those expected from the x-ray structure (Imoto, et al., 1972). On a quantitative basis the degree of similarity remains unknown. Indeed, the exact meaning of protein conformation is difficult to define when the situation in solution is considered, because the constraints which could result in the existance of a single immobile conformation are less than these operating in the crystalline state. For example, even if on a time-average the solution conformation closely resembles the x-ray structure, the groups of the protein may have considerable freedom of movement, which is independent of the overall molecular tumbling. This independent freedom of movement could be of considerable importance when considering the mechanism of enzymic action, which is conventially considered using a static model of protein.

The structure and dynamics of enzyme-substrate complexes is one of the most important areas of biophysical chemistry. Much experimental work has been done on the interaction of lysozyme-substrate complex of HEWL and work continues to be done by using some modern instruments for example ITC, DSC, etc. as well as HEWL inhibitor studies. The classical HEWL inhibitors and substrates are oligomers of N-acetyl-glucosamine $(NAG)_n$ . Short chain saccharides (n=1 to 3) act as inhibitors whereas long chain saccharides (n = 4 to 6) act as enzyme substrates. The structural formula of $NAG_3$ is shown below (Figure 1.4).

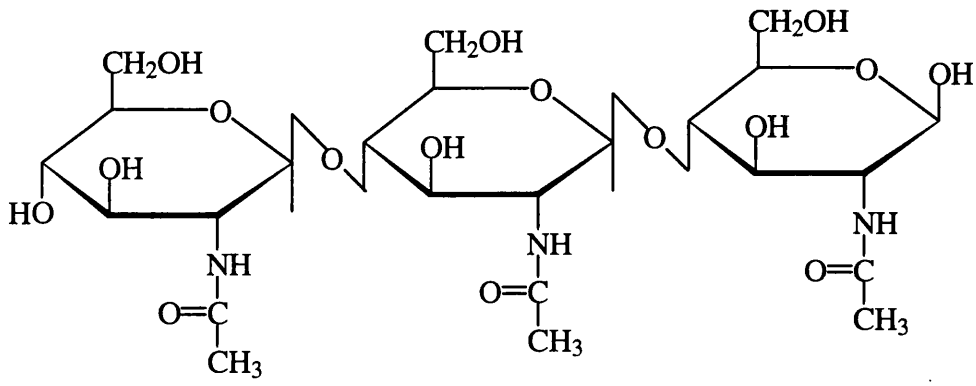


Figure 1.4: The structural formula of $NAG_3$

## 1:10:1 Three Dimensional Structure Of Lysozyme

The three-dimensional structure of HEWL was first determined by X-ray (Blake et al., 1965). It was the first crystal structure of an enzyme and since then the structure has been examined in various space groups and at higher resolution. The X-ray studies indicated the nature of the active site of the enzyme and and the mode of binding to inhibitors and substrate. The highly stable protein is cross-linked internally by four disulfide bridges. Lysozyme is a compact molecule, and the folding of this protein is complex. It has much less α-helix than many other proteins and, in a number of regions, the polypeptide chain is in an extended β-sheet conformation. The interior of lysozyme is almost entirely non polar. Hydrophobic interactions play an important role in the folding of lysozyme. The X ray studies indicated the nature of the active site of the lysozyme and the mode of binding to inhibitors and substrate.In summary, the main structural features of the domestic hen egg-white lysozyme molecule (Fig. 1.5) are as under:

(1) The molecule has approximately the shape of a prolate ellipsoid 45x30x30 Å (no allowance being made for bound water). It has a deep cleft on one side. The cleft divides the molecule roughly into two lobes. The first consists of the two ends of the chain (residues 1-39 and 85-129), while the second (comprising residues 40-84) is rather sheet-like and consists of residues either in the outer surface or lining the cleft.

(2) Lysozyme has a fairly small proportion of helix and reasonably long stretches of chain with essentially irregular conformation. Several parts of the chain have an extended conformation closely similar to the β-sheet.

(3) The first lobe (residues 1-39 and 85-129) contains four helices, and one single-turn $3_{10}$-type helix. There are short stretches (each five to nine residues) of backbone loops and turns connecting the helices. Three α-helices (helix A, residues 4-15; helix C, residues 88-99; helix D, residues 108-115) are on the protein surface and are partially exposed to solvent. The helix (B) consisting of residues 24-36 is totally buried. The $3_{10}$ helix (residues 119-124) is partially exposed to solvent. The second lobe (residues 40-84) contains a three-

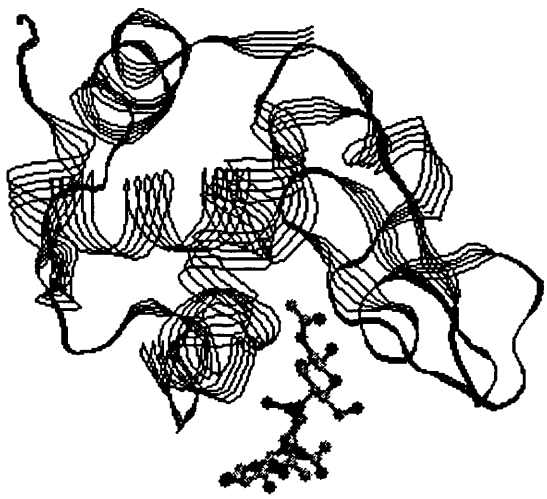

Figure 1.5: Ribbon diagram of the structure of hen egg white lysozyme, showing the position of the tri-NAG inhibitor in the active site cleft.

stranded antiparallel β-pleated sheet (residues 42-60), a small β-sheet (residues 1-2 and 39-40), and a single turn $3_{10}$ helix (residues 79-84). There is a long coiled loop region, residues 61-78, between the large β-sheet and the $3_{10}$ helix. Residues that line the cleft include β-sheet residues 43, 44, 46, 52, and 56-59, helix B residue 35, the loop connecting helices C and D (residues 98 and 101-103), helix D residues 107-110 and 112, and residues 62, 63 and 73.

(4) Cystine bridges occur between residues 6 and 127, 30 and 115, 64 and 80, and 76 and 94. The first two pairs have positive angles. All are the range $100^0 \pm 10^0$.

(5) The residues that line the cleft include Glu 35, Thr 43, Asn 46, Asp 52, Leu56, Glu 57, Ile 58, Asn 59, Trp 62, Trp 63, Arg 73, Ile 98, Asp 101, Gly 102, Asn 103, Ala 107, Trp 108, Val 109, and Ala 110. Between the active site cleft, with its flexible residues, and the rigid hydrophobic core lies a collection of residues known as the hydrophobic box. The hydrophobic box includes residues such as Trp 28, 108, and 111, Tyr 23 and Met 105. Recent studies have shown that the hydrophobic box plays a role in inhibitor binding and thermal denaturation (Miura *et al*, 1991; Bernard *et al*, 1990).

(6) HEWL can be crystallized in four different crystal space groups (triclinic, tetragonal, monoclinic and orthorhombic), but the structure is essentially the same in all four, with the exception of part of the β-sheet region and some of the longer side chains (Mckenzie and White, 1991).

## 1:10:2 Structural Changes Upon Inhibitor Binding

The substrate binding cleft has six sugar binding sites, A to F, and when $NAG_3$ binds to HEWL it binds to site A, B and C (see Figures 1.6 and 1.7). Each of the sugars is buried to a different extent with the order of solvent exposure being A > B > C, (Cheetham *et al*, 1992). The N-acetyl side chains of the sugar residues in sites A and B are both solvent accessible, and are therefore hydrogen bonded to solvent molecules. The polar side of the sugar bound and the A side (which contains the N - acetyl group) lies towards a mainly hydrophobic region of the cleft, defined by Arg 73 and Asp 101. Cheetham et al. (1992)

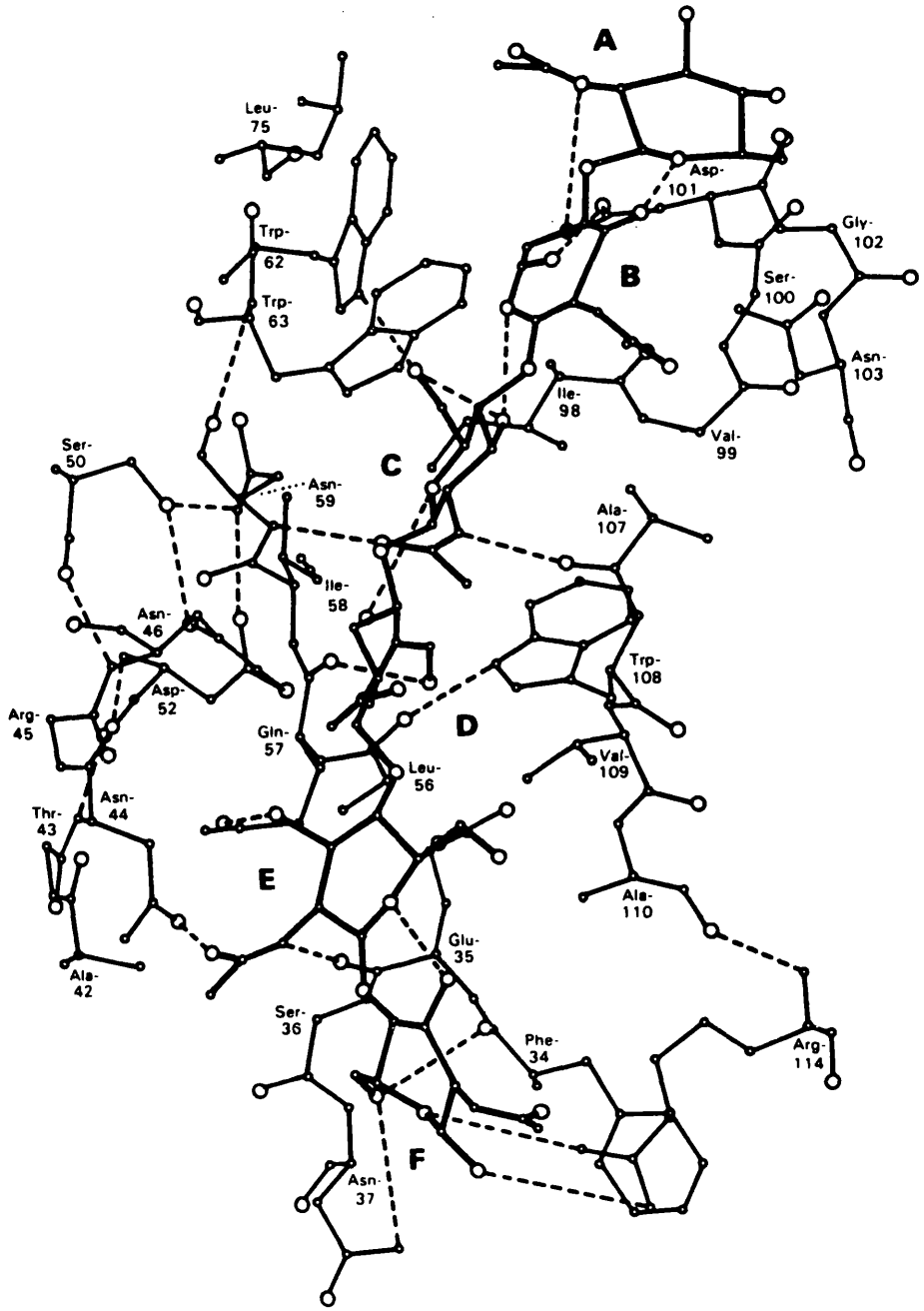


Figure 1.6: Diagram of the active site cleft region of hen egg white lysozyme, showing the disposition of the hexasaccharide substrate (adapted from McKenzie & White, 1991).

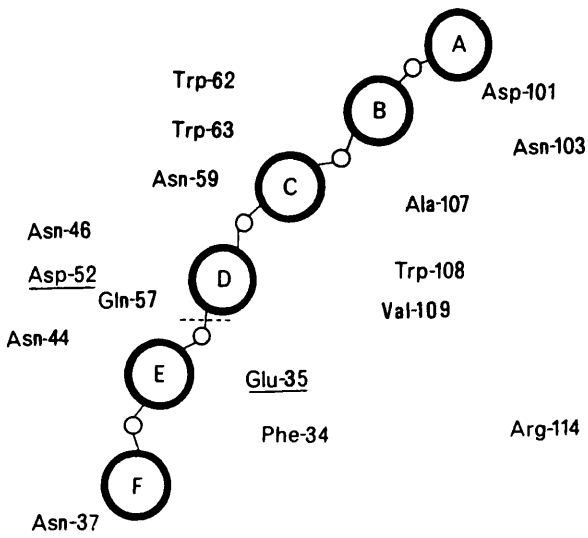


Figure 1.7: Sketch illustrating the lysozyme residues involved in hexasaccharide binding and cleavage. Cleavage takes place between sugars D and E. (Adapted from McKenzie & White, 1991).

discovered that the apolar face of the sugar in site B was directly above Trp 62, and proposed that this indicated a hydrophobic interaction. Similarly the hydrophobic face of the sugar in site C lies in a hydrophobic environmental generated by Ile 98, Ala 107, Trp 108 and Val 109.

The hydrogen bonding that occurs between $NAG_3$ and HEWL is summarised in the Table below

TABLE 1.1

The hydrogen bonding between $NAG_3$ and HEWL (Cheetham et al, 1992)

| Site | Sugar atom | Protein residue |
|---|---|---|
| A | $O_6$ | Asn 103 |
| B | $O_6$ | Asp 101 |
| C | $N_2$ | Ala 107 (amide C=O) |
| | $O_7$ | Asn 59 (amide N - H) |
| | $O_3$ | Trp63 |
| | $O_6$ | Trp 62 |
| | $O_1$ | 2 x$H_2O$ |

When the NAG binds Trp 62 and Trp 63 move by 1.0 and 0.7 Å, respectively, towards sites B and C, closing around the $NAG_3$ and maximizing the potential for intermolecular interactions. Similarly Ala 107, Asp 101, Asn 103 and Trp 108 all undergo slight conformational changes for the same reason. In the crystal structure regions of the protein remote from the active site show small perturbations. A comparison of the temperature factors show that residues involved in binding the $NAG_3$ stiffen up, while at sites remote from the active site little variation in temperature factors are found (Cheetham et al, 1992). The $\beta(1\rightarrow4)$ glycosidic linkages are twisted in the bound trisaccharide. The linkages have an angle of $28^0$ and $70^0$ between the C and B and B and A site sugars respectively. This allows a hydrogen bond to form between $O_5$ of sugar B and the $O_3$ hydroxyl of sugar C. This hydrogen bond is is not found between sugars A and B or in the chitobiose, where the degree of twist about the glycosidic link is $54^0$ (Cheetham et al, 1992).

The detailed NMR study of HEWL-$NAG_n$ was produced by the Dobson group (Lumb et al., 1994). The chemical shifts induced in HEWL by NAG, $NAG_2$ and $NAG_3$ binding are very similar with only a small increase in the effect as the oligosaccharide size increases. The largest chemical shifts are found at binding site C, with small shifts being observed in site B for $NAG_2$ and $NAG_3$. Residues further away from the active site are also changed. They include the main chain resonances of Asp 66, Leu 75, Cys 76, Ile 78, and residues in the C-terminal loop from 122—128. The side chain residues of Trp 62, Trp 63 and Trp 108 also change. The chemical shift of the hydrophobic box residue Trp 28 alters because of the change in conformation of Trp 108 (this change was also observed by Fukamizo et al., 1992). However, the predicted chemical shifts of remaining resonances in the hydrophobic box region are not found in this NMR study. The $C^{13}$ NMR study (Bernard et al., 1990) showed completely different results as observed by Oxford group. They concluded that conformational rearrangement occured in both the active site and hydrophobic box regions of the protein and that the effects increased as oligomer size increases from NAG to $NAG_3$. Also the three active site residues of Trp 62, Trp 63 and Trp 108 were found to be particularly sensitive to $NAG_n$ binding. The recent NMR study of NAG oligomers bound to Trp 62 mutants has shown that the major changes in the chemical shifts of HEWL occur in the β-sheet region (41-60) and the loop region (61-78). They suggested that these two regions also play a role in substrate binding (Kumagai et al., 1993).

The overall conclusion of the effects of NAG oligomer binding appears to be inconclusive. But the changes in the active site, the Trp 62, Trp 63 and Trp 108 residues and the loop residues 70 to 75 seem to be similar. Consequently HEWL is a well studied system and so we can apply this information in our ITC and DSC experiments to study the interaction of NAG in presence of penicillin-G (see later).

## 1:10:3 Microcalorimetry Studies of Lysozyme

Sabulal and Kishore (1996) have used high sensitivity differential scanning calorimeter (DSC) to study the thermodynamics of the interactions of some chloro-substituted alcohols

with hen egg-white lysozyme. They observed that the deconvolution of DSC curves in the absence and presence of alcohols showed thermal unfoldings behave as a reversible two-state process. The $T_m$ was decreased as concentration of alcohol increases. In case of unfolding reaction, the structure of protein changes, and therefore protein-solvent interactions may also change, because new extensive non-polar regions and peptide groups become exposed to the solvent and the distance between the charges increases greately. They also indicated that the hydrophobic effects of alcohols are greater on the denatured state than in the native state, since more groups are exposed to solvent in the former than in the latter. The unfolded state of protein consists of conformations in which the hydrophobic side chains are exposed to the solvent, therefore alcohols would interact favourably with hydrophobic side chains made available when the protein is unfolded, leading to a preferential stabilization of the unfolded state. Hence when the protein molecule undergoes a globular to random coil transition, alcohol molecules are competitively bound by the non polar groups exposed and hence reduce the effect of these groups on the organization of the solvent, leading to an increase in the total net entropy of denaturation. These effects are manifested as a lowering of the thermal denaturation temperature. Sabulal and Kishore (1995) studied the thermal denaturation of lysozyme at pH 2 in aqueous mixtures of amino acids and oligopeptides by high sensitivity differential scanning calorimetry. The most obvious effect of all the amino acids and peptides was to raise the temperature of denaturation. Both the calorimetric and van't Hoff enthalpies of denaturation increased in the presence of these systems, the ratio of the two enthalpies being nearly unity in each case, indicating the validity of the two-state approximation for the unfolding of lysozyme in these cosolute systems. They explained that these compounds preferentially hydrate proteins, increasing the chemical potential of the protein with increasing amino acid concentration. It has been suggested that the preferential hydration favours the more compact native state by opposing the increase of surface area of the proteins, which could increase the transition temperature. The observed thermal stabilization of lysozyme by the amino acids and oligopeptides indicates that small oligopeptides may be better protein stabilizing agents than their corresponding free amino acids.

The interactions of protein with urea have been studied by Makhatadze and Privalov (1992) using DSC and isothermal titration calorimetry. They have concluded in their studies that the urea molecule having four proton donor and one acceptor group, is interacting mainly

with the polar groups of the protein and there is polyfunctional hydrogen bonding between the peptide groups and denaturant molecules. The unfolded polypeptide chain of lysozyme has 229 binding sites for urea, compared with 119 in the folded form, and binds 58 molecules of urea in 6M solution (Makhatadze & Privalov, 1992). The contribution of each of the binding sites to the total Gibbs energy change of proteins was found to be a negative quantity increasing in magnitude with increase of denaturant activity in solution. These results indicate that the protein unfolding, due to these binding sites, should be a thermodynamically favourable process in the presence of "urea-type" molecules.

## 1:11 PENICILLIN

### 1:11:1 Introduction

Penicillin was discovered by Alexander Fleming in 1928, when he observed by chance that bacterial growth was inhibited by contaminating mold (Penicillium). He also observed that the extract from mold was not toxic when he injected into animals. Penicillin consists of a thiazolidine ring fused to a β-lactam ring, to which a variable R group is attached by a peptide bond. If R is a benzyl group then this is called benzyl penicillin (also known as Penicillin-G).

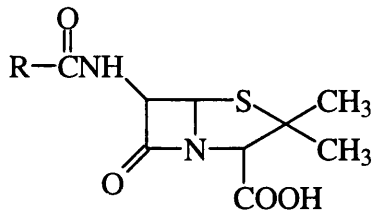


Penicillin

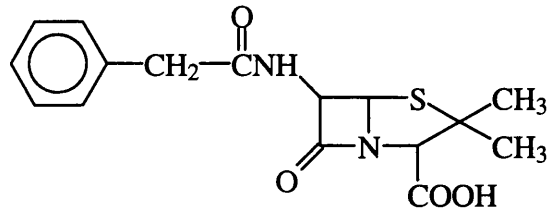


Benzyl Penicillin (Penicillin-G)

## 1:11:2 Benzyl Penicillin (Penicillin-G)

Several stains of Aspergillus and penicillium, particularly p. Notatum, yield this potent antibiotic when cultivated on suitable media. The parent acid, 6-phenylacetamido-penicillanic acid, is an amorphous white powder having no definite melting point. It is dextrarotatory with a specific rotation of $[\alpha]_D$ $+282^0$ and is normally isolated as the potassium or sodium salt. Both salts are freely soluble in water, moderately soluble in the lower alcohols and virtually insoluble in $Et_2O$, $CHCl_3$ and liquid paraffin. Benzyl penicillin is inactivated by oxidizing and reducing agents, glycerol and alcohols in the cold although it is possible that under these conditions the presence of impurities may be responsible for the deactivation. When highly purified, the parent acid is stated to be quite stable. In the cold dilute acids produce benzylpenicillic acid and penicillamine. Hot alkalis yield γ-phenyllevulinic acid and when treated with alcohols it gives a series of alkylbenzylpenicilloates. In cold alkaline solution it is rapidly inactivated by cystein and other aminothiol compounds. Dehydrogenation with selenium produces phenylacetamide. Benzyl penicillin posesses bacteriostatic and bactericidal activity, depending on concentration, against the majority of gram-positive bacteria and gram-negative cocci and also against some actinomycetes and spirochaetes (Glasby, 1979).

Penicillin blocks cell wall synthesis by inactivating a transpeptidase that catalyzes the formation of essential cross links between peptide units. The antiobiotic is believed to act by interfering with the utilization of certain substances required for the synthesis of the bacterial cell wall and accordingly exerts its effect against bacteria during cell division. This action is inhibited by the enzyme penicillinase which is produced during the growth of certain microorganisms. It is not, however, inactivated by pus, serum or the products formed by autolysis of tissue. A large number of organisms are normally sensitive to the antibiotic including Actinomyces israelii, Bacillus anthracis, Clostridium species, Corynebacterium diphtheriae, Erysipelothrix rhusiopathiae, Haemophilus influenzae, Leptospira species, Listeria monocytogenes, Neisseria species, Spirillum minus and Treponema species at minimum inhibitory concentrations between 0.006 and 2.0 μg/ml. In common with most of the penicillin antibiotics, benzylpenicillin produces toxic symptoms in

allergic patients. When administered to hypersensitive patients, anaphylactic shock with collapse and sometimes death may occur within minutes (Glasby, 1979).

The cross linking reaction is the target for the action of two important classes of antibiotics, the penicillins and the cephalosporins. Penicillin is thought to react irreversibly with the transpeptidase that catalyzes cross-linking. That enzyme normally forms an acyl-enzyme intermediate, via the penultimate residue of the pentapeptide chain (Figure 1.8). Penicillin evidently resembles the terminal dipeptide of this structure to the point that it can also react with the transpeptidase. The reaction is driven in part by the strain built into the four-membered lactam ring, for that ring opens during the reaction. Penicillin has been widely studied as an ideal antibiotic, because the cross - linking reaction has no counterpart in animal metabolism. Since the bacterial cell must continue to synthesize cell wall in order to grow and divide, inhibition of a step in this process provides a completely specific way to interfere with the growth of bacterial pathogens. Unfortunately, resistance to penicillin can be acquired. This resistance usually involves the synthesis, directed by an extra-chromosomal gene, of lactamase, an enzyme that hydrolyzes the lactam ring of penicillin and destroys its ability to interfere with peptidoglycan synthesis. The penicillin is an effective inhibitor of the transpeptidase because penicillin resembles acyl-D-Ala-D-Ala, one of the substrates of this enzyme. Secondly, the four membered β-lactam ring of penicillin is strained which makes it highly reactive. Therefore penicillin is a transition state analog, a striking example of molecular mimicry executed with perfection. Penicillin also acts as an irreversible inhibitor of serine-containing enzymes used in bacterial cell wall synthesis.

More brief details about penicillin: Large amounts of penicillin are also used in animal health products; for instance, it is used in intramammary preparations in efforts to overcome mastitis in the dairy herd. Pneumococcal resistance to penicillin-G and other β-lactam antibiotics is a reality but to think of these antibiotics as being ineffective for pneumococcal infections is a mistake. When penicillin minimum inhibitory concentration (MICs) higher than 8mg/L become prevalent in the community, the value of β-lactams will start to decline. Only then should other families of antimicrobials (glycopeptides, new quinolones) become first line agent (Goldstein & Garau, 1997).

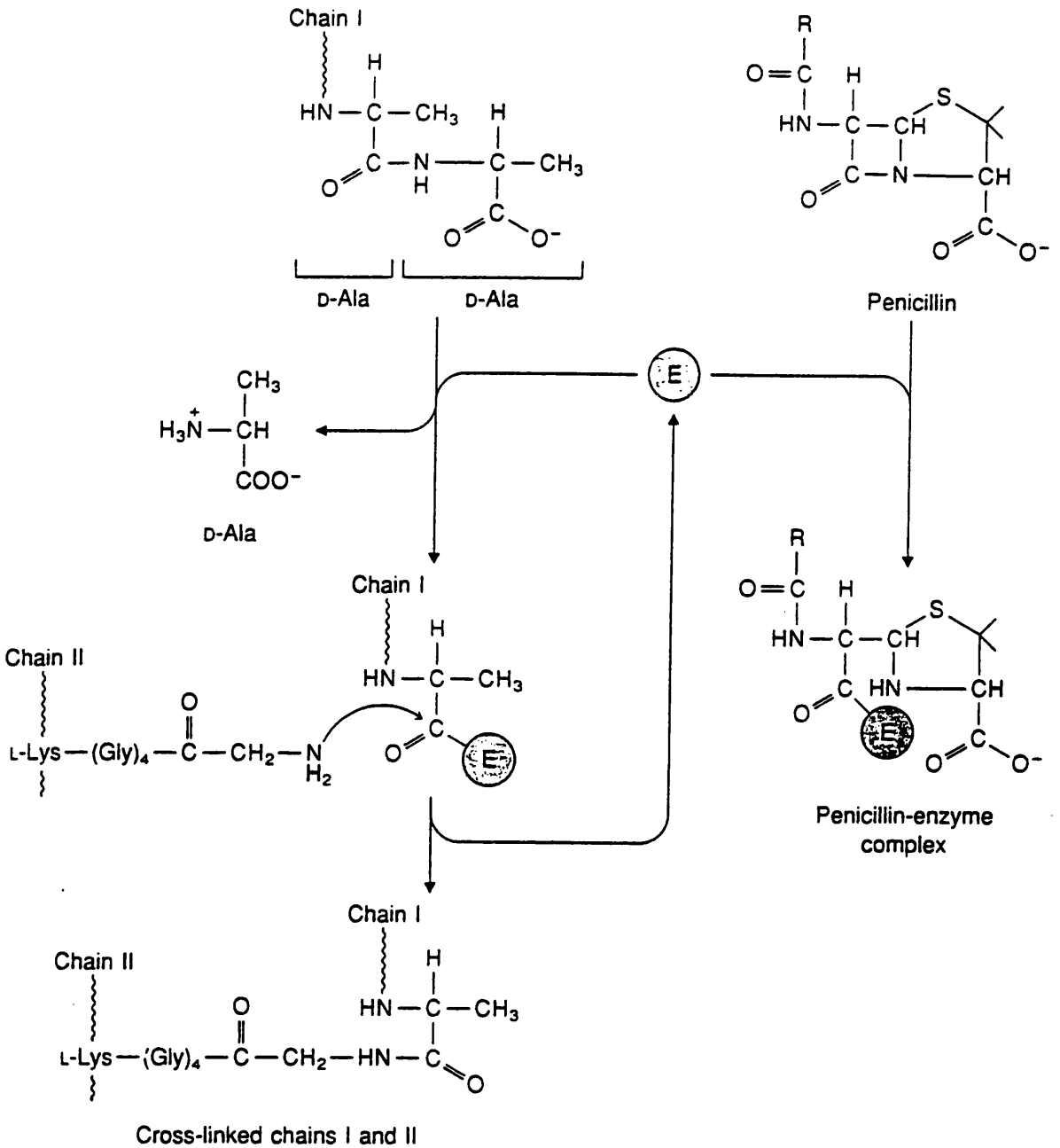


Figure 1.8: Sketch illustrating the cross-linking reaction in the enzyme-catalysed synthesis of peptidoglycan and how it is inhibited by penicillin. (Adapted from C.K. Mathews and K.E. van Holde (1990) "Biochemistry", Benjamin/Cummings.)

## 1:12 Interaction between Lysozyme and Penicillin

### 1:12:1 Introduction

Study of interaction of penicillin with proteins is important in order to understand the behaviour of penicillin in biological systems such as its transportation, antibacterial activity and allergy. The antibacterial activity of penicillin is closely related to the fact that penicillin becomes an inhibitor of enzymes which synthesize the cell wall of bacteria (Flynn, 1972).

As the reactive groups of penicillin N-acetyl-muramic acid have close structural similarity, Blake et al (1965) suggested that penicillin might bind to HEWL. They found that penicillin bound specifically to the cleft in the enzyme surface which had been located as the active site of the molecule by using X-ray diffraction at 6 Å resolution. The penicillin binding site is removed about 12 Å towards the top of the molecule from the site to which N-acetyl muramic acid itself and other saccharides bind, and the binding appears to be weaker by comparison. Possible amino acid residues which may be involved in the interaction include tryptophan, leucine, arginine and aspartic acid but at low resolution precise interactions could not be established.

Several papers have been published on the penicillin-lysozyme interaction by means of X-ray diffraction (Johnson, 1967), inhibition of lysozyme activity (Felsenfeld & Handschumacher, 1967), equilibrium dialysis (Klotz et al., 1950), radioisotope labeling (Corran & Waley, 1975) and pulse radiolysis (Phillips & Richards, 1973).

Johnson (1967) found that both penicillin V and para-iodophenoxymethyl-penicillin potassium salt inhibited lysozyme action on suspensions of Micrococcus lysodeikticus cells, the iodine derivative being very much more reactive. Later experimental work showed that α-benzyl-N-acetyl muramic acid bound to the same site as penicillin V, possibly involving hydrophobic contacts to the benzene ring.

Tipper and Straminger (1965) suggested that penicillin inhibits the reaction which cross links the mucopeptide chains through glycine bridges in the normal bacterial cell wall, and

that no similarity between penicillin and N-acetyl muramic acid is involved in the explanation of antibiotic activity of penicillin. Structural similarity were suggested between penicillin and D-alanyl-D-alanine group in the substrate in the cross linking reaction.

The hydrolytic action of lysozyme and penicillin was studied by Felsenfield and Handschumacher (1967). They demonstrated that hydrolytic action of lysozyme was inhibited 50% by benzylpenicillin (24mM) in 0.1M phosphate buffer at pH 7.0 using fluorescence measurements and ultraviolet difference spectroscopy. They indicated that an enzyme-inhibitor complex was formed and also reported that penicillin and N-acetylglucosamine produced a perturbation peak at 293nm when mixed with enzyme. N-Bromosuccinimide oxidation of the tryptophan residue in position 62, one of six tryptophan units in the enzyme molecule, destroyed enzymatic activity. This modification reduced the size of the perturbation peak induced by penicillin and eliminated the peak caused by N-acetylglucosamine.The experimental result agreed with previous work showing that penicillin bears a similar structure to that of the bacterial cell wall, N-acetylmuramic acid (Collins & Richmond, 1962), and penicillin and N-acetylmuramic acid was expected to show similar behaviour towards lysozyme. They have also reported that benzylpenicillin inhibits the lysis by lysozyme of the cells of M. Lysodeikticus. This inhibition was only observed in potassium phosphate buffer. In contrast with the results with N-acetylglucosamine, the inhibitory effect of penicillin was not observed in other buffers, which suggests that important differences in the binding of these inhibitors exists. The ultraviolet and fluorescence spectroscopic evidence for complex formation between lysozyme and either N-acetylglucosamine or penicillin corresponds closely with the data obtained by Hayashi et al., (1963, 1964) and Laskowski (1966). When penicillin or N-acetylglucosamine was mixed with lysozyme, a characteristic peak was observed at 293 nm, but the peak was seen at 291 nm when penicillin and free tryptophan were mixed. These results support the view that the inhibitors associate with one or more of the tryptophan residues of the enzyme. The perturbation produced by N-acetylglucosamine was completely abolished by oxidation of the tryptophan residue in position 62 of the lysozyme molecule, and the enzyme activity was completely destroyed. The perturbation induced by penicillin, however, was reduced by only one-sixth, a finding which reinforces the idea that important differences exist in the binding of these two compounds. It suggests that penicillin may bind to all (six) tryptophan residues of the enzyme; this result is also consistent with the additive

effect of penicillin and N-acetylglucosamine on the size of the perturbation peak (Felsenfeld & Handschumaker, 1967).

The X-ray crystallographic study reported by Johnson and Phillips (1965) indicated that penicillin was bound at only one site in the crystalline state. This may reflect the special nature of this binding site on the protein. Its location near to the N-acetylglucosamine-binding site was also based on this hypothesis. This specific binding of penicillin may involve the formation of a complex between the ring system of tryptophan and the phenacyl group of benzylpenicillin, plus bonding of the strongly acidic carboxyl group with basic amino acid sequences such as lysine-14, arginine-15, histidine-16, asparagine-44, arginine-45, asparagine-46, or arginine-112, asparagine-113, arginine-114. The association, involving the tryptophan residue at position 62, may induce a conformational change in the enzyme that results in the retention of one molecule of penicillin in the crystalline state (Felsenfeld & Handschumacher, 1967).

The activity of the penicillin series suggests that an aromatic side chain and a free carboxyl group are necessary for inhibitory activity. Modifications of the functional groups of either penicillin or related compounds with a resultant decrease in their structural similarity to N-acetylmuramic acid, either eliminated or reduced their inhibitory activity. Prior cleavage of the β-lactam ring may prevent acylation of a site of action associated with the bactericidal effect of penicillin, such as the transpeptidase cross-linking enzyme (Wise et al., 1965; Tipper & Strominger, 1965), but it does not interfere with the association of the molecule and lysozyme. The opening of the ring does not change the position of the nitrogen atom and does not eliminate the binding potential of the C-8 carbonyl group. Therefore lysozyme is not the site (Izaki et al., 1966) at which penicillin acts as a bactericidal agent since a much greater concentration of penicillin is required for inhibition of lysozyme. The antibiotic action of penicillin may require an association with an N-acetylmuramic-like receptor site that posess some of the structural features of the site on lysozyme to which the drug is bound (Felsenfeld & Handschumacher, 1967).

It has been reported that penicillin V binds to lysozyme in the ratio of one to one in the crystalline state (Johnson, 1967). It has been reported that an irreversible binding of penicillin-G with lysine-116 of lysozyme occurs when a mixture of penicillin-G and lysozyme is incubated for 48h at 37°C (Corran & Waley, 1975). It has also been reported that no complex formation between penicillin-G and lysozyme can be detected by means of equilibrium dialysis, whereas naphthylazopenicillin strongly interacts with lysozyme (Klotz et al., 1950). Stoichiometry and binding constant of the interaction between penicillin-G and hen egg white lysozyme were determined by Mitsumori, et al. (1980) using NMR and gel chromatography. The result showed that stoichiometry of interaction between penicillin-G and lysozyme is one to one, and the binding constant is approximately $1.9 \times 10^2$ $M^{-1}$. Fischer & Jardetzky (1965) used the broadening of the phenyl and methylene peaks of penicillin-G in the presence of albumin and concluded that the phenyl part of the penicillin molecule is involved in the interaction between penicillin-G and albumin and also observed that that the chemical shift values of these peaks are dependent on the concentration of penicillin-G. Thakkar & Wilham (1971) suggested that this concentration dependence of chemical shift values was caused by the self association of penicillin-G. Mitsumori et al. (1980) did experiments keeping the penicillin-G concentration constant, i.e. 32mM, whereas the concentration of lysozyme was varied from 0 to 10mM and observed that as lysozyme concentration increased, the phenyl peak showed an upfield shift of 0.098ppm, the methylene peak an upfield shift of 0.079ppm, and the $\beta$–$CH_3$ and 6-H peaks small upfield shifts of 0.035ppm and 0.022ppm, respectively. On the other hand, very little shift was observed in the $\alpha$-$CH_3$, 3-H and 5-H protons. The result that 3-H was not affected by the presence of lysozyme suggests that no electrostatic interaction involving the carboxyl group at C-3 of penicillin-G occurs between penicillin-G and lysozyme. They also suggested that phenyl and methylene peaks in the side chain are probably caused by the interaction with lysozyme and also small shift in the $\beta$-$CH_3$ protons may be due to the change in the intramolecular interaction with lysozyme. They also showed that $\beta$-$CH_3$ signal is a temperature dependent shift whereas 6-aminopenicillanic acid did not show any temperature dependent shift because it has no side chain. They concluded on this basis that temperature dependent shift of $\beta$-$CH_3$ of penicillin-G is primarily due to the phenacyl side chain. Furthermore the larger temperature dependent shift of $\beta$-$CH_3$ as compared to $\alpha$-$CH_3$ group suggests that in an aqueous solution the penicillin-G molecules tend to be less

extended in shape, with the phenacyl side chain approaching from the side of the β-$CH_3$ group to the heterocyclic ring. They assumed that the shift caused by the addition of lysozyme is due to the fast exchange between the free and bound penicillin molecules. The binding constant and the chemical shift difference between the two states can be estimated to be in the range 10-250 $M^{-1}$, and the chemical shift differences for the phenyl and methylene groups in the ranges 0.4-1.3 ppm and 0.3-1.1 ppm, respectively. They also investigated using C2-H proton of histidine-15 and NH protons of the indole ring of tryptophan residues as probes, and observed that C-2H proton of His-15 does not show any change in chemical shift in the presence and absence of penicillin-G, indicating that this histidine residue is not responsible for the interaction of penicillin-G with lysozyme. The NMR result shows that only one of the peaks, that which is at the lowest field, shows an upfield shift with an increasing concentration of penicillin-G. This result indicates that the tryptophan residue giving rise to this same peak is involved in the interaction with penicillin-G. On the other hand Glickson, Phillips and Rupley (1971) have reported other peaks show a large shift in the presence of N-acetylglucosamine. The NMR study therefore shows that penicillin-G is different from NAG in its way of interaction with lysozyme. It has also been shown that the phenacyl side chain of penicillin-G is interacting with the tryptophan-123 residue of the lysozyme molecule with higher affinity than NAG.

Mitsumori et al. (1980) results are different from Johnson (1967) because Trp-123 is not in the cleft of lysozyme molecule and the binding of penicillin-G is stronger than that of NAG. They suggested that there are two possibilities for this discrepancy. One is the difference in the molecular structure of penicillin-G and penicillin V; in the penicillin V molecule the phenoxymethyl side chain is substituted for the benzylside chain of penicillin-G. Another possible source of this discrepancy is that the experiments of Mitsumori et al. (1980) were done in solution, whereas Johnson (1967) studied the crystal state. It is likely that in the crystalline state, where the lysozyme molecules are presumably more closely packed than in the case of solution, the penicillin molecule is hindered from approaching to Trp-123, which is in the dominant binding site of lysozyme (Mitsumori et al., 1980).

The interaction of lysozyme with the antibiotics such as penicillin-G (benzyl penicillin), penicillin-V (phenoxy methyl penicillin), and methicillin (2,6-dimthoxy phenyl penicillin) at different concentrations and pH was studied by equilibrium dialysis (Subramanian et al.,

1983). Cooperative binding isotherms were observed at pH 5, 7, and 9 with all the penicillins and the binding ratios decreased slightly with increasing of pH. This was due to the decrease in the net positive charge on the protein with the increase of pH and the number of available binding sites on lysozyme was 4 at pH 5, 3 at pH 7 and 2 at pH 9 for all the penicillins. It was observed that the magnitude of $\Delta G$ decreased slightly with the increase of pH for all penicillins, indicating a slight decrease in the strength of binding at higher pH. The UV difference spectra of lysozyme-penicillin complexes at pH 5 showed peaks of low intensity of penicillin-G (284-286 nm) complex, penicillin-V (296-297 nm) and methicillin (300nm) complex, indicating a red shift in the peaks with the variation in the nature of the side chain group of penicillins. None of the penicillin complexes showed any peaks in the 284-300 nm region at pH 7 and 9 except in the case of lysozyme-penicillin-G complex at pH 7 which showed a peak of lesser intensity around 290nm. Since the penicillins differ only in the nature of their side chains, only penicillin-V and methicillin exhibit intramolecular hydrogen bonding between the side chain and the amide group of penicillin nucleus due to stereochemical considerations. This effect of hydrogen bonding would render these compounds more hydrophobic (Bird & Marshall, 1967). Therefore penicillin V and methicillin exhibit a higher binding strength compared to penicillin-G as the latter exhibits lower hydrophobicity since no intramolecular hydrogen bonding is possible in it. The appearance of peaks in the difference spectra of all these complexes at pH 5 and with only penicillin-G complex at pH 7 in the aromatic region indicated hydrophobic interactions with tryptophan residues at the binding sites (Mitsumori et al., 1980). In addition, electrostatic interaction of carboxyl group of penicillins will occur with the cationic residues such as lysines or arginines of the enzyme. Since all the penicillins dissociate into carboxylate anions with $pK_a$ values around 2.7 (Rapson & Bird, 1963), this ion binding of penicillins with lysozyme would be occuring at all pH values, but the non-involvement of tryptophans at pH 9 with all penicillins and with penicillin-V and methicillin complexes at pH 7 indicates that these cationic sites for ionic interactions could be lysines and not arginines (Philips et al., 1970).

The CD spectra of lysozyme-penicillin complexes in the near UV and far UV regions show that the penicillin-G at pH 5 and 7 bind at the tryptophan residues, probably Trp-108 lying at the entrance to the cleft of the hydrophobic box and/or Trp-123 lying on the molecular

surface involving hydrophobic interactions, and also at the lysine residues, possibly Lys 96, 97 or 116, the former two lying at the entrance to the cleft of the hydrophobic box and the latter on the molecular surface involving electrostatic interactions. But all the penicillins at pH 9 and only penicillin-V and methicillin at pH7 bind at these lysine residues involving only ionic interactions (Subramanian et al., 1983).

The binding of the α- and β-anomers of N-acetyl-D-glucosamine to hen egg white lysozyme and to the Trp-62 oxidized lysozyme was determined using sensitive microcalorimeter at $5^0$ and at pH 5 and at pH 3 and also binding of mutarotated mixtures of saccharide was determined at pH 5 and temperature 25 °C. The α-anomer binds more strongly than β-anomer to native lysozyme at pH 5. Specific oxidation of Trp-62 markedly reduces the binding of β-anomer as compared to α-anomer. It is, therefore, suggested that α-N-acetylglucosamine might bind in two orientations to site C of the lysozyme active cleft while β-anomer binds only one orientation (Cooper, 1974).

Felsenfeld & Handschumacher (1967) suggested that, on addition of penicillin-G, the native fluorescence of the enzyme was quenched with a significant shift in the emission maxima (red shift).

Imoto et al. (1972) found that the binding constant of penicillin-G was greater than that for NAG and other saccharide monomers; however it is smaller than those for dimers and trimers such as $(NAG)_2$ and $(NAG)_3$. It is known that various pigments such as Biebrich scarlet, which have aromatic rings in the molecular structure, bind to lysozyme with high affinity (Rossi et al., 1969).

# CHAPTER TWO

## 2 TECHNIQUES FOR STUDYING THE INTERACTION OF PROTEINS WITH LIGANDS

There are many techniques for studying the interaction of biological macromolecules with ligands etc. Examples are Spectroscopy, Optical activity, Microcalorimetry, Equilibrium dialysis, Chromatography, etc. We have mainly used the following three techniques in the present work:

(1) Fluorescence spectroscopy

(2) Microcalorimetry

(a) Differential scanning calorimetry

(b) Isothermal titration microcalorimetry

## 2:1 FLUORESCENCE

When a molecule absorbs light energy, it goes to the higher electronic energy level. If a molecule from excited state returns to the ground state by releasing its energy in the form of heat, it is called non-radiative decay. But on the other hand if part of the energy absorbed can be reemitted, as radiation usually of longer wavelength (red shift) than that of exciting light, this is known as fluorescence. It involves excitation ($10^{-15}$ s) followed by emission. There is a finite lifetime ($10^{-6}$ to $10^{-9}$ s) in the excited state. Fluorescence occurs at a lower frequency than that of the incident light. Since the detection frequency is different from the incident frequency, experimental sensitivity of fluorescence measurements is high because there is no background signal from the excitation source. It is often possible to measure fluorescence at concentrations in the $10^{-8}$ M. If the spontaneous emission may persist for long time it is called phosphorescence. The difference suggests that fluorescence is an immediate conversion of absorbed light into reemitted energy whereas phosphorescence involves formation of the electronic triplet state from which it slowly leaks.

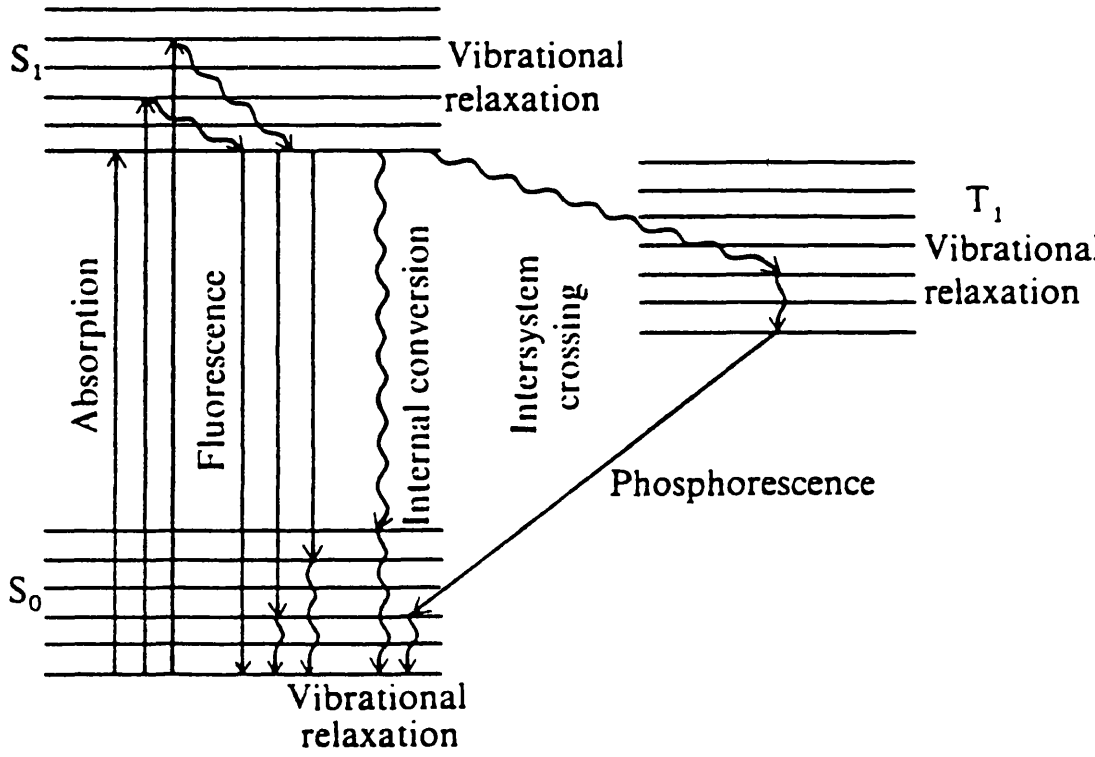


Figure 2.1: Jablonski diagram showing electronic excitation and possible routes of deexcitation.

## 2:1:1 Factors Affecting Fluorescence Intensity

The following factors affect the intensity of fluorescence..

(i) Internal conversion: In this process excitation energy in $S_1$ is lost either by collision with solvent or through internal vibrational modes. In general rate of internal conversion ($k_{ic}$) increases as the temperature rises (Figure 2.1).
(ii) Deexcitation also occurs due to collisions or complexes with solute molecules and in this way the excited state is quenched with a rate of $k_q[Q]$, where [Q] is the concentration of quenching species. Quenching is bimolecular process; aromatic chromophores usually have radiative lifetimes in the range of $1 \times 10^{-9}$ to $100 \times 10^{-9}$ seconds.
(iii) Intersystem crossing: In this process, the forbidden spin exchange converts an excited singlet into an excited triplet state. This excited state converts to the ground singlet state ($S_o$) either by phosphorescence or by internal conversion. This triplet state generally is lower in energy than the excited singlet.

There are different fluorescent molecules, natural and synthetic involving distinctive spectroscopic properties. Many treatises on fluorescent molecules are available for the interested reader (Czarnik, 1993; Griffiths, 1976; Krasovitskii & Bolotin, 1988; Lakowicz, 1994; Melamed et. al., 1990; Tyutyulkov et. al., 1991).

## 2:1:2 Applications

Many of the uses of fluorescence are similar to those of UV/vis spectroscopy - for example measuring binding, monitoring conformational changes, or following of a reaction. In addition, fluorescence is a particularly powerful technique because there are many reactions, solvent rearrangements, and molecular motion processes that take place on the same time scale as the lifetime of the excited state. The resulting sensitivity of fluorescence to this time scale and to environment is the basis of many of its applications to biochemistry.

Fluorescence spectroscopy is used to study the conformation and dynamics of the macromolecules by the following three ways:

(a) Dependence of the fluorescence properties of a chromophore on its environment to study the polarity of active sites and to detect conformational changes.
(b) The second uses excitation transfer to measure the distances between interesting sites on a macromolecule.
(c) The use of the polarised fluorescence to determine the size, shape and flexibility of macromolecule in solution and to determine orientation in complex molecular systems. (Yguerabide, 1978)
A few applications are listed below:
(i) Nucleic acid length and mass analysis (Clark & Mathies, 1997; Rye & Glazzer, 1995; Zeng et al.,1995).
(ii) DNA, RNA sequence analysis, sequence probes (Chee et al., 1996; Ju et al., 1996; Tyagi & Kramer, 1996).
(iii) Chromosome analysis (Swiger & Tucker, 1996; Yurov et al., 1996).
(iv) Enzyme Kinetics, protease activity (Lee et al., 1995).
(v) Cell differentiation, embryology (Gard et al., 1995; Spitzer et al., 1995).
(vi) Apoptosis (Fraker et al., 1995).
(vii) Membrane potential analysis (Gonzaliz & Tsien, 1995).
(viii) Analysis of ion dynamics; $Ca^{+2}$, $K^{+}$, $Na^{+}$,pH, $Cl^{-}$ (Tsien, 1989).
(ix) Cell signal transduction and propagation, regulation of cellular states (Tsien, 1992).
(x) Cell viability analysis (Palmeria et al. , 1996; Wrobel et al. , 1996).
(xi) Immuno detection (Rabbany et al. , 1994; Vredenburgh et al. ,1996).
(xii) Sub cellular organelle analysis (Rizzuto et al. ,1996).
(xiii) Protein, Carbohydrate analysis (Jackson 1996).

## 2:1:3 Limitations

Fluorescence intensity is ultimately limited by the times it takes an excited molecule to relax to a ground state from which each further excitation cycles can occur. Fluorescence methods are limited in sensitivity by light scattering from the external illumination and

background fluorescence that can not be effectively blocked by the optical filters. Photobleaching also limits the total amount of information available from a fluorescent molecule (Song et al.,1995; 1996). Not all molecules are themselves fluorescent, and small traces of fluorescent impurities might interfere to give erroneous results. In cases where artificial fluorescent probes are used, these themselves might interfere with the system under study.

## 2:2 PROTEIN FLUORESCENCE QUENCHING

Fluorescence quenching is the means by which some compounds have the ability to decrease the fluorescence intensity of some fluorophores (Eftink & Ghiron, 1980). There are two kinds of quenching, i.e. static and dynamic or collisional. In case of static quenching a complex is formed between the quencher and the fluorophor, while in dynamic quenching a collision occurs between the two substances. The contact between the quencher and the fluorophore during the lifetime of the excited state causes the fluorophore to return to the ground state. This transfer of the energy of the fluorophore to the quencher results without fluorescence occuring. So fluorescence intensity and lifetime decreases equivalently which is an important characteristic of collisional quenching. Quenching experiments are performed by titrating quencher into the sample under study, and measuring the decrease in intensity or life time. Data analysis is based on the Stern-Volmer equation

$$F_0/F = t_0/t = 1 + K_q\, t_0[Q] \quad \text{---------- (2. 1)}$$

Where $F_0$ and F are the fluorescence intensity in the absence and presence of quencher, [Q] is the concentration of quencher, $t_0$ and t are the lifetime in the absence and presence of quencher. $K_q$ is quenching rate or bimolecular rate constant. The product $K_q t_0$ is called Stern-Volmer quenching constant. If we plot a graph between $F_0/F$ vs [Q] or $t_0/t$ *vs* [Q] we get a straight line having slope equal to the quenching constant. For example the binding of xylazine to bovine serum albumin (BSA) was studied by fluorescence quenching, as a function of temperature. The temperature dependence of the Stern-Volmer constant suggests that the mechanism of the quenching process is mainly dynamic in origin. The

thermodynamic activation parameters were estimated based on such temperature dependence. The positive values of activation enthalpy and entropy changes indicate that the hydrophobic contribution is the predominant intermolecular force stabilising the xylazine-BSA complex (Jimenez et. al, 1995). The analysis is more complicated in case of static quenching and therefore its use is limited.

## 2:3 Protein Intrinsic Fluorescence

Protein fluorescence mainly derives from two amino acids, i.e. tryptophan and tyrosine. The fluorescence of most of proteins is dominated by the tryptophan residues. The emission spectra of proteins are sensitive to the binding of substrates, association and denaturation. Tryptophan is quenched by oxygen, iodide, acrylamide, succinimide, and other substances (Lakowicz, 1983).

We mainly used this technique in our present work. Protein fluorescence is inhibited by the same factors which affect the indole moiety and tryptophan residues. The absorption of protein at 280nm is due to tryptophan and tyrosine, but at 295nm, the absorption is due mainly to tryptophan alone. A variety of reasons have been suggested for the absence of tyrosine fluorescence in proteins. These include energy transfer to the tryptophan residue and quenching by nearly groups on the peptide chain. Tryptophan fluorescence is also sensitive to the polarity of the solvent used. As free tryptophan in solution depends upon the nature of the solvent (e.g. $\lambda_{max}$ = 297 in cyclohexane and 347 nm in water; Sun & Song, 1977). In general the tryptophan residues of a protein are buried in the non-polar region of the molecule. In many cases the association of proteins with substrates or other macromolecules results in shifts of their emission spectra. For example the emission spectra of lysozyme shifts from 342nm to 332nm when N-acetyl-D-glucosamine binds to lysozyme. These shifts are due to the shielding of tryptophan residues in the active site from contact with water. Other factors such as self-association of proteins and association of proteins with membranes can also yield substantial changes in the spectral properties of tryptophan. In short fluorescence generally is much more sensitive to the environment of the chromophore than is light absorption. The sensitivity of fluorescence is consequence of the relatively long time a molecule stays in an excited state singlet state before deexcitation. Therefore all kinds of processes can occur including protonation or deprotonation

reactions, solvent cage relaxations, local conformational changes and any processes coupled to translational or rotational motion.

## 2:4 MICROCALORIMETRY

Calorimeters form a broad and heterogeneous group of scientific instruments. Different measurements principle have been used and a large number of calorimetric designs and experimental procedures have been reported since the first calorimeter was designed more than 200 years ago by Joseph Black in Glasgow (Armstrong, 1964). A large number of methods are available to study the interaction of biological macromolecules with ligands, but a more direct method to measure the thermodynamic parameters is through calorimetry. Therefore calorimetry or microcalorimetry is the measurement of the heat evolved or adsorbed by a chemical or physical processes, so we can study the rate and extent of reaction. Almost all biological processes that involve physical and/or chemical reaction can also be studied by means of microcalorimetry. There are various types of microcalorimeters but two of them are most important i.e. Differential Scanning Calorimeters (DSC) (Privalov, 1974; Sturtevant, 1974; Privalov & Potkhin, 1986; Sturtevant, 1987; Chowdhry & Cole, 1989; Cooper & Johnson, 1992) and Isothermal Titration Microcalorimeter (ITC) (Sturtevant, 1974; Wiseman et al., 1989; Cooper & Johnson, 1992).

## 2:5 DIFFERENTIAL SCANNING CALORIMETER

In biological systems the temperature induced transitions such as thermal unfolding (denaturation) of proteins, lipid membrane phase transitions, nucleic acid and metal binding to proteins, inhibitors, etc., may be studied by differential scanning calorimeter. The DSC measures the apparent specific heat of a system as a function of temperature (Privalov, 1974; Sturtevant, 1974). We can measure $T_m$ and energetics of the transitions, cooperativity, association of the process etc. (Ricker,et al., 1971).

Although denaturation of proteins seems to be reversible in principle, the condition under which it can be achieved, and the proteins on which it has been done, are rather limited. According to the data from NMR spectroscopy, the state of amino acid residues in

denatured protein does not differ from that of free amino acids in solution (Jardetzky & Wade-Jardetzky, 1971). This difficulty was removed by using a sensitive scanning calorimeter (Privalov, et al., 1964, 1975; Danford et al., 1967). One of the greatest advantages of the calorimetric methods compared to other methods is that the effective , as well as the calorimetric, enthalpy of denaturation can be obtained from the same experimental curve of heat absorption. If the ratio of these enthalpies is deviate from unity, then we must conclude that this is the indication of some intermediate states (Tsong & Baldwin, 1972).

## 2:5:1 INSTRUMENTATION

The instrument MC-2D DSC designed by Microcal Inc. has been used to study the folding/unfolding of proteins. It consists of two tantalum metal cells (i.e. sample and reference cells) having volume of around 1.3ml and filled via a capillary tube. The cells are suspended in an adiabatic chamber. Sensitive thermopiles monitor the cell-cell and cell-jacket temperature difference, while feedback heaters maintain these differences nearly close to zero. The difference in the amount of energy supplied, which is directly proportional to the apparent specific heat, to the sample and reference cells, is recorded as a function of temperature by an external circuit. During the experiment the cells are maintained under a nitrogen gas of 2 atm. pressure for avoiding bubble formation. The instrument is also connected with an EM electronics N2a DC nano voltmeter as a pre-amplifier and circulating water bath which reduces the temperature when the scan is finished. The apparatus is connected to a PC which is used for instrument control as well as data recording (Figure 2.2).

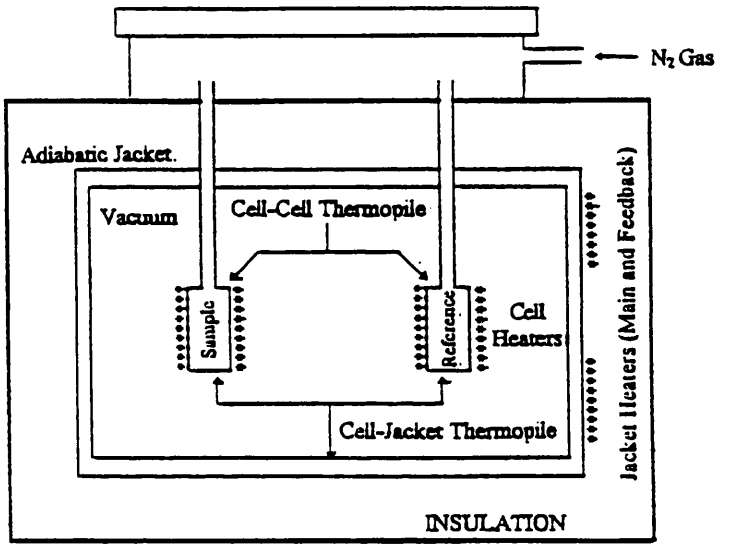


Figure 2.2: Schematic view of the Microcal MC2-D differential scanning calorimeter (DSC).

## 2:5:2 ADVANTAGES

The study of protein folding/unfolding and stability is very important both in the academic field and in biotechnology. The equilibrium between folded and unfolded states of small proteins is usually a two state process (Privalov, 1979); i.e. protein is either in the native, folded state or in the unfolded, denatured state. The stability of the folded state is only about 20-60 kJ/mol higher than that of the unfolded state. This small value is the result of a compromise balance between large enthalpy and entropy values. Protein stability can be affected by many factors, such as pH, concentration of solute, inhibitors, nature of ligands, etc. This stability change is obviously related to the energetics of the protein ligand interaction. Therefore high sensitivity differential scanning calorimetry is a very suitable technique for characterizing the thermal stability of protein since it provides the calorimetric and van't Hoff enthalpy and other thermodynamic values, and may lead to the analysis of multi domain proteins, as long as the denaturation process occurs under equilibrium conditions (Privalov, 1979, 1982).

Secondly with the help of DSC we may obtain the excess apparent specific heat of dilute sample with respect to a solvent baseline. However, in some cases aggregation of unfolded protein may occur during the transition, giving rise to exothermic processes that can distort the baseline.

A typical DSC thermogram (i.e. heat capacity vs temperature) consists of one or more peaks indicating a $\Delta C_p$ associated with transitions. The mid point temperature ($T_m$) of the transition gives a measure of the thermal stability of the system. In a two state process it is the temperature at which equal number of molecules will be in either state or it is the temperature at which any of the molecule will spend exactly half of its time in each state. Therefore $T_m$ is very useful when we consider the thermal stability of the protein.

The other main advantage of this technique is that we may understand the cooperativity of the process by considering the shape of transition. Highly cooperative process gives sharp transition while a less cooperative show a broader transition. Therefore the apparent size of the cooperative unit may be expressed by the equation

$$m = \Delta H_{vH}/\Delta H_{cal} \quad \text{---------- (2. 2)}$$

Where $\Delta H_{vH}$ is called van't Hoff enthalpy per mole, $\Delta H_{cal}$ is called absolute enthalpy per gram and m is the molar mass of the cooperative unit.

From DSC we can obtain the different thermodynamic parameters by using the following equations:

As $\Delta H(T_1) = \Delta H(T_0) + \Delta Cp(T_1 - T_0)$ ---------- (2. 3)

and $\Delta S(T_1) = \Delta S(T_0) + \Delta Cp.\ln(T_1/T_0)$---------- (2. 4)

Therefore great care must be taken when measure the $\Delta Cp$ values. As we know that:

$$\Delta H = {}_{T0}\int^{T} \Delta Cp(T)dT$$

or, at the mid-point temperature $T_m$ , $\Delta H_m = \Delta H_{298} + {}_{298}\int^{T} \Delta Cp(T_m)dT$

Suppose $\Delta Cp$ is constant at any temperature T, then we get

$\Delta H_{298} = \Delta H_m - \Delta Cp\ (T_m - 298)$ ---------- (2. 5)

By definition $\Delta S_m = \Delta H_m/T_m$

and $\Delta S_{298} = \Delta H_m/T_m - \Delta Cp.\ln(T_m/298)$

As $\Delta S_m = {}_{T0}\int^{T} \Delta Cp/T.\ dT$

Similarly $\Delta S_{298} = \Delta S_m - \Delta Cp\ \ln(T_m/298)$ ---------- (2. 6)

Substituting the values of $\Delta S_{298}$ and $\Delta H_{298}$ from equations 2.5 & 2.6 and inserting into the following equation, we get

$\Delta G_{298} = \Delta H_{298} - T\Delta S_{298}$---------- (2. 7)

Therefore $\Delta G_{298} = \Delta H_m - \Delta Cp(T_m - 298) - T(\Delta H_m/T_m) - \Delta Cp\ \ln(T_m/298)$

On rearranging the above equation, we have, at T = 298,

$\Delta G_{298} = \Delta H_m(1 - 298/T_m) + \Delta Cp(298 - T_m - 298\ \ln(298/T_m))$ --(2. 8)

In all the above equations $\Delta Cp$ is a very useful quantity for measuring other thermodynamic parameters. Therefore DSC has this major advantage to measure $\Delta Cp$ directly as large heat changes occur during thermal transitions.

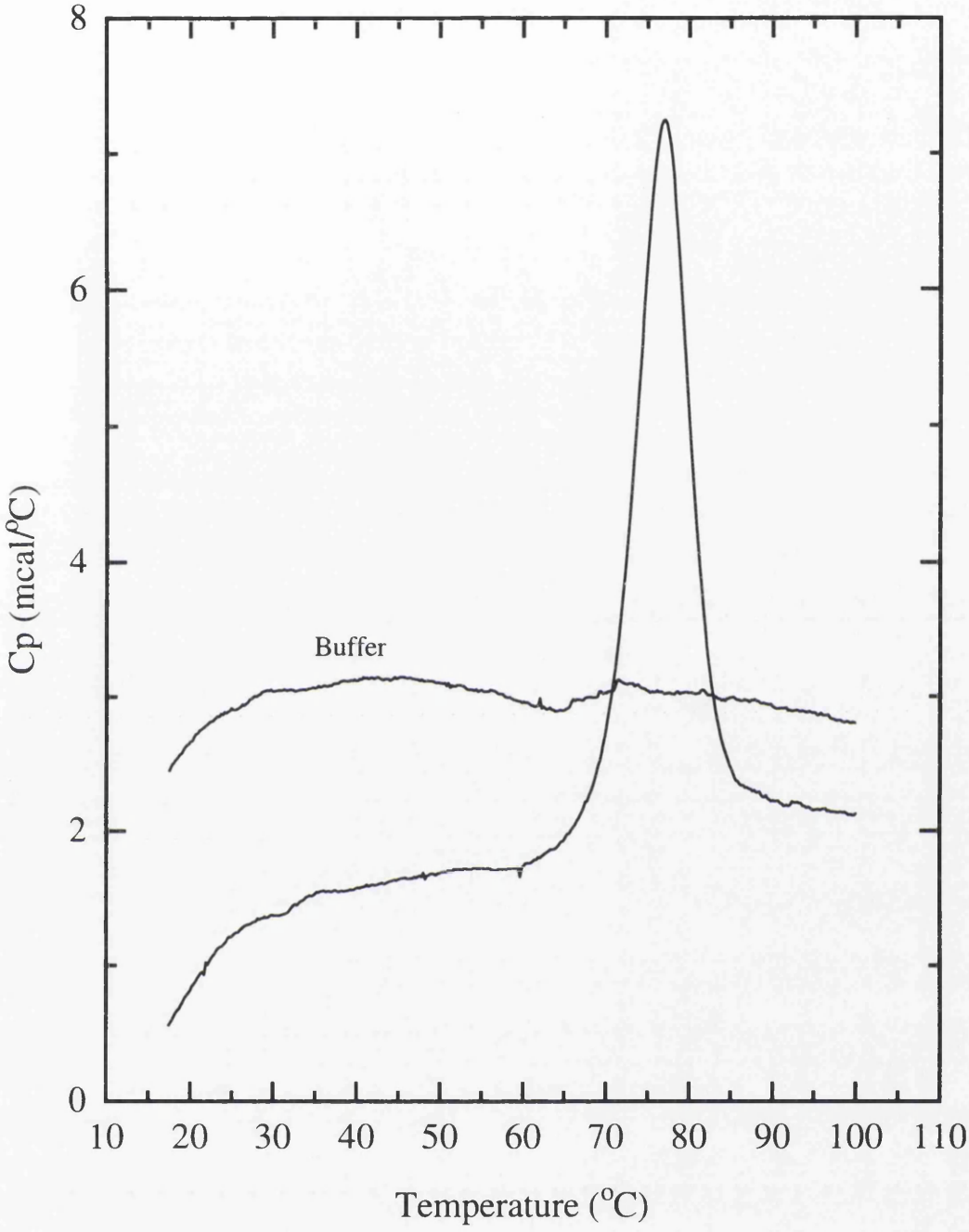


Figure 2.3: Typical DSC traces showing thermal unfolding of lysozyme (0.3 mM) in 0.1M acetate buffer pH 4.5 (containing 1.4mM $AlCl_3$). The buffer baseline is also shown.

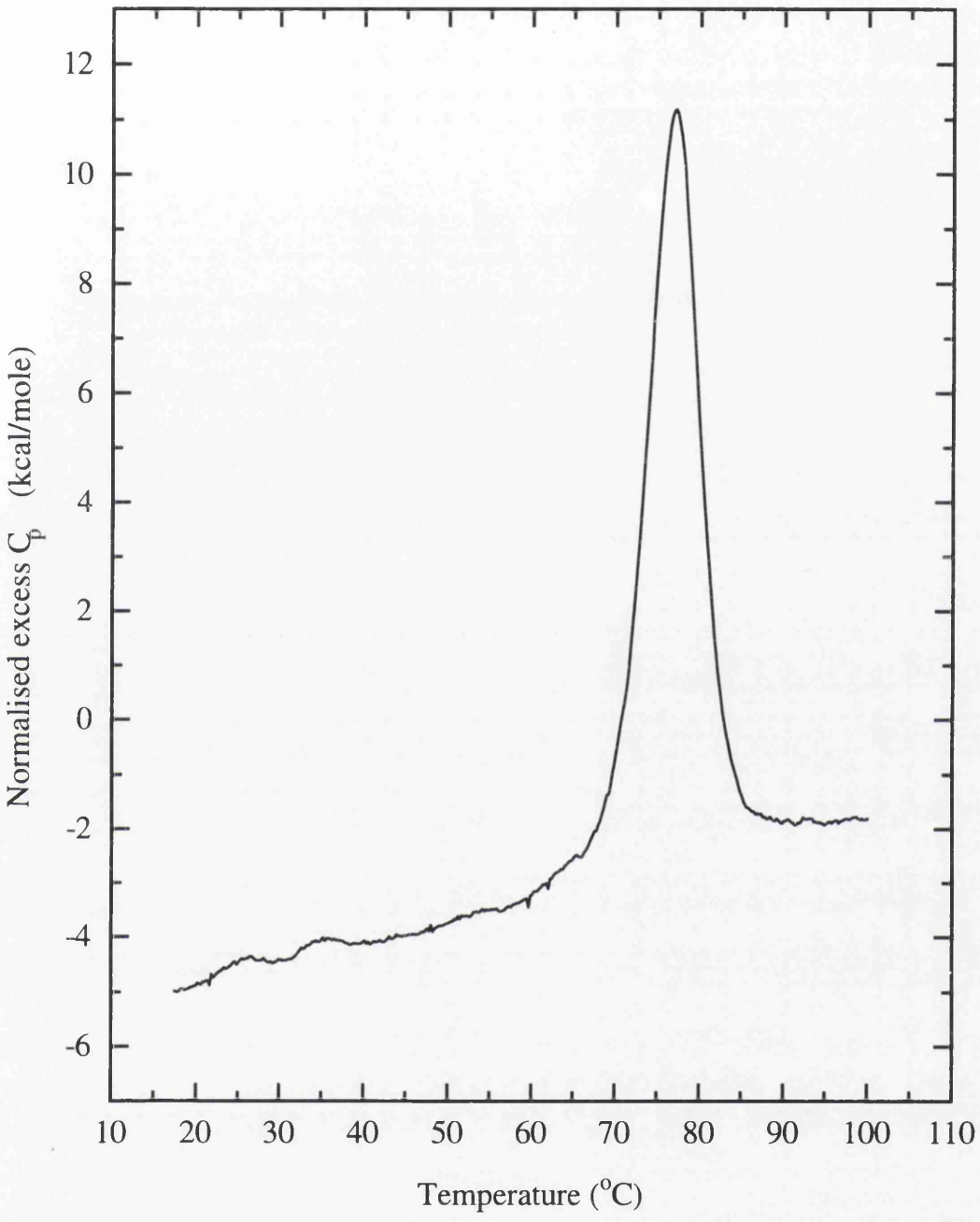


Figure 2.4: Normalized DSC data with buffer baseline subtracted (data from Fig. 2.3)

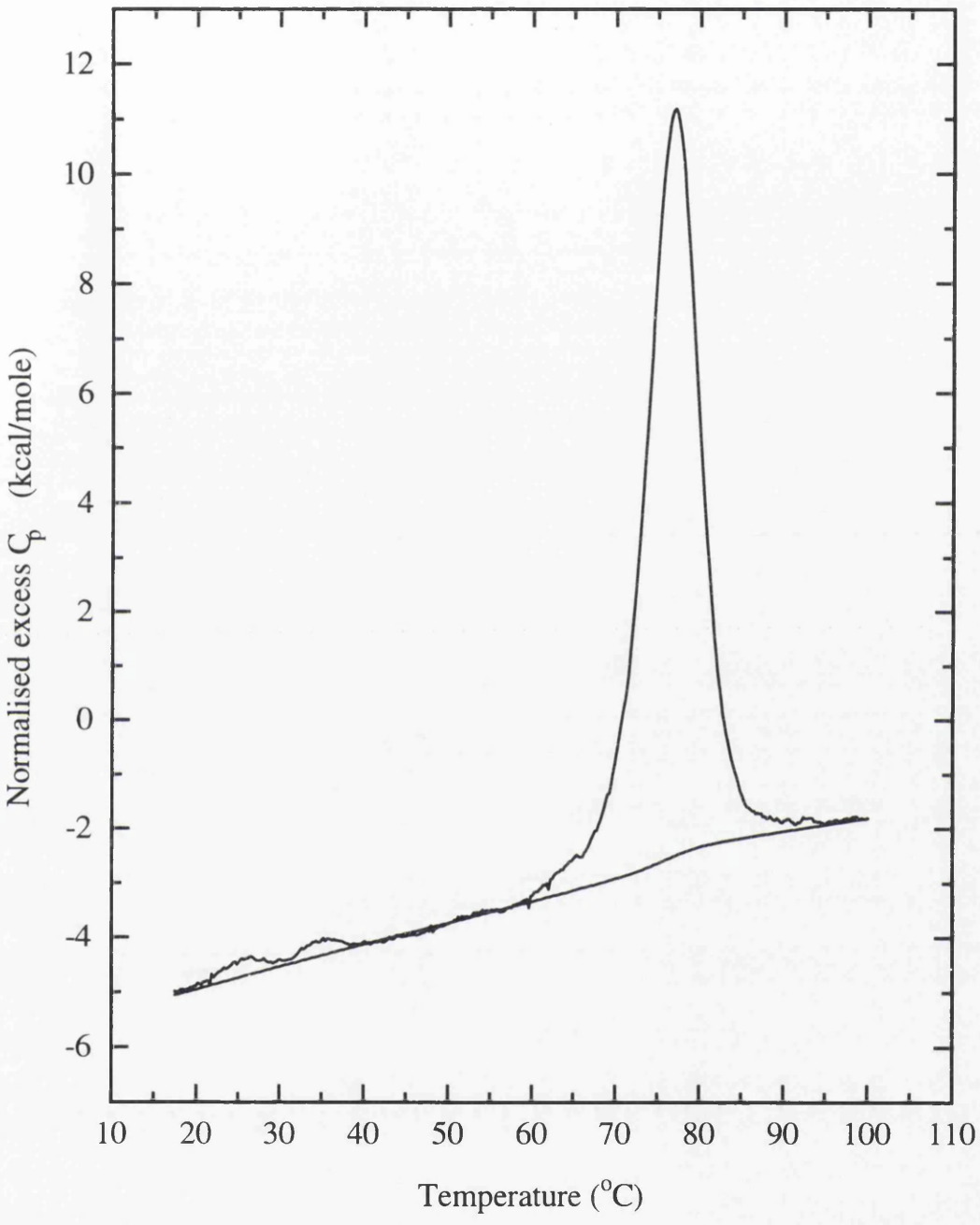


Figure 2.5: Normalized DSC data with buffer baseline subtracted (data from Fig. 2.3) and with a progress baseline draw for integration.

## 2:5:3 Data Analysis

All data analysis depends on the type of sample and the model used but some basic operations play a key role in every experiment.

(i) Normalization to heat capacity: Raw data, obtained by collecting differential thermal energy data as a function of time (mcal/min), are converted to differential heat capacity (mcal/degree) by dividing by the mean scan rate at each point (Figure 2.3). The actual scan rate varies slightly due to variation in the total heat capacity and heat losses in the instrument.

(ii) Baseline correction: Subtracting the buffer baseline from the actual experiment to remove the most of the artefact and non linearity arising from the instrumental problem such as mismatch of cell volumes, etc. (Figure 2.4).

(iii) Concentration/volume normalization: The differential excess heat capacity per mole is obtained by dividing by the actual amount of sample in the cell during the experiment, using the exact sample cell volume determined by the manufacturer.

(iv) Construct an appropriate baseline to take account of the change in heat capacity before and after the transition (Figure 2.5). The data are now ready for deconvolution in terms of the various models that might apply to the particular transitions involved such as multiple, overlapping transitions etc.

## 2:5:4 Models used in DSC analysis (taken from "DSC Data Analysis Tutorial Guide", Microcal Inc.)

Generally all proteins (or macromolecules) consists of number of structural domains A, B, C, - each of which is involved independently in a transition between the folded and the unfolded forms ($A=A^{'}$, $B=B^{'}$, ...). Equilibrium constants are expressed in terms of fractions ($K_a=f_{A'}/f_A$, $K_B=f_{B'}/f_B$ , ...). The actual calorimetric molar enthalpy change is written as $\Delta H_A$ , $\Delta H_B$ , ...

The total molar enthalpy of the system is now given by

$$H = H_N + f_A\Delta H_A + f_B\Delta H_B + \quad \text{---------- (2. 9)}$$

Where $H_N$ is the total enthalpy of the native state and all other $\Delta H$ values are measured relative to the folded form. The total molar heat capacity of the system is as follows

$$Cp = Cp_N + [f_A\Delta Cp_A + \Delta H_A(\partial f_A/\partial T)] \quad \text{---------- (2. 10)}$$

Where $Cp_N$ is the molar heat capacity of the totally folded state and $\Delta Cp_A$ is the change in heat capacity for unfolding the A domain.

As $f_A = 1-f_A'$ and $K_A = f_A'/f_A$ , $\therefore f_A = f'_A/K_A$

we get $f'_A = 1 - f'_A/K_A$

or $f'_A = K_A/1+K_A$ ---------- (2. 11)

Differentiating equation 2. 11 w.r.t. temperature we get

$$\partial/\partial T(f'_A) = [K_A/(1+K_A)^2]\ \partial/\partial T(\ln K_A) \quad \text{---------- (2. 12)}$$

$$\text{As } \partial/\partial T(\ln K_A) = \Delta H^*_A /RT^2 \quad \text{---------- (2. 13)}$$

where $\Delta H^*_A$ is the van't Hoff heat change from the reaction which corresponds to the heat change for the cooperative unit which actually participate in the reaction

Putting equations 2.11, 2.12,& 2.13 into equation 2.10 yields

$$Cp = Cp_N + [K_A\Delta Cp_N /1+K_A + K_A\Delta H^*_A\Delta H_A/ (1+K_A)^2RT^2] + \quad \text{--------- (2. 14)}$$

This is a general form of the equation and can be applied either two state or non-two state transitions as long as all parameters are evaluated at the same temperature T.

## 2:5:5 Model for independent two-state including ΔCp effects:

If we assume that each transition is two-state then $\Delta H^*_{van't\ Hoff}$ values become equal to $\Delta H_{calorimetric}$ values. If we assume further that $Cp_N$ is a linear function of temperature, i.e. $Cp_N = \beta_0 + \beta_1 T$, then equation 2. 14 becomes

$$Cp(T)=\beta_0+\beta_1(T)+[K_A(T)\Delta Cp_N\{1+K_A(T)\}+ K_A(T)\Delta H_A T^2 /\{(1+K_A(T)\}^2RT^2]$$

---------- (2. 15)

Where the temperature dependent parameters Cp(T), $K_A(T)$ and $\Delta H_A(T)$ have been indicated. We can express $\Delta H_A(T)$ in terms of its temperature-independent value at the mid point $T_{mA}$ and the heat capacity changes for the transition $\Delta Cp_A$ , i.e.

$$\Delta H_A(T) = \Delta H_{mA} + \Delta Cp_A\ (T - T_{mA}) \quad \text{---------- (2. 16)}$$

Integrating equation 2. 13 for $T_{mA}$ where $K_A(T)$ is unity at an unspecified temperature T.

$$K_A(T) = \exp(-\Delta H_{mA}/RT[1-(T/T_{mA})](\Delta Cp_A/RT[T-T_{mA}-T\ln(T/T_{mA})] \quad \text{----(2. 17)}$$

Putting values of $\Delta H_A(T)$ and $K_A(T)$ from equations2. 16 and 2. 17 into equation 2.15, we get Cp(T) values to which DSC data can be fitted. To begin curve fitting with Origin, the operator indicates the number of transitions needed to fit the experimental DSC heat capacity curve and then all $T_m$ values, so Origin can provide guesses for fitting all other parameters.

## 2:5:6 Model for independent two-state transitions excluding ΔCp effects

When all heat capacity changes are assumed to be zero and $\Delta H_A(T)$ is replaced by temperature-independent heat $\Delta H_{mA}$ then equations 2.15, 2.16 and 2.17 reduce to

$$Cp(T) = K_a(T)\Delta H_A(T^2)/[1+K_A(T^2)]RT^2 \quad \text{---------- (2. 18)}$$

$$K_A(T) = \exp[\{-\Delta H_{mA}/RT\}\{1-(T/T_{mA})\}] \quad \text{---------- (2. 19)}$$

The curve fitting procedure is the same as in the previous equations.

## 2:5:7 Modified independent non two-state transitions

This model is only applied to transitions with no ΔCp values. Before curve fitting with this model, a progress baseline must be subtracted from the experimental data to remove ΔCp effects, then equation 2. 14 reduces to

$$Cp(T) = K_A(T)\Delta^*H_{mA}\,\Delta H_{mA}/[1+K_a(T)]^2RT^2 \quad \text{---------- (2. 20)}$$

We can calculate equilibrium constant like equation 2. 19 but we substitute here Van`t Hoff heat instead of calorimetric heat

$$\therefore\ K_A(T) = \exp[\{-\Delta^*H_{mA}/RT\}\{1-(T/T_{mA})\}] \quad \text{---------- (2. 21)}$$

## 2:5:8 Single two-state transition with subunit dissociation

In case of biological macromolecule shaving subunits, the subunit dissociation occurs simultaneously with thermal unfolding

i. e. $A_n \rightleftharpoons nA$

$$K = [A]^n/[A_n] \quad \text{---------- (2. 22)}$$

Where n is the number of dissociation subunits. If f is the fraction in state A and 1–f is the fraction in An state;

then $1-f = [A_n]/C_t$ and $f = [A]/nC_t$ ---------- (2. 23)

Where $C_t$ is total molar concentration. Substituting values from equation 2. 23 into equation 2.22, we get K as follows

$$K = \{ f^n/^n n^n C_t \}/\{(1-f)/C_t\}$$

or $K = f^n n^{n\ n-1} C_t / 1-f$ ---------- (2.24)

Using equation 2. 24 And the following expressions:

$$\partial \ln K(T)/\partial(1/T) = -\Delta H_a(T)/R$$

and $\Delta H(T) = \Delta H_{mA} + \Delta Cp_A\ (T - T_{mA})$ ---------- (2.25)

Integrating between $T_{mA}$ to T when f=0. 5, then we get

$$K(T) = 5^{n-1} n^{n\ n-1} C_t \exp[\{-\Delta H_{mA}/RT(1-T/T_{mA})\} - \Delta Cp_A/RT\{T-T_{mA}-T\ln T/T_{mA}\}]$$

---------- (2.26)

$$Cp(T) = \beta_0 + \beta_1(T) + f(T)\ \Delta Cp + [\Delta H_A(T)/RT^2][\{1-f(T)\}]/[1-n+\{n/f(T)\}]$$

---------- (2.27)

Equation 2.14 is a general equation for any value of n so long as the bulk concentration $C_t$ is expressed as n-mer. For systems which associate when unfolding occurs i. e.

$A = 1/J(A_J)$ ---------- (2.28)

the same equations are valid, providing the bulk concentration $C_t$ is expressed as monomer equivalents and that n in the above equation is equal to 1/J.

## 2:6 ISOTHERMAL TITRATION MICROCALORIMETRY

All biological processes depend on the binding of ligands by specific proteins such as enzymes, receptors, antibodies, inhibitors, etc., and transport proteins, and therefore the determination of binding affinity for such molecular recognition processes plays a key role in biochemistry. But there are relatively few, fast, convenient and accurate methods to measure heat effects at constant temperature and among them isothermal titration microcalorimeters is the most suitable technique, we can determine heat of reaction as well

as the equilibrium constant and stoichiometry in a single experiment. Later on by using simple thermodynamic relationships we can determine all the thermodynamic parameters without applying the Van't Hoff equation. High sensitive microcalorimeter is very important to measure the changes in weak non-covalent forces and small amount of sample is required for this purpose. The recent development of sensitive instruments allows the measurement of heat effects from reactions involving as little as nanomole amounts of reactants (Spokane & Gill, 1981; Donner, et al., 1982; Mckinnon, et al., 1984; Ramsay, et al., 1986; Myers, et al., 1987; Schon & Freire, 1989; Wiseman, et al., 1989). The types of biological studies carried out using microcalorimetry have included such diverse topics as the measurement of enzyme activities (Monk & Wadso, 1969), thermodynamics of proton binding to proteins, such as chymotrypsin, lysozyme and ribonuclease (Shiao & Sturtevant, 1970) and the study of conformational changes such as the acid denaturation of lysozyme by guanidine hydrochloride (Atha & Ackers, 1971). More recently, it has been employed to investigate a range of processes from peptide and antibiotic interactions to protein folding (Cooper & McAuley-Hecht, 1993).

The two most important microcalorimeters to study the binding processes are Thermometric (LKB) and the Omega reaction microcalorimeter from Microcal Inc.

The Omega reaction microcalorimeter is very sensitive and measures binding constant upto $10^8$. This instrument was recently designed specifically for measuring the binding constant and heats of binding for biological associations (Wiseman et. al., 1989). The PC software package-Origin is used for analyzing the results. A titration experiment can be achieved in a very short time and also equilibrium of samples occurs within a few minutes after loading the sample and this fast response time of the calorimeter depends on the injection of the ligand within two or three minutes of interval of time.

The calorimeter consists of two coined-shaped cells, sample cell and reference cell, contained within an adiabatic jacket. The cells have volume of approximately 1.4ml made of Hastelloy C. Heaters are positioned on the surface of both cells as in the case of DSC. Samples are loaded using long narrow access tubes. The injection syringe has a long needle with a stirring blade at the end and this is suspended into the sample cell as shown in Figure 2.6. The injection syringe is coupled to a motor which rotates the syringe during the experiment to mix the contents of the sample cell. The plunger of the syringe is connected

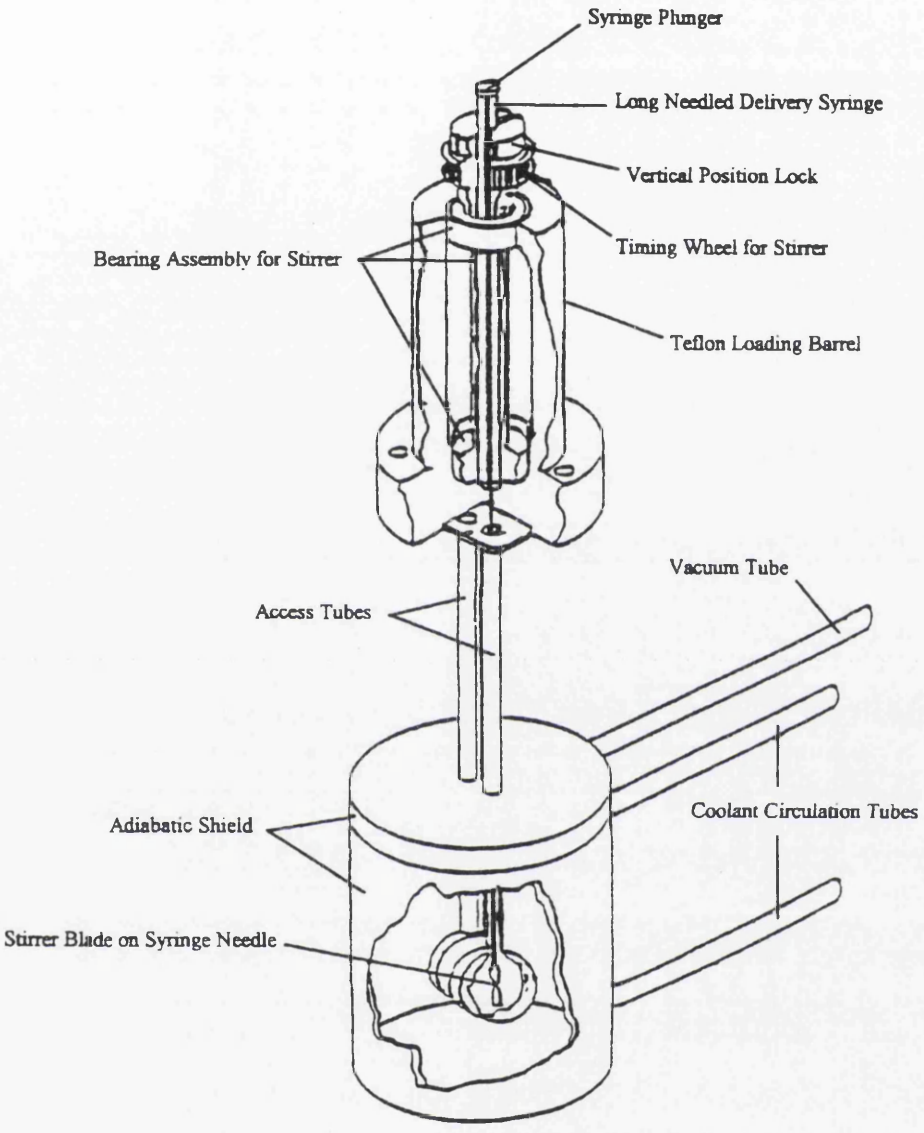


Figure 2.6: Schematic view of the Microcal OMEGA isothermal titration microcalorimeter (ITC) cell and injection/stirrer assembly.

to a stepping motor which controls the volume to be injected. A thermometric device is located between the sample and reference cell which measure the temperature difference ($\Delta T_1$) between the two cells. Similarly the temperature difference ($\Delta T_2$) between the cells and the adiabatic jacket is also measured using a thermopile.

When a sample is introduced into the sample cell, heat is either evolved or absorbed. This heat effect is monitored by the calorimeter using a feedback system. The reference cell is continuously heated at a slow constant rate which makes of $\Delta T_1$ non zero; this activates a feed back system which supplies power to the sample cell to return $\Delta T_1$ to zero. A PC running suitable software controls the action of the syringe stepper motor and the operator is able to set parameters such as duration of injection, time interval between the injection and volume of injection. The speed of the rotating, stirring syringe is not controlled by PC. Therefore speed is generally set at about 400 RPM to minimise the heat of mixing. Typical data are illustrated in Figure 2.7.

## 2:6:1 Calculations of thermodynamic parameters from experimental data

In case of an association experiment the observed heat effects are related by the following equation

$$Q_{obs} = Q_r + Q_{dil} + Q_{mix} \qquad \text{---------- (2.29)}$$

Where $Q_r$ is equal to heat of binding of enzyme and substrate, $Q_{dil}$ is called heat of dilution and therefore the values of all the components of the experiment have to be measured and $Q_{mix}$ is heat of mixing. We have to perform the following experiments to reach to the conclusion for obtaining the enthalpy

| | contents of sample cell | contents of syringe |
|---|---|---|
| $Q_{obs}$ | macromolecule | ligand |
| $Q_1$ | macromolecule | buffer |
| $Q_2$ | buffer | ligand |
| $Q_{mix}$ | buffer | buffer |

where $Q_{dil} = Q_1 + Q_2 - 2.Q_{mix}$

In practice the value of $Q_{dil}$ may be very small and so it can be neglected. But this is not always the case, so we may have to perform all the four experiments.

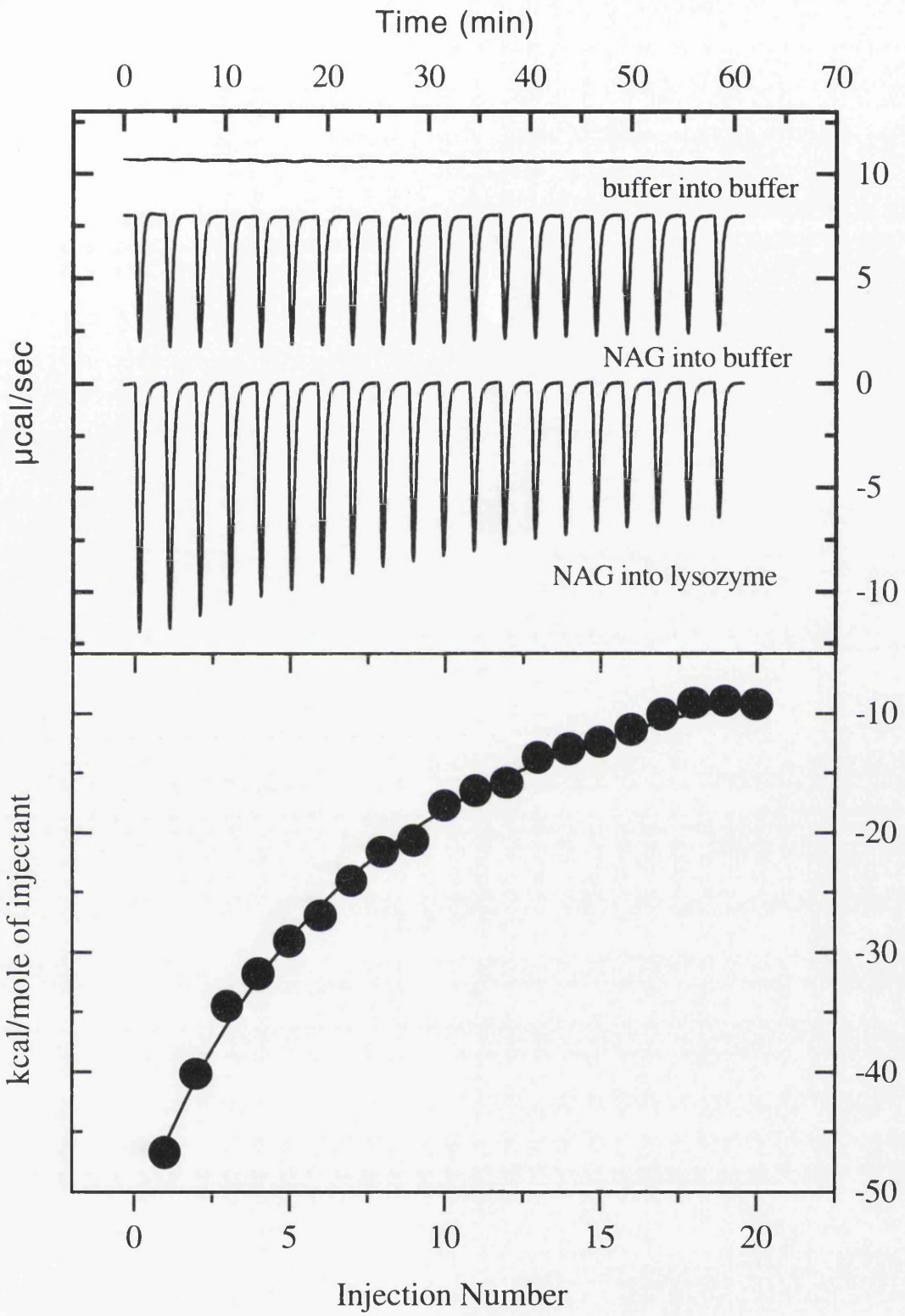


Figure 2.7: A typical ITC profile produced by the binding of lysozyme toNAG in 0.1M acetate buffer pH 5. The upper panel shows the raw data, including dilution controls. The lower panel shows integrated heat data after correction for dilution, together with the theoretical fit.

If an enzyme is saturated with ligand then the enthalpy is equal to the total heat divided by the concentration.

$$\Delta H^0 = Q_r / [M] \quad \text{----------} \quad (2.30)$$

The isothermal titration microcalorimeter can be used for measurement of enthalpy and association constant using heat production or uptake as a measure of the extent of the reaction.

$$Q_r = [ML]\Delta H^0/[M]_t \quad \text{----------} \quad (2.31)$$

Where $[M]_t$ is total concentration of protein and [ML] is the concentration of complex.

In case of 1:1 binding

$$Q = K_a[L]\Delta H^0/\{1+K_a[L]\} \quad \text{----------} \quad (2.32)$$

Equation 2. 32 can be rearranged as follows

$$1/Q = 1/\Delta H^0 + 1/K_a[L]\Delta H^0 \quad \text{----------} \quad (2.33)$$

If we plot a graph between 1/Q vs 1/[L] ,we get a straight line having slope equal to $1/K_a\Delta H^0$ and intercept equal to $1/\Delta H^0$. We have assumed in the above equation that there is a weak binding, but experimentally binding is too strong for this approximation to hold and free ligand concentration at equilibrium is not equal to the ligand concentration.

Another useful method is the hyperbolic relationship for the observed heat as a function of total enzyme and ligand concentration;

$$Q = -\Delta H^0(n[M]_t+[L]_t+1/K_a)\{1-(1-4n[M]_t[L]_t/(n[M]_t+[L]_t+1/K_a)^2\}^{1/2}/2[M]_t \quad \text{----------} \quad (2.34)$$

Where n is the number of binding sites. For multiple binding the above equation will be as follows

$$Q = \sum_{i=1}^{j} n_i \Delta H_i[L] K_i / 1 + K_i \quad \text{----------} \quad (2.35)$$

Where j is the set of number of distinct binding sites. $K_i$, $\Delta H_i$ and $n_i$ are the apparent association constant, enthalpy change and number of each set of sites. The calorimetric titration curves can be analyzed using two sets of sites. But the complications arise if we use more than two set of sites because the single fitting data may not be obtained since there are then three variable parameters exist for each set of sites. Further complications

arise when the binding sites are interactive, e.g. in case of inhibitor, because the binding of one ligand may increase or decrease the binding affinity of second ligand. In this case the thermodynamic parameters may be measured in presence and absence of other ligand and then changes in $\Delta H^0$ and $K_a$ may be estimated.

## 2:6:2 Data Analysis

All of the data analysis steps can be performed using the Origin software package from Microcal Inc. We can obtain $\Delta H^0$, $K_a$ and n values per mole of protein from ITC analysis. The raw data obtained is a record of the heat required to maintain the temperature of the cells and jacket equal as a function of time. First step is to integrate the peaks in both experiments i.e. enzyme-ligand and dilutions. The dilution heats are then subtracted from the enzyme ligand titrations to get the correct values for titration. The heats of each injection are then plotted against the number of injection. Then apply theoretically to fit the data using a least square approach to obtain the values of n, $K_a$ and $\Delta H^0$. The data may be fitted either one set of binding sites or two set of binding sites. In case of weak binding we may fix any one of the parameters but usually we fix the value of n equal to one. Two mathematical models used in the Origin software to analyze the experimental data are explained below.

## 2:6:3 Model for one set of sites (taken from "ITC Data Analysis Tutorial Guide", Microcal Inc.)

In case one to one binding process, the binding constant K is given by

$$K = \theta/(1-\theta)[L] \quad \text{----------} \quad (2.36)$$

Where $\theta$ is the fraction of sites occupied by ligand L.

Also $[L]_T = [L] + N\theta[M]_t$ ---------- (2. 37)

Where $[L]_t$ and $[M]_t$ are the bulk ligand and bulk macromolecule concentration respectively.

By combining equations 2. 36 and 2. 37

$\theta^2-\theta[1+\{[L]_t/n\{M]_t\} + \{1/nK[M]_t\}] + \{[L]_t/n[M]_t\} = 0$ ---------- (2. 38)

The total heat content of the solution is given by

$Q = n\theta[M]_t\Delta HV_0$ ---------- (2. 39)

Where $\Delta H$ is molar heat of ligand binding and $V_0$ is the active cell volume.

Solving quadratic equation and putting the value of (into equation 2. 39, we get the final result as

$Q = \{n[M]_t\Delta HV_0 /2 \}\{1 + ([L]_t/n[M]_t) + (1/nK[M]_t) ([\{1+([L]_t/n[M]_t)+ 1/nK[M]_t\}^2 - 4[L]_t/n[M]_t]^{1/2}$ ---------- (2. 40)

The equation 2. 40 can be solved for Qi by putting values of n. K and $\Delta H$ at the end of the ith injection. The ITC actually measures the $\Delta Q_i$ value between i and i (1 injections which leads to, $Q_i = Q_i - Q_{i-1}$ ---- (2. 41)

This expression is only valid for volume $V_0$. Therefore some corrections are made in the calculations to account for the volume of liquid which is displaced from the cell on injection.

Initial guesses of the fitting parameters n, K, and $\Delta H$ are made automatically and are substituted into equation 2.40 to find values for $\Delta Q_i$ for each injection. These calculated values for $\Delta Q_i$ are compared with the corresponding experimental values of $\Delta Q_i$ and new values of the fitting parameters are found using statistical methods until there is an optimum fit between experimental and calculated $\Delta Q_i$ values.

## 2:6:4 Model for two sets of independent sites

When ligand binds to a macromolecule having two non-interacting sites, we have

$K_1 = \theta_1/(1-\theta_1)[L]$ ---------- (2.42)

and $K_2 = \theta_2/(1-\theta_2)[L]$ ---------- (2.43)

$[L]_t = [L] + [M]_t (n_1\theta_1 + n_2\theta_2)$ ---------- (2.44)

Solving equations 2.42, 2.43 and 2.44 and then rearranging , we get the cubic equation as given below

$[L]^3 + p[L]^2 + q[L] + r = 0$ ----------(2.45)

Where $p = 1/K_1 +1/K_2+ (n_1 +n_2)[M]_t-[L]_t$

and $q = \{n_1/K_2 + n_2/K_1\}[M]_t (\{1/K_1 + 1/K_2\}[L]_t . 1/K_1K_2$

and also $r = -[L]_t /K_1 K_2$ ---------- (2. 46)

Equations 2. 44 and 2. 45 can be solved for [L], numerically , once the value of $[L]_t$ , $[M]_t$ ,$n_1$, $n_2$ , $K_1$, and $K_2$ are assigned. Putting this value of [L] into equation 2. 42 gives values for $\theta_1$ and $\theta_2$. The heat content of the solution after the ith injection, $Q_i$ , is given by

$$Q_i = [M]_tV_0(n_1 \theta_1\Delta H_1 + n_2\theta_2\Delta H_2)$$ ---------- (2. 47)

Initial guesses of the fitting parameters $n_1$ , $n_2$ , $K_1$ , $K_2$ , $\Delta H_1$, $\Delta H_2$, are made and are substituted into equations 2. 45 and 2. 46 to find a value for [L] and then $\theta_1$ and $\theta_2$ using equation 2. 42 and 2. 43. Values for $\Delta Q_i$ are then found using equation 2. 47. The parameters are optimised using statistical methods until there is an optimum fit between experimental value and theoretical value.

## 2:6:5 More about ITC

Using ITC we can determine in principle the binding constant, free energy, enthalpy, entropy and stoichiometry for binding of a ligand to a protein in a single experiment. Thermodynamic parameters with the combination of other information such as three dimensional structures of the complexes provides valuable information about ligands, proteins and their interactions. Another main advantage of ITC is that only a small amount of protein/ligand is required for analysis. Most of the experiments stated in this thesis required only 3-6mg of protein per experiment. The material can be recovered if appropriate purification procedures for the particular system are available. It is not necessary to determine the exact concentration of the protein because the apparent stoichiometry can be determined in the non linear least squares analysis. However, the overall accuracy is improved if the binding site concentration is determined independently. A titration experiment can be carried out in a couple of hours including equilibration, cleaning, data analysis and plotting etc.

The major difficulty arising in this technique to determine binding constant is that if the binding constant is too strong ($K > 10^8 M^{-1}$) or too weak ($K< 10^4 M^{-1}$). The enthalpy component is always obtainable if the process is saturated. Independent enthalpy measurements can also be obtained by single injections of ligand into excess protein or protein into excess ligand.

As heat effects can also be dependent upon the impurity of the protein, sometimes erroneous results may occur. In case of enzyme the problem is more complicated. This problem is usually solved by examining the binding of an inhibitor to the enzyme or by using an enzyme which requires two or more substrates to bind before the catalytic reaction occurs. Other heat effects may arise due to the release or uptake of protons by the enzyme or substrate, or change in the aggregation state of the species or even conformation changes during association. Therefore, in addition to ligand binding, calorimetry can also give information about these processes.

Calorimetric heat effects can depend on the buffer salts used. Generally the pH of the buffer solutions containing proteins remain constant. During association process, if protons are released and then these protons are picked up by the buffer, this will produce a heat effect. By varying buffers, the observed enthalpy of binding will also vary. These parameters obtained can be used to calculate the number of moles of protons being released to the buffer. The observed enthalpy ($\Delta^0H_{obs}$) will equal the enthalpy of the association reaction plus an additional heat contribution from the association of the protons and buffer molecules

$$\Delta^0H_{obs} = \Delta^0H_0 + \Delta N\Delta^0H_b$$

Where $\Delta^0H_0$ represents the enthalpy changes in the absence of buffer effects and $\Delta^0H_b$ is the heat of protonation of the buffer. The plot of $\Delta^0H_{obs}$ versus $\Delta^0H_b$ gives a straight line with a slope equal to $\Delta N$ (number of protons released) and intercept equal to $\Delta H^0$.
Although microcalorimetry is non destructive, sometimes denaturation may also occur during long periods of stirring and/or equilibration in the calorimeter, and samples should be tested for conformation after the experiment.

Microcalorimetry has been used to study the interactions of drugs and foods, cancer cells, micro-organisms, blood, excipients (pharmaceutical additives), and cyclodextrins. The effect of drug on the growth rate of micro-organisms can be determined by measuring the heat output before and after the addition of the drug. Microcalorimetry has been used to measure degradation rate of drugs as solids or in solution (Suurkuusk & Wadso, 1982). The stability of ampicillin in an aqueous solution as a function of concentration of ampicillin, pH, and temperature was studied by Oliyai & Lindenbaum (1991). The observed

rate constant was found to agree with published values. The mechanism for degradation was pH dependent (with maximum stability at pH4) and the molal enthalpy change of the reaction varied with pH. The ITC has also been applied to study the binding of cations to ATP (Wilson & Chin, 1991). The cations which were investigated by calorimetry were $Mg^{+2}$, $Ca^{+2}$, and $Sr^{+2}$. In all cases the binding occurred with a positive enthalpy change and an increase in entropy. $Mg^{+2}$ was found to have the highest association constant followed by $Ca^{+2}$ and then $Sr^{+2}$. Monovalent cations such as $Na^{+1}$, $Li^{+1}$, and $K^{+1}$ were found to compete with $Mg^{+2}$ for complexation with ATP.

Microcalorimetry as a non specific technique has both limitations and advantages. Non specificity can result in the measurement of the wrong physical chemical interactions but it can also be used to study many different interactions that may be too complex to be studied by a simple specified technique.

# CHAPTER THREE

# 3 MATERIALS AND METHODS

## 3:1 Materials

Bio-materials and general chemicals used in this work are listed below and, unless otherwise indicated, were used without further purification. Reagents were normally of Analar or equivalent grade. These are shown in the following table.

| Chemical Name | Product/Lot Number | Molecular/Formula Weight | Chemical Company |
|---|---|---|---|
| Lysozyme | L-6876/65H7025 | 14,315 | Sigma |
| M. Lysodeikticus | M-3770/109F68081 | - | Sigma |
| L-Tryptophan | 270422/93659 | 204.33 | Fluka |
| N-acetyl-D-glucosamine | A-8625/43H04351 | 221.2 | Sigma |
| Penicillin-G, Na salt | PEN-NA/86H0534 | 356.4 | Sigma |
| MOPS | M-1254/40H5618 | 209. 3 | Sigma |
| MES | M-8250/46H5725 | 195. 2 | Sigma |
| Glycine | 28458/K22073013 | 75. 07 | BDH |
| (Tris[hydroxymethyl]-aminomethane-HCl) | T-3253/112H5602 | 157. 6 | Sigma |
| Piperazine | P4,590-7/50503022 | 86. 14 | Aldrich |
| Tin(II) Chloride | 20,825-6/30712032 | 189. 60 | Aldrich |
| Copper(II) Chloride | 20,314-9/08727TG | 134. 45 | Aldrich |
| Gallium(III) Sulfate | 25,420-7/09321DZ | 427. 63 | Aldrich |
| Cobalt(II) Chloride | 25,559-9/51219 | 237. 97 | Aldrich |
| Zinc Chloride | 20,808-6/40929 | 136. 28 | Aldrich |
| Nickel(II) Chloride hexahydrate | 22,338-7/50921 | 237. 71 | Aldrich |
| Ferric Chloride hexahydrate | 10110/9604210E | 270. 30 | BDH |
| Iron(II) Sulfate | 24240. 262/89321 | 278. 01 | Prolabo |
| Manganese Chloride | 54258/225309 | 197. 9 | Hopkin & Williams |
| Cadmium acetate | 10063/8444160 | 266. 52 | BDH |
| Lead Chloride | 26869-0/2318455 | 278. 10 | Aldrich |
| Barium Chloride | 191800 | 244. 28 | Hopkin & Williams |
| Magnesium Chloride | Mo600/19086399 | 203. 31 | FSA |
| Aluminium Chloride hexahydrate | 23,707-8/LN10519LN | 241. 43 | Aldrich |
| Europium(III) Chloride hexahydrate | 20,325-4/12313AN | 360. 41 | Aldrich |
| Lanthanum Chloride heptahydrate | 26,207-2/02719HQ | 371. 4 | Aldrich |
| Potassium Chloride | 101984L/ TA198038 | 74. 55 | BDH |
| Indium(III) Chloride | 20344-0/04311HF | 221. 18 | Aldrich |

## 3:2:1 Estimation of protein concentration

All proteins containing the aromatic residues, tyrosine and tryptophan, have a significant absorbance maximum at about 280nm (Creighton, 1984). By applying Lambert-Beer law ($A = \varepsilon cl$, where A is absorbance, $\varepsilon$ is the molar extinction coefficient, c is the molar concentration of the sample and l is the path length of the cell in cm.) we can then determine the concentration of protein, if we know the extinction coefficient of protein. In the case of lysozyme the $A^{280}_{1mg/ml} = 2.65$ (Mckenzie & White, 1991; Cooper, 1974), and molecular weight is 14315 amu, giving $\varepsilon_{280} = 37{,}900$.

## 3:2:2 Estimation of protein Extinction Coefficients

When the value of the extinction coefficient is not available from the literature, the method of Gill and von Hippel (1989) can be applied to calculate the extinction coefficient. We can only apply this method when the number of tryptophan, tyrosine and cysteine residues is known. This is an empirical rule and is only applicable in principle for denatured proteins. This method is based on the following equation

$$\varepsilon_{protein} = \alpha\varepsilon_{Tyr} + \beta\varepsilon_{Trp} + \gamma\varepsilon_{Cys}$$

where $\alpha$, $\beta$, and $\gamma$ are the number of residues of tyrosine, tryptophan and cysteine, respectively, and $\varepsilon_{Tyr}$, $\varepsilon_{Trp}$, and $\varepsilon_{Cys}$ are their molar extinction coefficients.

Summary of extinction coefficients of the amino acids which absorb light in the UV region at 280nm:

| Residues | $\varepsilon_{280}$ |
|---|---|
| Trp | 5690 |
| Tyr | 1280 |
| Cys | 120 |

## 3. 3 FLUORESCENCE SPECTROSCOPY

All the fluorescence binding and quenching experiments were carried out at 25°C using the Spex FluoroMax Spectrofluorometer, fitted with a circulating thermostatted water bath. Control of the instrument and data acquisition were carried out using a PC running dM3000 software package from Spex Inc. The samples were diluted using appropriate buffer to give an absorption maximum of about 0.1 absorbance units (or less) to prevent complication by internal filtering effects. The protein emission spectra were obtained by exciting the sample at 280nm and in some cases at 295nm. All the data were collected at 1nm wavelength steps and interval of one second. The initial volume of each sample in the cuvette was 3ml. First we measured the fluorescence intensity of protein alone, then adding appropriate amount of the quencher or other ligand (NAG, PG, salt, etc.) in the cuvette keeping the concentration of protein constant. In this way we measured the fluorescence intensity of each sample. The maximum fluorescence intensity was measured and plotted as a function of concentration to give a fluorescence titration curve. These data were analysed by non-linear regression in terms of a standard hyperbolic binding equation (Origin software, with function programmed by A.Cooper) to give estimates of n and $K_d$ values, where n is the number of (identical) binding sites and $K_d$ is the dissociation constant ($K_d = 1/K_a$). In our case, for most of the experiments reported here, the binding affinity is not very strong and the curvature of the titration plots is usually insufficient to define n values unambiguously. Consequently the value of n was normally set to unity (n = 1) to allow meaningful comparison of data.

## 3:4 DIFFERENTIAL SCANNING CALORIMETRY

Millimolar solutions of lysozyme were prepared by dissolving lysozyme in the appropriate buffer, then dialysing against this buffer at 4 °C overnight. Buffers used were: 0.1M sodium acetate-acetic acid buffer pH 5.00 and pH 4.12; 0.1M phosphate buffer pH 7.00; 0.1M sodium citrate-citric acid buffer pH 3.05 and pH 4.00; 0.1M Tris hydroxy-methylamino

methane-HCl (Tris) buffer pH 7.00; and 0.1M glycine-NaOH buffer pH 10.00. Protein concentration was determined spectrophotometrically as given above. Solutions of substrate-lysozyme complex were prepared by dissolving known mass of NAG or penicillin , a sample of the dialysed lysozyme solution. In some experiments, the penicillin G was also dissolved in appropriate buffer and this solution was heated to about 100 °C prior to mixing in lysozyme solution.

The DSC experiments were carried out using a Microcal MC-2D ultrasensitive calorimeter, fitted with an EM Electronics N2a nanovolt pre-amplifier. A PC was used to collect the data and to control the DSC. A typical procedure was as follows. First the buffer solution was degassed by placing the solution under vacuum in a small desiccator fitted with a water aspirator, and gently stirred using a magnetic stirrer. Secondly both reference and sample cells were cleaned and then loaded with the degassed buffer in both cells using a syringe fitted with a length of narrow gauge Teflon tubing. It is very important that cells may be free from any air bubbles. Nitrogen gas pressure is applied to the cells to inhibit bubble formation. Thirdly, scan parameters were introduced into the computer, for example, number of scan = 1, scan rate = 60 deg/hour, initial temperature = 20 °C, final temperature = 100 °C, filter = 15 seconds, file name = $MC_1$. DAT. The fourth step was to equilibrate the cell temperature until the difference in temperature between the cells and the adiabatic jacket was less than 1 °C. At this stage the scan was initiated and allowed to run to completion. When this baseline scan was completed, and the DSC cooled to the original temperature, this procedure was repeated with degassed protein solution in the sample cell, carefully keeping all other parameters as same. This scan was also recorded using the computer.

The final step was then to analyze the data using Origin software package from Microcal, with the DSC add on installed, as follows:

(i) normalise the thermogram with respect to the actual scan rate.

(ii) subtract buffer baseline from the sample scan.

(iii) normalise the data for protein concentration and cell volume.

(iv) fit to a non-two-state model(in this thesis). The mathematical basis for this model is stated in section (2:5:4 & 2:5:5).

## 3:5 ISOTHERMAL TITRATION MICROCALORIMETRY

The ITC experiments were carried out at about 25 (±0.5) °C using a Microcal Omega instrument. The general procedure is as follows. The reference cell was filled with distilled degassed water containing 0.05% sodium azide (this is an unstirred cell and rarely needs re-filling). The sample cell was filled with degassed sample (lysozyme, etc.) solution using a syringe with tubing attachment. Care was taken to avoid air bubbles being trapped in the cell. Then the temperature of the cells was raised (usually to 25 °C. as in this thesis) and the system was allowed to reach thermal equilibrium for a few minutes. The injection syringe was rinsed and filled with ligand solution (e.g. metal chloride, NAG, PG, etc.), mounted in the calorimeter and stirred at a constant 400 rpm. As soon as the baseline was stable (RMS noise 0.04μJ/s or less) the experiments were started. An injection schedule was set up (number of injections = 25, volume = 10μl, interval between injections = 3 minutes, etc.) which was under PC control. The control experiments were also carried out under the same conditions. The experimental data were stored on disk drive A for later evaluation of the results. The sample cell was daily cleaned with detergent (5% SDS, 1mM NaEDTA. pH8. 3). The experimental data were then analysed using Origin software package. The data were corrected by subtracting the heats of dilution of the ligand (PG, NAG, $LaCl_3.6H_2O$, etc.) from the titration experiment. In this thesis the heats of dilution of lysozyme/buffer and buffer/buffer were very small and therefore usually neglected in the analysis without affecting the results. The data were then analyzed using one set of sites model to give values of n, $\Delta H^0$ and K. In case of weak binding usually we have fixed the value of n as unity. Finally the $\Delta G^0$ values and $\Delta S^0$ values can be calculated using the appropriate equations as stated in chapter two.

### 3.6 Lysozyme Enzyme Assay

Lysozyme assay were done using the standard Sigma procedure of cell wall hydrolysis of Micrococcus lysodeikticus as follows.

Approximately 1.5 mg of Micrococcus lysodeikticus was dispersed in 10ml of 0.066M potassium phosphate buffer, pH 6.24. The absorbance of the solution (2.5ml) was measured using a quartz cuvette (1cm light path) at 25°C. The $A_{450nm}$ of this suspension was between 0.6 and 0.7. After equilibration in the cuvette at 25°C, the initial absorbance at 450 nm was monitored until constant, and then 0.1 ml of lysozyme solution (200-400 units, in the same buffer) were added. The subsequent decrease in absorbance at 450 nm was followed, and the rate of decrease ($\Delta A$ /min) was used to calculate the activity.

Lysozyme specific activity = $(\Delta A_{450}/min)/(0.001 \times mg\ solid/reaction\ mix)$

For a typical lysozyme specific activity of 47530 units/mg solid, 400 units in 0.1 ml corresponds to 4000 units per ml, equivalent to about 0.08 mg/ml of protein.

Experiments to investigate the effect of inhibitors (penicillin-G or N-acetyl-glucosamine) involved addition of the appropriate compound to the reaction mixture, comparing the relative rates of hydrolysis under otherwise identical conditions.

Note: Calorimetric data are usually quoted in calories throughout, since the Microcal instruments are so calibrated. For comparison, 1 calorie = 4.184 J.

# CHAPTER 4

# 4 Thermodynamics of Interaction of Penicillin-G and Lysozyme

## 4:1 UV Difference and Activity Measurements

Previous studies on the possible interaction between lysozyme and penicillin have involved UV difference spectra and enzyme activity measurements (Felsenfeld & Handschumacher, 1967). Attempts to reproduce these experiments here were only partially successful.

The UV difference experiments (240-400nm) were as follows: samples of lysozyme (approximately 0.1 to 0.5mg/ml), dissolved in 0.1M acetate buffer, pH 5, were used as both reference solution and to make up various concentrations of penicillin-G (upto 10mM) for UV absorbance measurements. This ensured that the protein concentration was the same in both sample and reference cuvettes. Despite this, the UV difference spectra observed (using a Shimadzu UV-160A spectrophotometer) were ambiguous. The high absorbance of the lysozyme solutions (A = 2.65 for 1 mg/ml at 280nm) leads to large stray light errors in the UV region. Moreover, the broad UV absorbance of penicillin-G itself in this region ($\lambda_{max}$ = 323nm) obscures any small changes that might arise from binding. Consequently no further experiments of this type were attempted.

The effects of both penicillin-G and N-acetyl-glucosamine (for comparison) on the enzyme activity of lysozyme in solution at pH 6.24 and 25°C are shown in Tables 4.1 and 4.2, and in Figure 4.1.

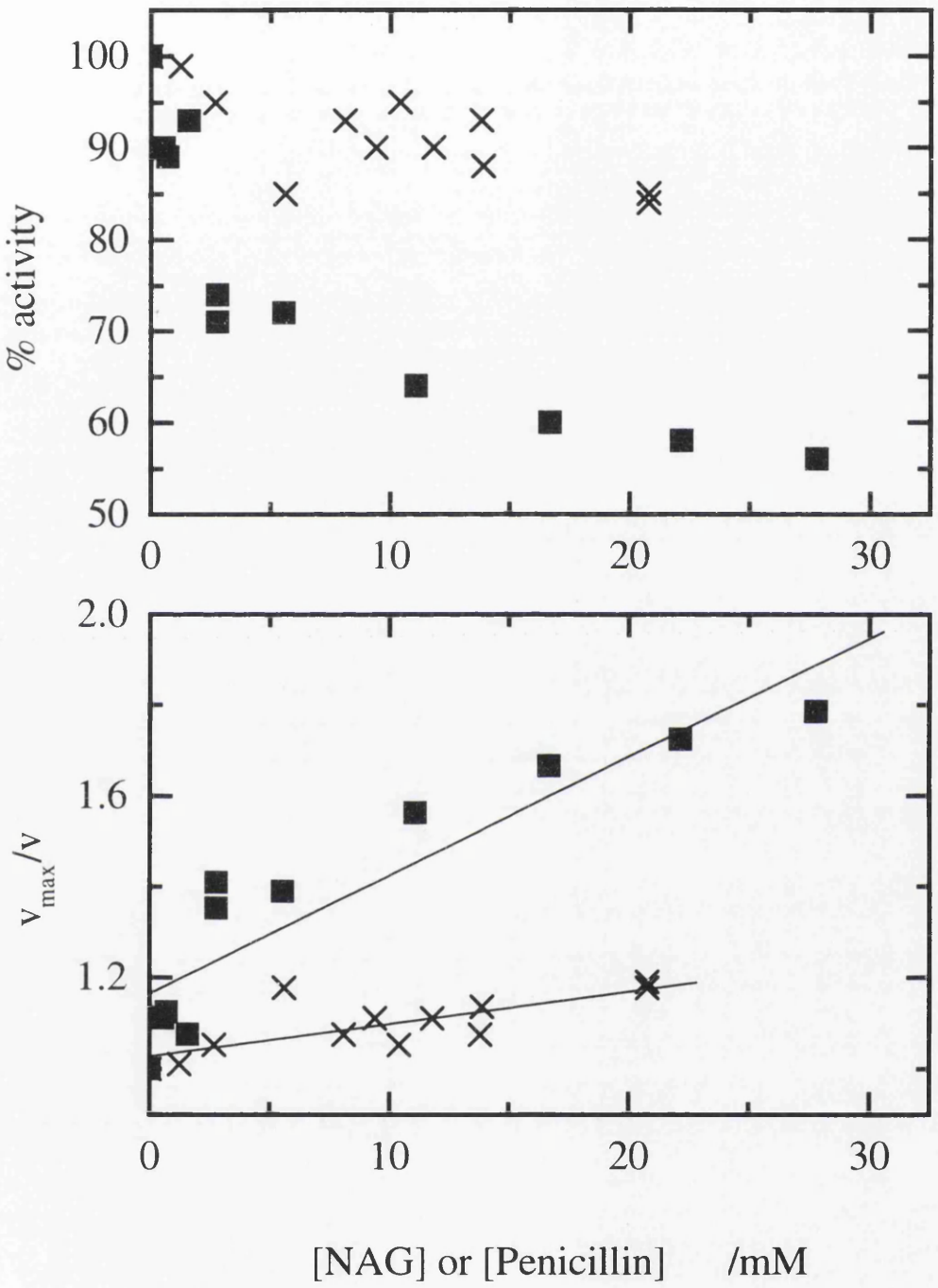


Figure 4.1: Effects of NAG ( ■ ) and penicillin-G ( × ) on the enzymic activity of lysozyme. The upper panel shows the raw data. The lower panel shows data plotted in a reciprocal form (see text) with best fit straight lines of slope corresponding to $K_i$ = 38 mM (NAG) and 140 mM (penicillin).

Table 4.1: Effect of Penicillin-G on relative activity of lysozyme

| [Penicillin-G] /mM | % Lysozyme Activity |
|---|---|
| 0 | 100 |
| 1.25 | 99 |
| 2.7 | 95 |
| 5.6 | 85 |
| 8.1 | 93 |
| 9.4 | 90 |
| 10.4 | 95 |
| 11.8 | 90 |
| 13.8 | 93 |
| 13.9 | 88 |
| 20.8 | 85 |
| 20.8 | 84 |

Table 4.2: Effect of NAG on relative activity of lysozyme

| [NAG] /mM | % Lysozyme Activity |
|---|---|
| 0 | 100 |
| 0.55 | 90 |
| 0.71 | 89 |
| 1.6 | 93 |
| 2.8 | 74 |
| 2.8 | 71 |
| 5.55 | 72 |
| 11.1 | 64 |
| 16.7 | 60 |
| 22.2 | 58 |
| 27.8 | 56 |

Considering first the NAG data (Table 4.2), it is clear that this known competitive inhibitor has a significant effect on lysozyme activity, giving 50% inhibition at around 25-30mM concentration. This is consistent with the known $K_d$ for binding of NAG in the lysozyme active site under similar conditions (Cooper, 1974). Penicillin however gives much less of an effect over the same concentration range. This implies that either penicillin does not bind to lysozyme (or rather binds with a much lower affinity than NAG), or that the binding of

penicillin is not in the active site and does not markedly affect enzyme activity. These observations contrast with those of Felsenfeld & Handschumaker (1967), who showed upto 50% inhibition by 24mM penicillin-G in phosphate buffer at pH 7. However, they were unable to show the same effect in several other buffers, for reasons which remain unclear.

The substrate for the lysozyme assay reaction is a complex material and conventional enzyme kinetic theory probably does not apply. However, a very simple analysis of inhibition effects might be as follows. Assuming simple competitive inhibition of the enzyme (E) by inhibitor (I):

$$E + I \rightleftharpoons EI \qquad ; \qquad K_I = [E][I]/[EI]$$

and assuming that the rate of substrate hydrolysis (v) is proportional to the free enzyme concentration [E], then:

$$v_{max}/v = ([E] + [EI])/[E] = 1 + [EI]/[E] = 1 + [I]/K_I$$

where $v_{max}$ is the rate in the absence of inhibitor.

This shows how the rate of the reaction is expected to be halved when $[I] = K_I$ . Furthermore, a plot of $v_{max}/v$ versus [I] should be linear with slope equal to $1/K_I$ . This is shown in Figure 4.1. The plot for NAG inhibition does not show the expected linearity, for reasons that are not clear but probably related to the oversimplicity of this model with the M. lysodeikticus substrate. Nevertheless, the least-squares slope of the data give an estimated $K_I(NAG) \approx 38$ mM, in line with other estimates. The penicillin data are roughly linear (at least within the rather large experimental errors) and do at least give an indication of the order of magnitude of any inhibition constant. The value found from the slope of the penicillin data in Fig. 4.1 corresponds to $K_I(penicillin) \approx 140$ mM. This is consistent with Klotz et al. (1950) who suggested that penicillin binding to lysozyme was much weaker than NAG.

## 4:2 Study of the Interaction of Lysozyme and Penicillin-G by Fluorescence techniques

Fluorescence spectroscopy is useful for investigating protein-ligand interactions because of the known sensitivity of tryptophan residues to their environment (Lehrer & Fasman, 1966). The relative exposure of the Trp residues in a protein to the solvent (water) will play a significant role in determining the wavelength of the emitted light in an intrinsic fluorescence measurement. This means that it is possible to use fluorescence measurements to determine rapidly whether or not a protein (e.g, lysozyme) adopts the native or molten globule state. The molten globule state has an expanded structure resulting in more penetration of the solvent, and therefore greater exposure of the Trp residues to water. This in turn results in the $\lambda_{max}$ of the protein being red shifted. Lala and Kaul (1992) found that $\lambda_{max}$ shifted from 328nm in the N state to 343 nm in the molten globule state. As hen egg white lysozyme has six tryptophan residues, it is therefore possible to use these as fluorescence probes in intrinsic protein fluorescence and protein fluorescence quenching measurements. This gives us useful information about the binding constant of penicillin-G and lysozyme and also lysozyme and NAG.

### 4:2:1 Results

The solution of penicillin-G and NAG was also prepared in different buffers and at different pH according to experimental conditions. Then series of solution was prepared to study the interactions of protein and ligand using the fluorescence method as described elsewhere in chapter 3. Care was taken to ensure that the protein concentration remained constant throughout and to eliminate any extraneous factors which may cause either a drop or an increase in intensity with addition of the inhibitor, such as temperature fluctuations or impurities in the sample thus ensuring that the observed intensity changes result purely from inhibitor quenching of the Trp fluorescence.

The binding of both penicillin-G and NAG to lysozyme was examined by fluorescence measurements as described in Chapter 3, using Trp excitation at 280 or 295 nm. The lysozyme concentration in these experiments was always in the range 0.002-0.005 mM. The changes in fluorescence emission with increasing concentration of NAG or penicillin were analysed in terms of a single-site binding model, and the results are summarised in Table 4.3, with examples of data shown in Figures 4.2 and 4.3 (for penicillin) and Figures 4.4 and 4.5 (for NAG). In all cases, a sharp emission peak was found near 342nm (in case of lysozyme alone) and around 357nm (in case of lysozyme-penicillin-G solutions). Similar quenching effect was observed in tryptophan-penicillin-G interaction and lysozyme-penicillin-G in presence of NAG at all pH. As the protein is titrated with penicillin-G the fluorescence intensity drops as stated above.

Firstly, these results indicate that titration of lysozyme with penicillin in the absence of NAG gives changes in the fluorescence emission spectra consistent with binding with $K_d$ values ranging from around 1-2 mM at neutral or acid pH (pH 4-7), rising to 26.6 mM at pH 9. This suggests that basic amino acid residues (e.g. lysine or arginine) may be involved in the binding, either directly or indirectly. This binding is unaffected, at least at pH 4.12, by the presence of NAG, which might have been expected to act as a competitive inhibitor to binding of penicillin. Similar fluorescence binding experiments using NAG alone (Table 4.3) give $K_d$ values for NAG consistent with published data, confirming the adequacy of the technique used here. This suggests that whatever binding process may be involved with penicillin, it is not competing with binding of the known saccharide inhibitor in the active site cleft of lysozyme.

In these experiments the binding curves were too shallow (weak binding) to allow determination of stoichiometry (n) values, and n was set equal to unity for analysis.

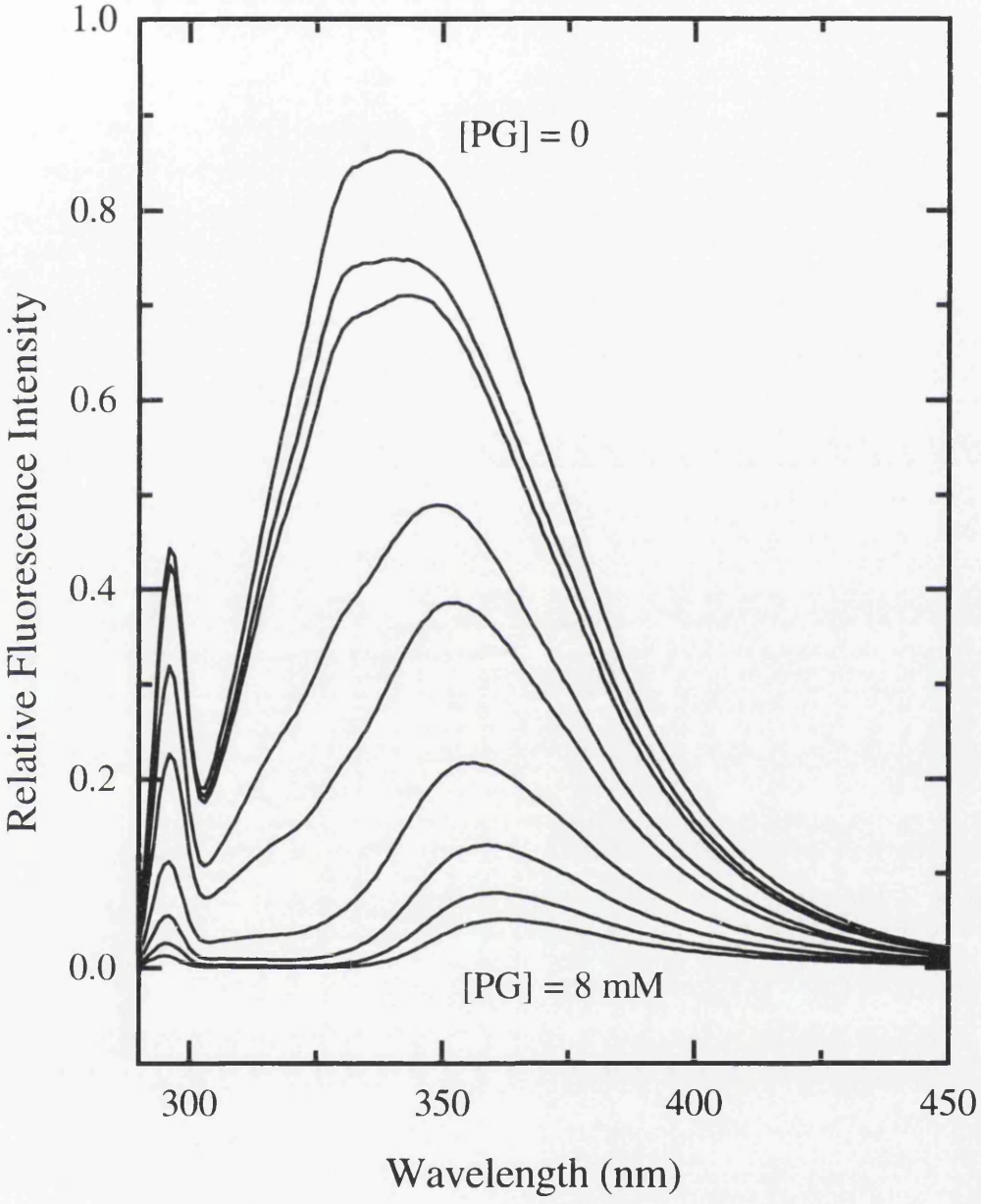


Figure 4.2: Example of typical fluorescence emission spectra for Lysozyme binding penicillin-G in 0.1M acetate buffer pH 4.12. The excitation wavelength was 295 nm and penicillin concentrations range from 0 to 8 mM. Note that the fluorescence intensity is quenched by increasing penicillin, [PG].

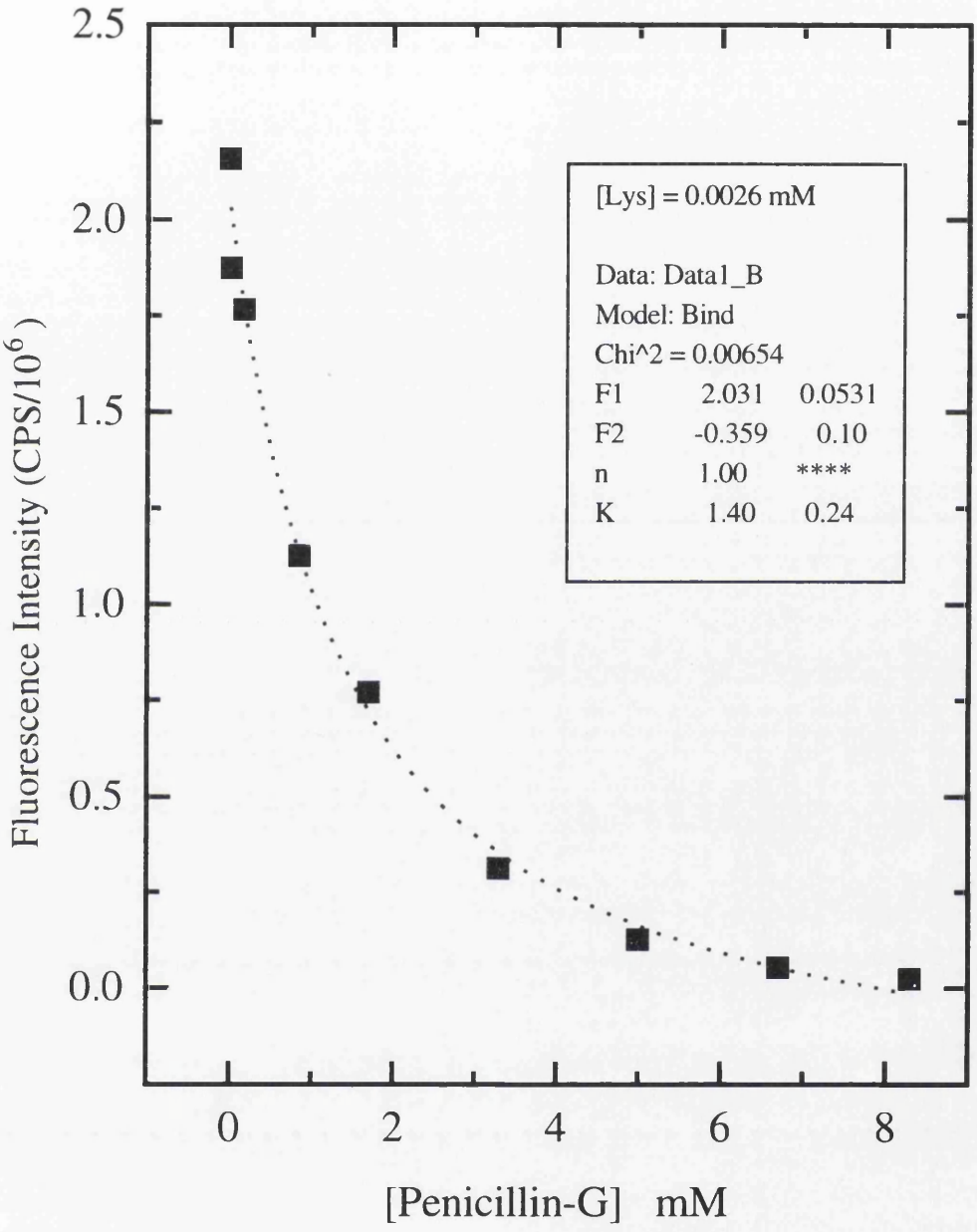


Figure 4.3: Decrease in fluorescence intensity at 340nm (from Fig. 4.2) with increasing concentrations of penicillin-G. The dotted line is a least-squares fit of the data to a single-site binding model, giving K = 1.4 mM in this instance.

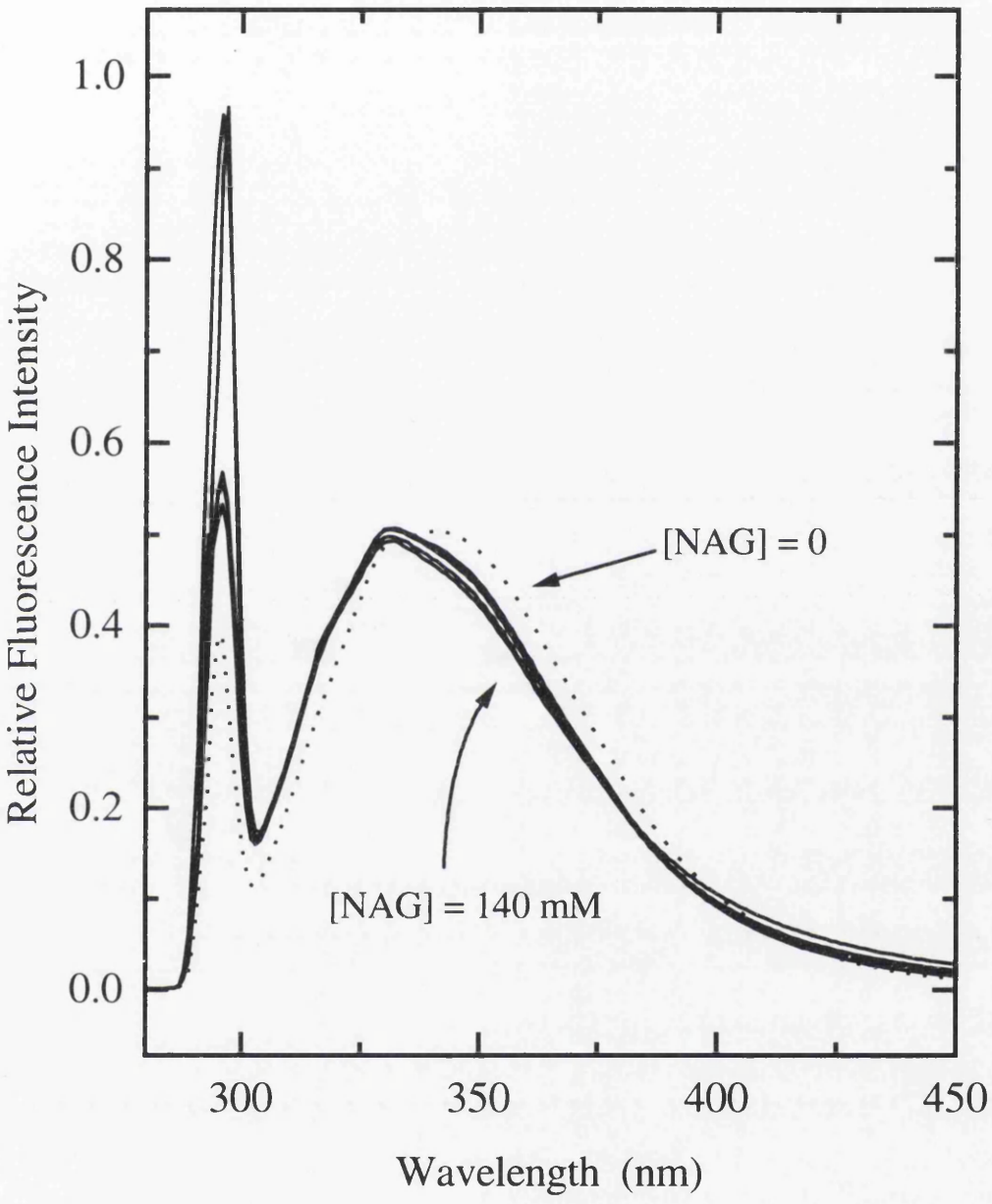


Figure 4.4: Florescence emission spectra of lysozyme in the presence of increasing concentrations of NAG (0 - 140 mM).

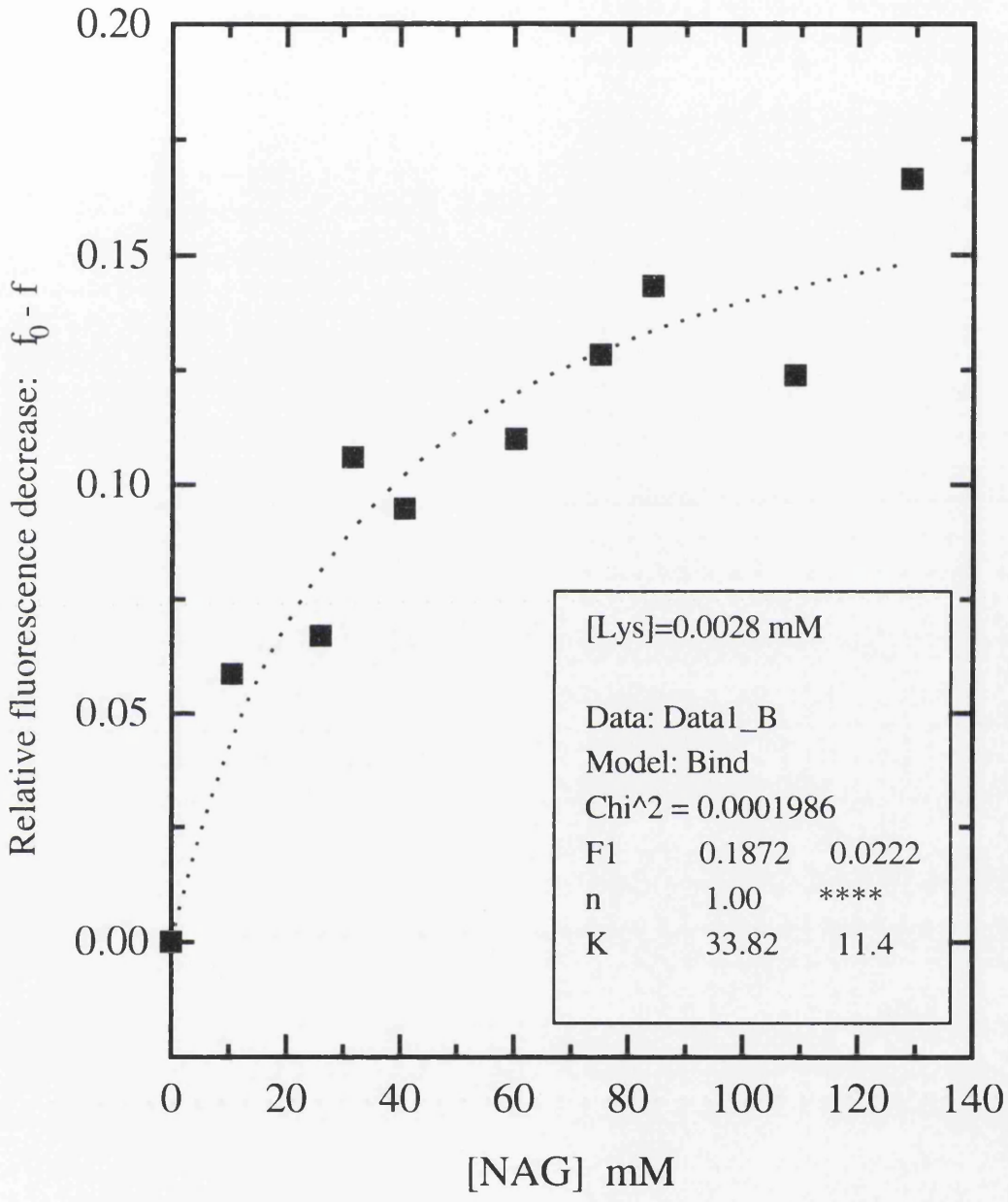


Figure 4.5: Change in relative fluorescence intensity of lysozyme at 360nm (from Fig. 4.4) with increasing NAG concentration. The dotted line is aleast-squares fit of the data with K = 33.8 mM

Table 4.3: Fluorescence binding parameters for NAG and penicillin at 25 °C

| pH | Buffer | [NAG] /mM | [PG] /mM | $K_d$ /mM |
|---|---|---|---|---|
| | | | | |
| 4.12 | acetate | x | 0 - 8 | 1.4 |
| .. | .. | x | 0 - 5 | 1.1 |
| .. | .. | 3.33 | 0 - 5 | 1.3 |
| .. | .. | 33.3 | 0 - 5 | 1.1 |
| | | | | |
| 5.0 | acetate | 0 - 140 | 0 | 33.8 |
| .. | .. | x | 0 - 100 | 1.8 |
| | | | | |
| 6.24 | phosphate | x | 0 - 17 | 2.0 |
| | | | | |
| 9.0 | glycine | x | 0 - 50 | 26.6 |
| | | | | |

x = this ligand not present during the titration.

The possibility that the effect of penicillin on lysozyme fluorescence might be due to a direct interaction with tryptophan residues, or due to non-specific internal filtering effects, was tested by repeating the fluorescence titration at pH 6.24 using free tryptophan in solution rather than lysozyme. The addition of penicillin to this solution did indeed lower the Trp fluorescence in a similar manner to lysozyme (Fig. 4.6), but with an apparent $K_d$ of order 40 mM, much weaker than for lysozyme under the same conditions.

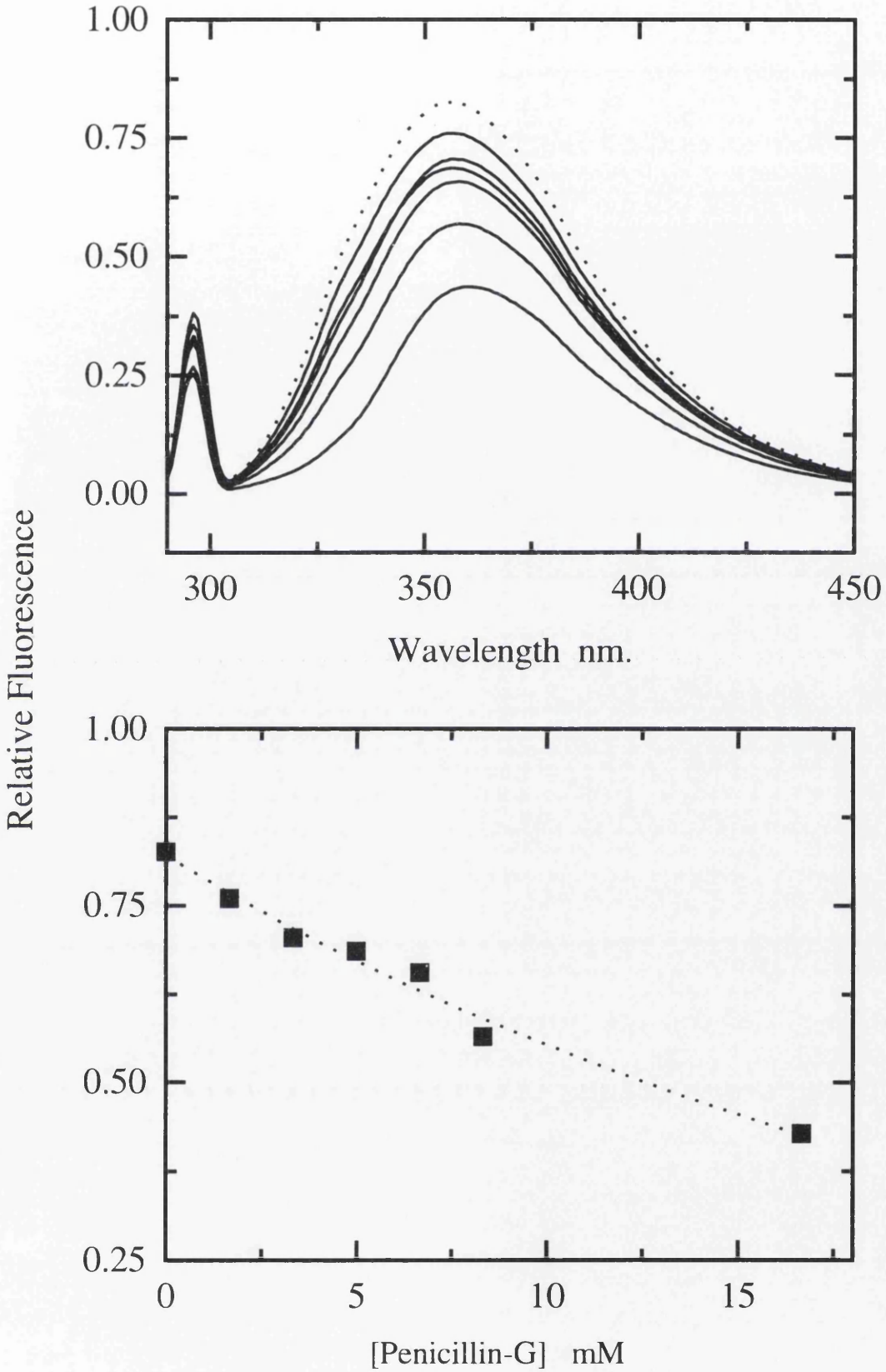


Figure 4.6: Effect of penicillin-G on the fluorescence of free Tryptophan in phosphate buffer, pH 6.24. The upper panel shows the decrease in fluorescence intensity as the penicillin concentration is raised to about 15 mM. The bottom panel shows the same data at 360 nm together with the theoretical fit for Kd = 41.5 mM.

The possibility of irreversible, time-dependent effects of penicillin on lysozyme was examined by repeating the fluorescence titration with identical samples after storage at room temperature for 24 hours, but no change in binding parameters was observed (Table 4.4). Interestingly, similar time-course experiments using NAG showed an apparent decrease in $K_d$ over several hours. This is probably due to the known mutarotation of α- and β-anomers of NAG, as seen by Cooper (1974).

Table 4.4: Time dependence of apparent binding constants at pH 5.0, acetate buffer, 25 °C.

| Ligand | Time /h | $K_d$ /mM |
|---|---|---|
| | | |
| Penicillin | 0 | 1.8 |
| | 24 | 1.8 |
| | | |
| NAG | 0 | 45.4 |
| | 0.25 | 44.9 |
| | 2 | 32.5 |
| | 5 | 30.4 |
| | 6 | 21.9 |
| | 14 | 19.3 |
| | 30 | 11.9 |
| | | |

## 4:3 DIFFERENTIAL SCANNING CALORIMETRY

Differential scanning calorimetric technique was used to measure the thermodynamic unfolding parameters for lysozyme in the presence of NAG and penicillin-G under a range of conditions. Data analysis was performed using Microcal Origin software, which is based on standard deconvolution procedure (Sturtevant, 1987; Privalov & Potekhin, 1986), and transitions were fit to single-peak non-two-state thermal unfolding models as stated in chapter 3.

## 4:3:1 RESULTS & DISCUSSION

DSC measurements of lysozyme in aqueous solutions using different buffers having same ionic strength and different pH values have been carried out under different conditions including protein concentration, variation in concentration of inhibitors, etc. Repeat DSC scans were used to examine the refolding and reversibility of the process and an example is shown in Figure 4.7. Initial scans of lysozyme alone show a single endothermic transition under all conditions. With repeat scans, each successive heating/cooling cycle shows two or more additional transitions at lower temperatures together with a decrease in magnitude of the main transition. These less stable species are probably mis-folded, or incorrectly folded forms of the polypeptide brought about by the build up of chemical changes (proline isomerization, side chain de-amidation) with repeated unfolding and exposure to high temperature (A.Cooper, S.Barron & M.Nutley, unpublished). As proline isomerization is reversible (Stein, 1993; Schmidt et al., 1993), but it may be depend on time and on cooling the polypeptide gets trapped with wrong proline conformers. Because lysozyme contains two proline residues, so four cis/trans conformations are possible. On this ground Cooper (1996) suggests that the appearance of four possible misfolded species in the DSC experiments is due to proline residues and not due to disulphide effects because the process is unaffected by the presence of reducing agents (Cooper, 1996).

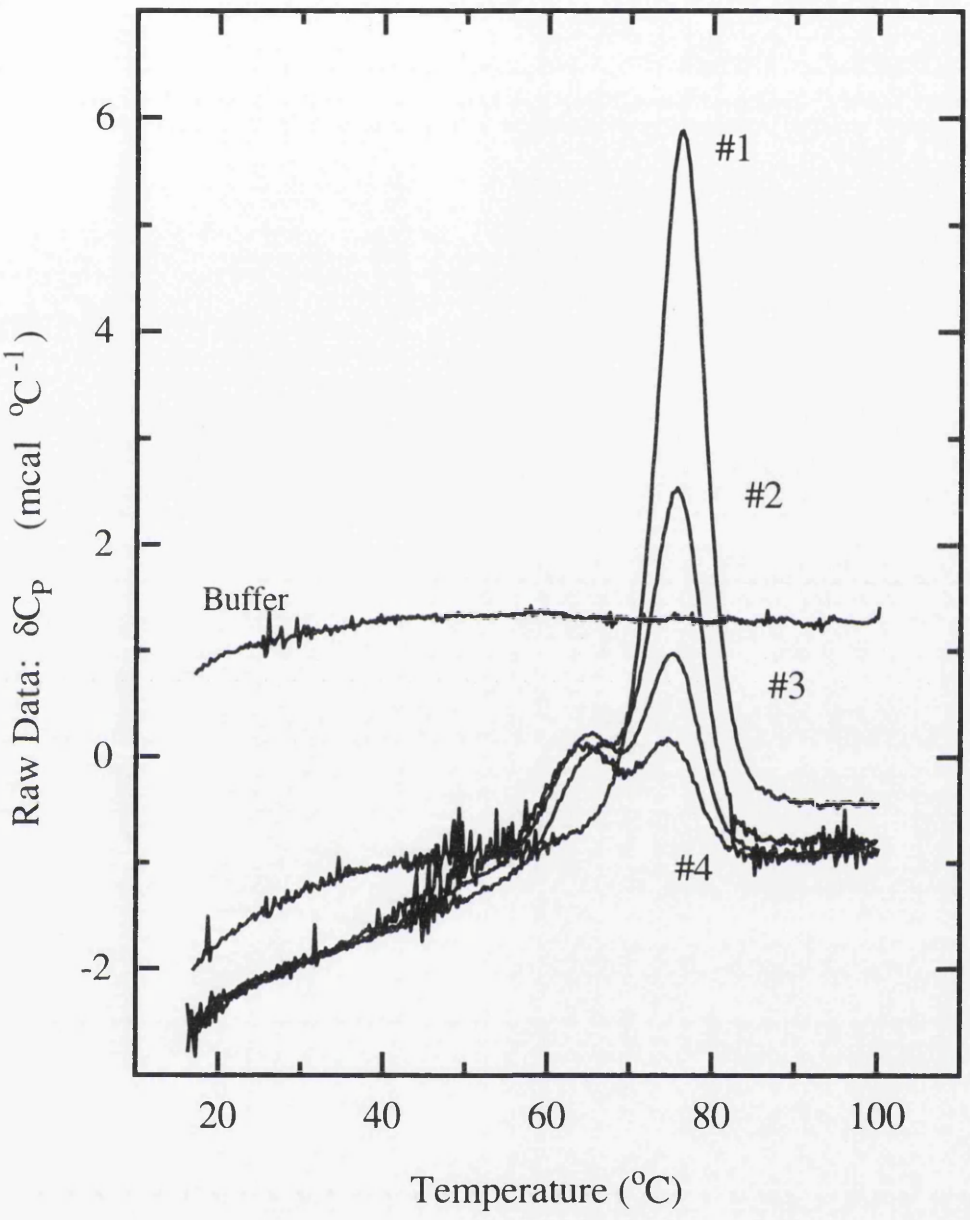


Figure 4.7: Repeat DSC scans of lysozyme (0.34mM) in acetate buffer pH 4.0, showing the accumulation od "mis-folded" forms of the protein during repeated heating and cooling.

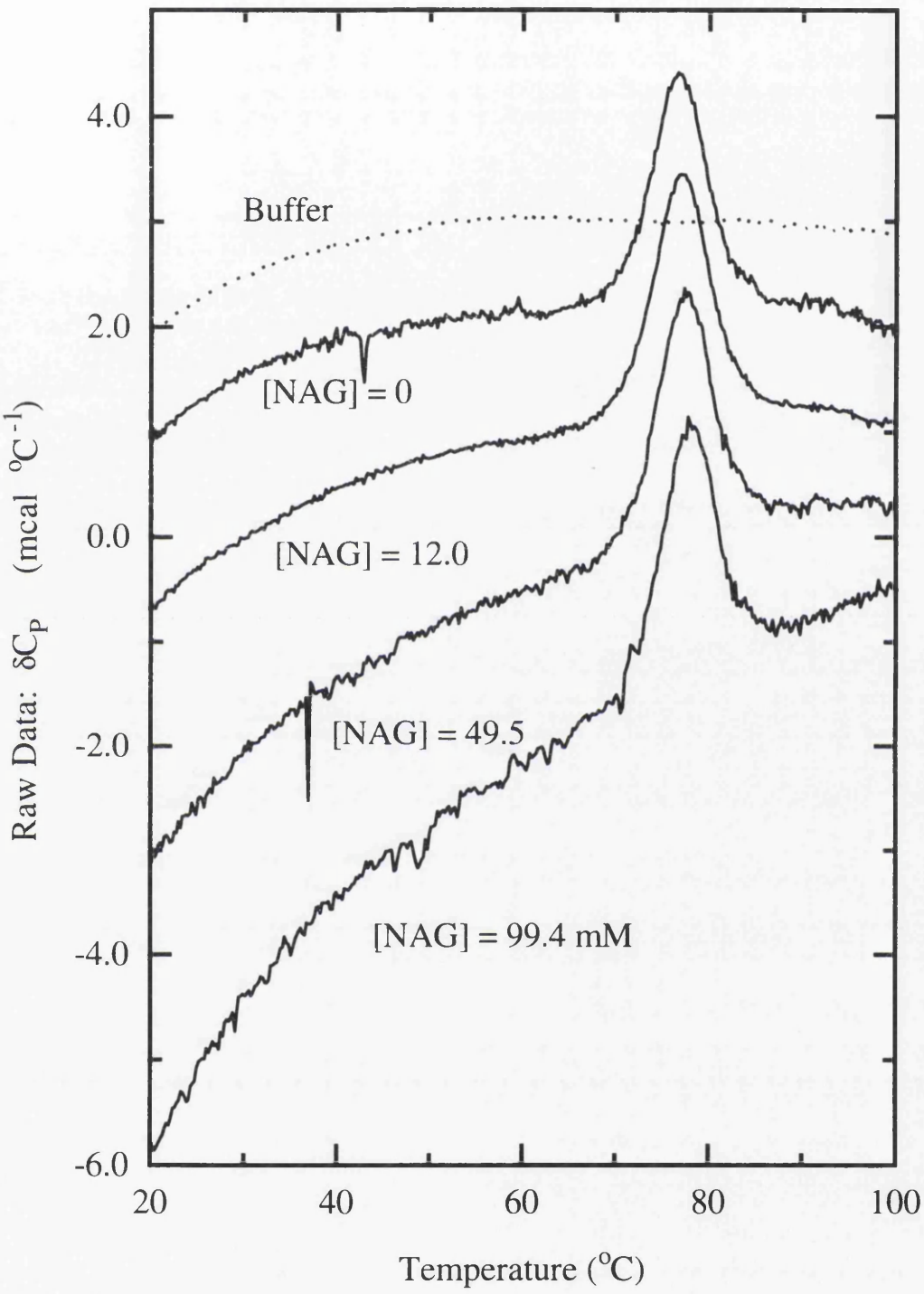


Figure 4.8: Raw DSC data for thermal unfolding of lysozyme (0.12mM, 0.1M acetate, pH 5) with increasing concentrations of NAG. The buffer baseline is shown for comparison.

The thermal denaturation of lysozyme at pH 5 in the presence of increasing concentrations of NAG is shown in Figure 4.8. Thermodynamic parameters, denaturation temperature $T_m$, etc. are shown in Table 4.5. On reheating, the already scanned solutions of complexed and uncomplexed lysozyme show that the transitions are reversible. The denaturation transition of lysozyme in NAG solutions is thus a two-state transition. In the absence of NAG the values of the transition temperature, $T_m$ , and enthalpies of denaturation are nearly close to the values reported in the literature (Privalov, 1979; Gopal & Ahluwalia, 1994). The effect of NAG is to bring about a small increase in $T_m$ , but with no significant increase in $\Delta H$ (at least within experimental uncertainty). This is consistent with binding of NAG to the native state of the protein:

$$PL \underset{+L}{\overset{-L}{\rightleftharpoons}} P \rightleftharpoons U$$

where P is the protein in native state, L is the ligand, PL is the protein ligand complex, and U is the protein in unfolded or denatured state. When the concentration of P+PL increases relative to the concentration of U, the protein is by definition more stable. The results in Table 4.5 show that $T_m$ increases as the concentration of NAG increases and hence the stability of lysozyme also increases.

TABLE 4.5: Thermal stability of lysozyme with varying concentrations of NAG in 0.1M acetate buffer pH 5. Concentration of lysozyme = 0.119mM

| [NAG]mM | $T_m$ (°C) | $\Delta H_{cal}$ (kcal $mol^{-1}$) | $\Delta H_{VH}$ (kcal $mol^{-1}$) |
|---|---|---|---|
| 0 | 76.6 | 113 | 125 |
| 12.0 | 76.9 | 109 | 131 |
| 49.5 | 77.3 | 108 | 134 |
| 99.4 | 77.9 | 115 | 134 |

These experiments with NAG therefore show, as anticipated, that the binding of a ligand to native lysozyme increases $T_m$ , and we should expect similar behaviour if penicillin also

binds in a similar manner. However significantly different results were seen in DSC experiments in the presence of penicillin.

The effects of penicillin-G on the thermal denaturation of lysozyme were performed using acetate buffer pH 5; phosphate buffer pH 7; glycine buffer pH 10; citrate buffer pH 3, pH 4; tris buffer pH 7 and MOPS buffer pH 7. We observe in all cases that the DSC thermograms show significant downward (exothermic) curvature (see for examples Figures 4.9 to 4.11) upon which is superimposed the endothermic unfolding transition of the protein. This baseline behaviour was observed also in simple control experiments using buffer and penicillin-G alone (Fig.4.10). Rescanning did not show any peak, nor did it show the exothermic baseline effects. This strongly suggests that penicillin-G in solution is undergoing irreversible thermal decomposition with increasing temperature in the DSC, and furthermore that either penicillin itself, or its decomposition products, are interacting irreversibly with the lysozyme to prevent even partial refolding upon cooling. Consistent with this, protein samples removed from the DSC after scanning in the presence of penicillin were turbid due to presence of aggregated protein. Also, in those experiments where unfolding transition could be seen, the apparent $T_m$ of the transition was lower than observed in the absence of penicillin under otherwise identical conditions.

In order to examine whether these effects are due to penicillin itself, or to its decomposition products, some experiments were performed using solutions in which the penicillin was heated to 100°C and cooled prior to addition of the lysozyme. DSC measurements were performed on the thermal denaturation of lysozyme and lysozyme-penicillin-G (heat treated) in 0.1M citrate buffer pH 4 and in MOPS buffer, pH 7 (Figure 4.12). The results show that, even though the exothermic baseline effects no longer appear, as the concentration of heat-treated penicillin-G increases, the $T_m$ of lysozyme unfolding decreases. Moreover, in these experiments, thermal unfolding curves are strongly affected by exothermic aggregation concomitant with the unfolding transition of the protein. These observations suggest that the major effect here is the interaction of thermally-decomposed penicillin with the unfolded polypeptide of lysozyme rather than with the folded form of the

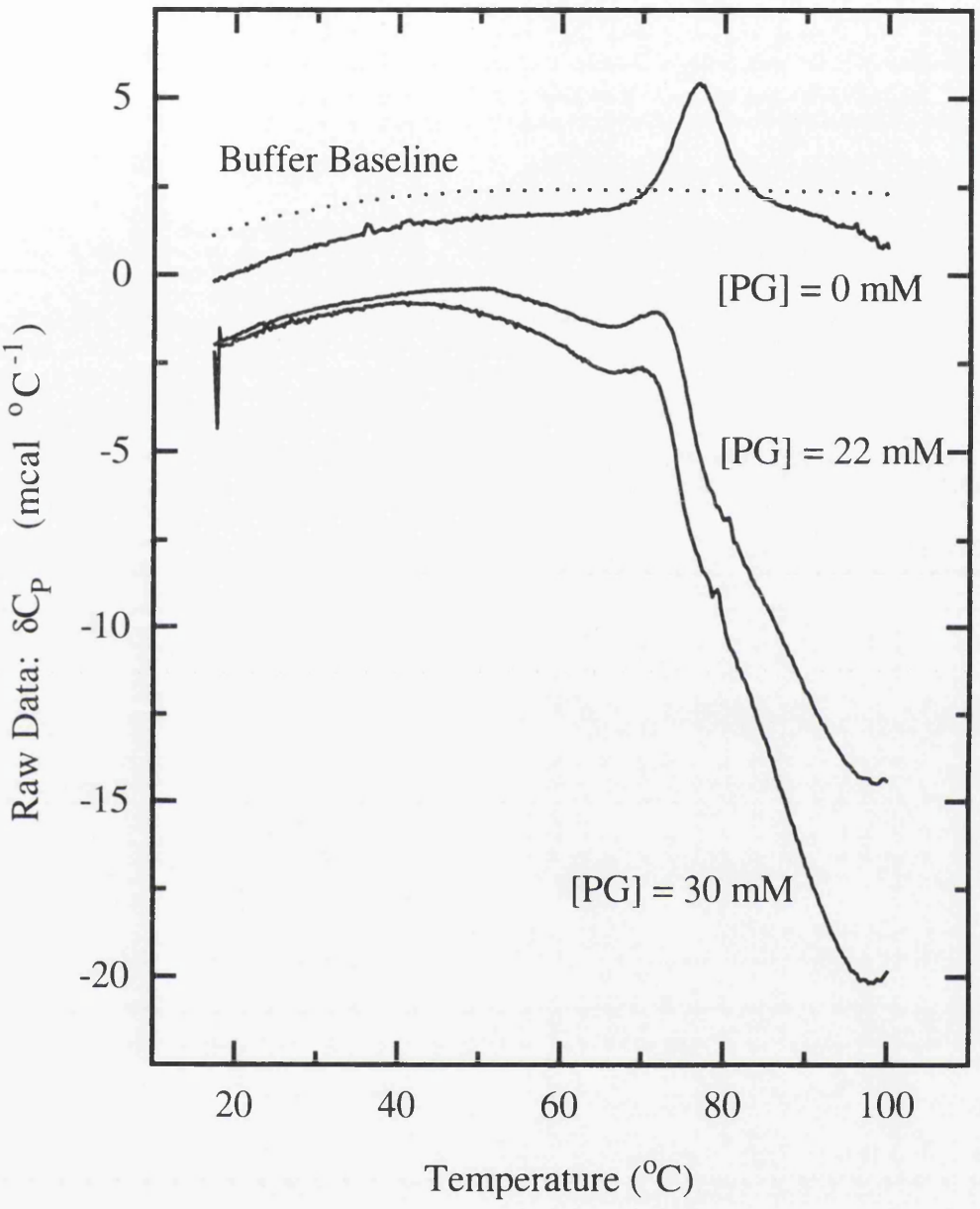


Figure 4.9: Raw DSC traces of lysozyme in 0.1M acetate pH 5.0, in the presence and absence of penicillin-G at the indicated concentrations. The exothermic baseline drift in the presence of penicillin is due to decomposition of the antibiotic.

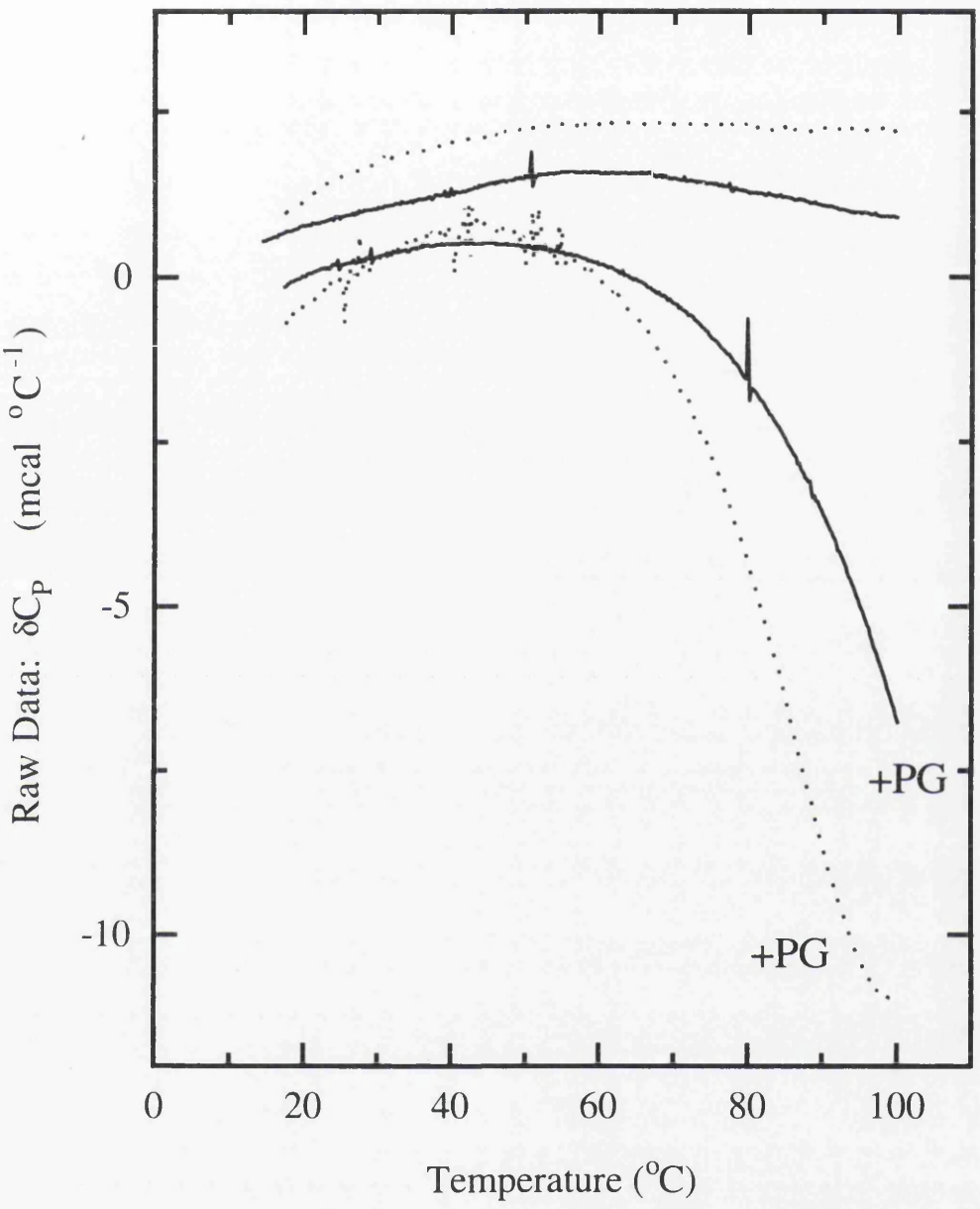


Figure 4.10: DSC scans of buffer solutions (acetate, dotted; phosphate, solid) with and without added penicillin-G, showing that the exothermic drifts are due to decomposition of the antibiotic at higher temperatures, even in the absence of protein.

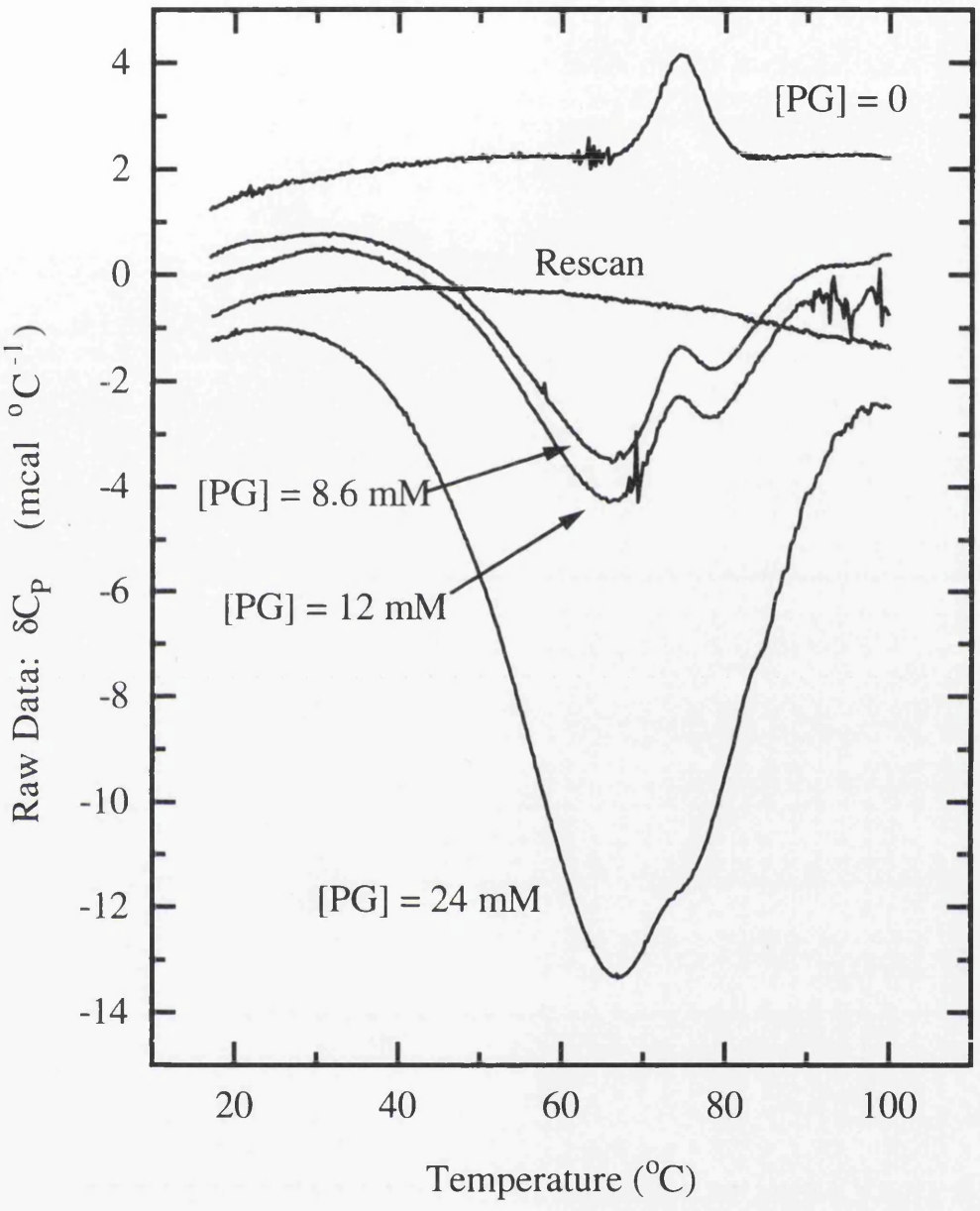


Figure 4.11: DSC scans of lysozyme in 0.1M citrate pH 4.0 showing the greater thermal decomposition effects of penicillin-G at lower pH. The re-scan shows that decomposition is complete during the first scan under these conditions, and that thermal unfolding of the lysozyme is also irreversible.

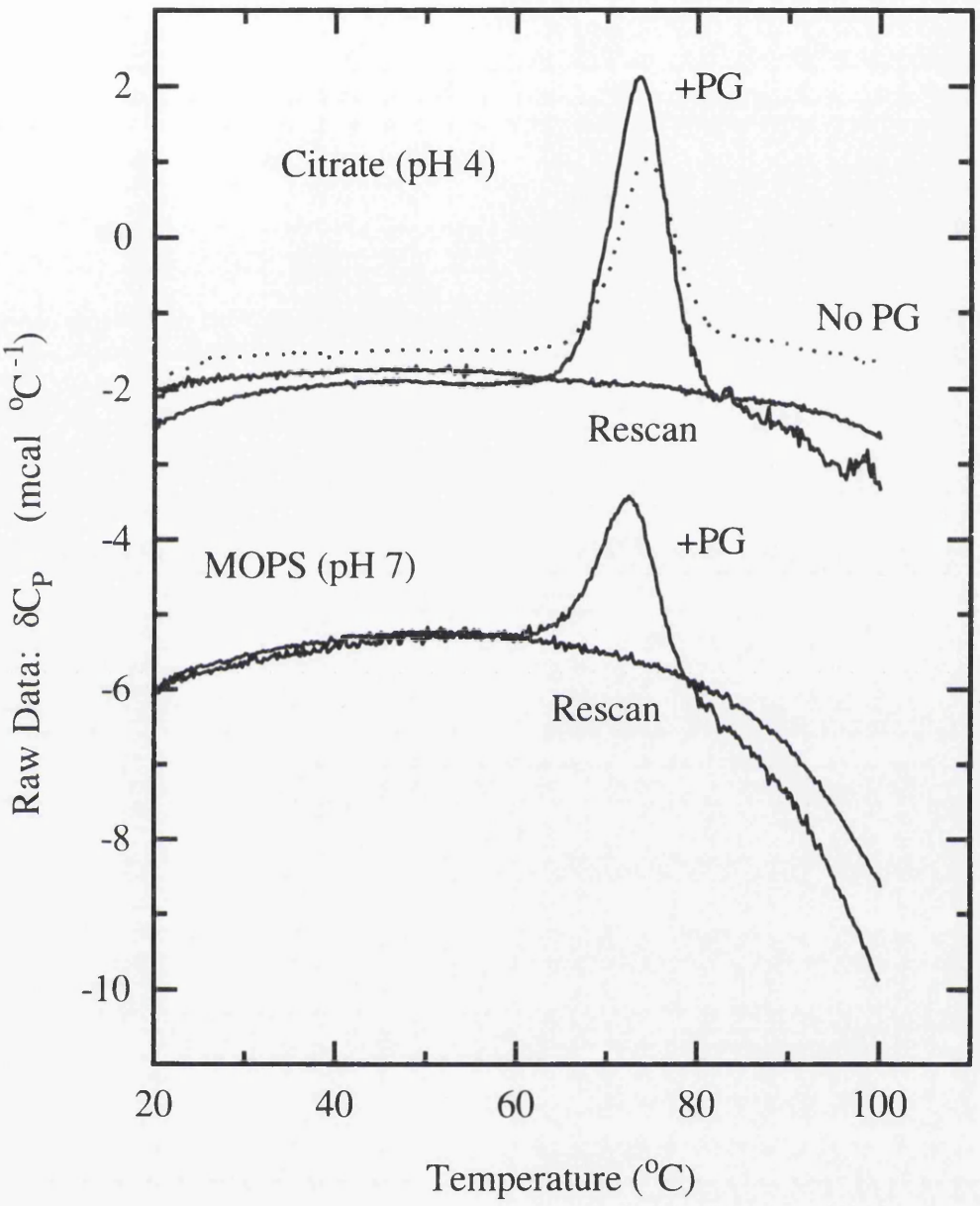


Figure 4.12: DSC scans of lysozyme in two different buffers containing penicillin-G previously heated to 100 °C. The dotted line is for lysozyme in acetate without penicillin. The rescans show that although the baseline drift effects are reduced by pre-heating the penicillin solutions, the decomposition products still induce irreversible effects in the protein.

protein. Aggregation in DSC thermograms leads to artificial sharpening of the transition, resulting in difficulties when estimating the $T_m$ and $\Delta H_m$ from these traces. $T_m$'s and other data quoted in Table 4.6 are therefore approximate only.

TABLE 4.6: Lysozyme with varying concentrations of heat-treated penicillin-G in 0.1M MOPS buffer pH 7, and citrate pH 4.

| | [Penicillin-G]mM | $T_m$(°C) | $\Delta H_{cal}$ (kcal/mol) | $\Delta H_{VH}$ (kcal/mol) |
|---|---|---|---|---|
| pH 7, MOPS buffer | 0.00 | 73.7 | 94.0 | 115.7 |
| | 5.33 | 72.5 | 83.0 | 127.7 |
| | 11.22 | 72.7 | 109.0 | 98.6 |
| | | | | |
| pH 4, citrate buffer | 0 | 74.4 | 97.8 | 134.5 |
| | 12.26 | 73.5 | 124 | 116.5 |
| | 24.8 | 73.2 | 106 | 117.9 |
| | 31.12 | 73.3 | 95.1 | 132.7 |

Notes: (a) In the case of MOPS buffer, the actual pH was reduced by addition of penicillin by about 0.2 pH units. (b) The samples in citrate buffer + penicillin after DSC were turbid, indicating aggregation of the unfolded protein in this case.

Another relevant observation is that high concentrations of penicillin-G can produce aggregation (or reduced solubility) of lysozyme even at room temperature. For example, in buffers containing up to 50mM penicillin, native appears soluble. However, with higher penicillin concentrations (> 50mM) lysozyme solutions (2-3 mg/ml) are turbid. This is of practical importance because it limits the concentrations that might be used for ITC experiments (see below), and might indicate that the penicillin is inducing some protein unfolding even at relatively low temperatures.

## 4:4 ISOTHERMAL TITRATION CALORIMETER

Direct studies on the possible binding of penicillin to lysozyme (with similar experiments using NAG for comparison) were attempted using isothermal titration calorimetry under a range of conditions following the procedures described in Chapter 3.

### 4:4:1 RESULTS AND DISCUSSION

The initial microcalorimeteric experiments were concerned with measuring the association constants for inhibitor (substrate analogue) binding to hen egg-white lysozyme under various conditions such as different buffers, different concentrations of N-acetyl-D-glucosamine, penicillin-G and lysozyme. Preliminary trials indicated that the binding (if any) of penicillin-G was weak, and it was therefore necessary to check experimental procedure using the known properties of NAG. Typical ITC experiments for NAG binding to lysozyme are illustrated in Figures 4.13 and 4.14, and data listed in Table 4.7.

Although the binding parameters obtained for the NAG/lysozyme interaction are comparable to previously published data (Cooper, 1973), there appears to be a small but significant of lysozyme concentration on both the observed K and $\Delta H$ values (see Table 4.7). The reason for this is not entirely clear, though it might reflect some effect of protein-protein interactions at higher concentration. It is puzzling that NAG binding seems to be tighter, though less exothermic, for higher lysozyme concentrations. Regardless of the reasons for this effect, it is clear that for comparative purposes the ITC experiments are best done using the same protein concentrations where possible.

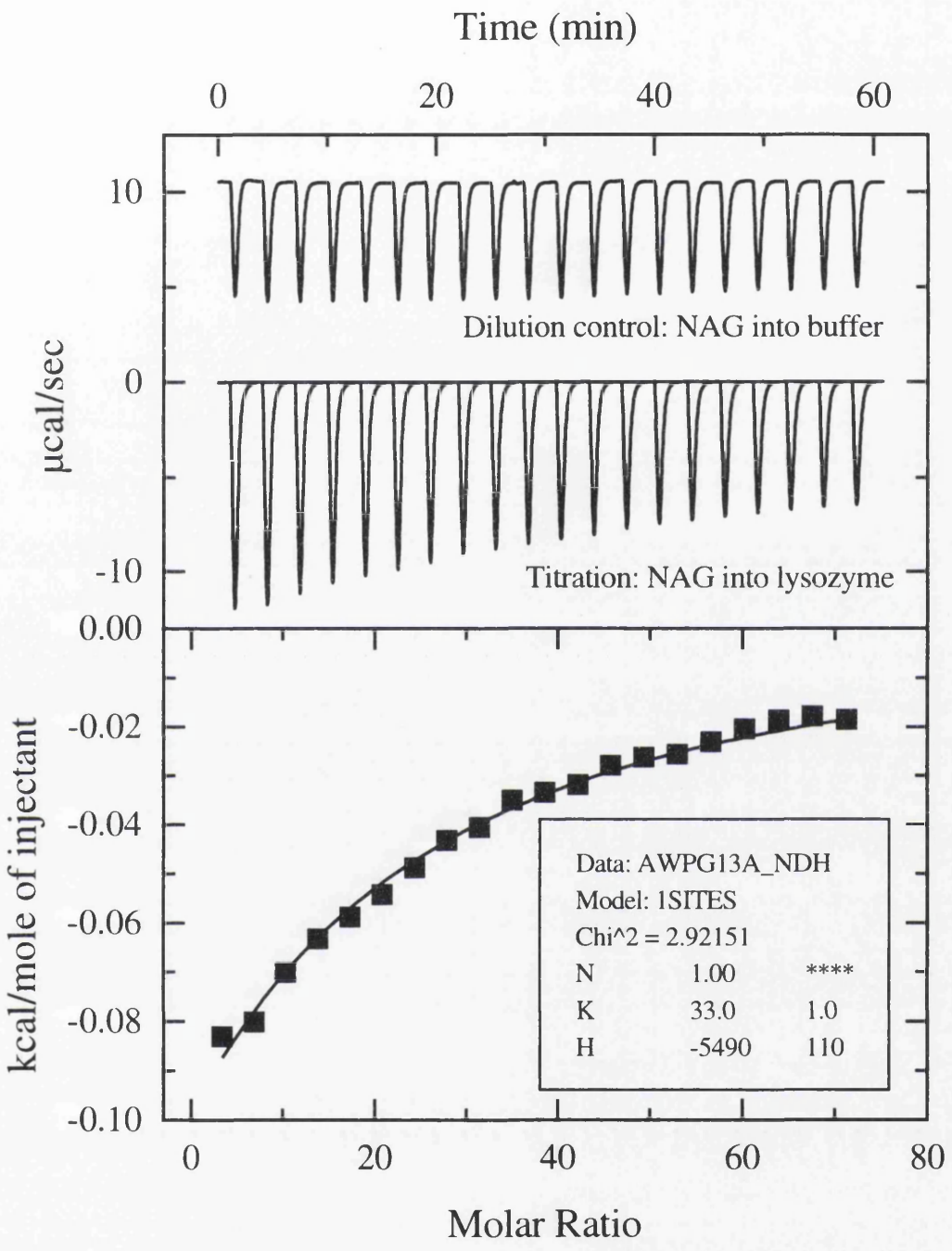


Figure 4.13: Typical ITC data for binding of NAG to lysozyme in acetate buffer, pH 5, 25.4 $^{o}$ C. 20 x 5µl injections of NAG (500mM) into lysozyme (0.52mM).

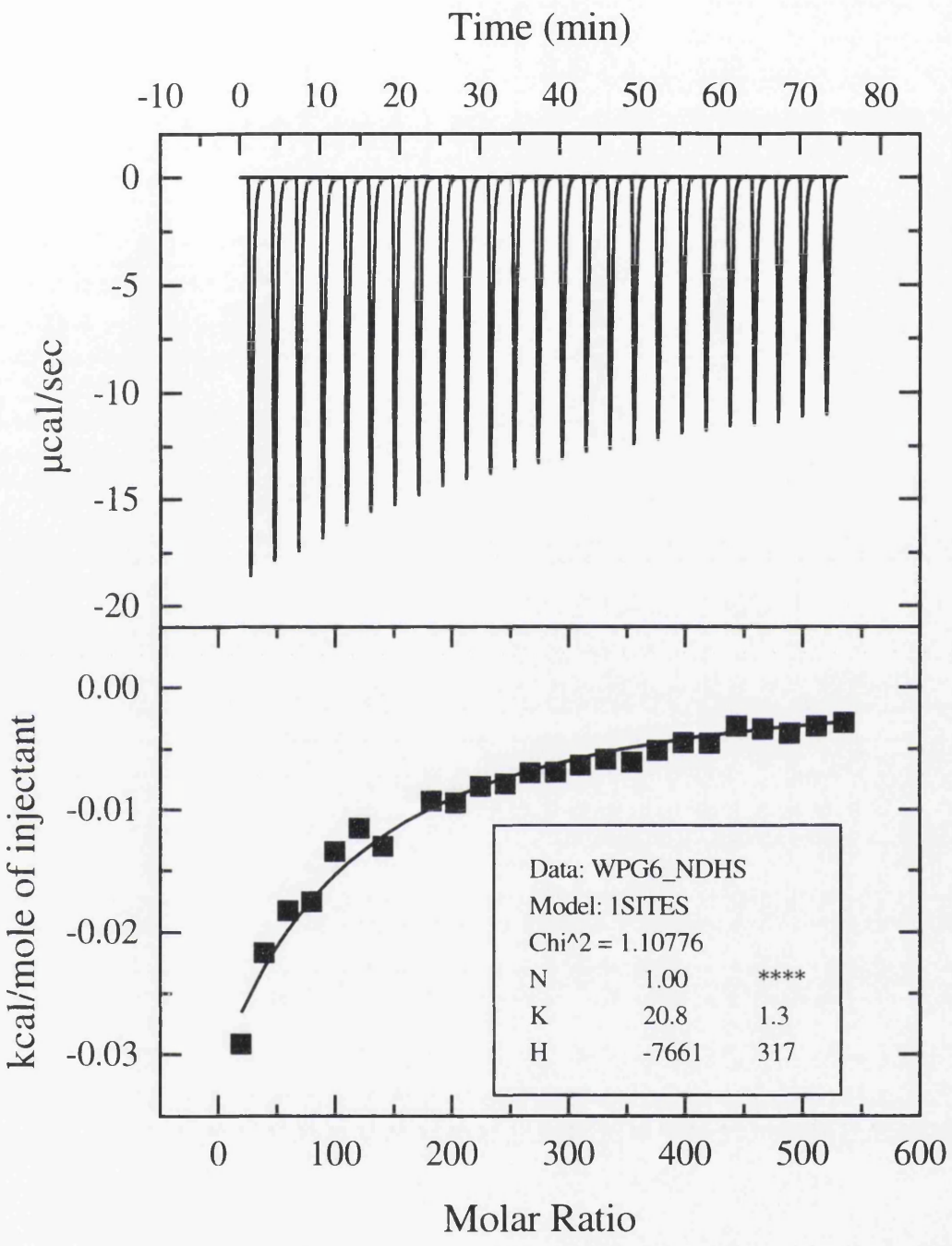


Figure 4.14: ITC data for NAG binding to lysozyme using lower protein concentrations (0.18mM). Other conditions as in Fig. 4.13.

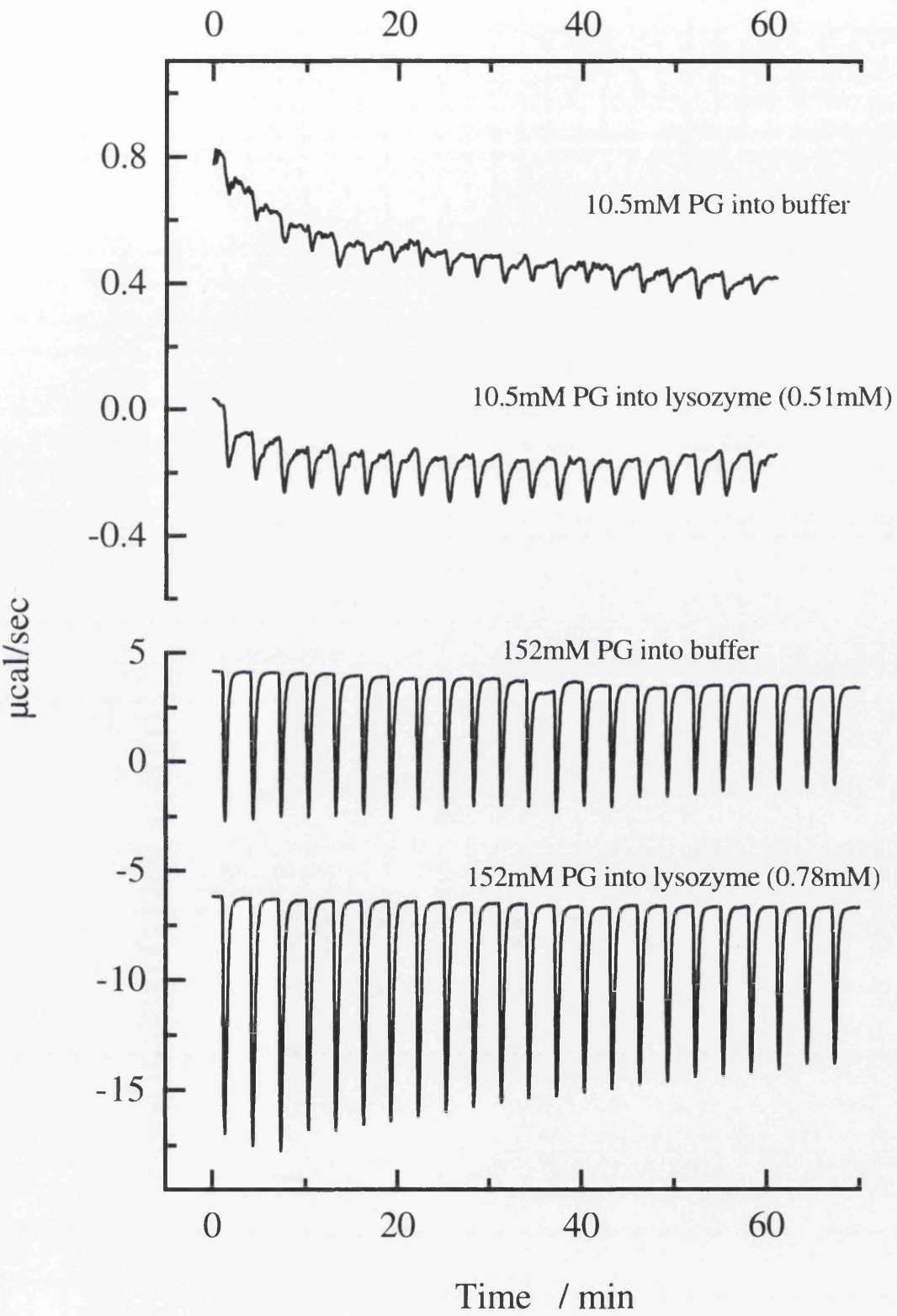


Figure 4.15: Examples of trial ITC experiments for binding of penicillin-G to lysozyme (acetate, pH 5, 25 $^{o}$ C), 5µl injections.

TABLE 4.7: Thermodynamic parameters for binding of N acetyl D glucosamine and hen egg-white lysozyme at 25 °C , pH 5, acetate buffer.

| [Lysozyme] mM | N (kept fixed) | K / $M^{-1}$ | ΔH (kcal/mol) |
|---|---|---|---|
| 0.5201 | 1 | 36.5 | -5.3 |
| 0.5860 | 1 | 32.2 | -6.5 |
| 0.4836 | 1 | 24.5 | -6.6 |
| 0.4790 | 1 | 30.2 | -6.5 |
| 0.4839 | 1 | 30.4 | -5.9 |
| | | | |
| 0.1805 | 1 | 19.7 | -8.0 |
| 0.1718 | 1 | 21.3 | -7.9 |

Attempts to measure binding of penicillin to lysozyme directly using ITC were unsuccessful, despite many trials, because of the apparent weakness of the effect and the very high heats of dilution of penicillin at the required concentrations. An example of typical ITC data is given in Figure 4.15. In all cases examined, over a range of pH and concentration values, injections of penicillin into lysozyme solution were consistently more exothermic than for penicillin injected into buffer alone. This is clear indication of some sort of interaction between lysozyme and penicillin. However, even at the highest available penicillin concentrations (approx. 200mM in the injection syringe), there was no evidence of binding saturation, and attempts to fit the data (after dilution correction) to the standard binding model were largely unsuccessful. The indication from these fitting attempts is that the binding affinity ($K_{PG}$) for penicillin is no better than 20 $M^{-1}$ (i.e. 50mM dissociation constant) at pH 5, and probably less at higher pH.

Following on from this, although it does not appear possible to measure binding of penicillin directly by ITC experiments, it is possible to study this indirectly by observing the possible inhibitory effect of penicillin on the binding of NAG. Consequently a series of experiments was performed in which the binding of NAG to lysozyme was measured by ITC titration in the presence of increasing amounts of penicillin-G. The results for pH 5 at 25 °C, using 0.5mM lysozyme, are summarized in Figures 4.16 and 4.17. Similar qualitative results were also seen using lower lysozyme concentrations. These data show that

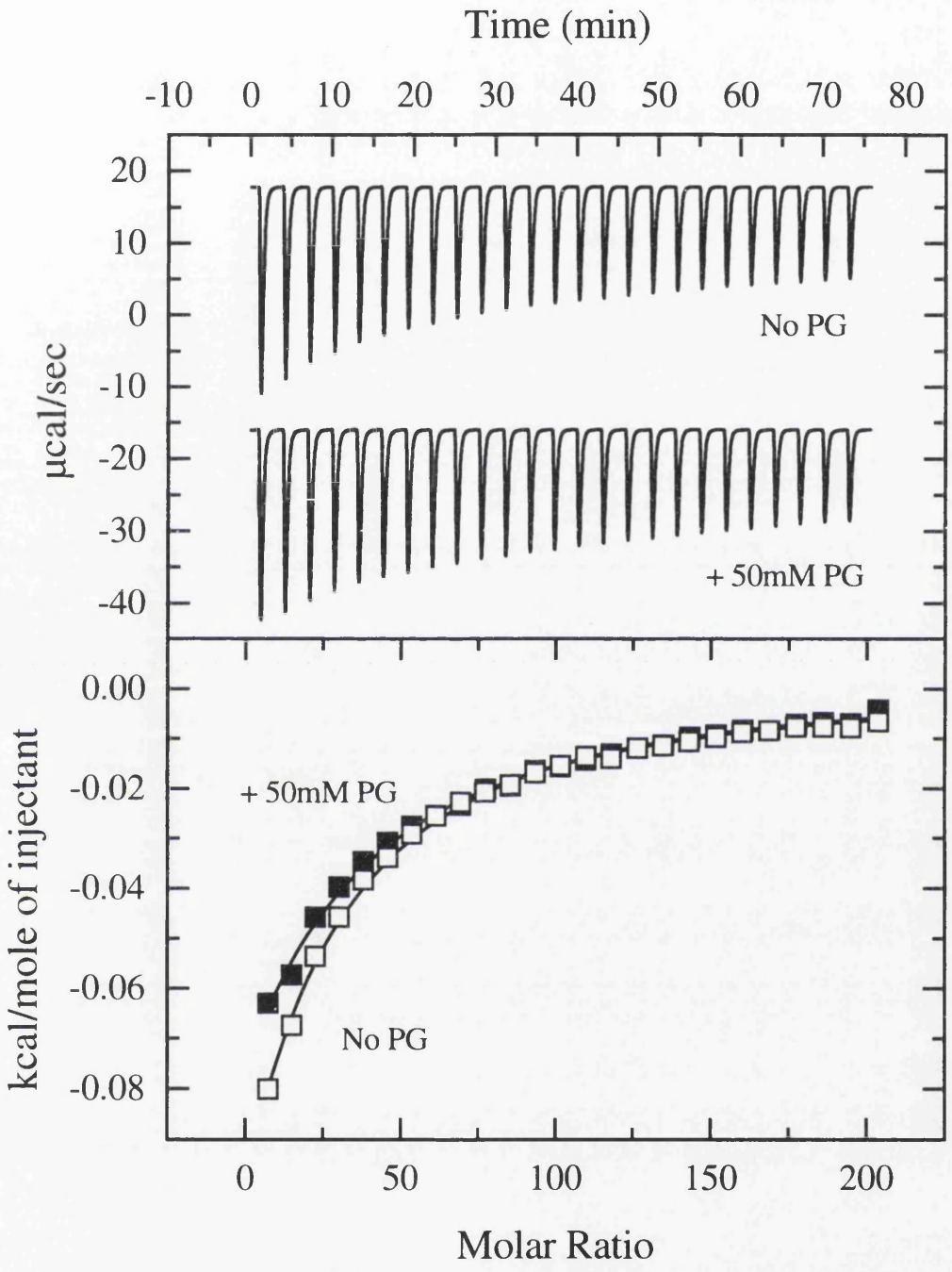


Figure 4.16: ITC comparison of binding of NAG to lysozyme (0.5mM) in the presence and absence of 50mM penicillin-G, 0.1M acetate, pH 5. The data in the bottom panel are corrected for dilution heats and fit to the simple binding model. Open squares are for binding without penicillin, and the solid symbols show data in the presence of 50mM penicillin with all other condition identical.

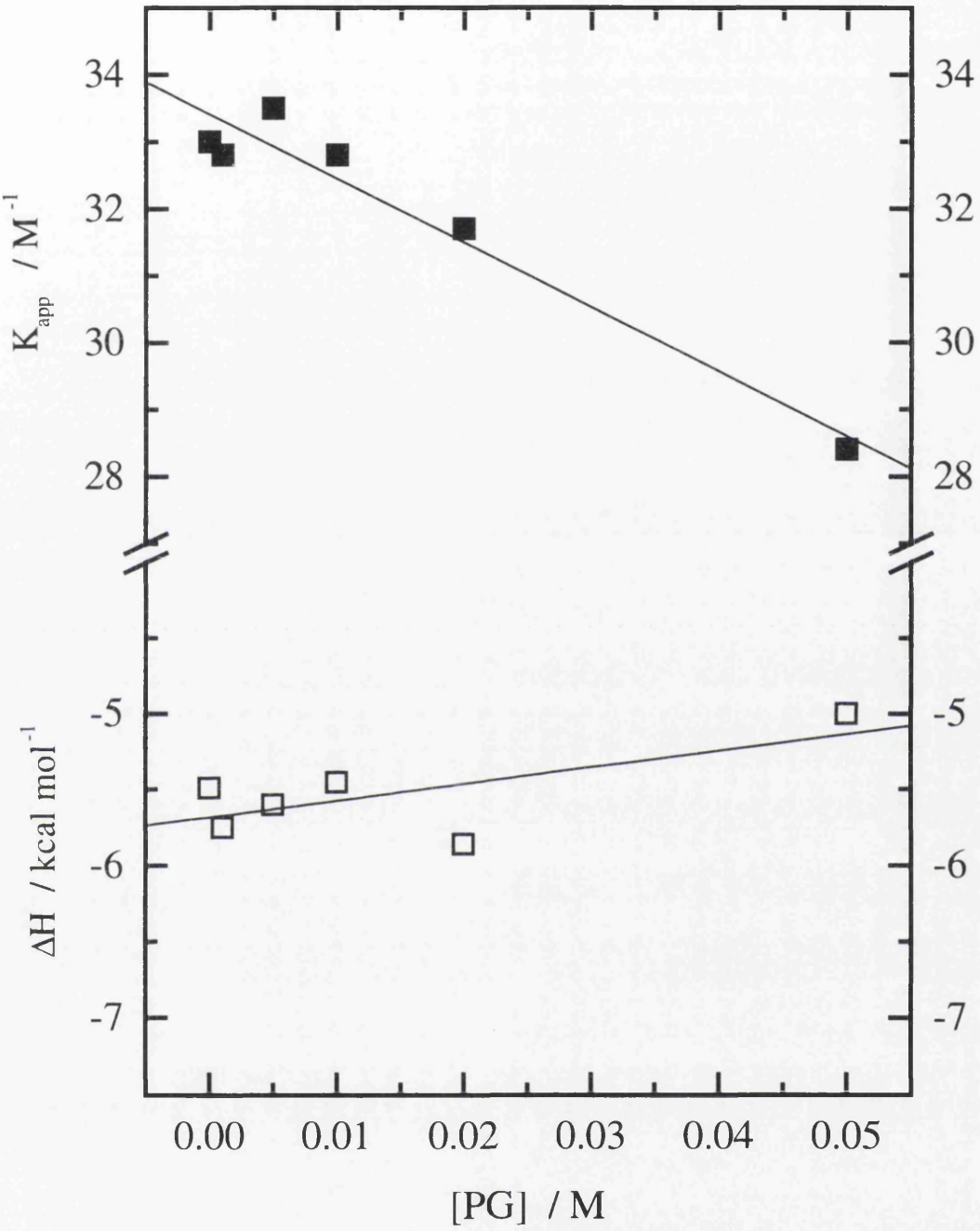


Figure 4.17: Effect of penicillin-G concentration on the apparent binding constant ($K_{app}$) and enthalpy of binding ($\Delta H$) of NAG to lysozyme at pH 5 in acetate buffer. The line through $K_{app}$ data shows the least-squares fit for $K_{PG} = 2.9\ M^{-1}$ (350mM).

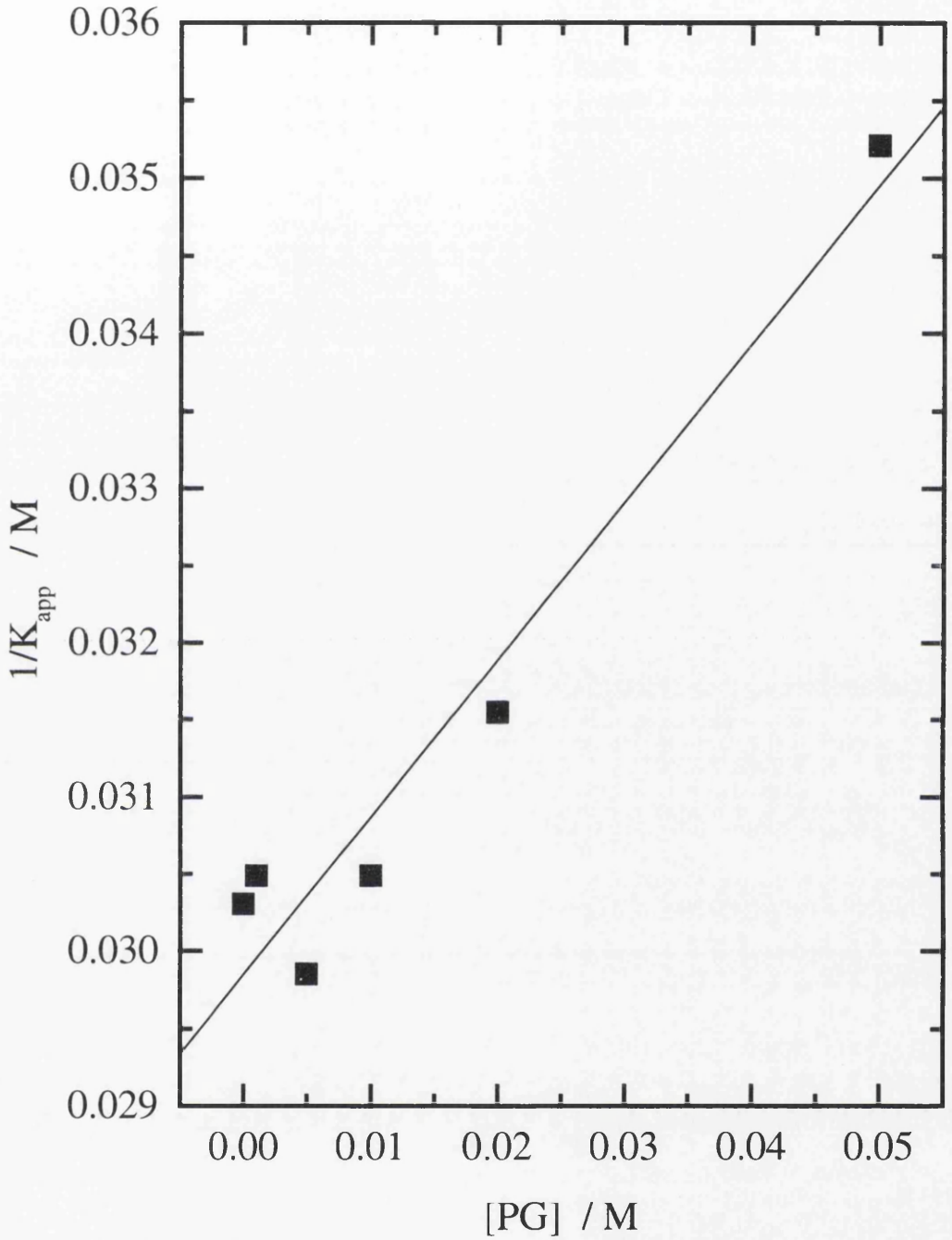


Figure 4.18: Alternative reciprocal plot of $K_{app}$ data from Fig. 4.17. The line shows the least-squares fit for $K_0$(NAG) = 29.8 mM, and $K_{PG}$ = 300mM.

penicillin has a small but consistent effect on the apparent binding constant for NAG under these conditions. Increasing concentrations of penicillin (up to 50mM) in solution produce a small linear decrease in $K_{NAG}$ consistent with weak competitive inhibition. There is a similar, though less pronounced, decrease in magnitude of the apparent enthalpy of NAG binding, see Figure 4.17. (Higher concentrations of penicillin could not be used because of the precipitation of protein that this produced under these conditions.)

If penicillin is acting as a simple competitive binding inhibitor in the active site cleft of lysozyme, then we should expect that the apparent binding constant for NAG should depend on the penicillin concentration in the following way (obtained from simple binding equilibrium expressions):

$$K_{NAG} = K_0/(1 + K_{PG}[PG])$$

where $K_0$ is the binding affinity for NAG in the absence of penicillin inhibition, and $K_{PG}$ is the apparent binding constant for penicillin in the same site.

For very weak binding ($K_{PG}[PG] << 1$) this can be approximated as:

$$K_{NAG} \approx K_0(1 - K_{PG}[PG] + ...)$$

so that a plot of $K_{NAG}$ versus [PG] should be linear with intercept equal to $K_0$ and the ratio of slope/intercept equal to $K_{PG}$. This is shown in Figure 4.17 where the linear least-squares fit gives a value of $K_0 = 33.4\ M^{-1}$ (consistent with direct measurement reported in Table 4.7) and $K_{PG} = 2.9\ M^{-1}$ ($\approx$ 350 mM dissociation constant).

Alternatively, the above equation can be written in its reciprocal form:

$$1/K_{NAG} = 1/K_0 + [PG].(K_{PG}/K_0)$$

This plot is shown in Figure 4.18, and gives estimates of $K_0 = 33.5\ M^{-1}$ and $K_{PG} = 3.4\ M^{-1}$ (300 mM), essentially identical to the above.

This very low value for $K_{PG}$ is consistent with both the DSC experiments that showed no stabilising effect of penicillin on native lysozyme, and with the failure to observe direct binding using ITC. It is difficult to be sure that this very weak binding is anything other than a non-specific binding or inhibition effect. It is clear, at least from these experiments, that penicillin-G does not bind competitively in the lysozyme active, at least not very strongly, under these conditions.

It is however possible that penicillin might be binding at some other site on the enzyme that does not compete with NAG binding, and such effects would not be picked up in these competitive NAG binding ITC experiments. It is also interesting that these results seem to be in direct contradiction both to some of the earlier published observations (Subramanian et al., 1983; Mitsumori et al., 1980) and to the fluorescence binding studies reported here. This maybe indicates that penicillin binding is occurring at some other site or sites. Also in this context, Mitsumori et al. (1977) suggested that small degradation products of penicillin bound to lysozyme, and Corran and Waley (1975) suggested an irreversible complexation of penicillin to the ε-amino group of lysine-116 of the enzyme.

# CHAPTER 5

## 5:1 INTERACTION of Lysozyme and Metal Ions

### 5:1:1 INTRODUCTION

Metal ion binding to proteins such as lysozyme has been investigated to obtain information about the behaviour of these proteins in biological media and the effect of metal ions on their structure (Ramadan & Porath, 1985; Kuroki et al., 1989). Various metal ions including $Mn^{2+}$, (Gallo et al., 1971; Ikeda & Hamaguchi, 1973), $Co^{2+}$ (Mcdonald & Phillips, 1969), $Ni^{2+}$ (Ikeda & Hamaguchi, 1973), $Cu^{2+}$ (Teichberg, et al., 1974) and $Gd^{2+}$ (Secemski & Lienhard, 1974) and similarly other metal ions bind to lysozyme, and the binding modes have been studied in some detail. These interactions were studied using techniques such as immobilized metal ion affinity chromatography (Ramadan & Porath, 1985; Belew et al., 1987), circular dichroism (Desmet et al., 1989), nuclear magnetic resonance (Tsuge et al., 1991; Aramini et al., 1992). However the interaction of lysozyme with metal chlorides using differential scanning calorimeter was not considered in most of the cases.

The first systematic investigations of the binding of metal ion by lysozyme is probably that by Fiers and Klotz (1952), who found the affinity of five proteins for $Cu^{2+}$ in acetate buffer at pH 6.5 including hen egg white lysozyme. Some years later, McDonald and Phillips (1969) studied a shift in the NMR spectrum of HEWL induced by $Co^{2+}$ and concluded that this cation participates in coordinative binding to a single site. Gallo et al. (1971), using electron paramagnetic resonance (EPR), studied the binding of $Mn^{2+}$, as well as, $Co^{2+}$, to lysozyme. The binding of each involved Asp-52 and Glu-35. Both metal ions are inhibitors of lysozyme activity, but $Mn^{2+}$ binds more strongly than $Co^{2+}$. Jori et al. (1971) coordinated $Zn^{2+}$ as well as $Co^{2+}$ to lysozyme and again found Glu-35 and Asp-52 to be involved.

Ikeda and Hamaguchi (1973) investigated the interaction of lysozyme and divalent cations $Mn^{2+}$, $Co^{2+}$, and $Ni^{2+}$ and also studied the lysozyme bound with a substrate, glycol chitin, or inhibitors, N-acetylglucosamine (NAG), di-NAG, and tri-NAG. The binding constant of

$Mn^{2+}$ to lysozyme was increased by a factor of about two when di-NAG or tri-NAG had been bound with lysozyme. The binding constant of $Mn^{2+}$ to NAG bound lysozyme was, however, only slightly larger than that for free lysozyme. The binding constants of di- and tri-NAG to $Mn^{2+}$-bound lysozyme were also about two times as large as the constant in the absence of $Mn^{2+}$, while the binding constant of NAG in the presence of $Mn^{2+}$ was almost the same as that in its absence. In the case of $Co^{2+}$, the binding of the saccharides was suggested to be independent of the binding of the metal ion. The enzymic activity of lysozyme toward glycol chitin in the presence of these metal ions was also explained.

Divalent copper ion was found to inhibit non-competitively the lysis of Micrococcus lysodeikticus cells by hen egg white lysozyme, with an inhibition constant ($K_a$=3.8 x $10^2$ $M^{-1}$), studied by Teichberg et al. (1974). The association constant of $Cu^{2+}$ for lysozyme and for a derivative of lysozyme in which tryptophan residue 108 was selectively modified, were measured spectrofluorimetrically and found to be 1.8x$10^2$ $M^{-1}$ and 1.0x$10^3$ $M^{-1}$, respectively. The electron spin resonance spectrum of $Cu^{2+}$ was not affected by the addition of lysozyme. They demonstrated that $Cu^{2+}$ was bound in the neighbourhood of tryptophan 108. The crystals of lysozyme soaked in $Cu^{2+}$ were examined by X-ray crystallography and observed that $Cu^{2+}$ was found to be near to the carboxyl side chain of aspartic acid 52, one of the carboxyl groups believed to be involved in the catalytic action of the enzyme. They also investigated that the addition of a saccharide inhibitor to lysozyme was found to increase the association constant of $Cu^{2+}$ for lysozyme from a value of 1.8x$10^2$ $M^{-1}$ to 6.0x$10^2$ $M^{-1}$. This finding was interpreted as indicative of a change in conformation around tryptophan 108 and glutamic acid 35 induced by the interaction of saccharides with the enzyme, which affects the metal binding properties of aspartic acid 52.

Imoto et al. (1981) determined the $Ca^{2+}$ stability (association) constant ($40M^{-1}$) and found that lysozyme is inhibited in the presence of $Ca^{2+}$, showing only 20% of the activity of the free enzyme toward hexa-N-acetyl glucosamine. They predicted that $Ca^{2+}$ shifts the native-denatured transition in lysozyme toward the native state, and this has some preservative effect on the protein. The stabilization mechanism of the mutant human lysozyme with a calcium binding site (D86/92 means human lysozyme in which Glu-86 and Ala-92 were replaced with aspartic acid) was investigated by using calorimetric approaches. By differential scanning calorimetry, the enthalpy change in the unfolding of holo-D86/92 was

found to be 6.8 kcal/mol smaller than that of the wild-type and apo-D86/92 lysozymes at 85 °C. However, the unfolding Gibbs energy change of the holo mutant was 3.3 kcal/mol greater than the apo type at 85 °C, indicating a significant decrease of entropy in the presence of $Ca^{2+}$. Subsequently, the $Ca^{2+}$ binding process in the folded state of the mutant was analyzed by using titration isothermal calorimetry. The binding enthalpy change was calculated to be 4.5 kcal/mol, and free energy change was -8.1 kcal/mol at 85°C, which indicates that the binding was caused by a large increase in entropy ($T.\Delta S$=12.6 kcal/mol). From these analyses, the unfolded holo mutant was determined to bind $Ca^{2+}$ with a binding $\Delta G°$ of -4.8 kcal/mol ($\Delta H$ = -2.6 kcal/mol, $T.\Delta S°$ = 2.6 kcal/mol) at 85 °C. Therefore, the major cause of stabilization of holo-D86/92 is the decrease in entropy of the peptide chain due to $Ca^{2+}$ binding to the unfolded protein (Kuroki et al., 1992).

Differential scanning calorimeter was used to study the unfolded behaviour of equine lysozyme by Van Dael et al.(1993). They demonstrated that equine lysozyme undergoes a two-stage unfolding transition upon heating or in the presence of guanidine hydrochloride that is highly dependent on the state of calcium binding. Differential scanning calorimetry shows the two transitions to be particularly well resolved in the calcium free protein, where the first transition occurs with a mid point at 44 °C at pH 4.5 and the second occurs at 70 °C. In the presence of calcium, the first transition takes place with a mid point of 55 °C but the parameters for the second transition remain unchanged. They demonstrated that apo equine lysozyme does not unfold in the highly cooperative manner found for human (Barel et al., 1972) and HEWL (Khechinashvili et al., 1973) and apo equine lysozyme is much less stable than human and HEWL which have transition temperatures of 78 and 76 °C, respectively. They found a single peak of protein unfolding when the concentration of calcium was 2mM and 10mM, suggesting a lesser degree of cooperativity but in the presence of 0.1mM calcium, the first transition is shifted to higher temperature and the second transition coincides with the one observed in the absence of $Ca^{2+}$, indicating that the binding site is only partially occupied.

The temperature dependence of the partial heat capacity of equine lysozyme in 10mM acetate buffer (pH 4.5) in the presence of various concentrations of $CaCl_2$ was investigated by Griko et al. (1995). They found that as the concentration of $CaCl_2$ increases, the first absorption peak was shifted to a higher temperatures without affecting the second peak.

They concluded that first peak of heat absorption was associated with the disruption of the calcium binding domain and correspondingly, results in the loss of the ability of lysozyme to specifically bind $Ca^{2+}$. The second heat absorption peak should be associated with the cooperative disruption of the rest of the molecule, i.e. with the α-domain which is rich in α-helical conformation. The stability of this domain was not affected by the stability of the $Ca^{2+}$ binding β-domain. This conclusion is in agreement with the experimental observation that the far UV CD spectra of EL changes significantly in the temperature region of the second transition (Van Dael et al., 1993). A similar conclusion was recently reached by Dobson and co-workers in the study of the refolding kinetics of HEWL by pulse NMR techniques (Dobson et al., 1994; Hooke et al., 1994). According to these authors the α-domain in HEWL folds first and appears to be more stable than the β-domain. The binding of $Ca^{2+}$ by the mutant human lysozyme is an entropically driven process and the same is true for lactalbumin (Griko et al., 1994a) and equine lysozyme.

More recently, a new technique, electrospray ionization mass spectrometry (ESI-MS), was used to evaluate the interactions of metal ions with HEWL (Moreau et al., 1995). They demonstrated that the protonation states are the same with a HEWL-metal ion mixture as with HEWL taken alone. They also investigated that HEWL binds from 1 to 8 ions of $Cu^{2+}$, where the ratios of $Cu^{2+}$ varied from 1 to 86 ions of $Cu^{2+}$ per molecule of HEWL within the mixture. HEWL was also able to bind from 1 to 6 ions of $Zn^{2+}$ where the ratio of this metal ion varied in the same manner as copper. No effect on the enzyme activity was provoked by $Cu^{2+}$ or $Zn^{2+}$.

The native structure of EL is very similar to that of HEWL and LA. However, the unfolding behaviour of these three proteins is quite different. EL unfolds in two distinct cooperative stages with two distinct heat absorption peaks. LA also unfolds in two stages, however in this case only the first transition is highly cooperative; the second transition is probably cooperative and occurs with only diffuse heat absorption (Griko et al., 1994a). In the case of HEWL the unfolding transition always occurs in a single cooperative peak. In this case experimental conditions have never been bound in which the two domains behave independently in equilibrium unfolding. The difference in unfolding behaviour between HEWL, EL and LA are not due to the existence of a calcium binding site in the latter two

proteins. The calcium binding site in the b-domain of EL is formed by three closely located Asp residues and two main chain carbonyl groups(Tsuge et al., 1992). HEWL and human lysozyme do not have the calcium binding site and unfold as a single cooperative unit; also the enthalpy of their unfolding is somewhat higher than that of EL and LA (Privalov & Khechinashvili, 1974; Kuroki et al., 1992b). According to the observations obtained, it shows that significant differences of three proteins depend upon their packing at the interface between the a and b domains. In HEWL the interface is tightly packed forming a single extended densely packed cluster. In contrast the groups at the interface in EL are loosely packed, defining two well defined densely packed clusters. The overall volume of these two clusters is lower than that of the single cluster in HEWL. These observations explain the differences in total unfolding enthalpy for these two proteins. It is also noteworthy, that in EL the densely packed cluster corresponding to the $\alpha$ domain is smaller in volume than that of the $\beta$ domain(Griko et al., 1995).

T7 lysozyme has a lytic activity similar to that of HEWL or T4 lysozyme, but it cuts a different bond in the peptidoglycan layer and, even though all three proteins have a cleft (Mathews et al., 1981), is structurally very different from them. The critical residues for catalysis by HEWL and T4 lysozyme are glutamic and aspartic residues located on opposite sides of the cleft, but no acidic residues are found inside the cleft of T7 lysozyme. In contrast to the other lysozymes, T7 lysozyme had no apparent activity against the Gram-positive bacterium Micrococcus lysodeikticus, a usual substrate in lysozyme assay. The bifunctional T7 lysozyme has a single domain globular protein, the cleft is clearly the site of amidase activity. Therefore the $Zn^{2+}$ binds to HEWL in the unfolded state because HEWL and T7 lysozyme have different behaviour towards metal site.

Blanco et al. (1996) have studied the functional, conformational and thermodynamic aspects of lysozyme-lithium chloride interactions using viscometric, densitometry, solubility, activity and kinetic techniques. The results showed that LiCl-protein interaction depends on the salt concentration and therefore they concluded that lysozyme can undergo a weak conformational transition implying the preferential interaction between salt and protein, as lysozyme was in a more packed conformation in salt than in water. When salt concentration was less than 70mM then the preferential binding of salt inside the protein was observed. When salt concentration was greater than 70mM, a total salt exclusion from

the lysozyme internal domain was observed. They demonstrated that thermodynamic stability is greater at higher salt concentration in the medium. They have not observed any direct interaction of salt with the active site of the enzyme, and LiCl did not show any competitive inhibitory effect at any salt concentration studied.

The interaction of lysozyme with Zn, Cd, and Hg acetates using UV/vis, chromatography, and DSC techniques was studied by Olmo et al. (1996). The UV/vis spectra was not changed by the addition of Zn or Cd, but there was a great change in the presence of mercury salt. They suggested that this change might be due to the interaction of mercury with the disulphide bridges of the protein. The chromatographic studies indicated the aggregation state of the enzyme changes at 10 and 15mM Cd acetate and 5, 10, and 15mM Zn acetate, and dimeric structure of lysozyme was postulated. The DSC result showed that the $T_m$ of lysozyme was decreased in the presence of these salts which suggested that the interaction of these salts with the protein gives a thermal destabilisation effect on the protein.

## 5:2 Effect of Metal Ions on Lysozyme Stability

Our main aim of doing these unfolding experiments was only to compare the $T_m$ values of the interaction of lysozyme and metals. Because in most of the binding experiments (lysozyme and metals) the pH value changes as the concentration of salt (metal chloride) increases, it was necessary first to explore the effect of pH changes. The behaviour of metals and lysozyme is shown in next section.

### 5:2:1 Effect of pH on lysozyme unfolding

The effect of pH on the stability of protein (lysozyme) folding is similar to ligand binding behaviour. So the ligands in such special case of ligand binding are the hydrogen ions ($H^+$) that bind to specific protein sites (acidic or basic groups) in both folded or

unfolded states. The stability of protein is affected only if the binding affinity of proton is different in both states. Therefore differential scanning calorimeter is used to study the lysozyme unfolding in various buffers over a wide range of pH. The buffers used were KCl/HCl (pH 1.52-2.03), glycine/HCl (pH 2.56-3), sodium citrate/citric acid (pH 3.51), sodium acetate/acetic acid (pH 4.03-5.46), MES (pH 6.09 - 6.77) and MOPS (pH 7 - 7.46). The data obtained and graph are shown in Table 5.1 and summarized in Figures 5.1 and 5.2. The lysozyme concentration was in the range 0.3-0.4 mM for these experiments.

TABLE 5.1
Differential Scanning Calorimetry study of Lysozyme in various buffers

| Buffer 0.1M | pH | $T_m$ (°C ) | $\Delta H_{cal}$ kcal $mol^{-1}$ | $\Delta H_{VH}$ kcal $mol^{-1}$ |
|---|---|---|---|---|
| KCL/HCl | 1.54 | 48.5 | 64.1 | 75.9 |
| KCl/HCl | 2.19 | 54.4 | 84.1 | 85.4 |
| Glycine/HCl | 2.61 | 62.2 | 92.7 | 100.4 |
| Glycine/HCl | 3.09 | 70.1 | 104.0 | 108.6 |
| Citrate | 3.56 | 70.8 | 109.5 | 108.5 |
| Acetate | 4.04 | 76.3 | 111.8 | 120.0 |
| Acetate | 4.46 | 76.8 | 114.0 | 116.9 |
| Acetate | 5.01 | 76.3 | 117.5 | 115.5 |
| Acetate | 5.5 | 75.4 | 106.1 | 119.4 |
| MES | 6.09 | 75.3 | 101.2 | 115.2 |
| MES | 6.77 | 72.9 | 110.9 | 104.0 |
| MOPS | 6.94 | 73.4 | 102.1 | 118.8 |
| MOPS | 7.46 | 72.7 | 104.3 | 115.0 |

The results (Table 5.1) show that that the major changes in $T_m$ are at low pH region. This is due to the protonation of the carboxylate side chains. The value of $T_m$ is maximum at pH 4 to pH 5, after this a slight decrease in $T_m$ with increasing pH occurs. This may reflect ionization of histidine residues. However, at pH values close to neutral the protein aggregates immediately after unfolding, releasing heat in an irreversible fashion. This may also have the effect of reducing the apparent $T_m$ of the protein.

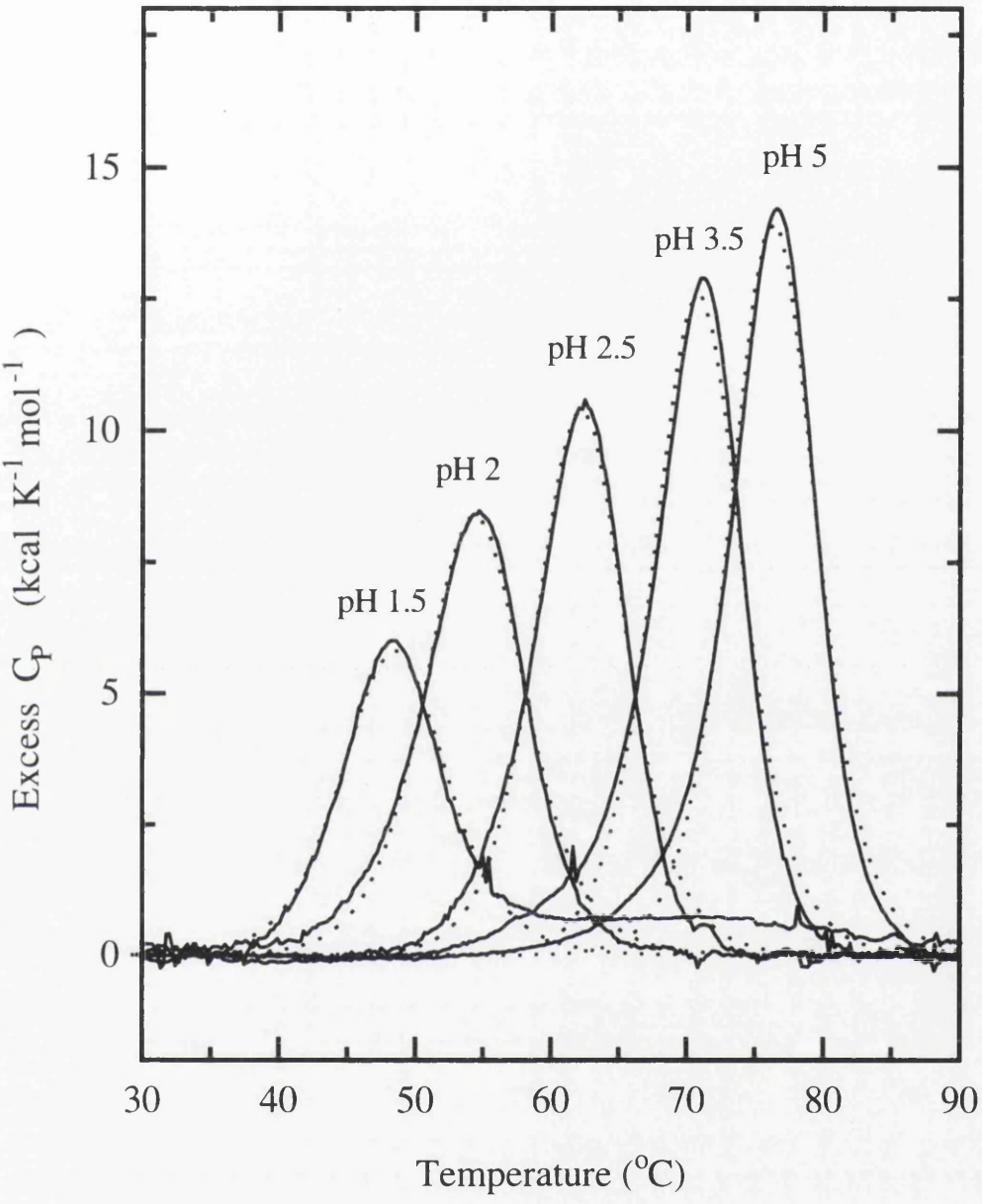


Figure 5.1: Normalized DSC data for thermal unfolding of lysozyme as a function of pH.

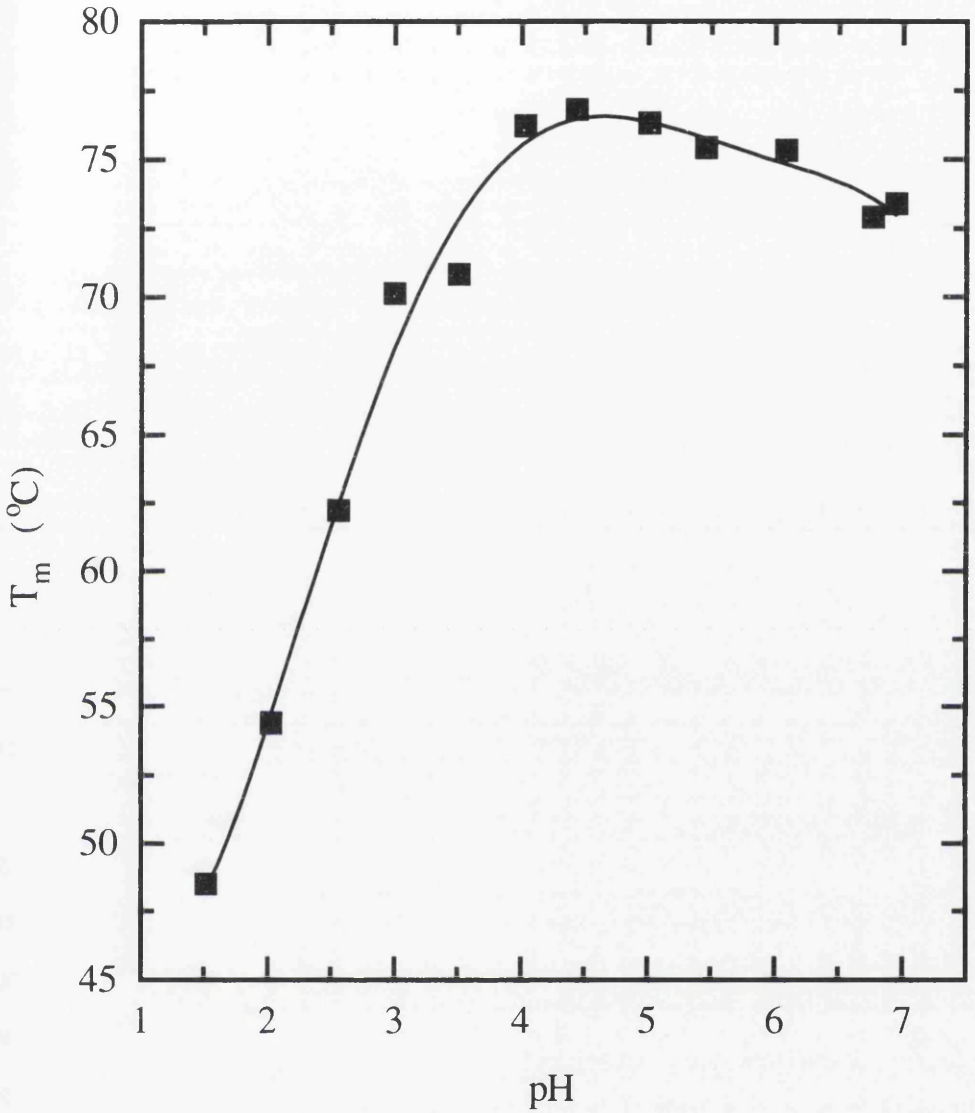


Figure 5.2: Variation with pH in the $T_m$ of lysozyme determined by DSC.

## 5:3 Effect of Metal Ions

We have studied in detail the unfolding behaviour of lysozyme in the presence of Group I, Group II, Group III and Group IV metal ions using differential scanning calorimeter. DSC experiments were performed as described earlier over a range of pH values with inclusion of different concentrations of various metal ion salts (usually the chlorides) in the appropriate buffer, and this buffer was also used for reference and baseline controls. Addition of metal chloride to lysozyme solution sometimes led to a decrease of the pH, in particular at higher concentrations. Consequently the pH of each sample was checked immediately prior to DSC, and actual pH's are quoted in the results below.

Table 5.2 summarises the effects of some Group I-IV metal ions on the $T_m$ of lysozyme in acetate buffer, originally at pH 4.05. The general trend is that all metal chlorides decrease the $T_m$ with increasing concentration, but some metals are much more effective than others, and in some cases the effects may simply be due to changes in ionic strength. For example, both the simple monovalent (K+, Rb+, Cs+; Fig. 5.3) and most divalent ($Mg^{2+}$, $Ba^{2+}$, $Pb^{2+}$; Fig.5.4) metal ions produce similar changes in $T_m$ that probably reflect increasing ionic strength (i.e. both metal ion plus chloride concentration) rather than any specific metal-protein interaction. The one exception seen is for tin ($Sn^{2+}$) which gives a massive decrease of around -21 °C in the $T_m$. However, this is accompanied by precipitation in the mixture and probably indicates strong irreversible interaction between $Sn^{2+}$ ions and the unfolded polypeptide (Fig. 5.5). Tin has two oxidation states, II and IV, and both are reasonably stable. $Tin^{2+}$ in acid is well known as a mild reducing agent, whereas $Pb^{2+}$ is a stable state and Pb(IV) is unstable, and therefore Pb(IV) is a strongly oxidising agent as compared to $Sn^{2+}$.

Table 5.2: Effect of metal ions on the $T_m$ of lysozyme in 0.1M acetate, pH 4.05

| Metal Ion | [ion] /mM | Sample pH | $T_m$ /°C | $\Delta T_m$ /°C | Comments |
|---|---|---|---|---|---|
| | | | | | |
| None | - | 4.0 | 76.5 | - | ±0.3 (mean & sd of 10 expts.) |
| | | | | | |
| K+ | 12.8 | 4.0 | 76.2 | -0.3 | |
| | 44.1 | 4.0 | 75.8 | -0.7 | |
| | 98.2 | 4.0 | 75.4 | -1.1 | |
| | 154.2 | 4.0 | 74.2 | -2.3 | |
| | | | | | |
| Rb+ | 44.2 | 4.0 | 75.3 | -1.2 | |
| | | | | | |
| Cs+ | 73.8 | 4.0 | 74.8 | -1.7 | |
| | 118.1 | 4.0 | 74.7 | -1.8 | |
| | | | | | |
| $Mg^{2+}$ | 13.5 | 4.0 | 75.8 | -0.7 | |
| | 28.5 | 4.0 | 75.3 | -1.2 | |
| | 57.0 | 3.9 | 74.2 | -2.3 | -1.3 anticipated from pH change |
| | 75.3 | 3.8 | 73.5 | -3.0 | -1.7 .. .. |
| | | | | | |
| $Ba^{2+}$ | 100.4 | 3.9 | 72.7 | -3.8 | -1.3 .. .. |
| | | | | | |
| $Sn^{2+}$ | 19.0 | 4.05 | 55.5 | -21.0 | Slight precipitate |
| | | | | | |
| $Pb^{2+}$ | 6.0 | 4.05 | 76.1 | -0.4 | |
| | 9.9 | 3.8 | 75.0 | -1.5 | -1.7 anticipated from pH change |
| | | | | | |
| $Al^{3+}$ | 22.6 | 3.9 | 64.0 | -12.5 | See Tables 5.5 - 5.7 for more data on $Al^{3+}$ |
| | | | | | |
| $In^{3+}$ | 5.2 | 3.7 | 74.8 | -1.7 | -2.2 anticipated from pH change |
| | 8.2 | 4.06 | 76.1 | -0.4 | pH adjusted back to 4.06 |
| | 9.9 | 3.5 | 72.8 | -3.7 | -3.3 anticipated from pH change |
| | 21.5 | 3.4 | 66.5 | -10.0 | -4.7 .. .. |
| | 62.4 | 3.3 | 63.1 | -13.4 | -5.6 .. .. |
| | 92.5 | 3.1 | 61.1 | -15.4 | -7.4 .. .. |
| | | | | | |
| $Tl^{3+}$ | 19.6 | 4.0 | 76.3 | -0.2 | |
| | 21.0 | 4.0 | 76.3 | -0.2 | |

Trivalent metal ions ($Al^{3+}$, $In^{3+}$) give somewhat greater changes in $T_m$ , part of which arises from the decrease in buffer pH in the presence of these salts at high concentration (Figs. 5.6

and 5.7). However, even when the effects of pH are taken into account (Table 5.2), there does seem to be an additional destabilising effect of these ions. The effects of $Al^{3+}$ ions are explored in more detail below. Interestingly, thallium ($Tl^{3+}$) ions do not have such a great effect on $T_m$ (Fig. 5.8), and this probably reflects the differences in stability of the level III oxidation of these metals. That is, for Al and In the level III state is most stable, but the reverse is true for Tl (Mackay and Mackay, 1981). Consequently it is likely that in the course of the experiment the $Tl^{3+}$ ions decompose to $Tl^{+}$, such that their effect on lysozyme $T_m$ is much reduced. The I oxidation state is most important in thallium chemistry where it is the most stable state. Thallium(I) compounds are stable and show some resemblance to both lead(II) compounds and those of alkali metals.

TABLE 5.3: Thermodynamic parameters associated with the thermal unfolding of lysozyme in 0.1M acetate buffer pH 4.05, plus selected salts.

| Salt | [Salt]/ mM | $T_m$ °C | $\Delta H_{cal}$ kcal $mol^{-1}$ | $\Delta H_{VH}$ kcal $mol^{-1}$ |
|---|---|---|---|---|
| None | 0 | 76.5 | 115.3 ± 3.1 | 123.3 ± 2.9 |
| | | | | |
| KCl | 12.8 | 76.0 | 117.8 | 122.7 |
| | 44.1 | 75.3 | 114.6 | 122.1 |
| | 98.2 | 75.1 | 117.7 | 123.1 |
| | 154.2 | 74.7 | 139.9 | 109.6 |
| | | | | |
| $MgCl_2$ | 13.5 | 75.4 | 114.2 | 120.4 |
| | 28.5 | 74.9 | 112.5 | 123.3 |
| | 57.0 | 73.8 | 111.5 | 120.4 |
| | 75.2 | 73.2 | 109.8 | 121.0 |
| | | | | |
| $AlCl_3$ | 11.2 | 70.0 | 116.0 | 122.0 |
| | 22.6 | 64.0 | 114.9 | 124.7 |
| | | | | |
| $InCl_3$ | 5.2 | 74.4 | 102.0 | 117.5 |
| | 62.4 | 62.7 | 94.7 | 118.6 |
| | 92.5 | 60.9 | 90.6 | 117.0 |
| | 8.2* | 76.2 | 105.7 | 129.4 |

* pH adjusted to 4.05

Note: $T_m$ here refers to the fitted curve.

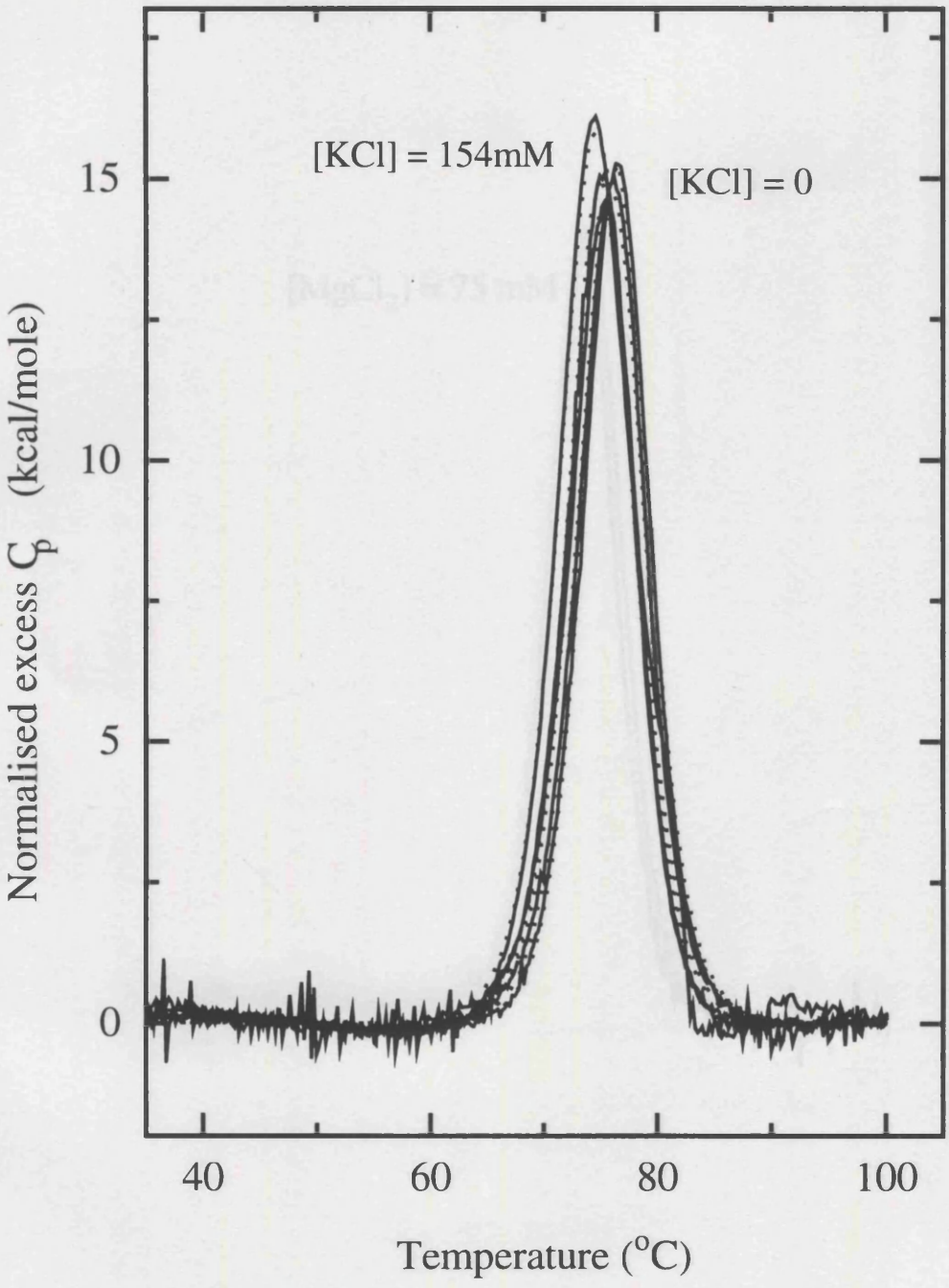


Figure 5.3: DSC traces for lysozyme in 0.1M acetate buffer, pH 4.05, with varying concentrations of KCl (0-154 mM).

Date: 6/7/98
File: FIG5-3.org
Origin v. 2.9

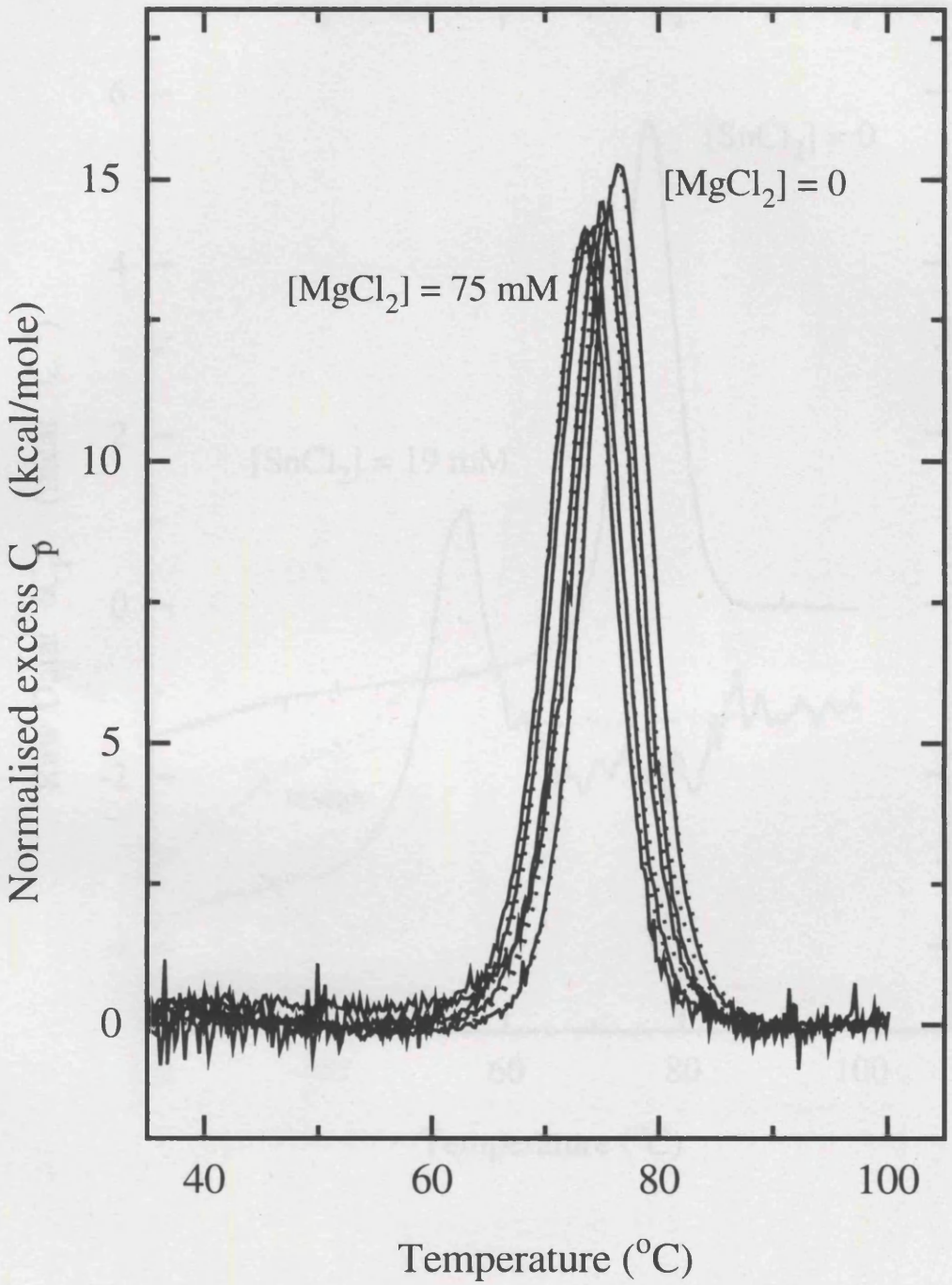


Figure 5.4: DSC traces for lysozyme in 0.1M acetate buffer, pH 4.05, with varying concentrations of $MgCl_2$ (0-75 mM).

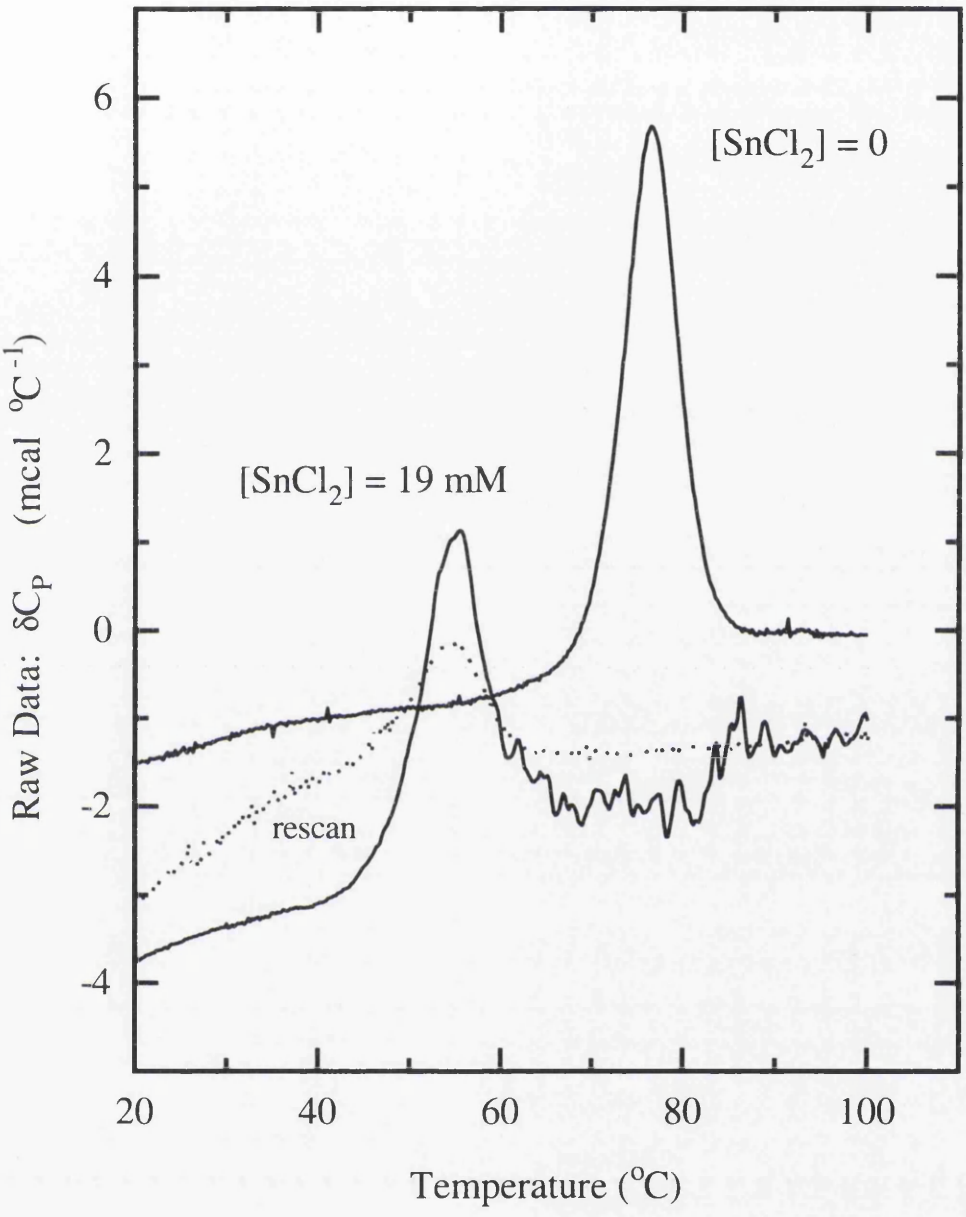


Figure 5.5: DSC scan and rescan (dotted) of lysozyme with and without Tin Chloride (19 mM) in 0.1M acetate buffer pH 4.05 (raw data).

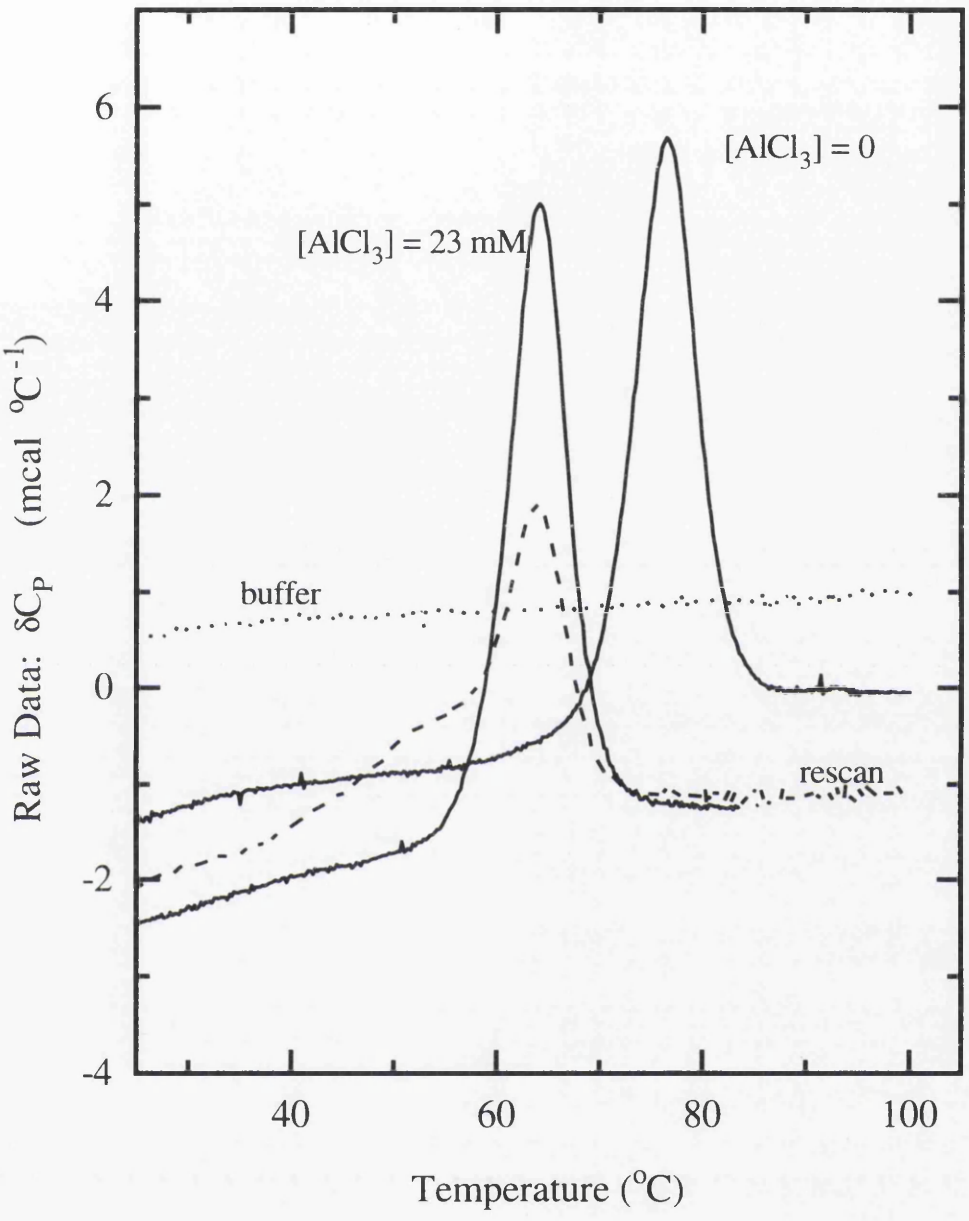


Figure 5.6: Raw DSC data for unfolding of lysozyme in the presence or absence of Al3+ ions, 0.1M acetate, pH 4.05. The rescan is shown dashed.

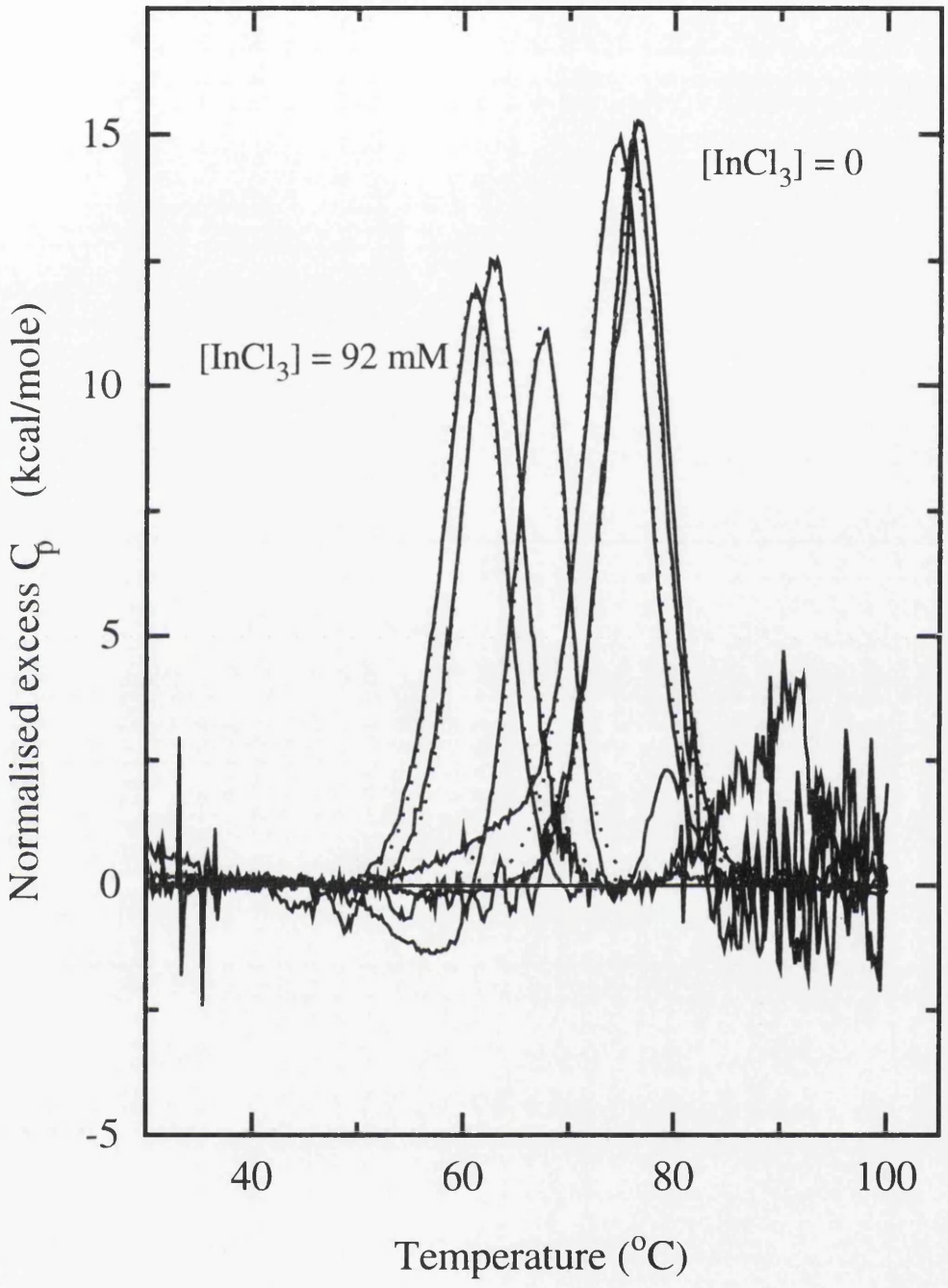


Figure 5.7: Normalized DSC data for unfolding of lysozyme in the presence or absence of $In^{3+}$ ions (5-93mM), 0.1M acetate, pH 4.05.

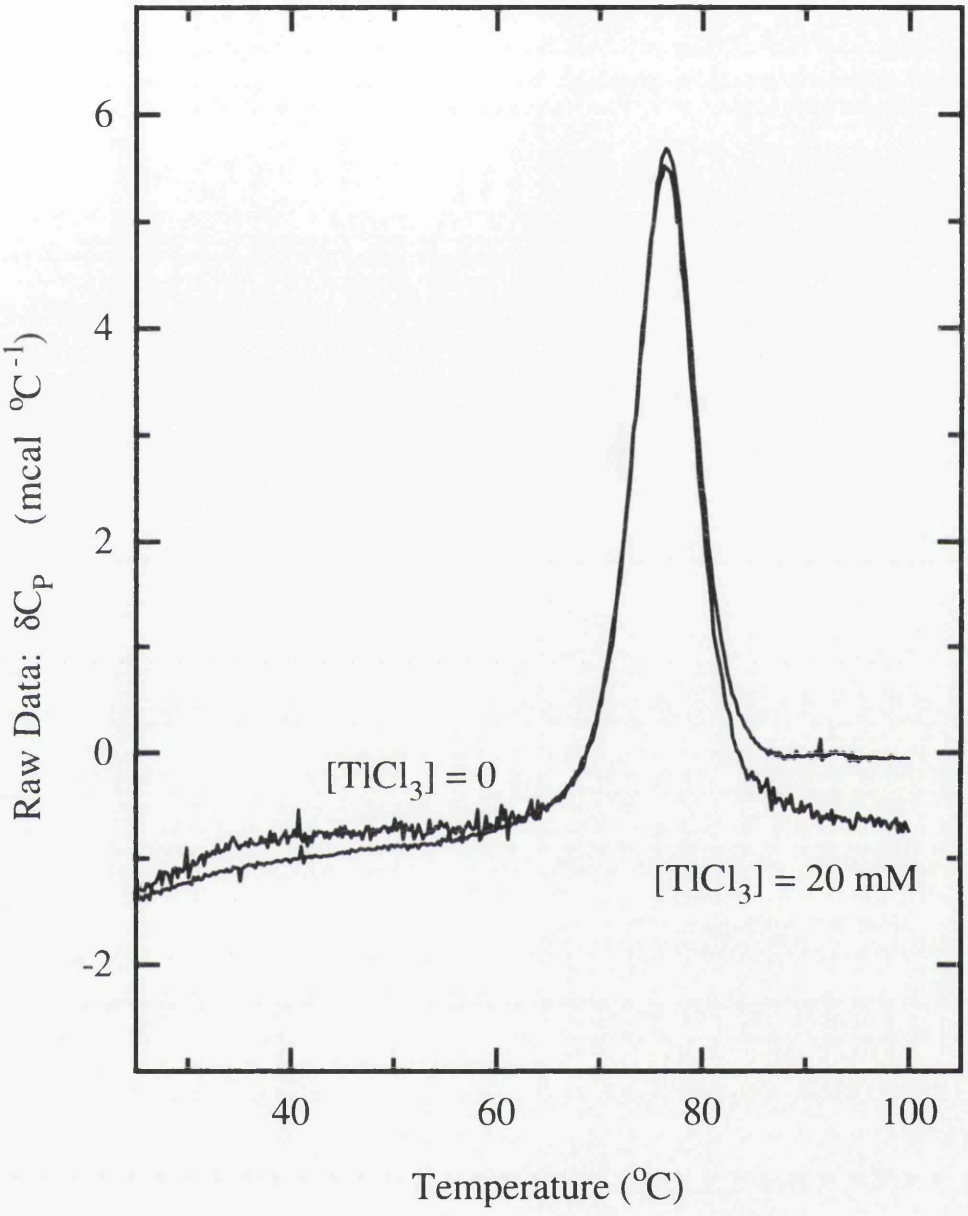


Figure 5.8: DSC scan of lysozyme with and without Thallium(III) Chloride (20 mM) in 0.1M acetate buffer pH 4.05 (raw data).

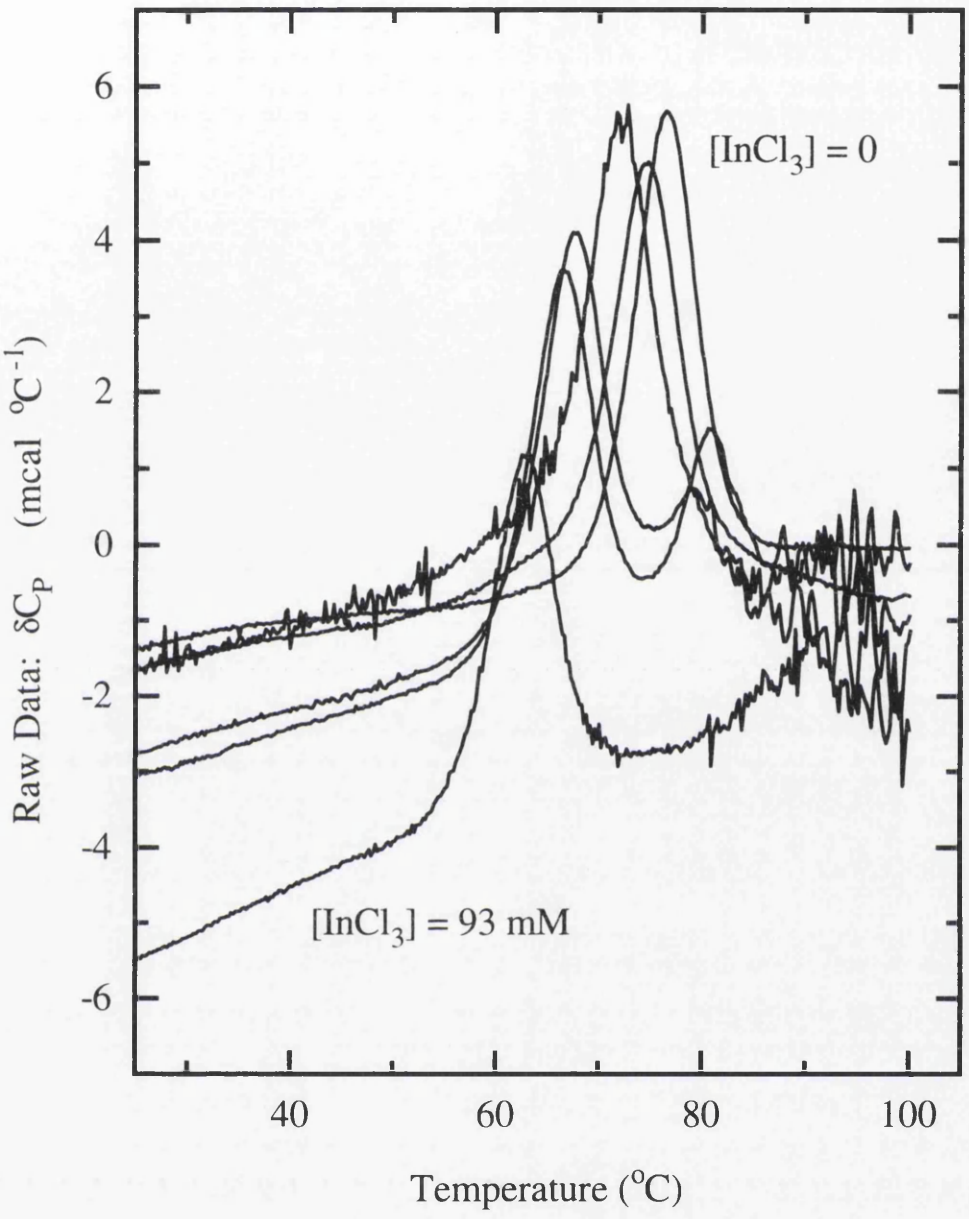


Figure 5.9: DSC scans of lysozyme with and without indium(III) chloride (5-93 mM) in 0.1M acetate buffer pH 4.05 (raw data).

Table 5.3 shows representative data for the effect of selected metal salts on the enthalpies of unfolding of lysozyme in acetate buffer. Generally speaking, the change in $\Delta H_{cal}$ reflects the changes in $T_m$ in that lower $T_m$ values induced by the presence of metal salts is accompanied by a lower $\Delta H_{cal}$ . This illustrates the well known effect of $\Delta C_p$ on the enthalpies of unfolding, i.e. $\Delta H_{cal}$ is temperature dependent and unfolding at lower temperatures takes place with lower enthalpy. This is partly, but not totally reflected in the trends seen for $\Delta H_{VH}$ which, although they show some decrease in most cases, are not as marked as might be expected from $\Delta H_{cal}$ . This is probably due to the effect of aggregation in such cases (e.g. $In^{3+}$, see Fig. 5.9), since this has the effect of artificially sharpening the DSC thermogram and therefore gives an over-estimate of the transition enthalpy in the van't Hoff analysis.

### 5.3.1 Effect of Transition Metal Ions

We have investigated the interaction of HEWL with manganese nitrate hexachloride, manganese chloride, cobalt chloride, zinc chloride, nickel chloride, copper sulphate, copper chloride, cadmium acetate, iron sulphate and iron chloride in 0.1M sodium acetate/acetic acid buffer pH 4.05 unless otherwise stated. These salts were selected on the basis of their solubilities in aqueous buffers. The results are shown in Table 5.4 and illustrated in Figures 5.10 to 5.15. The pH value of the solution was sometimes significantly altered by addition of metal salts, so the actual pH is quoted in Table 5.4 together with the anticipated change in $T_m$ where relevant.

Overall, taking into account both pH and ionic strength changes, it can be seen that the only transition metal ions observed to give significant changes in $T_m$ of lysozyme are $Mn^{2+}$ and $Cu^{2+}$. The effect in all such cases is to reduce the $T_m$ , indicating as before a significant interaction between the metal ions and groups on the unfolded polypeptide. The effect of $Cu^{2+}$ was further explored by addition of KCl to the mixture. As can be seen from Table 5.4, $Cu^{2+}$ ions produced significant decreases in $T_m$ even in the presence of 100mM KCl (Fig. 5.16), suggesting that the interaction of $Cu^{2+}$ with exposed protein or peptide groups is not simply electrostatic. This is consistent with the known complexation properties of

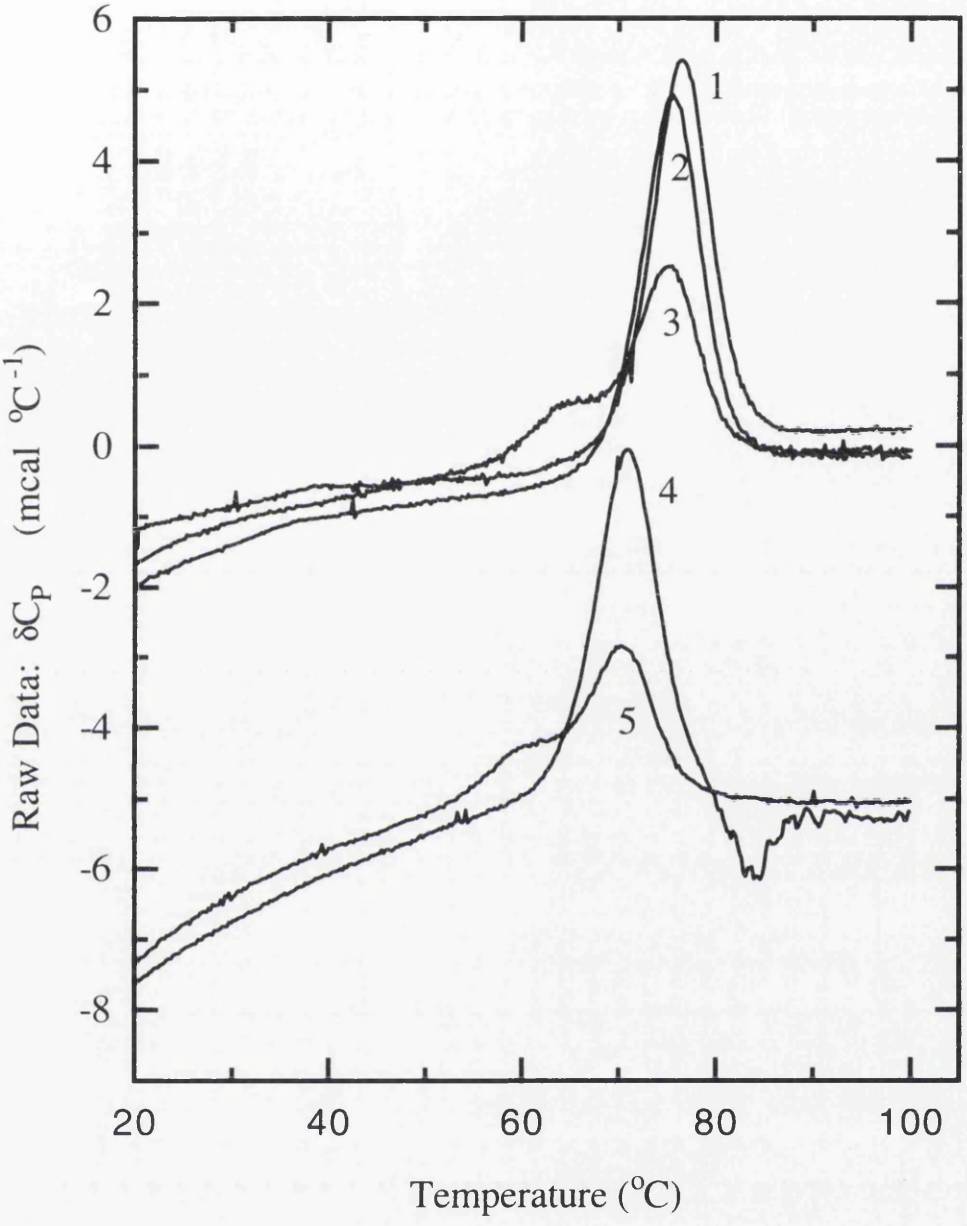


Figure 5.10: Raw DSC scan and rescan data of lysozyme with Manganese Nitrate Hexahydrate in 0.1M acetate pH 4.05: (1) No Mn, (2) + 13.8 mM Mn, (3) rescan of #2, (4) + 75 mM Mn, (5) rescan of #4

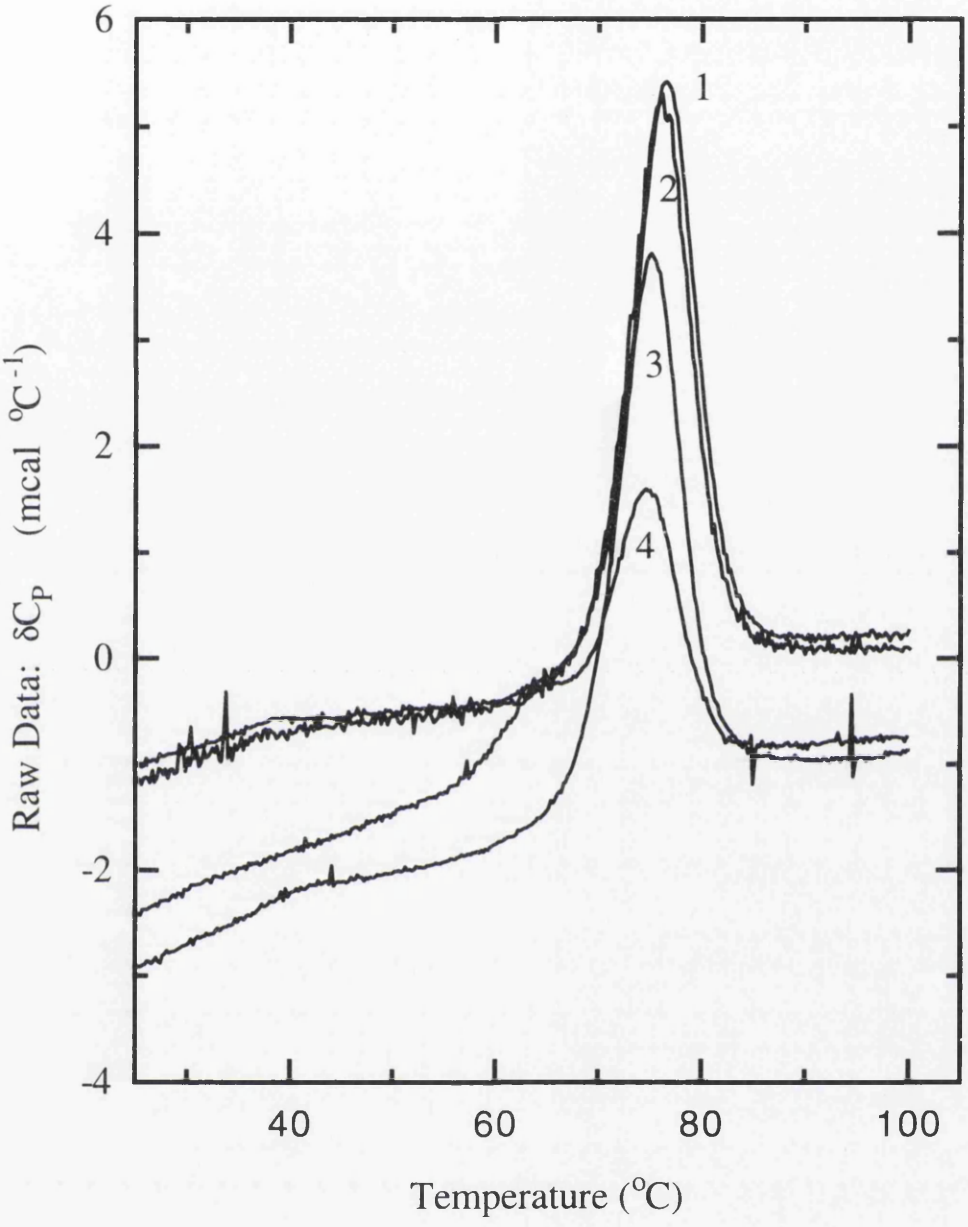


Figure 5.11: Raw DSC scan and rescan data of lysozyme with Cobalt Chloride Hexahydrate in 0.1M acetate pH 4.05: (1) No Co, (2) + 7.5 mM Co, (3) + 21 mM Co, (4) rescan of #3

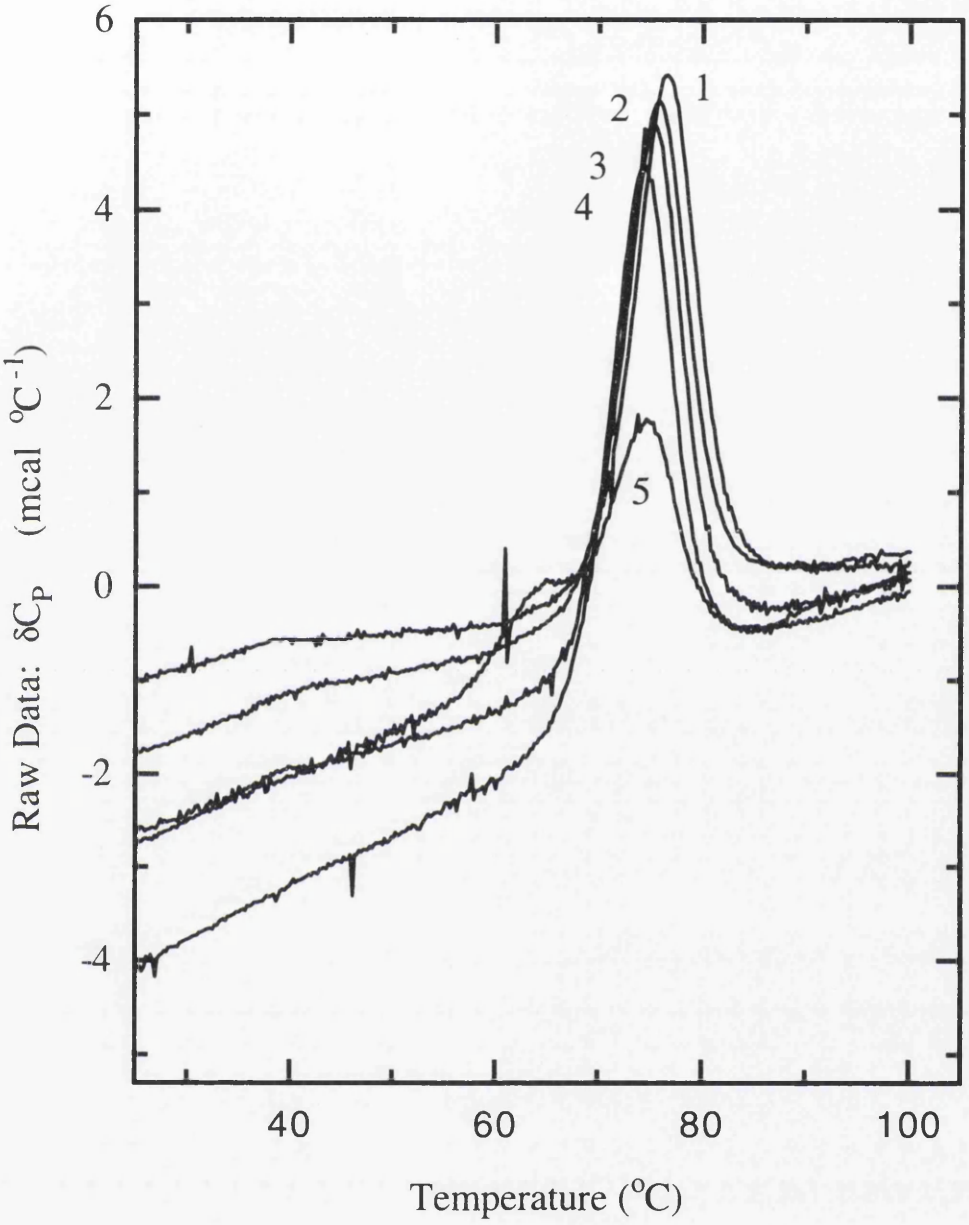


Figure 5.12: Raw DSC scan and rescan data of lysozyme with Zinc Chloride in 0.1M acetate pH 4.05: (1) No Zn, (2) + 10 mM Zn, (3) +18 mM Zn, (4) + 34 mM Zn, (5) rescan of #2

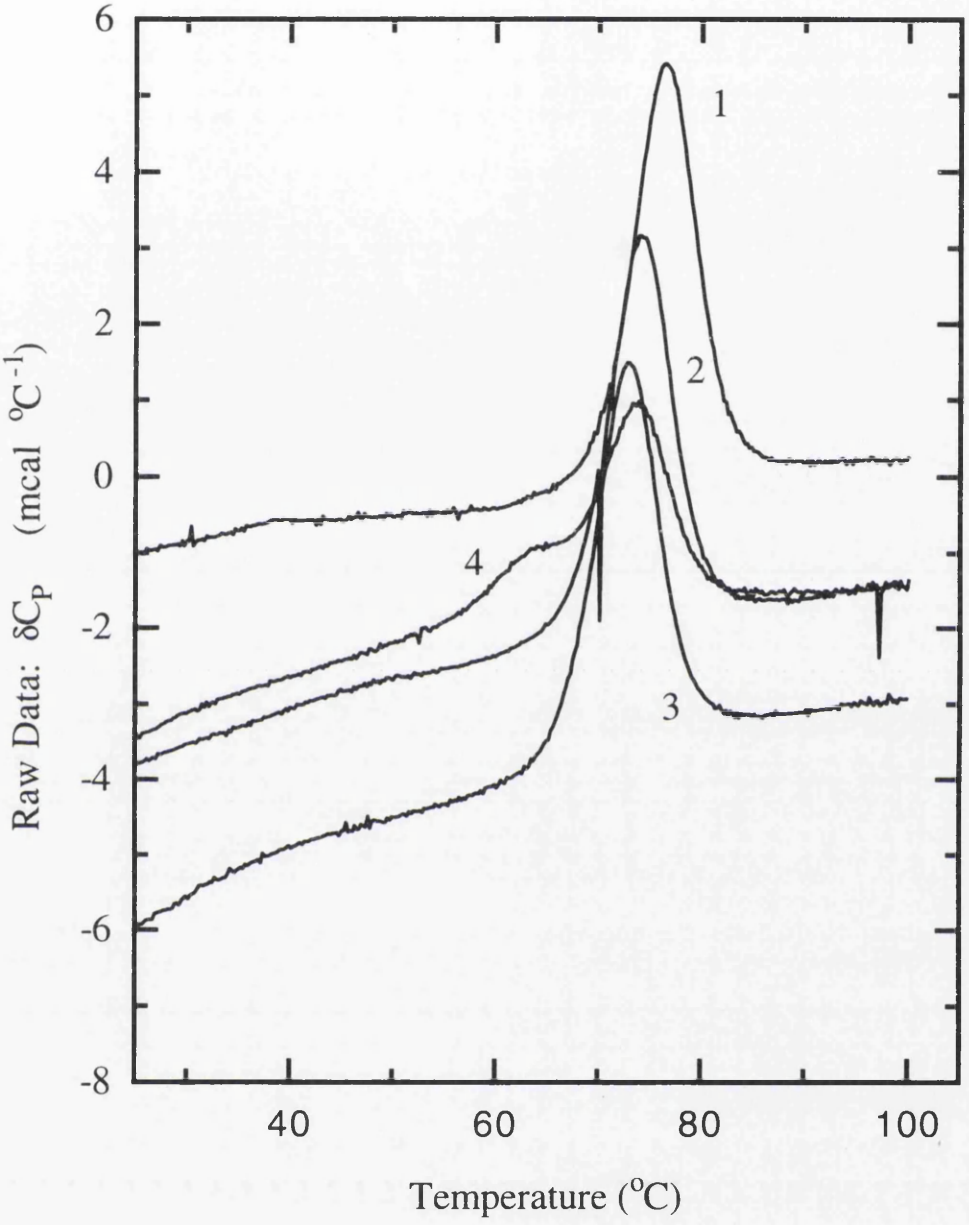


Figure 5.13: Raw DSC scan and rescan data of lysozyme with Nickel(II) Chloride Hexahydrate in 0.1M acetate pH 4.05: (1) No Ni, (2) +36 mM Ni, (3) +59 mM Ni, (4) rescan of #3

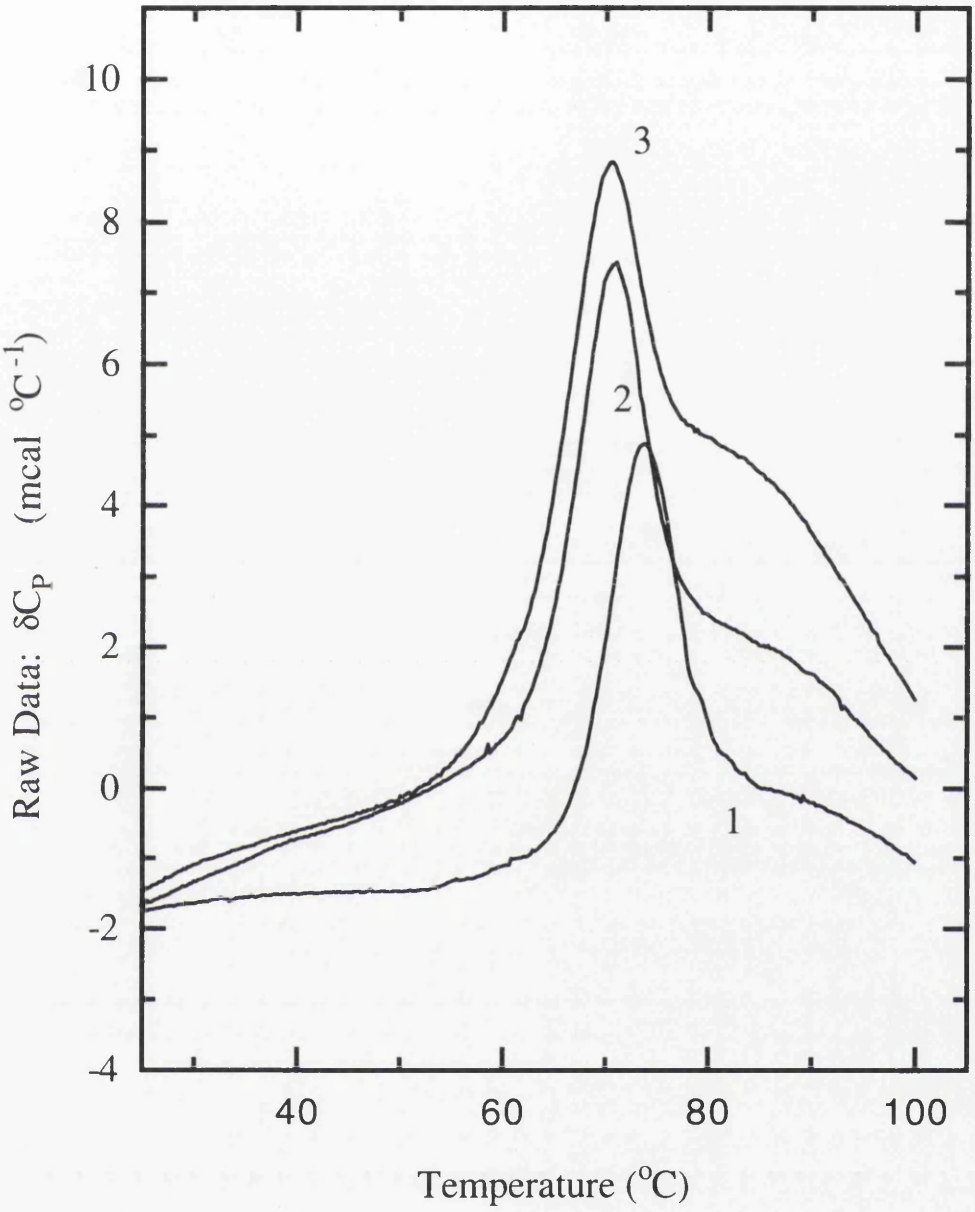


Figure 5.14: Raw DSC scan and rescan data of lysozyme with Copper Sulfate in 0.1M acetate pH 5.4: (1) No Cu, (2) + 13 mM Cu, (3) + 20 mM Cu.

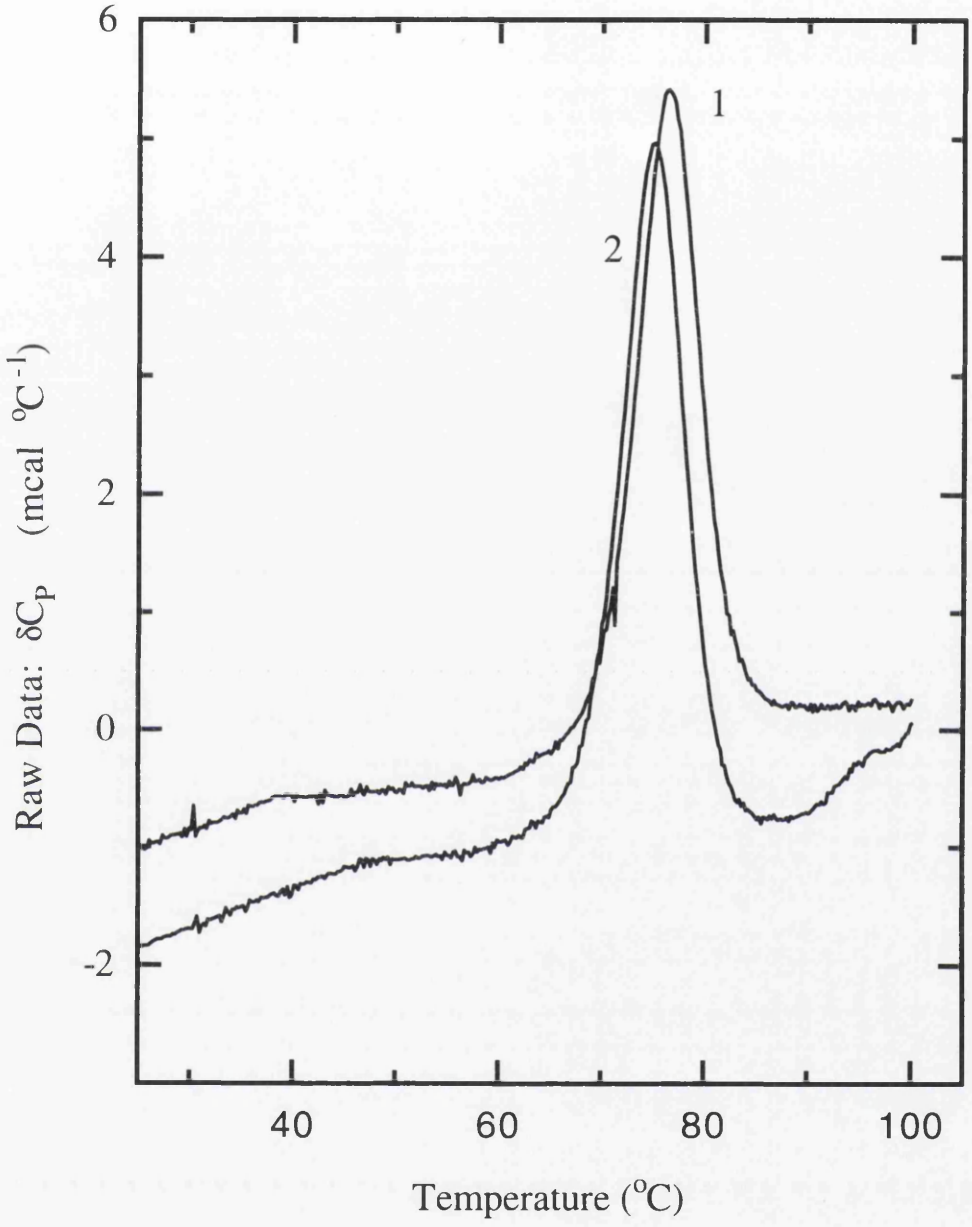


Figure 5.15: Raw DSC scan data of lysozyme with Iron(II) Sulphate in 0.1M acetate pH 4.05: (1) NoFe, (2) + 74 mM Fe.

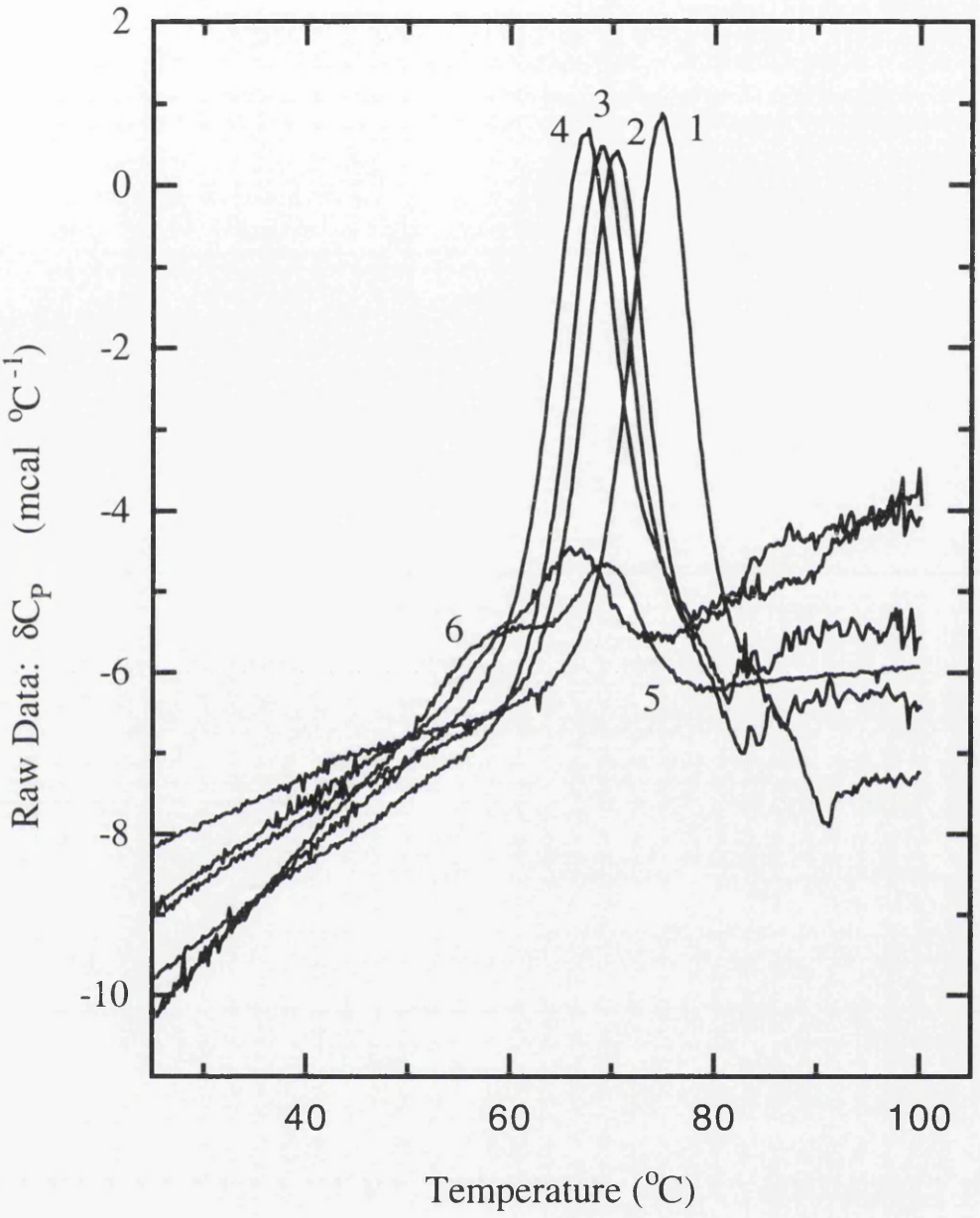


Figure 5.16: Raw DSC scan and rescan data of lysozyme with Copper Sulphate in 0.1M acetate pH 4.05, in presence of ).1M KCl: (1) No Cu, (2) + 25 mM Cu, (3) + 42 mM Cu, (4) + 72 mM Cu, (5) rescan of #2, (6) rescan of #4

$Cu^{2+}$ with peptide groups, known classically as the "biuret reaction" (Creighton, 1993). It is conceivable that $Mn^{2+}$ interacts with peptide groups in a similar manner.

Interestingly a very recent study has shown specific binding of $Cu^{2+}$ ions to prion protein (Stockel et al., 1998). They investigated the CD spectra of prion proteins in the absence and presence of $CuCl_2$ and observed changes in the minima at 208nm and 222nm which showed that binding of $Cu^{2+}$ to prion protein might induce conformational change. A slight decrease in intensity after addition of $Cu^{2+}$ was due to either a minor unfolding of the molecule or an aggregation of the prion protein. The protein shows a prominent band at 295nm and protein-copper complex shows at 295nm and 260nm, suggesting a change in the tertiary structural environment of the aromatic residues in PrP. This was further studied using fluorescence spectroscopy and observed that addition of $CuCl_2$ into prion protein induced a quench of the tryptophan fluorescence of 30% of the initial intensity with the development of a shoulder in the original peak indicating a second maximum at 346.5nm, suggesting that tryptophan indoles move to a more hydrophobic environment. They also compared the quenching of fluorescence with other metal ions like $Co^{2+}$ and $Zn^{2+}$, and found that fluorescence intensity was only quenched in the presence of $CuCl_2$, suggesting that a high selectivity of the binding sites for copper. Because the binding titrations change around pH 6 this suggests that histidine plays a role in this copper-protein complex.

Table 5.4: Effect of transition metal ions on the $T_m$ of lysozyme in 0.1M acetate or MOPS buffer

| Metal Salt | [ion] /mM | Sample pH | $T_m$ /°C | $\Delta T_m$ /°C | Comments |
|---|---|---|---|---|---|
| | | | | | |
| None | - | 4.0 | 76.5 | - | ±0.3 (mean & sd of 10 expts.) |
| | | | | | |
| $Mn(NO_3)_2$ | 13.8 | 3.9 | 75.5 | -1.0 | |
| | 74.6 | 3.7 | 70.9 | -5.6 | -2.2 anticipated from pH |
| | | | | | |
| $MnCl_2$ | 5.7 | 4.9 | 75.9 | -0.6 | -0.1 .. .. .. |
| | | | | | |
| $NiCl_2$ | 35.8 | 4.0 | 73.9 | -2.6 | |
| | 57.1 | 3.9 | 72.8 | -3.7 | |
| | | | | | |
| $CoCl_2$ | 7.5 | 4.1 | 76.2 | -0.3 | |
| | 21.3 | 4.1 | 75.1 | -1.4 | |
| | 4.5 | 7.1 | 76.4 | -0.1 | -3.5 .. .. .. |
| | | | | | |
| $ZnCl_2$ | 10.1 | 4.0 | 75.8 | -0.7 | |
| | 18.0 | 4.0 | 75.2 | -1.3 | |
| | 33.7 | 3.9 | 74.3 | -2.2 | |
| | 53.7 | 4.1 | 73.0 | -3.5 | |
| | | | | | |
| $CuSO_4$/KCl | 25.2/100 | 3.7 | 70.4 | -6.1 | -2.2 .. .. .. |
| | 42.1/100 | 3.6 | 69.0 | -7.5 | -2.8 .. .. .. |
| | 72.3/100 | 3.5 | 67.6 | -8.9 | -3.3 .. .. .. |
| | | | | | |
| $CuSO_4$ | 2.8 | 5.4 | 72.6 | -3.9 | -0.6 .. .. .. |
| | 13.6 | 5.5 | 71.0 | -5.5 | -0.8 .. .. .. |
| | 20.1 | 5.4 | 70.6 | -5.9 | -0.4 .. .. .. |
| | | | | | |
| Cd acetate | 13.3 | 5.4 | 74.3 | -2.2 | -0.4 .. .. .. |
| | 40.3 | 5.7 | 75.1 | -1.4 | -1.1 .. .. .. |
| | | | | | |
| $FeCl_2$ | 18.1 | 4.1 | 75.3 | -1.2 | |
| | | | | | |
| $FeSO_4$ | 74.0 | 4.1 | 75.0 | -1.5 | |
| | | | | | |

### 5.3.2 Further Studies of $Al^{3+}$ and related ions

In view of the relatively large effect of $Al^{3+}$ ions on lysozyme stability, and because of the possibly important role of aluminium in physiology and disease, these effects have been explored in more detail by DSC together with $Mn^{2+}$ and $Cd^{2+}$ for comparison.

Aluminium is a trivalent metal, belonging to the third period. It is a very common metal with a large number of applications. It is usually present in an organism but it does not accumulate, although its elevated level in an organism can be related to a variety of diseases such as those related to encephalopathy (Ganrot, 1986).

The general effect of addition of $Al^{3+}$ on the DSC of lysozyme is illustrated in Figures 5.17 and 5.18 and data summarized in Tables 5.5 and 5.6. Interestingly the effect of $Al^{3+}$ is not just to progressively reduce $T_m$, as seen with other metal ions. At certain concentrations (upto 10-20mM) the DSC thermograms show two discrete transitions, one close to the original and a second at lower or higher temperature. At higher concentrations the unfolding transition appears as a single peak with reduced $T_m$ . The reason for this unusual behaviour is not clear, although it appears to come from a combination of both stabilising and destabilising effects. Thus the higher temperature transition may reflect the binding of $Al^{3+}$ to the native molecule which, at higher concentrations, is counteracted by ion binding to the unfolded form. This is broadly consistent with the non-specific thermodynamic effects observed by Socorro et al. (1995), which showed that the effects of $AlCl_3$ on lysozyme properties in solution were different above and below $Al^{3+}$ concentrations of around 10mM. Socorro et al. (1995) demonstrated that aluminium chloride behaves as a salting-in agent to lysozyme. At low salt concentrations, a conformational transition is observed that brings about greater preferential binding of the aluminium salt and its smaller solubility power, in accordance with the larger preferential hydration and interaction. Despite all this a drastic change in enzyme activity does not occur, because the protein is in a good solvent medium and aluminium cation binding does not take place on the active site residues.

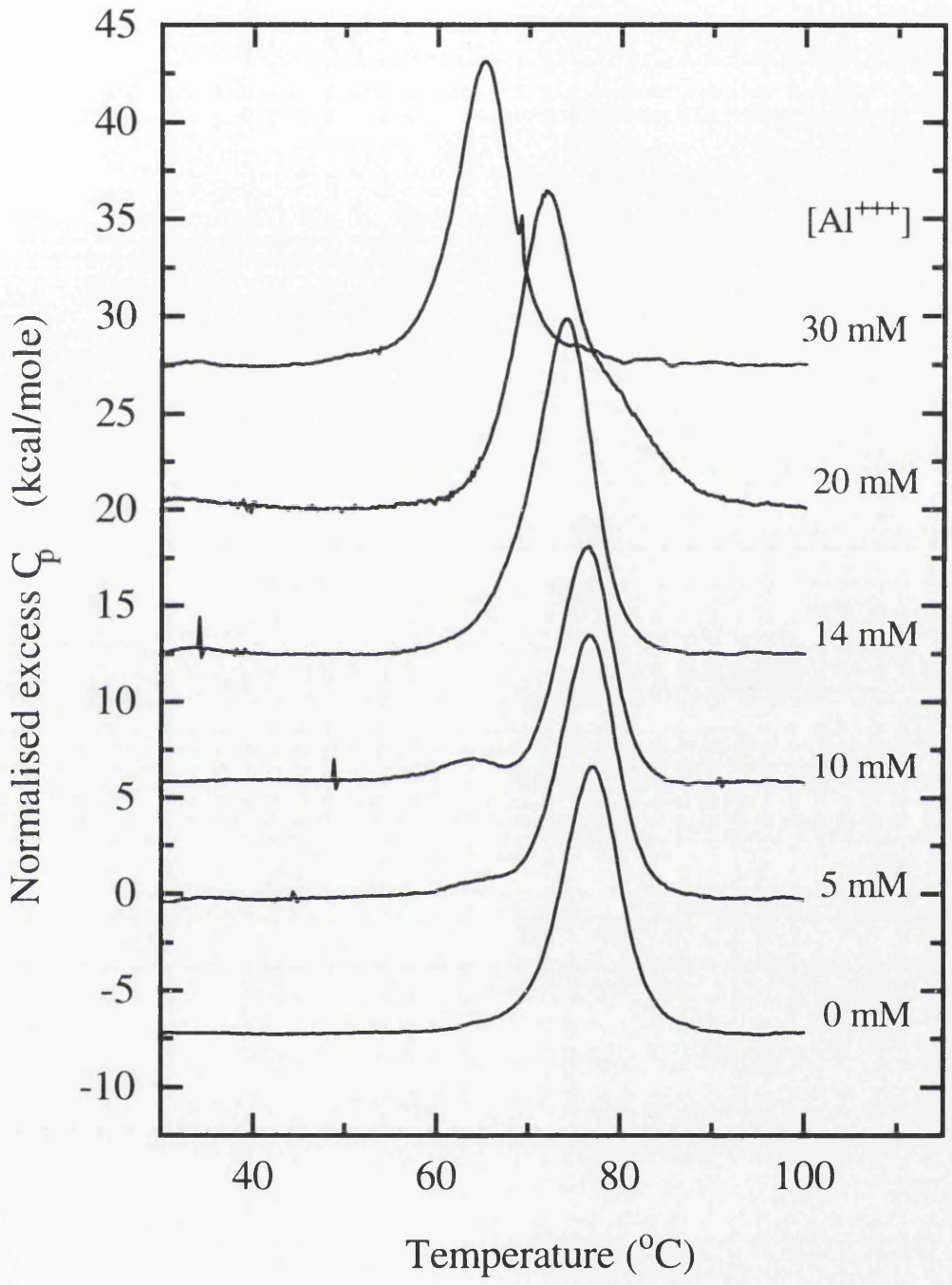


Figure 5.17: Normalized DSC scans for lysozyme in the presence of increasing concentrations of $Al^{3+}$ ions (0.1M acetate, pH 4,5).

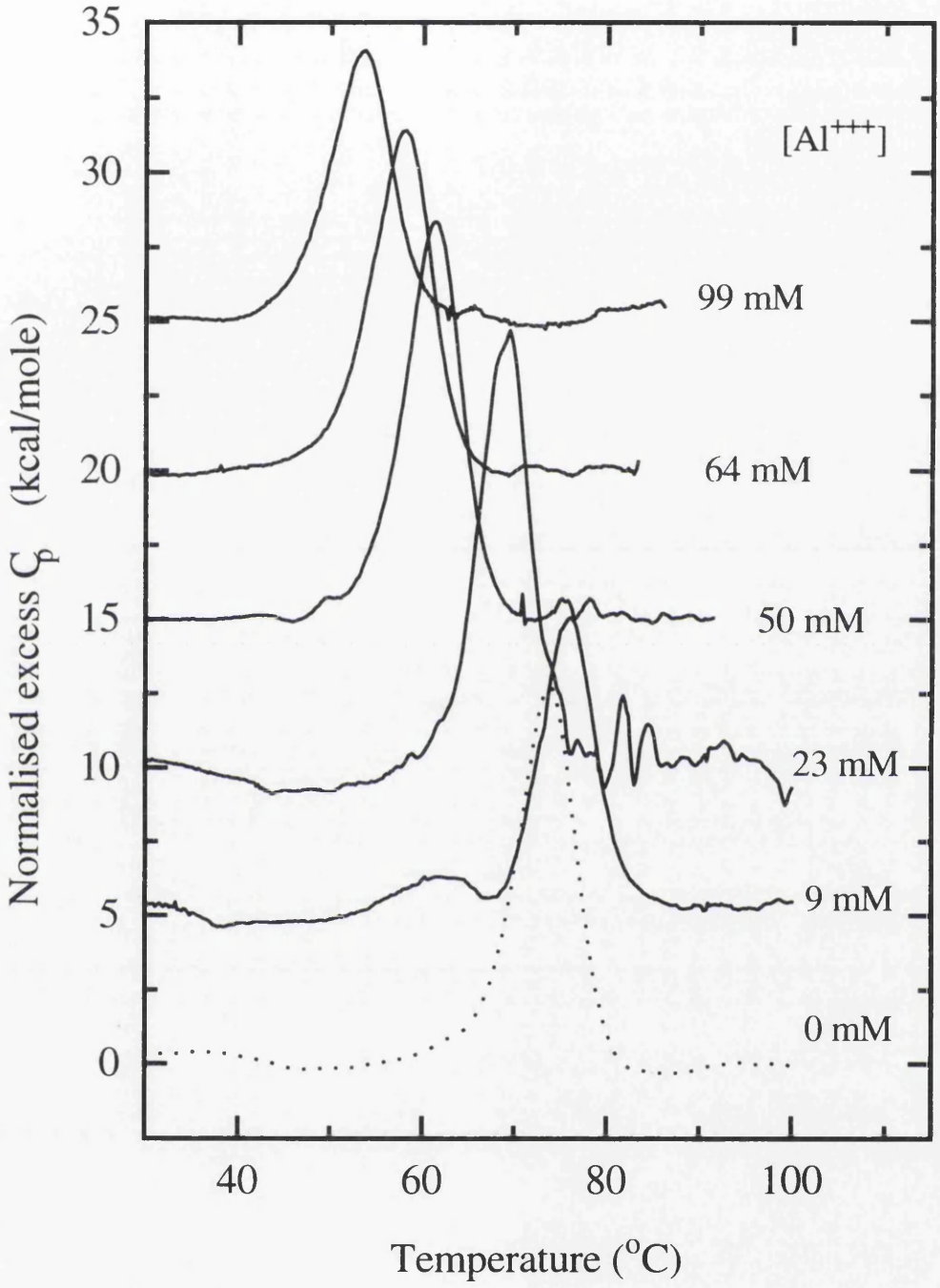


Figure 5.18: Normalized DSC scans for lysozyme in the presence of increasing concentrations of $Al^{3+}$ ions (0.1M MOPS, pH 7).

TABLE 5.5: Thermodynamic parameters associated with the thermal unfolding of lysozyme with aluminium chloride in 0.1M acetate buffer

| $[Al^{3+}]$ mM | pH | $T_m$ °C | $\Delta H_{cal}$ kcal $mol^{-1}$ | $\Delta H_{VH}$ kcal $mol^{-1}$ | $T_m$ °C ** | $\Delta H_{cal}$ ** | $\Delta H_{VH}$ ** |
|---|---|---|---|---|---|---|---|
| 0 | 4.5 | 76.8 | 114 | 116 | | | |
| 1.4 | 4.53 | 76.7 | 110 | 121 | | | |
| 3.1 | 4.33 | 76.7 | 109 | 121 | | | |
| 3.5 | 4.37 | 75.8 | 116 | 124 | | | |
| 5.0 | 4.26 | 76.3 | 110 | 120 | | | |
| 9.2 | 4.06 | 76.2 | 90 | 133 | 63.4 | 11 | 90 |
| 10.1 | 4.16 | 75.6 | 105 | 128 | 67.3 | 29 | 68 |
| 11.6 | 4.00 | 75.2 | 120 | 125 | | | |
| 14.4 | 3.89 | 74.3 | 102 | 137 | 70.3 | 50 | 87 |
| 20.9 | 3.74 | 71.8 | 132 | 108 | 80.1 | 50 | 87 |
| 22.1 | 3.78 | 71.4 | 171 | 90 | 80.0 | 37 | 89 |
| 29.6 | 3.53 | 64.8 | 122 | 111 | | | |
| 30.4 | 3.67 | 66.6 | 117 | 119 | | | |
| 49.6 | 3.39 | 61.1 | 120 | 113 | | | |
| 60.6 | 3.39 | 59.7 | 109 | 116 | | | |
| 70.9 | 3.26 | 58.5 | 101 | 113 | | | |
| 91.8 | 3.22 | 56.8 | 114 | 107 | | | |
| 92.1 | 3.21 | 56.9 | 130 | 105 | | | |

** values for second peak, where present

TABLE 5.6: Interaction of lysozyme and aluminium chloride in presence of 0.1M MOPS buffer

| $[Al^{3+}]$ mM | pH | $T_m$ °C | $\Delta H_{cal}$ kcal $mol^{-1}$ | $\Delta H_{VH}$ kcal $mol^{-1}$ | $T_m$ °C ** | $\Delta H_{cal}$ ** | $\Delta H_{VH}$ ** |
|---|---|---|---|---|---|---|---|
| 0 | 7.0 | 73.4 | 102 | 119 | | | |
| 9.4 | 6.2 | 75.6 | 86 | 122 | 62.4 | 27 | 69 |
| 23.0 | 4.2 | 68.4 | 121 | 116 | | | |
| 49.7 | 3.9 | 61.0 | 106 | 111 | | | |
| 64.41 | 3.8 | 57.6 | 95 | 104 | | | |
| 85.39 | 3.7 | 74.2 | 105 | 107 | | | |
| 98.91 | 3.7 | 53.1 | 79 | 95 | | | |

** values for second peak, where present

We have also studied in detail the interaction of aluminium chloride and lysozyme using different buffer systems and different pH values. The results are shown in Table 5.7.

Examination of this table shows that at pH 2 and below there is very little apparent effect of $Al^{3+}$ on lysozyme stability. The effect become most marked between pH 2.5 and 5, and then falls off again at higher pH. Consequently the destabilising effects of $Al^{3+}$ peak in the same pH range in which the $T_m$ of lysozyme alone is most sensitive. This suggests that the groups responsible for the $Al^{3+}$ effect are the same groups on the protein that are responsible for pH sensitivity in this range, i.e. most likely the carboxylate side chains of glutamate and aspartate.

TABLE 5.7: Interaction of aluminium chloride and lysozyme in different buffers

| Buffer | $[Al^{3+}]$ mM | pH | $T_m$ °C | $\Delta H_{cal}$ kcal $mol^{-1}$ | $\Delta H_{VH}$ kcal $mol^{-1}$ |
|---|---|---|---|---|---|
| KCl/HCl | 0 | 1.5 | 48.5 | 59.8 | 80.2 |
| | 9.6 | 1.5 | 47.7 | 78.6 | 77.1 |
| | 18.4 | 1.5 | 47.8 | 66.1 | 81.5 |
| | 0 | 2.0 | 54.4 | 84.1 | 85.4 |
| | 9.9 | 2.0 | 54.1 | 69.7 | 93.2 |
| | 18.8 | 2.0 | 53.4 | 85.3 | 81.5 |
| | | | | | |
| Gly/HCl | 0 | 2.6 | 62.2 | 93.0 | 100 |
| | 11.2 | 2.5 | 59.6 | 95.3 | 95.2 |
| | 21.2 | 2.5 | 58.7 | 90.6 | 95.5 |
| | 21.4 | 2.5 | 58.3 | 90.7 | 95.3 |
| | 0 | 3.0 | 70.1 | 104 | 109 |
| | 22.2 | 3.0 | 64.0 | 104 | 111 |
| | | | | | |
| Citrate | 0 | 3.5 | 70.8 | 109 | 108 |
| | 20.3 | 2.7 | 58.0 | 92.4 | 101 |
| | | | | | |
| Acetate | 0 | 4.0 | 76.2 | 123 | 113 |
| | 11.2 | 3.6 | 69.7 | 122 | 109 |
| | 0 | 4.4 | 76.8 | 117 | 115 |
| | 16.0 | 3.9 | 73.2 | 152 | 110 |
| | 0 | 5.0 | 76.3 | 118 | 115 |
| | 9.5 | 4.7 | 76.0 | 137 | 103 |
| | 0 | 5.5 | 75.4 | 106 | 119 |
| | 10.0 | 5.0 | 76.1 | 107 | 124 |
| | 11.2 | 5.1 | 76.3 | 122 | 108 |
| | | | | | |
| MES | 0 | 6.1 | 75.3 | 101 | 115 |
| | 10.1 | 4.7 | 73.4 | 112 | 128 |
| | 0 | 6.8 | 72.9 | 111 | 104 |
| | 11.0 | 5.6 | 75.8 | 131 | 85.7 |
| | | | | | |
| MOPS | 0 | 7.0 | 73.4 | 102 | 119 |
| | 11.3 | 4.9 | 74.3 | 137 | 113 |
| | 0 | 7.5 | 72.7 | 104 | 115 |
| | 11.5 | 5.9 | 75.9 | 115 | 107 |

That $T_m$ varies with pH shows that the extent of protonation of the protein changes on denaturation, and this might in principle give rise to additional heat effects. However, this is unlikely in view of the low enthalpies and heat capacities associated with the ionization of

glycine, acetic acid and phosphoric acid (Edsall & Gutfreund, 1983; Kishore, et al, 1994). Further, the ionization effects of the groups of the protein being titrated in this pH range are partly compensated by the ionization effects of glycine, acetate and phosphate buffers (Privalov & Potekhin, 1986). This indicates that the buffers used do not appreciably modulate experimental observations. Results of all the experiments show that the van't Hoff and calorimetric enthalpies are almost equal (except in cases that show two transitions, see above) which shows the reversibility and the approximately two-state character of the thermal unfolding of lysozyme in the absence and presence of aluminium chloride.

Binding of manganese chloride and cadmium acetate to hen egg-white lysozyme were also studied using differential scanning calorimeter. The results obtained for the thermal denaturation of lysozyme in aqueous buffer with manganese chloride at pH 4.5 (0.1M acetate buffer) and pH 7.0 (0.1M MOPS buffer) are shown in Tables 5.8 and 5.9, and Figures 5.19 and 5.20, respectively.

TABLE 5.8: Lysozyme binding manganese chloride in 0.1M acetate buffer.

| $[Mn^{2+}]$ mM | pH | $T_m$ °C | $\Delta H_{cal}$ kcal $mol^{-1}$ | $\Delta H_{VH}$ kcal $mol^{-1}$ |
|---|---|---|---|---|
| 0 | 4.5 | 76.8 | 114 | 116 |
| 7.5 | 4.4 | 76.4 | 96 | 129 |
| 16.3 | 4.4 | 76.1 | 88 | 131 |
| 34.3 | 4.4 | 75.6 | 91 | 125 |
| 55.1 | 4.3 | 74.5 | 96 | 123 |
| 70.5 | 4.3 | 74.7 | 94 | 118 |
| 94.2 | 4.3 | 74.7 | 108 | 109 |

TABLE 5.9: Lysozyme binding manganese chloride in 0.1M MOPS buffer.

| $[Mn^{2+}]$ mM | pH | $T_m$ °C | $\Delta H_{cal}$ kcal $mol^{-1}$ | $\Delta H_{VH}$ kcal $mol^{-1}$ |
|---|---|---|---|---|
| 0 | 7.0 | 73.4 | 102 | 119 |
| 7.0 | 7.1 | 74.9 | 104. | 112 |
| 18.9 | 7.0 | 76.0 | 112 | 119 |
| 42.9 | 7.0 | 76.5 | 100 | 120 |
| 70.9 | 7.0 | 76.5 | 95 | 136 |
| 97.2 | 7.0 | 76.5 | 147 | 124 |

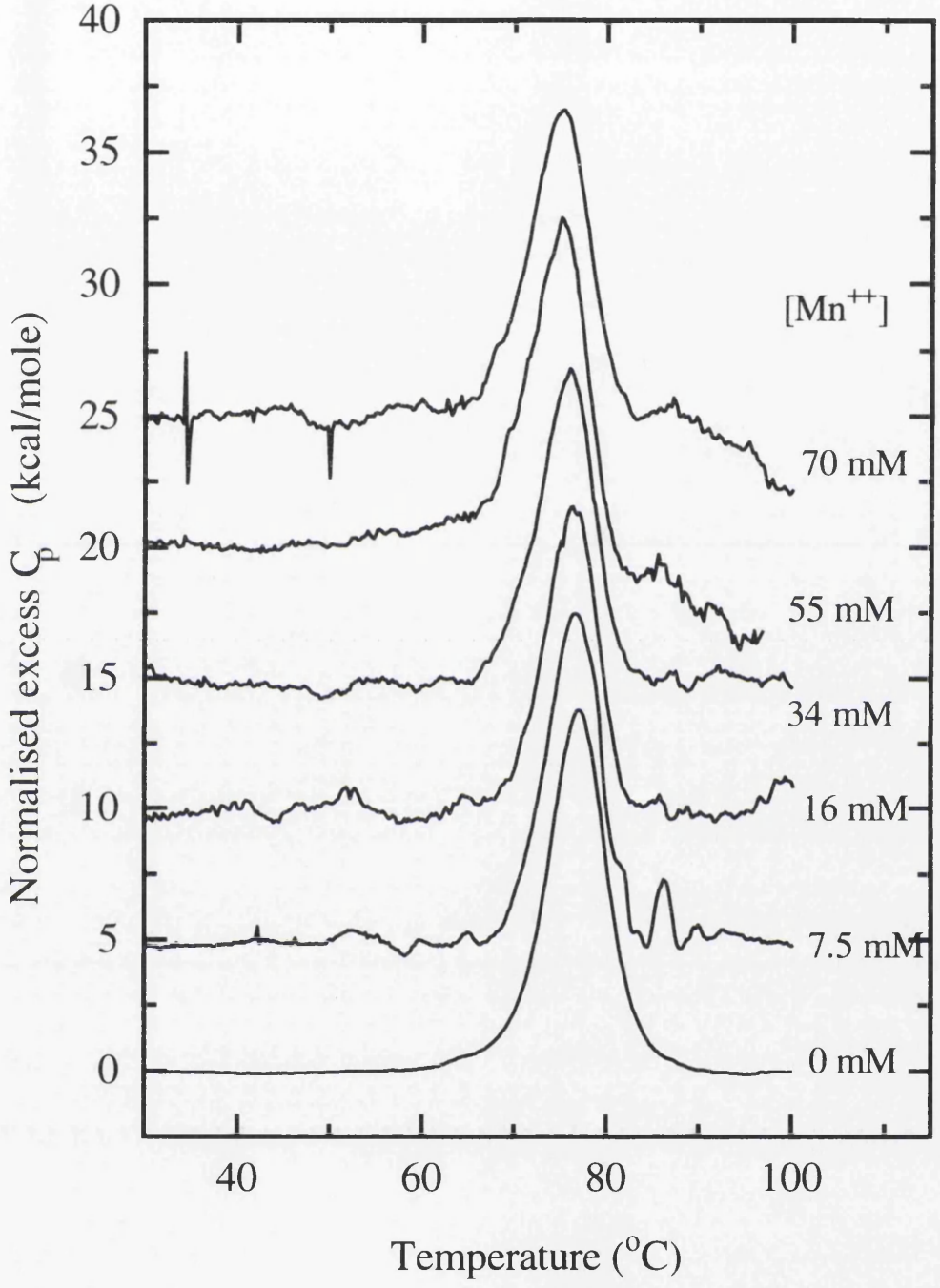


Figure 5.19: Normalized DSC scans for lysozyme in the presence of increasing concentrations of $Mn^{2+}$ ions (0.1M acetate, pH 4.5).

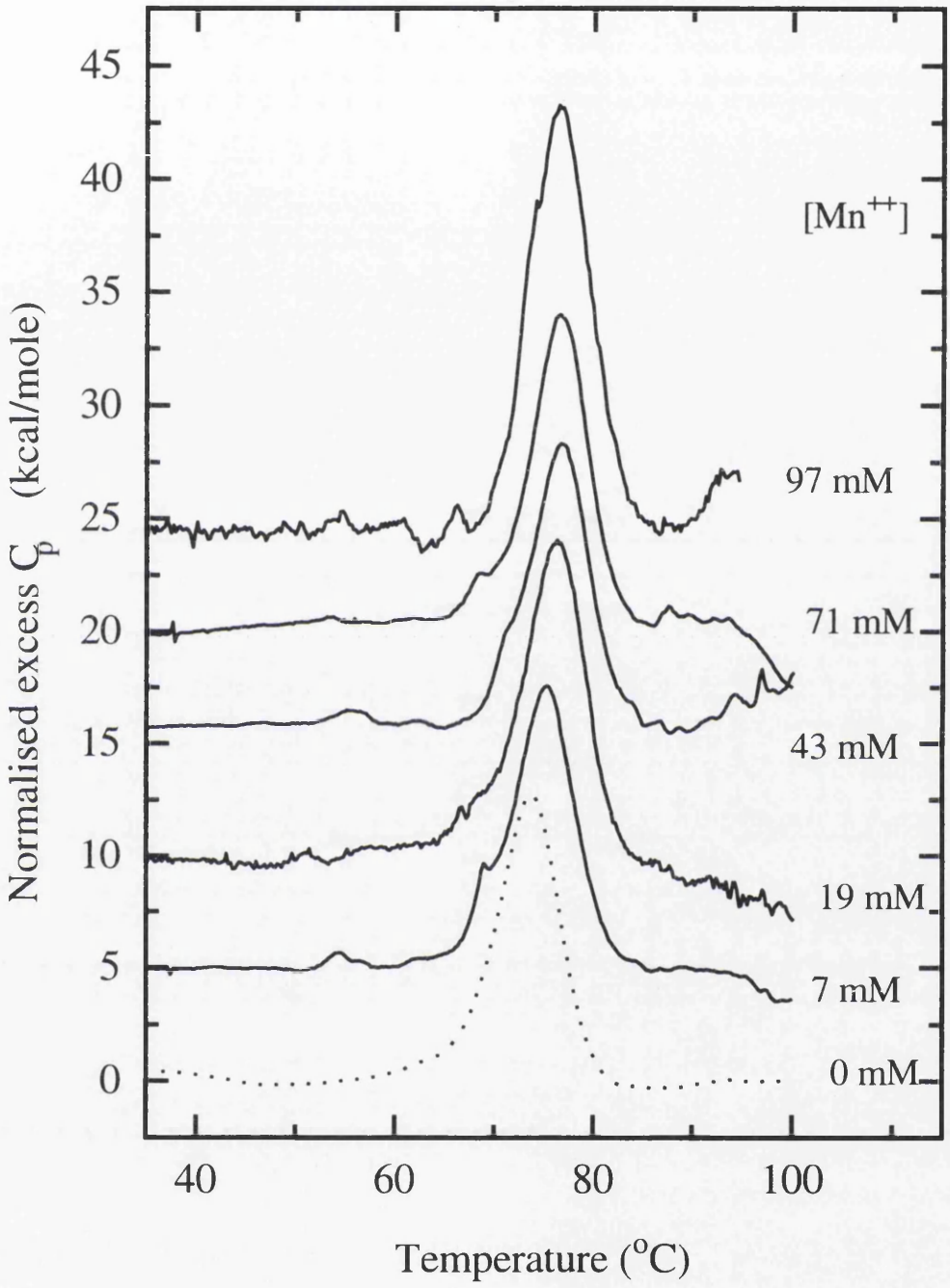


Figure 5.20: Normalized DSC scans for lysozyme in the presence of increasing concentrations of $Mn^{2+}$ ions (0.1M MOPS, pH 7).

At pH 4.4 the $T_m$ was decreased when the manganese chloride concentration was increased, but the opposite was seen at pH 7. This again indicates a balance of both stabilising and destabilising effects of the metal ions. This might be due to specific binding to folded or unfolded forms of the protein, alternatively it might just reflect non-specific ionic strength effects.

Previous work has shown that $Mn^{2+}$, like $Co^{2+}$, forms an association with HEWL at pH 7.0 and that this association occurs at the active site (Gallo et al., 1971). The enhanced stability of the $Mn^{2+}$ complex over that of $Co^{2+}$ could well arise from crystal field effects. Manganous ion possesses a spherically symmetric electronic ground state and as such derives no crystal field stabilization through complex formation involving any particular geometry. Such is distinctly not the case with $Co^{2+}$ which derives considerable stability from an octahedral ligand arrangement. A molecule such as lysozyme possesses its own structuring forces and the incorporation of a metal ion will be have to involve some compromise between what the ion prefers and what the protein prefers. Ions such as $Mn^{2+}$ and $Mg^{2+}$ with no crystal field requirements should thus be easier to incorporate than ions such as $Co^{2+}$ and $Ni^{2+}$. A similar argument has been presented by Bright (1967) in a comparison of the binding of $Co^{2+}$ and $Ni^{2+}$ to β-methylaspartase. Vallee and Williams (1968) demonstrated that irregular geometries of ligands around metal ions are often encountered among metalloproteins. Although $Mn^{2+}$ is a slightly less effective inhibitor of lysozyme activity than is $Co^{2+}$, it binds to the active site more strongly (Gallo et al., 1971). It was also found that the metal ions can interact with lysozyme bound with a substrate glycol chitin, or inhibitors, NAG, di-NAG, and tri-NAG. The binding constant of lysozyme was increased by a factor of about two when di-NAG or tri-NAG had been bound with lysozyme. The binding constant of $Mn^{2+}$ to NAG-bound lysozyme was slightly larger than that for free lysozyme. The binding constants of di- and tri-NAG to $Mn^{2+}$-bound lysozyme were also about two times as large as the constant in the absence of $Mn^{2+}$, while the binding constant of NAG in the absence of $Mn^{2+}$ was almost the same as that in its absence. In the case of $Co^{2+}$, the binding of the saccharides was suggested to be independent of the binding of the metal ion (Ikeda and Hamaguchi, 1973).

TABLE 5.10: Lysozyme binding cadmium acetate in 0.1M acetate buffer.

| $[Cd^{2+}]$ mM | pH | $T_m$ °C | $\Delta H_{cal}$ kcal $mol^{-1}$ | $\Delta H_{VH}$ kcal $mol^{-1}$ |
|---|---|---|---|---|
| 0 | 4.5 | 76.8 | 114 | 116 |
| 11.1 | 4.6 | 76.3 | 110 | 117 |
| 20.8 | 4.7 | 76.4 | 96 | 138 |
| 31.4 | 4.7 | 76.2 | 107 | 122 |
| 48.3 | 4.8 | 76.2 | 119 | 112 |
| 70.0 | 4.8 | 75.6 | 123 | 110 |
| 84.4 | 4.9 | 75.9 | 114 | 118 |
| 101.4 | 4.9 | 75.5 | 130 | 106 |

By comparison with aluminium and manganese ions, the effects of adding cadmium acetate are very small and entirely consistent with the simple pH effects resulting from addition of Cd acetate to the mixture. The results are, nevertheless, given in Table 5.10 and Figure 5.21 for completeness. Therefore we suggest that cadmium acetate binds to the unfolded state of lysozyme less strongly than other transition metal chlorides (Martins & Drakenberg, 1982).

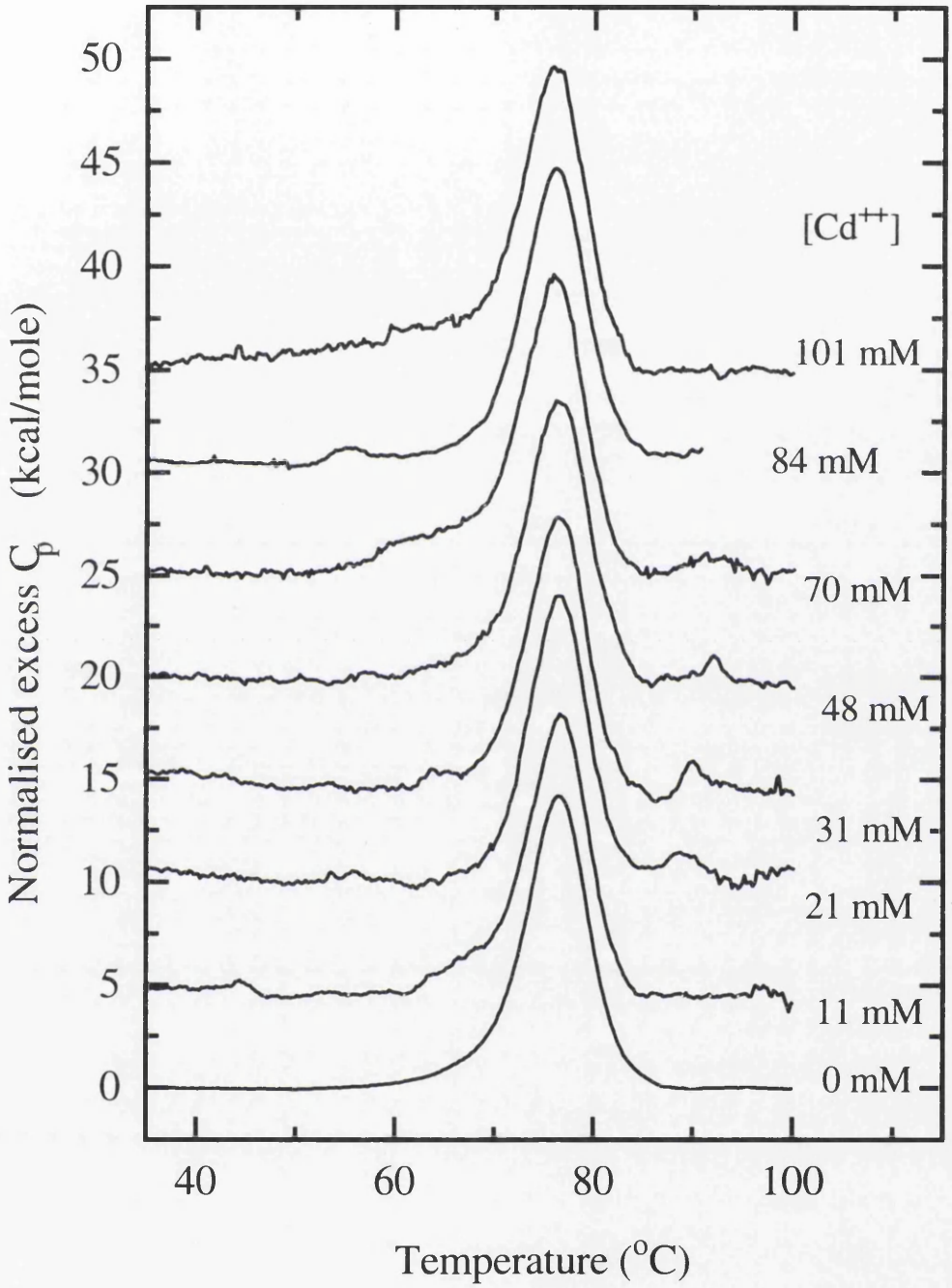


Figure 5.21: Normalized DSC scans for lysozyme in the presence of increasing concentrations of $Cd^{2+}$ ions (0.1M acetate, pH 5).

# CHAPTER 6

# 6 INTERACTION of LANTHANIDE IONS with LYSOZYME

## 6:1 INTRODUCTION

The binding of lanthanide cations to lysozyme in solution has been investigated by proton relaxation enhancement methods (Dwek, et al., 1971; Jones, et al., 1974) and by UV methods (Secenski & Lienhard, 1974). Both these types of study concluded that a single binding site exists but neither would have been able to detect sites of weak binding in the presence of this site. In the solid state, binding of lanthanide ions to lysozyme has been studied at low resolution (Blake & Rabstein, 1970) and binding at a single site (close to asp 52 and glu 35) was reported, although later studies (Kurachi, et al., 1975; Perkins, 1975) have indicated that several sites in this region of the protein could exist.

The use of paramagnetic lanthanide cations in complexes with biological macromolecules has attracted attention in view of their utility in nmr studies of macromolecules. They have been used as structural probes, aids to assignments, spectral simplifiers and probes of dynamic information (Dwek,1973; Nieboer, 1975; Reuben, 1975; Dobson & Levine, 1976). Applications for lysozyme and lysozyme-inhibitor complexes have been described (Butchard et al., 1972; Dwek et al., 1971; Jones et al., 1974; Campbell, et al., 1975a; Dobson & Williams, 1977).

The solution studies, with that of Ostroy et al. (1978), show that a 1:1 enzyme-metal ion complex is formed, and that the dissociation constants lie in the range 0.2-0.8mM. Proton relaxation enhancement studies, however, give a larger dissociation constant, about 13mM (Dwek, et al., 1971; Jones, et al., 1974). The activity of lysozyme is inhibited by lanthanide binding (Ostroy, et al., 1978). The high resolution crystallographic studies at pH 4.5-4.7 show that there are two $Gd^{3+}$ positions in one main binding site between Asp-52 and Glu-35 which are separated by 0.36nm in both triclinic and tetragonal lysozyme (Kurachi, et al., 1975; Perkin, et al., 1979). This observation has led to three different proposals to describe

the way in which lanthanides bind to lysozyme (Dobson & Williams, 1977; Perkins et al., 1979).

Diffraction methods cannot be applied to the determination of protein conformation in solution. Nuclear magnetic resonance has provided some types of necessary information (Campbell et al., 1973a; 1975a; 1975b). In order to obtain conformational information from nmr spectroscopy, the technique of paramagnetic lanthanide ion probe have been employed extensively to determine the conformations of small molecules in solution. The principles of the application of these probes are straightforward. When a paramagnetic lanthanide ion is bound to a ligand, the nmr spectrum of the ligand is perturbed. There are clearly a large number of possible conformations of a polypeptide chain of 129 residues. The conformation of lysozyme is of greatest interest in the region of the active site cleft, and particularly close to glu35 and asp 52. The lanthanide cations were found (Blake & Rabstein, 1970) to bind near to these groups in the crystal.
The binding of the lanthanides to lysozyme involving the definition of the number of binding sites, the strength of binding, the nature of the binding groups and the position of the metal ion in the protein structure was discussed by Dobson and Williams (1977).

The effect on the resonances in the nmr spectrum of lysozyme of varying concentrations of lanthanide ions have been measured. In these titrations the ionic strength was maintained constant by using KCl, and each experiment was done at a constant pH value and a constant concentration of lysozyme. The result indicates that a strong binding site exists, but also that weaker sites exist. When pH was varied in solutions containing various concentrations of a lanthanide ion up to 50mM and lysozyme concentration of 5mM keeping ionic strength at 0.4 as constant, the result shows that lanthanide binds to several sites in the molecule, although there is only one strong binding site. This major binding site involves glu-35 (pK value 6.0) but no other ionizable group with a pK value above 3.5. As the pH value is decreased, the fraction of lysozyme bound to the lanthanide ion decreases as $H^+$ competes for the binding group. This means that binding constant increases with pH (Dobson & Williams, 1977).

The shifting and broadening induced by the binding of paramagnetic lanthanides at the major site was measured for a number of assigned resonances by Dobson and Williams

(1977). By interpretation of these data the protein conformation and orientation of groups around the metal binding site have been shown to be similar in the solution and crystalline states. However, it was found that groups in the protein are not rigidly held in space, but are undergoing independent motion. In this way the solution conformation of lysozyme differs from the static model of the protein constructed from x-ray diffraction studies.

The simultaneous binding of lanthanide and N-acetylglucosamine inhibitors to hen egg-white lysozyme in solution using $^{1}H$ and $^{13}C$ nuclear magnetic resonance technique was studied by Perkins et al. (1981). They demonstrated that lanthanide ions and the N-acetylglucosamine (NAG) sugars are able to bind simultaneously to hen egg-white lysozyme. They also characterized the properties of the ternary complexes with lysozyme, which involve up to seven paramagnetic lanthanides and two diamagnetic lanthanides, together with α-NAG, β-NAG, α-MeNAG and β-MeNAG. They found that NAG sugars bind at least two independent sites and that one of them competes with La3+ for binding to lysozyme. Given the known binding site of lanthanides at Asp-52 and Glu-35, the competitive binding site of NAG was identified as subsite E. A simple analysis of the paramagnetic-lanthanide-induced shifts suggested that the NAG sugar binds in subsite C, in accordance with crystallographic results (Perkins, et al., 1979). This finding was refined by several computer analyses of the lanthanide induced shifts of 17 proton and carbon resonances of β-MeNAG. Good fits were obtained for all the signals, except for two that were affected by exchange broadening phenomena. No distinction could be made between a fit for a two-position model of Ln3+ binding with axial symmetry to lysozyme, according to the crystallographic result, or a one position model with axial symmetry where the $Ln^{3+}$ is positioned mid-way between Asp-52 and Glu-35 (Perkins, et al., 1981).

Bunzli and Pfefferle (1994) demonstrated the existance of at least two metal-binding sites in BLA (bovine α-lactalbumin). The site labelled 1 has a high affinity for $Eu^{3+}$. It is relatively rigid and may be identified as the $Ca^{2+}$ site reported for baboon milk α-lactalbumin (Asp-82, Asp-83, Asp-84, Asp-87, Asp-88, and Thr-86) (Stuart, et al., 1986). The presence of the $COO^{-}$ groups Asp-98 and Asp-88 in a calcium site is unusual for a Ca-binding protein. They have also investigated that site 1 is comprised of two different environments with similar affinities for the metal ion and found that these environments are similar and could

be related to the presence of $COO^-$ groups which may vary denticity, depending upon steric interactions (Pfefferle, 1989). They also explained that the second site is sequentially populated after saturation of site 1, its affinity is low, and its population is pH dependent, indicating that this site is more exposed to the solvent and less specific.. They tentatively assigned it to the distinct $Zn^{2+}$ site evidenced by other authors (Murakami, 1983; Musci & Reed, 1986).

Schomacker et al. (1988) showed that the lanthanide/protein stability complex is dependent on the ionic radii of the lanthanide ion after the complex formation both in the HSA (human serum albumin) solution and in the human plasma solution. They further demonstrated that dependence of the lanthanide/albumin binding constants on the ionic radius of the $Ln^{3+}$ (lanthanide) ion corresponds to the widely known chemical behaviour of lanthanide-ligand complexes in which electrostatic binding forces are predominant.

Proton nuclear magnetic resonance ($^1H$ NMR) has been employed to study the effects of the lanthanide ions $Lu^{3+}$ and $Yb^{3+}$ on both the apo- and $Ca^{2+}$- saturated forms of the porcine intestinal calcium binding protein (porcine ICaBP). Titration of the apoprotein with $Lu^{3+}$ showed the 2 mol equiv of $Lu^{3+}$ bound sequentially to the protein in the absence of $Ca^{2+}$. The two dissociation constants of the apoprotein for $Lu^{3+}$ were determined to be $K_{dI} < 10^{-6}$ M and $K_{dII} = (2.3 \pm 1.2) \times 10^{-4}$M. The addition of only 1 mol equiv of $Lu^{3+}$ to the apoprotein resulted in $^1$HNMR spectral perturbations that were very similar to those observed previously for the addition of 2 mol equiv of calcium (Shelling, et al., 1983). The binding of the second mole of $Lu^{3+}$ led to further changes in the $^1$HNMR spectra, indicating that this second mole of lanthanide had little effect on the overall conformation of porcine ICaBP. At a $[Lu^{3+}]/[ICaBP]$ ratio greater than 2, it was apparent that the protein began to aggregate as all of the resonances became significantly broadened. As with $Lu^{3+}$, titration of the apoprotein with $Yb^{3+}$ showed the sequential binding of 2 mol equiv of $Yb^{3+}$ to the protein. The two dissociation constants of the apoprotein for $Yb^{3+}$ were determined to be $K_{dI} < 10^{-7}$ M and $K_{dII}= (5.0 \pm 1.6) \times 10^{-5}$ M. The addition of $Yb^{3+}$ to the $Ca^{2+}$ saturated protein resulted in the displacement of only one mole equivalent of calcium ions, with a relative $Yb^{3+}/Ca^{2+}$ dissociation constant ratio of $0.023 \pm 0.015$. This ratio along with the known dissociation constant of the protein for $Ca^{2+}$, results in a value of $K_{dI} \sim 2 \times 10^{-9}$ M for

$Yb^{3+}$. The lanthanide-shifted $^1H$ NMR resonances, being sensitive structural indicators, showed that the species with $Yb^{3+}$ in one site and $Ca^{2+}$ in the other site differed in structure from the species with $Yb^{3+}$ in one site and no metal ion in the other site (Hoffman & Sykes, 1985).

The binding of lanthanide cations to lysozyme causes only a small conformational change. This change is fast, and probably involves merely a reorientation of binding groups to accomodate the metal ion. It was found that groups in the protein are not rigidly held in space, but are undergoing independent motion. In this way the solution conformation of lysozyme differs from the static model of the protein constructed from x-ray diffraction studies Dobson and Williams, 1977). It is instructive to compare this study of lysozyme and lanthanides complex with earlier studies (Campbell et al., 1975a). The two studies are complementary in the sense that different regions of the lysozyme molecule are perturbed by the lanthanide induced shifts. Because the lanthanides bind almost at the protein surface and not at the centre, the solid space of lysozyme that is perturbed by lanthanides corresponds to almost over half a-sphere. A large channel is missing from this half-sphere, and this corresponds to the lysozyme cleft above and below Asp 52 and Glu 35 (Stephen, et al., 1981).

As for as the nature of the binding of the lanthanide ions to the protein is concerned, the following points can be made. First, all binding of significant strength is to carboxylate groups rather than to other functional groups. Secondly, only one strong bonding site exists, and this is presumable due to the binding between two carboxylate groups (Asp-52 and Glu-35), whilst weak binding occurs to single carboxylate groups. Thirdly. No major conformational change takes place on binding which has allowed in this case the lanthanide cations to be used as probes of the structure of the nature protein (Dobson & William, 1977). The binding of lanthanide cations to lysozyme causes only a small conformational change. This change is fast, and probably involves merely a reorientation of binding groups to accomodate the metal ion.

## 6:2 METHOD

Interaction of lysozyme and lanthanide metal chloride (lanthanum chloride & europium chloride) was studied using three techniques:

(1) Fluorescence Spectroscopy

(2) Differential Scanning Calorimetry

(3) Isothermal Titration Microcalorimetry.

The general procedures of all these three techniques are fully explained in this thesis elsewhere. However, for the fluorescence experiments reported here, micromolar solutions of protein was prepared. Then a series of solutions of lanthanum or europium was prepared in lysozyme solution. We have also studied the interaction of lysozyme and lanthanide chloride in presence of NAG and penicillin-G in 0.1M MES buffer pH 6.8. In a similar way we have used the differential scanning calorimetric technique and isothermal titration microcalorimetric technique to study the behaviour of lysozyme and lanthanide in 0.1 M MES buffer pH 6.7. The detailed experimental procedure is explained in chapters 2 and 3 elsewhere in this thesis.

## 6:3 RESULT and DISCUSSION

### 6:3:1 Fluorescence Spectra.

The binding of $Eu^{3+}$ ions to hen egg-white lysozyme is evidenced by changes in both the intrinsic fluorescence of the protein, arising from tryptophan groups, and the luminescence of the $Eu^{3+}$ ion. The intensity of the intrinsic protein fluorescence decreases upon addition of Eu salt upto certain points and then remains approximately constant as shown in Figure 6.1. This is consistent with static quenching due to binding of the Eu ions to a site or sites on the protein. Similar effects were seen with La ions (Figure 6.2). Analysis in terms of a simple binding model (dotted lines in Figs. 6.3 and 6.4) gives an estimate of the apparent binding constant. Some typical numerical results are shown in Tables 6.1. This is similar in both the lanthanide ions which are under consideration.

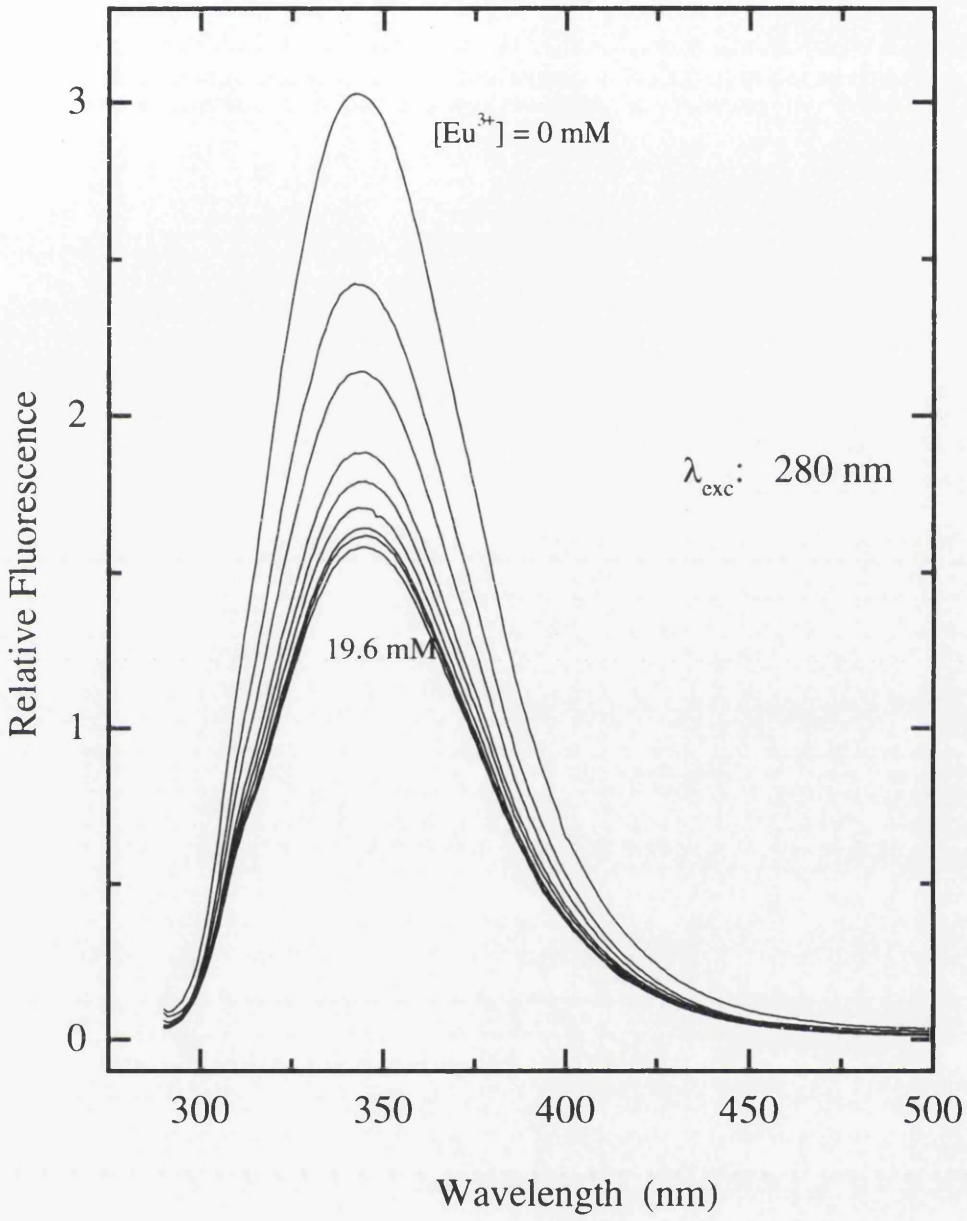


Figure 6.1: Emission spectra of lysozyme with increasing concentrations of $Eu^{3+}$ ions, 0-19.6 mM (see Table 6.1), in 0.1M MES, pH 6.7

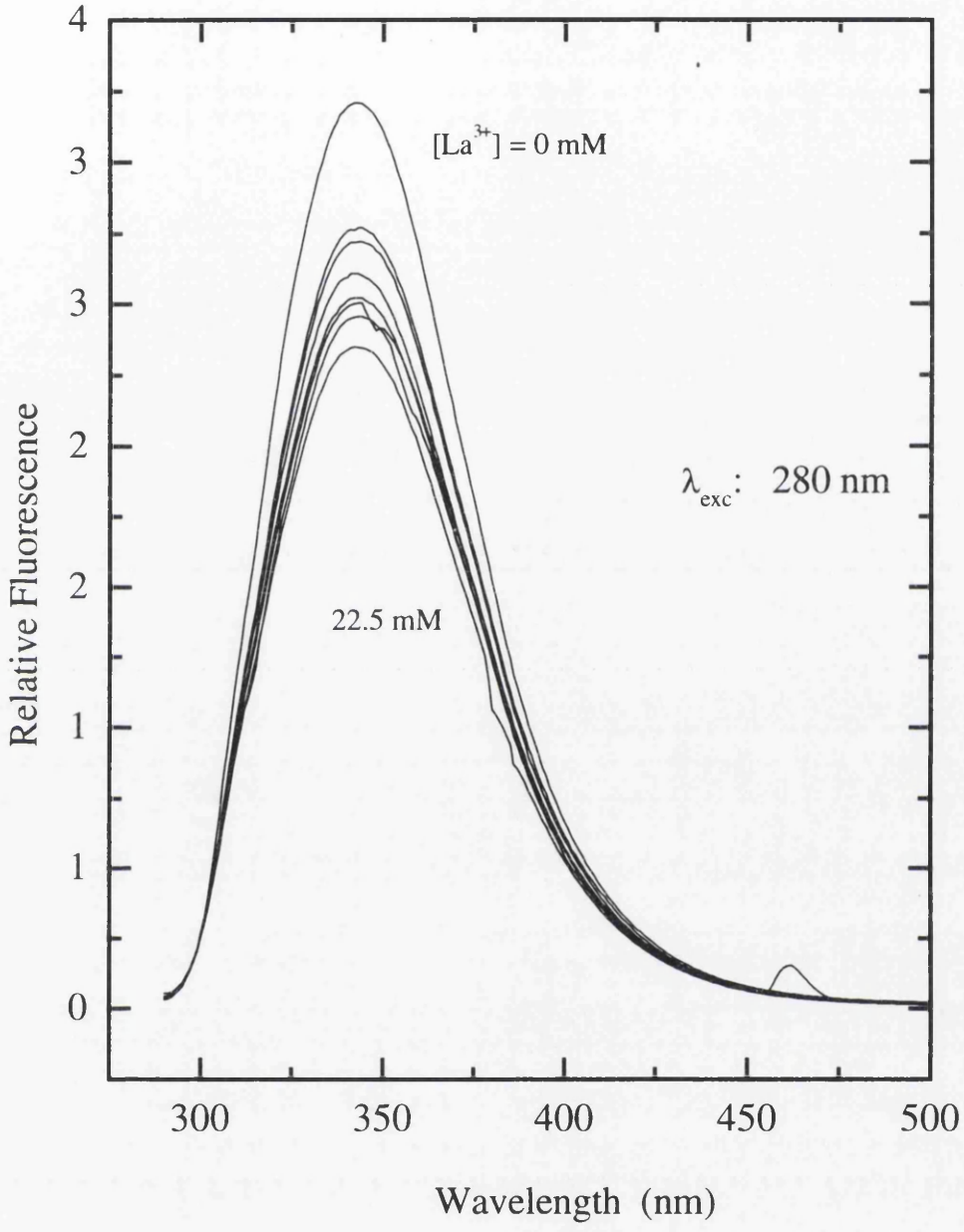


Figure 6.2: Emission spectra of lysozyme with increasing concentrations of $La^{3+}$ ions, 0-22.5 mM , in 0.1M MES, pH 6.7

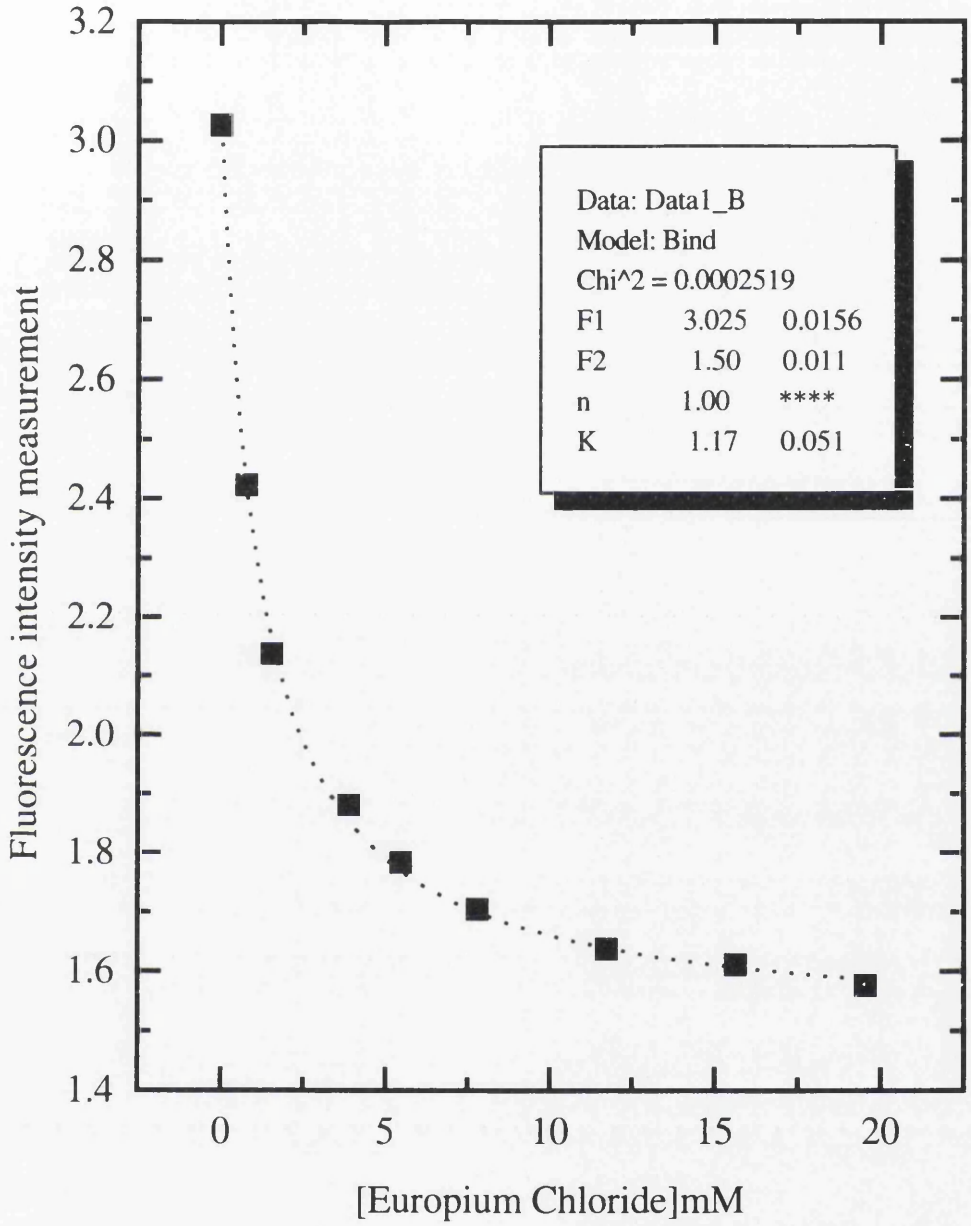


Figure 6.3: Intrinsic luminescence of lysozyme monitored during titration with $Eu^{3+}$ ions in 0.1M MES buffer pH 6.7. Conditions:Excitation wavelength=280nm, Analysis wavelength=342nm, [Lysozyme]=0.0026mM. The dotted line shows the theoretical fit to a simple binding model with the parameters shown.

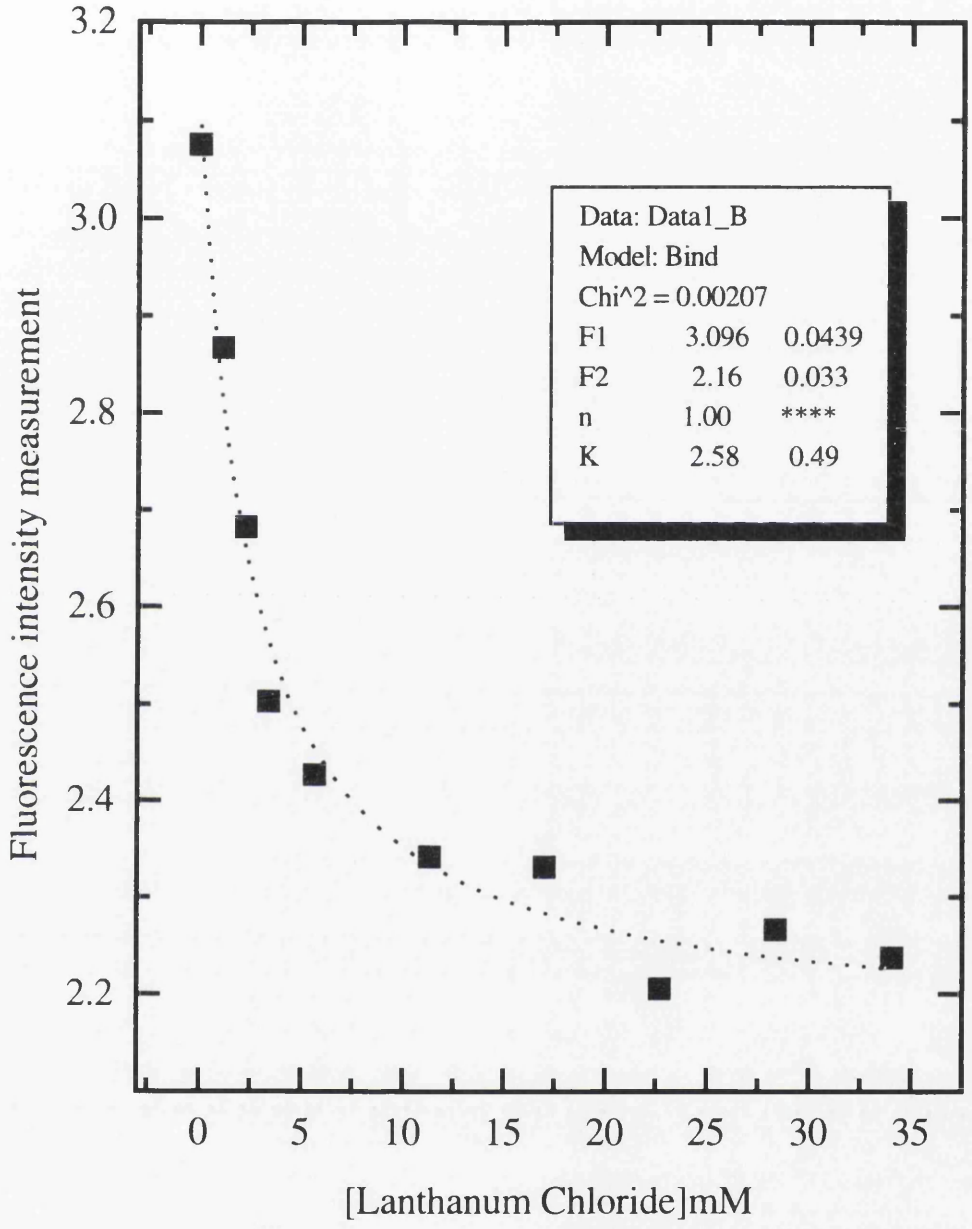


Figure 6.4: Intrinsic luminescence of lysozyme monitored during titration with $La^{3+}$ ions in 0.1M MES buffer pH 6.7. Conditions: Excitation wavelength=280nm, Analysis wavelength=342nm, [Lysozyme]=0.0031mM. The dotted line shows the theoretical fit to a simple binding model with the parameters shown.

TABLE 6.1: Quenching of fluorescence intensity of lysozyme with various concentrations of Europium chloride in 0.1 M MES buffer pH 6.7. Concentration of lysozyme = 0.0026mM. Excitation wavelength=280nm, Wavelength analysis=342nm.

| [Europium chloride] mM | Fluorescence intensity x $10^{-6}$ |
|---|---|
| 0.00 | 3.0267 |
| 0.78 | 2.4231 |
| 1.56 | 2.1368 |
| 3.91 | 1.8810 |
| 5.48 | 1.7831 |
| 7.82 | 1.7038 |
| 11.74 | 1.6364 |
| 15.65 | 1.6101 |
| 19.56 | 1.5754 |

Similar fluorescence quenching experiments were done in the presence of various concentrations of NAG (Tables 6.2 and 6.3) and penicillin-G (Table 6.3) to investigate any possible competitive binding effects.

TABLE 6.2: Interaction of lysozyme and europium chloride using 0.1M MES/NAG buffer. Excitation wavelength=280nm, Fluorescence analysis=342nm, Temperature=25 °C.

| [Lysozyme] mM | [NAG] mM | $k_d$ /mM | K /$M^{-1}$ |
|---|---|---|---|
| 0.0031 | 0 | 1.27 | 787.4 |
| 0.0027 | 10.00 | 1.47 | 680.3 |
| 0.0027 | 23.42 | 1.42 | 704.2 |
| 0.0027 | 36.37 | 1.58 | 632.9 |
| 0.0027 | 41.64 | 1.58 | 632.9 |
| 0.0031 | 45.73 | 1.73 | 578.0 |
| 0.0030 | 70.80 | 1.6 | 625.0 |
| 0.0028 | 93.55 | 1.77 | 565.0 |
| 0.0027 | 101.37 | 1.98 | 505.1 |

These results indicate that, in the absence of any inhibition, $Eu^{3+}$ binds to lysozyme with a dissociation around 1.3 mM. On the other hand in presence of NAG, acting as an inhibitor, the dissociation constant ($k_d$) increased slightly as the concentration of NAG increases (Table 6.2). In these experiments it was not possible from analysis of the fluorescence titration curves to get any estimate of the number of Eu binding sites per protein molecule. However, the inhibitory effects of NAG appear to show that at least some of the sites might

be in the active cleft of the enzyme. (Competitive binding experiments with penicillin were not possible in this case because of precipitation in mixtures of penicillin and Eu salts.)

TABLE 6.3: Interaction of lysozyme and lanthanum chloride using o.1M MES/NAG and 0.1M MES/PG buffer pH 6.7. Excitation wavelength=280nm, Fluorescence analysis=342nm, Temperature=25.1 °C

| [Lysoz]mM | [NAG]mM | [PG]mM | $k_d$/mM | K/[$M^{-1}$] |
|---|---|---|---|---|
| 0.0031 | x | x | 2.58 | 387.6 |
| 0.0027 | 10.04 | x | 2.78 | 359.7 |
| 0.0027 | 50.21 | x | 3.44 | 290.7 |
| 0.0028 | 70.08 | x | 3.72 | 268.8 |
| 0.0027 | 100.2 | x | 3.22 | 310.6 |
| 0.0027 | x | 10.00 | 2.41 | 414.9 |
| 0.0033 | x | 15.26 | 1.53 | 653.6 |
| 0.0024 | x | 15.26 | 1.53 | 653.6 |
| 0.0028 | x | 25.02 | 0.923 | 1083.4 |
| 0.0028 | x | 40.9 | 0.457 | 2188.2 |

Similar results were obtained using lanthanum chloride alone and in the presence of NAG or penicillin, to investigate any competitive binding effects. The results are summarised in Table 6.3. Binding of $La^{3+}$ alone gives an apparent dissociation constant of around 2.6 mM under these conditions. This is also increased in the presence of NAG, just as was the case with $Eu^{3+}$ ions, suggesting that $La^{3+}$ and NAG compete for some of the same binding sites. However, the effect of penicillin-G on $La^{3+}$ binding is just the opposite, that is the apparent dissociation constant decreases with increasing penicillin-G concentration. This indicates some kind of cooperative involvement of penicillin in La binding, but it is unclear what the molecular basis for this might be.

These results are in reasonable agreement with the solution studies of Ostroy et al. (1978) which show that a 1:1 enzyme-metal ion complex is formed, and that the dissociation constants lie in the range 0.2-0.8 mM. Proton relaxation enhancement studies, however, give a larger dissociation constant, about 13mM (Dwek et al., 1971; Jones et al., 1974). Our results here also support the findings of Perkin et al. (1981) that lanthanides and NAG sugars compete for the same binding site on lysozyme.

## 6:3:2 Differential Scanning Calorimetry

We have investigated the interaction of hen egg-white lysozyme with lanthanum chloride in 0.1M MES buffer pH 6.7. The results are shown in Table 6.4.

TABLE 6.4: Thermodynamic parameters associated with the thermal unfolding of lysozyme in 0.1M MES buffer pH 6.7, in the presence of lanthanum chloride.

| [Lysozyme] mM | $[La^{3+}]$ mM | $T_m$ (°C ) | $\Delta H_{cal}$ kcal $mol^{-1}$ | $\Delta H_{VH}$ kcal $mol^{-1}$ |
|---|---|---|---|---|
| 0.2942 | 0 | 73.5 | 112 | 119 |
| 0.3024 | 5.86 | 75.2 | 108 | 124 |
| 0.3024 | 11.92 | 75.0 | 114 | 122 |
| 0.3221 | 13.73 | 74.5 | 120 | 123 |
| 0.3035 | 25.11 | 73.3 | 128 | 117 |
| 0.3081 | 25.92 | 73.1 | 121 | 121 |
| 0.3081 | 50.08 | 71.0 | 115 | 122 |
| 0.3261 | 51.78 | 70.6 | 117 | 123 |
| 0.3075 | 70.26 | 68.0 | 113 | 118 |
| 0.3088 | 70.28 | 68.5 | 106 | 125 |
| 0.3043 | 99.93 | 66.8 | 117 | 119 |
| 0.3088 | 101.31 | 66.6 | 101 | 125 |

The deconvolution of DSC curves in the absence and presence of lanthanum chloride shows that the thermal unfolding behaves as a reversible two-state-process. The transition temperature decreases with the increase in the concentration of lanthanum chloride. We have also observed that on rescanning the sample, the lysozyme peak disappears which shows that at high temperature lanthanum chloride reacts with the lysozyme in such a way as to inhibit refolding (Figure 6.5). Such samples were turbid after DSC indicating irreversible aggregation of the polypeptide in the presence of $La^{3+}$, more particularly at higher concentrations. The values of $\Delta H_{cal}$ and $\Delta H_{VH}$ are nearly equal at all concentrations, though with a tendency for $\Delta H_{VH}$ to be the greater in most cases. This is consistent with a simple 2-state process in which the shape of the DSC transition is slightly sharpened by aggregation effects at high temperature.

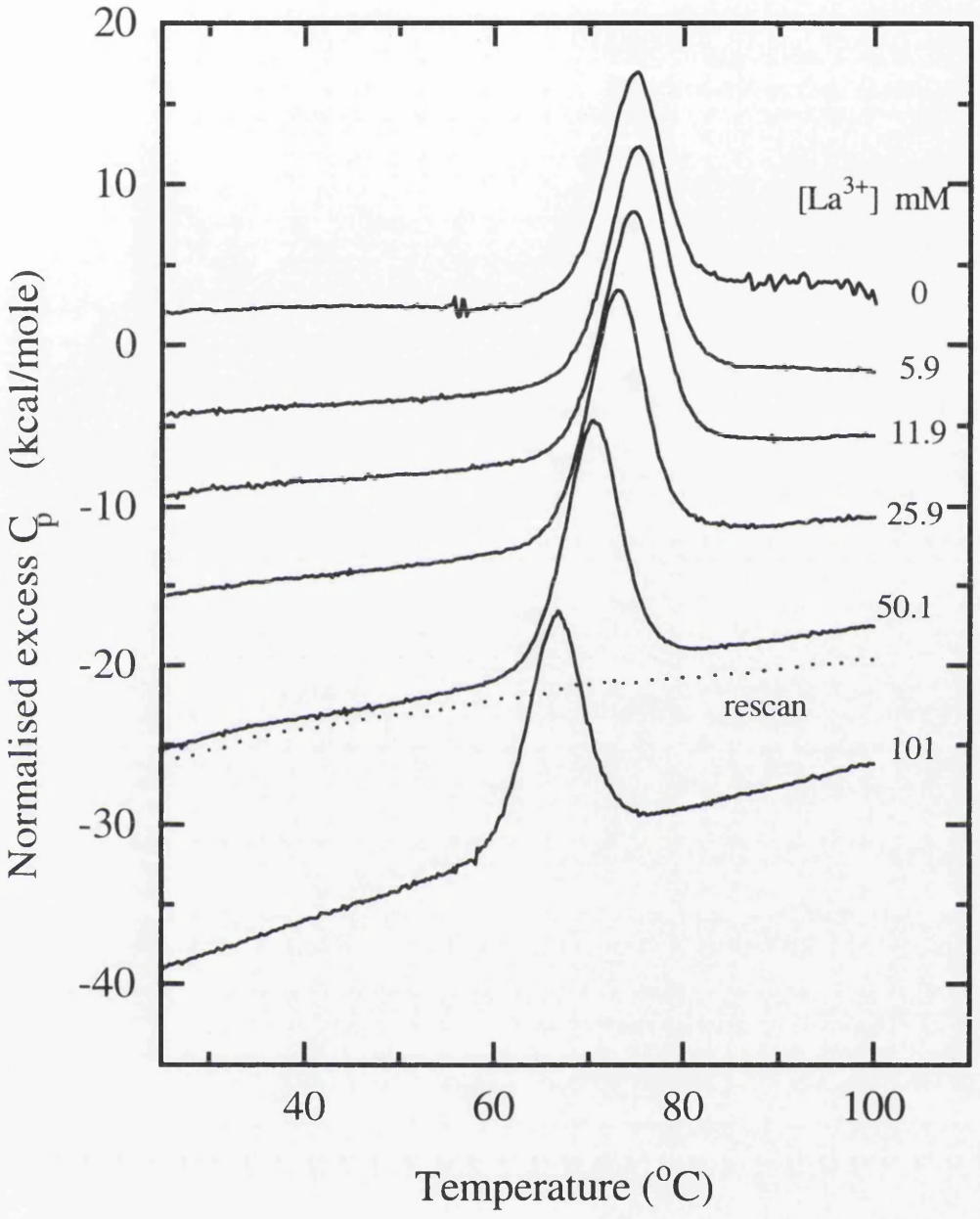


Figure 6.5: Normalized DSC data for unfolding of lysozyme in 0.1M MES buffer, pH 6.7, with increasing concentrations of lanthanum chloride.

In case of europium chloride the DSC results are less useful due to severe aggregation of the protein-lanthanide mixture, therefore at this stage we cannot get any useful result.

These results indicate that, like some of the other transition metal ions studied (Chapter 5), lanthanide ions interact more strongly with the unfolded form of lysozyme and therefore reduce the thermal stability of the native fold. This is in apparent disagreement with the observations made by Norton and Allerhand (1977) and Perkins et al. (1981) who suggested that lanthanides stabilize lysozyme in solution. It also seems to contradict the observations here using fluorescence methods (see above) which indicated quite strong lanthanide binding to native lysozyme. This paradox can be resolved by suggesting that lanthanide ions bind to both native and unfolded forms of the protein, but that the binding affinity and/or the number of binding sites for lanthanide ions is greater for the unfolded polypeptide. In this way, although lanthanide ions may bind to the native conformation at low temperatures, at higher temperatures the folded form is destabilised and $La^{3+}$ binds preferentially to the unfolded protein. If, as suggested earlier, the lanthanide ions are binding to available carboxylate groups, then the increased exposure of such groups in the unfolded state might be consistent with this interpretation.

## 6:3:3 Isothermal Titration Microcalorimetry

The main aim of these studies was to extend the previous work as stated in the beginning of this chapter with a view to obtaining a greater understanding of the interactions involved in proteins with metal ions. The binding of lanthanide chloride to protein has been carried out using a Microcal Omega Ultrasensitive Isothermal Titration microcalorimeter following procedures described earlier (Chapter 3). Titration of lanthanide chloride solutions with lysozyme and also lanthanide chloride into lysozyme in presence of NAG and PG were also studied in 0.1M MES buffer pH 6.7, at 25 °C. Enthalpy changes ($\Delta H$) and association constants ($K_a$) were determined from the Microcal Origin software package using the one set of sites model after correction for dilution controls. In some cases it was necessary to fix the binding stoichiometry, n, to unity in order to get rational fitting parameters for these weakly binding situations.

The initial microcalorimetric experiments were concerned with measuring the association constants for ion binding to hen egg-white lysozyme. The interaction of europium chloride in the absence of NAG and presence of various concentrations of NAG were also measured under the same conditions. The results of these experiments are given in Table 6.5 and typical binding isotherms are shown in Figures 6.6, 6.7 and 6.10. Similar data for lanthanum are given in Table 6.6 and Figures 6.8, 6.9 and 6.11.

In both cases the ITC experiments for lanthanide binding were complicated by relatively large and concentration-dependent exothermic heats of dilution of the metal ions (see Figs. 6.6 - 6.11). However, in all cases the addtion of lanthanide ions to lysozyme solution gave heat pulses that were initially endothermic, but became exothermic and approaching dilution values as the titration progressed. This indicates that interaction of these ions with lysozyme is endothermic.

TABLE 6.5: Thermodynamic parameters for binding of europium chloride with lysozyme in 0.1M MES buffer pH 6.7 in the presence of various concentrations of NAG at 25 °C.

| [NAG] mM | n (±) | $K/M^{-1}$ | $\Delta H$ kcal $mol^{-1}$ | $K/M^{-1}$ (n=1) | $\Delta H$ (n=1) kcal $mol^{-1}$ |
|---|---|---|---|---|---|
| 0 | 3.9 | 1160 | 0.85 | 550 | 3.8 |
| 0 | 2.5 (0.1) | 834 (18) | 1.57 (.03) | 590 (5) | 4.22 (.01) |
| 10.85 | 2.8 | 1100 | 1.17 | 630 | 3.64 |
| 22.46 | 2.7 (0.3) | 935 (64) | 1.41 (0.1) | 610 (64) | 4.17 (0.2) |
| 51.21 | 2.9 (0.1) | 792 (50) | 1.35 (.03) | 520 (28) | 4.29(.04) |
| 70.96 | 2.0 (0.2) | 700 (40) | 2.14 (.01) | 580 (30) | 4.52 (0.4) |
| 100.3 | 2.4 (0.3) | 730 (42) | 1.55 (.12) | 540 (35) | 4.00 (0.1) |
| 150.46 | 2.1 | 667 | 1.74 | 540 | 3.84 |

(±) values in brackets indicate standard deviations of several experiments.
Note: The two sets of data for 0 mM NAG relate to different lysozyme concentrations.

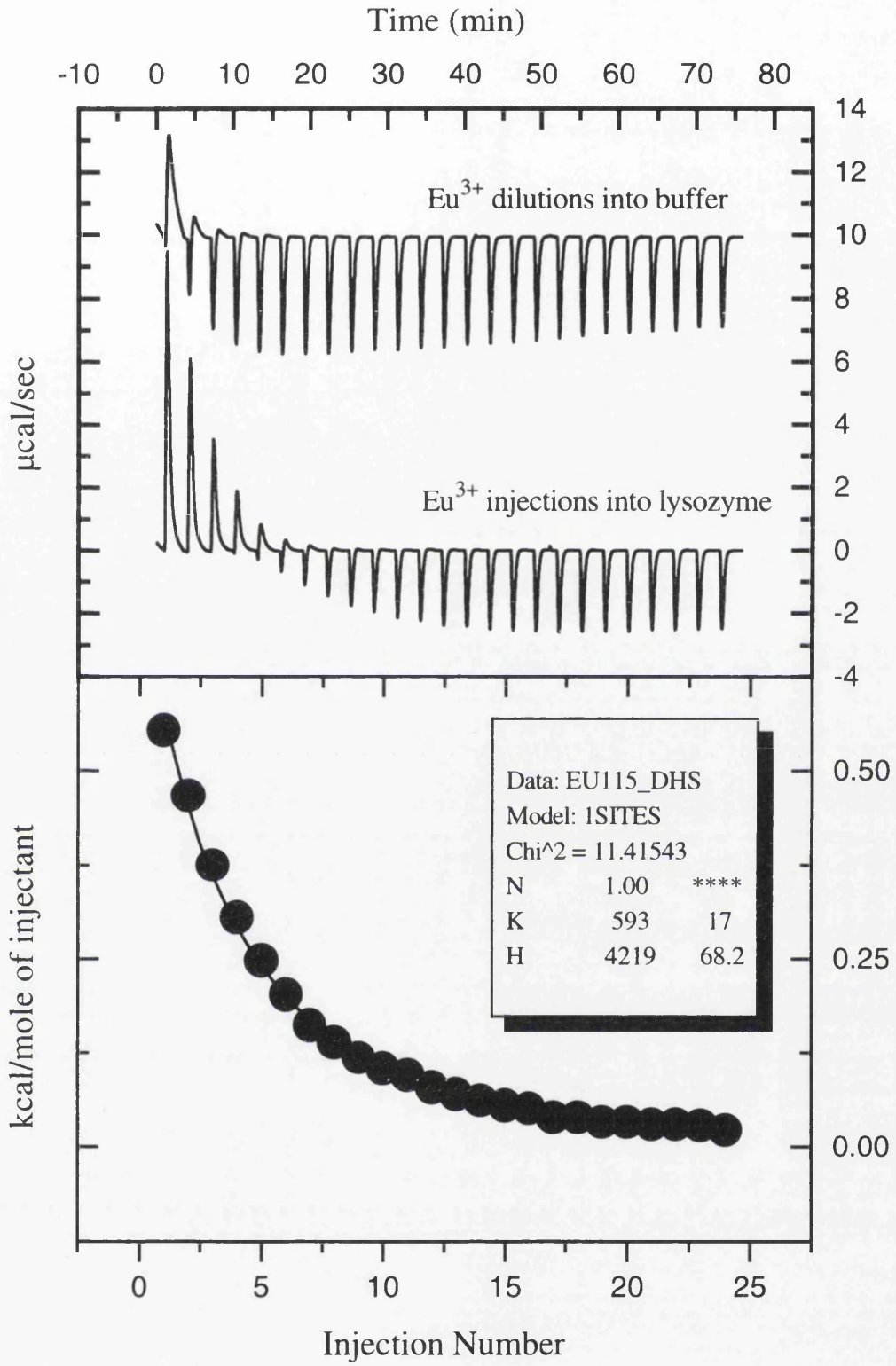


Figure 6.6: Example of ITC data for Lysozyme (0.3051mM) binding Europium chloride (40.23mM) in 0.1M MES buffer pH 6.7, Temperature = 25.2 C

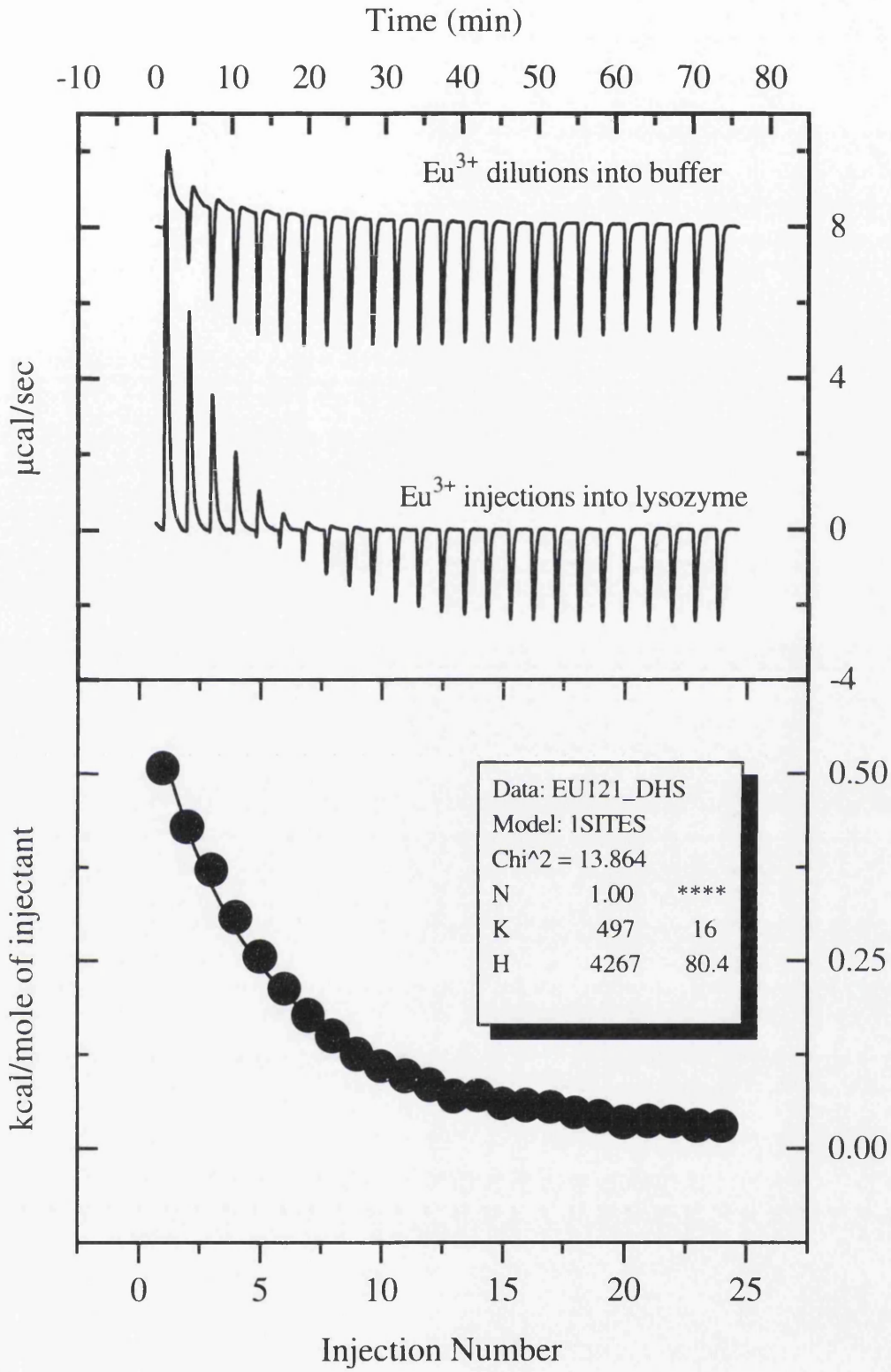


Figure 6.7: Example of ITC data for binding of Europium chloride to lysozyme in the presence of NAG (51.2 mM). Other conditions as in Fig.6.6

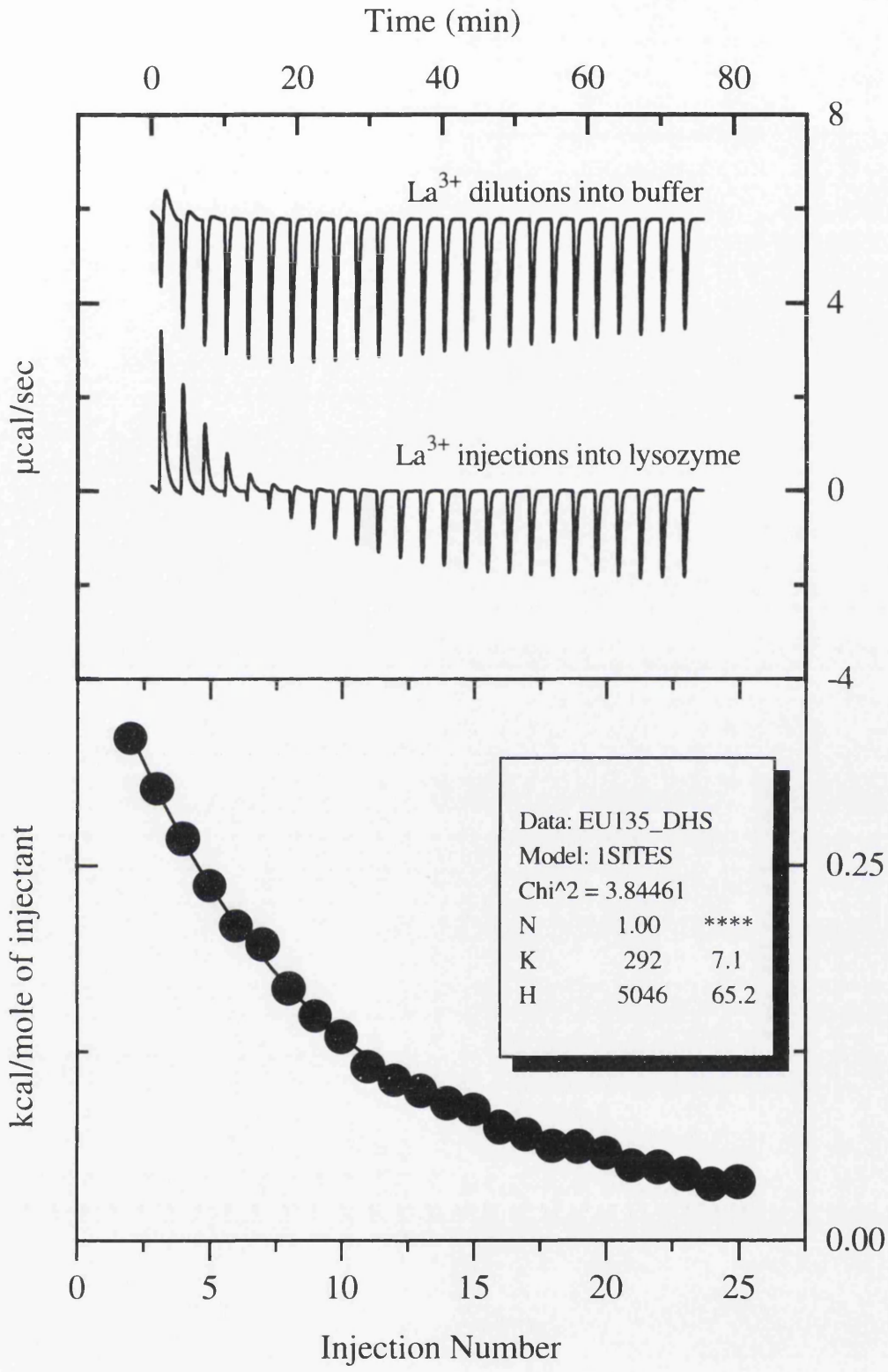


Figure 6.8: Example of ITC data for binding of Lanthanum chloride to lysozyme. Conditions as in Fig.6.6

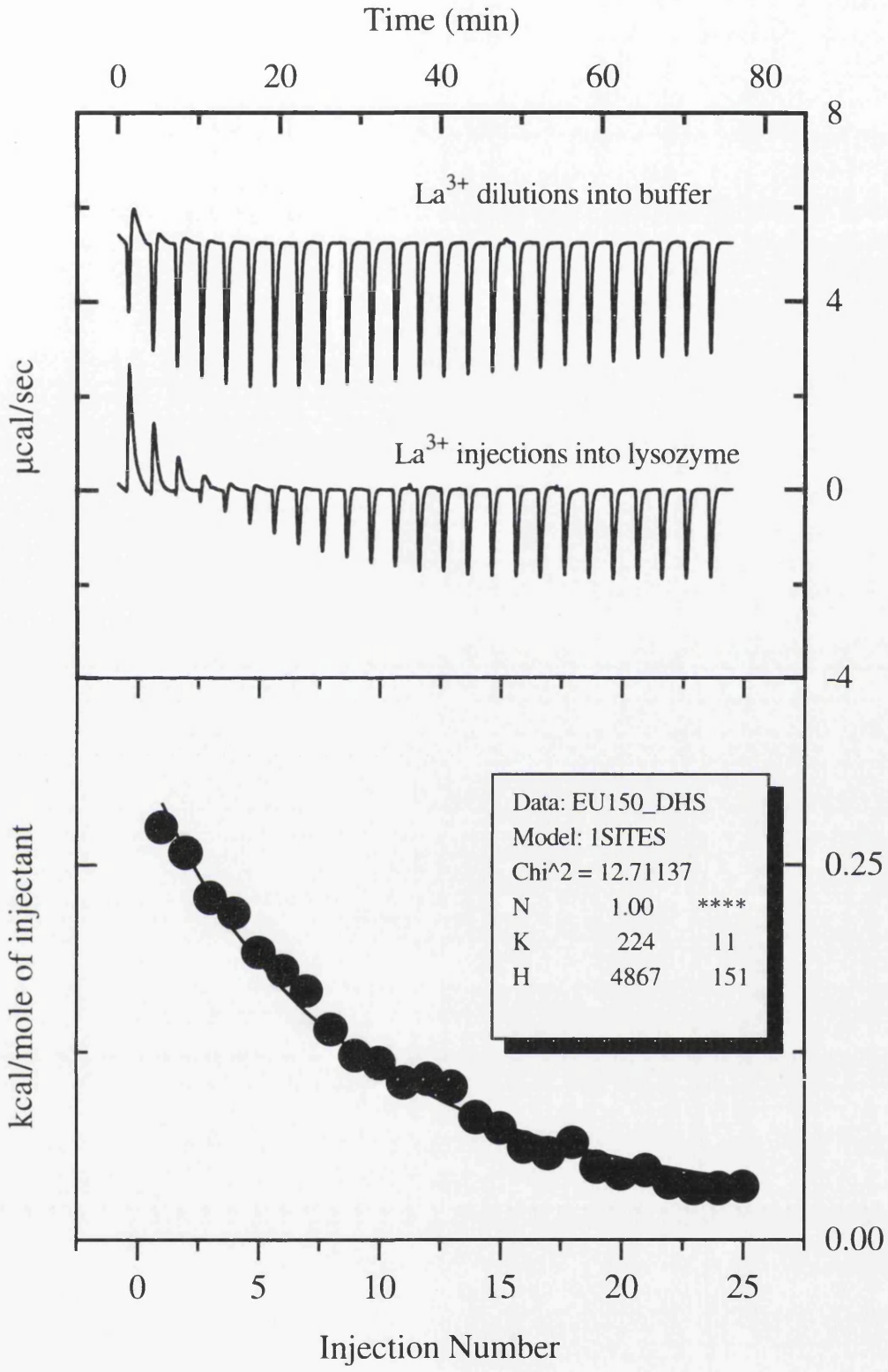


Figure 6.9: Example of ITC data for binding of Lanthanum chloride to lysozyme in the presence of NAG (40 mM). Other conditions as in Fig.6.6

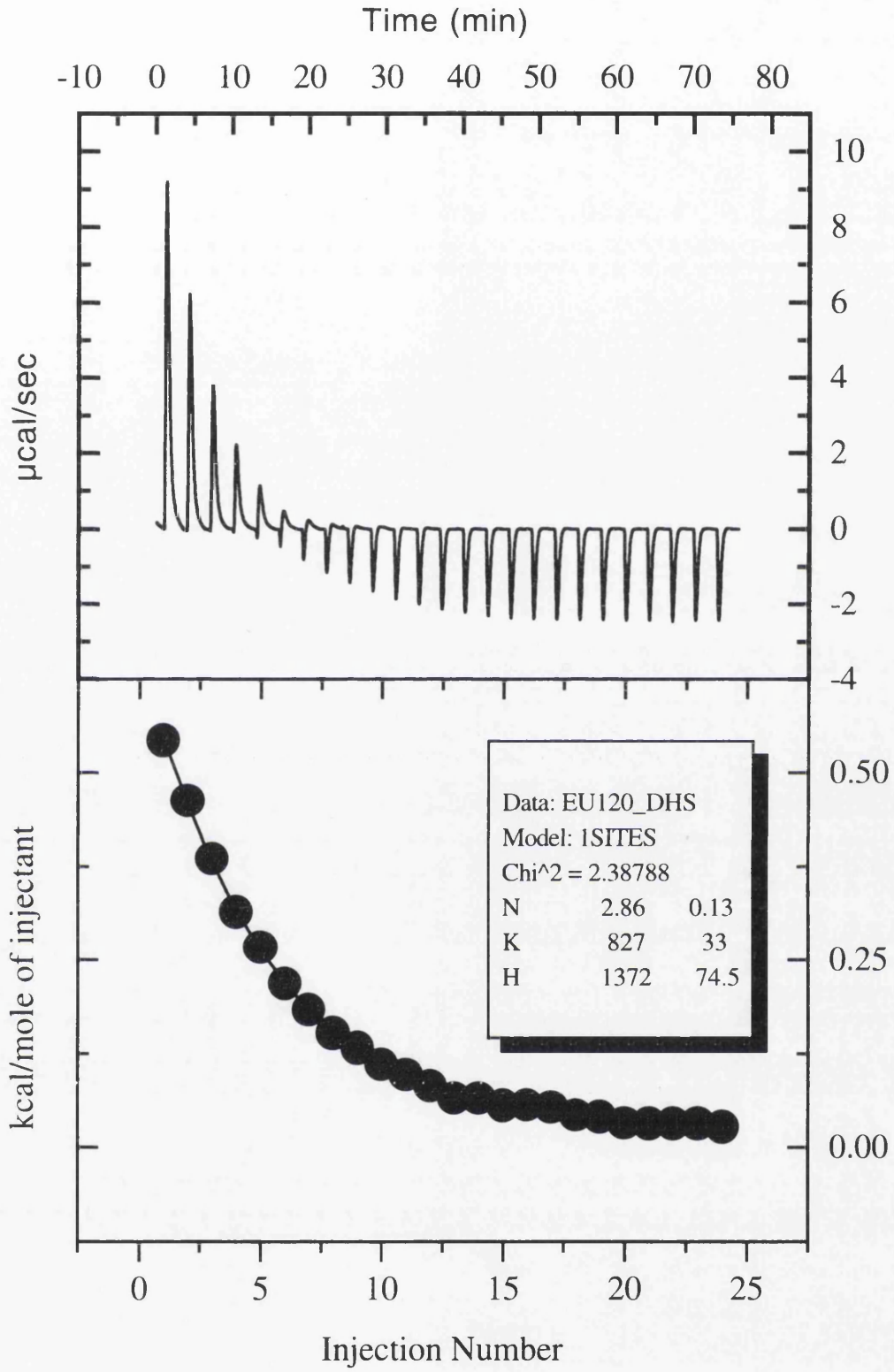


Figure 6.10: Example of ITC data for $Eu^{3+}$ binding to lysozyme in the presence of 51 mM NAG, other conditions as in Fig. 6.6. The data in this case have been fitted with N allowed to vary.

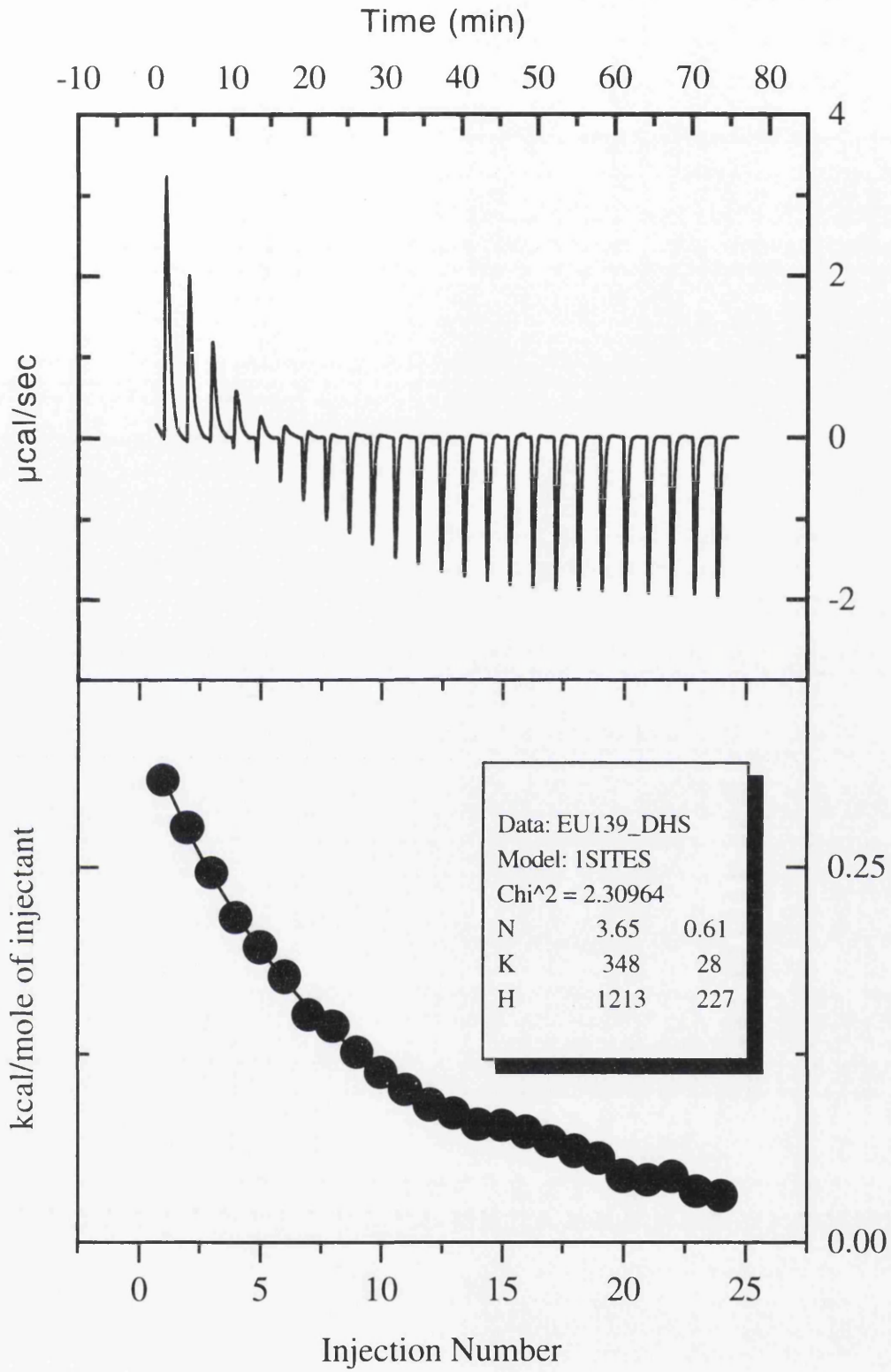


Figure 6.11: Example of ITC data for $La^{3+}$ binding to lysozyme in the presence of 7.2 mM NAG, other conditions as in Fig. 6.6. The data in this case have been fitted with N allowed to vary.

TABLE 6.6: Thermodynamic parameters of lanthanum chloride with lysozyme in 0.1M MES buffer pH 6.7 in the presence of various concentrations of NAG at 25 °C.

| [NAG] mM | n (±) | $K/M^{-1}$ | $\Delta H$ kcal $mol^{-1}$ | $K/M^{-1}$ (n=1) | $\Delta H$ (n=1) kcal $mol^{-1}$ |
|---|---|---|---|---|---|
| 0 | 4.7 (1.1) | 450 (55) | 1.01 (.24) | 280 (11) | 5.19 (.2) |
| 7.19 | 3.8 (0.2) | 370 (11) | 1.30 (.11) | 280 (1) | 5.31 (.1) |
| 16.17 | 1.7 (0.2) | 310 (7) | 2.93 (.35) | 290 (1) | 4.92 (.04) |
| 24.86 | 1.4 | 270 | 3.48 | 260 | 4.91 |
| 50.24 | 2.8 | 338 | 1.55 | 280 | 4.53 |
| 99.4 | 3.2 (0.2) | 345 (12) | 1.23 (.05) | 275 (1) | 4.28 (.15) |
| 157.76 | 3.6 | 338 | 1.09 | 260 | 4.24 |

(±) values in brackets indicate standard deviations of several experiments.

These ITC results show that, in the absence of NAG, there is some apparent binding of both $Eu^{3+}$ and $La^{3+}$ ions to lysozyme, with K values in the range 500-1000 $M^{-1}$ (1-2 mM $K_{diss}$) for $Eu^{3+}$, and slightly weaker at 250-500 $M^{-1}$ (2-4 mM) for $La^{3+}$. These binding affinities are in good agreement with those determined by fluorescence methods above, where $K_{diss}$ was found to be of order 1.3 mM for Eu (Table 6.2) and 2.6 mM for La (Table 6.3). The enthalpies of binding are positive (i.e. endothermic) with values that depend on assumptions regarding the number of lanthanide binding sites. For weakly binding systems such as this, it is not usually feasible to obtain unambiguous estimates of binding stoichiometry (n) from analysis of ITC titration data alone. However, in these experiments the n values consistently converged on values greater than 1 (Figures 6.10 and 6.11), suggesting the possibility at least of multiple binding sites for these ions on the protein. The endothermic nature of the binding probably arises from removal of solvated water from the lanthanide ions during the process. This would result in a positive entropy contribution from this released solvation that would make the overall binding process thermodynamically feasible (negative $\Delta G°$).

In the presence of NAG the binding of both Eu and La were significantly decreased (Tables 6.5, 6.6). Also the apparent n values were decreased as the concentration of NAG was increased. This suggests that at least one of the lanthanide binding sites might be competitive with NAG binding, presumably in the active site cleft. The most likely sites for lanthanide ion binding are those on the protein involving carboxylate groups, in particular the glutamate-aspartate pair (glu35-asp52) in the active site where NAG also binds. When

we used piperazine buffer at pH 5 we found that there is no apparent interaction of lanthanide ion and lysozyme at this pH value and the K value is smaller in more acidic medium, as might be expected from the protonation of the ligating groups (Bunzli and Pfefferie, 1994). Thus due to the acidic behaviour of Asp52, Glu35, and other carboxylate groups, europium and lanthanide ions does not bind to lysozyme at low pH. The major binding site involves Glu35 (pK value 6.0) but no other ionisable group with a pK value above 3.5. There is only indirect evidence for the involvement of Asp52 in the binding, and the pK value for this group is low (3.5±0.5). The lack of apparent lanthanide binding at pH 5 therefore indicates that Glu35 might be the major residue involved here. These findings are comparable to the results obtained from other groups (Johnson et al., 1981; Dobson & Williams, 1977).

Similar experiments investigating the possible inhibition by penicillin of lanthanide ion binding to lysozyme were unsuccessful because when we add the penicillin-G into lanthanide solution it forms a white precipitate. Therefore there is no point of using penicillin-G buffer because penicillin-G reacts with lanthanide at pH 5.

# CHAPTER SEVEN

## 7: SUMMARY

This thesis reports on studies of the interaction of lysozyme and penicillin-G using UV/Vis spectrophotometry, fluorescence spectroscopy, differential scanning calorimeter (DSC) and isothermal titration microcalorimeter (ITC), in comparison with the known lysozyme inhibitor, NAG. Similar techniques were applied to the possible interactions of metal ions in solution with this protein. The general conclusions are summarised here.

Using UV/vis spectroscopy we found that NAG has significant effect on lysozyme activity whereas penicillin-G has less inhibition activity. These initial experimental results appeared contrary to previous literature data, but could be rationalised by the varying effects of different buffers on the penicillin inhibition effects. UV difference experiments were inconclusive because of high absorbance by penicillin-G in this region, however there was no clear evidence for binding of penicillin in the enzyme active site under most conditions.

In the case of fluorescence spectroscopy the interaction of penicillin-G and lysozyme gives a change in the protein emission spectrum consistent with binding with $K_d$ values ranging from 1-2 mM at neutral or acid pH (pH 4-7), rising to 27 mM at pH 9. This binding did not seem to be competitive with NAG binding, suggesting that binding sites for penicillin-G lie outside the active site cleft of lysozyme.

DSC measurements of lysozyme in aqueous solution using various buffer systems having the same ionic strength were carried out in the presence of penicillin-G and/or NAG. In all penicillin-G experiments the thermograms gave a downward exothermic curvature. This behaviour was also observed in simple control experiments using penicillin alone. Rescanning did not show any further transition, which suggests that penicillin-G is undergoing irreversible thermal decomposition with increasing temperature in the DSC. When the penicillin-G solution was heated prior to DSC experiments, the lysozyme $T_m$ was reduced as the penicillin concentration increased. this suggests that the major effect is due

to the thermally decomposed penicillin-G interacting with unfolded lysozyme rather than (or better than) with the folded form.

The interaction of penicillin-G with lysozyme measured using ITC in different buffer systems was difficult to quantify because of the large heats of dilution of penicillin at the high concentrations required to test for binding. An alternative indirect approach, using the possible inhibitory effect of penicillin on NAG binding in the ITC was attempted. These experiments indicated a weak competitive binding of penicillin-G with $K_d$ of order 300 mM. Such very weak binding would not have been detected in the UV/vis and fluorescence experiments reported above because of the very high concentrations of penicillin required to produce a measurable effect. This weak binding may be non-specific, and the inhibitory effect on NAG binding might result from more general changes in protein conformation rather than direct binding of penicillin in the active site.

The unfolding behaviour of lysozyme in the presence of monovalent, divalent, and trivalent metal ions has been studied in detail using differential scanning calorimetry (DSC) in various buffers. Monovalent and most divalent metal ions produced a similar small decrease in $T_m$ probably as a simple non-specific ionic strength effect. However, in the case of trivalent metal ions (and some divalent transition metal ions) there is a much greater change in $T_m$ values, frequently accompanied by precipitation of the unfolded protein. This is probably because of strong interactions of highly charged ions with the unfolded polypeptide promoting aggregation of the unfolded chains and shifting the equilibrium away from the native fold state.

More specific interactions of lanthanide ions with lysozyme were investigated using fluorescence, DSC, and ITC techniques. Intrinsic protein fluorescence of lysozyme is quenched in the presence of europium and lanthanum ions in a manner consistent with binding to groups on the protein with an apparent $K_d$ of order 1-4 mM, depending on the metal. This binding is weakened slightly in the presence of NAG, but strengthened slightly by penicillin-G, suggesting some cooperative interaction involving penicillin and lanthanide binding sites. ITC studies indicate multiple binding sites for the lanthanide ions on native lysozyme, only some of which are affected by NAG binding. DSC experiments showed that the lanthanide ions had a similar effect to other metals in reducing the $T_m$ or causing

aggregation of the protein. This suggests that, even though these ions bind to the native state of the protein, at higher temperatures the binding to the unfolded state is more favourable.

# REFERENCES


Acharya, K. R. Stuart, D. I., Walker, N. P. C., Lewis, M., & Phillips, D. C. (1986), Nature (London), 324, 84.

Agresti, D. G., Lenkenski, R. E. & Glickson, J. D. (1977) Biochem. Biophys. Res. Commun. 76, 711-719.

Aramini, J., Drakenberg, T., Hiraoki, T., Ke, Y., Nitta, K. & Vogel, H. (1992) Biochemistry, 31, 6761-6768.

Armstrong, G. T. (1964) J. Chem. Educ., 41, 297.

Atha, D. H. & Ackers, G. K. (1971) J. Biol. Chem., 246, 5845

Barlow, D. J. & Thornton, J. M. (1983) J. Mol. Biol., 168, 867.

Barel, A. O., Prieels, J. P., Maes, E. , Looze, Y., & Leonis, J., (1972) Biochim. Biophys. Acta 257, 288.

Belew, M., Yip, T., Anderson, L. & Porath, J. (1987) J. Chromatogr. 403, 197-206.

Bernard, M., Canioni, P., Cozzone, P., Berthou, J., Jolles, P. (1990) Int. J. Peptide Protein Chem., 36, 46-55.

Bird, A. E. & Marshall, A. C. (1967) Br. J. Pharmacol., 25, 638.

Blake, C. C. F., Koenig, D. F., Mair, G. A., North, A. C. T., Phillips, D. C. & Sarma, V. R. (1965) Nature (London) 196, 1173-1176.

Blake, C. C. F., Johnson, L. N., Mair, G. A., North, A. C. T., Phillips, D. C. & Sarma, V, R. (1967) Proc. Roy. Soc., B167. 378.

Blanco, M. D., Martin, J. A., Garcia, O., Lozano, M. & Teijon, J. M. (1996) Journal of Physiology, 493P, 141S.

Brewer, M. & Scott, T. (1983). In Concise Encyclopaedia of Biochemistry (Jakubke, H.D., ed.), pp. 374-376, Walter de Gruyter & Co. Berlin 30.

Bright, H. J. (1967) Blochemistry, 6, 1191.

Bunzli, J-C. G., & Pfefferie, J-M. (1994) Helvetica Chimica Acta, 77 323-333.

Butchard, C. G., Dwek, R. A., Ferguson, S. J., Kent, P. W., Williams, R. J. P. & Xavier, A. V. (1972) FEBS Lett., 25, 91-93.

Campbell, I. D., Dobson, C. M. & Williams, R. J. P. (1975a) Proc. Roy. Soc., A345, 23.

Campbell, I. D., Dobson, C. M, & Williams, R. J. P. (1975b) Proc. Roy. Soc., A345, 41.

Canfield, R. E. (1963) J. Biol, Chem., 238, 2698-2707.

Cantor, C. R. & Schimmel, P. R. (1980) Biophysical Chemistry, Part 111, p 849.

Chaudhuri, D. & Horrocks.Jr. W. DeW. (1997) Biochemistry, 36, 9674-9680.

Chee, M., Yang, R., Hubbell, E., Berno, A., Huang, X. C., Stem, D., Winkler, J., Lockhart, D. J., Morris, M. S. and Fodor, S. P. A. (1996) Science, 274, 610-614.

Cheetham, J. C., Artymiuk, P. J., Phillips, D. C. (1992) J.Mol.Biol., 224, 613-628.

Cheng, X., Chang, X., Pflugrath,J. W.& StudierF. W. (1994) Proc. Natl. Acad.Sci. USA; 91, 4034-4038.

Chowdhry, B. Z. & Cole, S. C. (1989) TIBTECH, 7, 11.

Clarke., Johnson, J. R. & Robinson, R. (1949) The Chemistry of Penicillin, Princeton, University Press, Princeton, New jersey, 440-454.

Clark, S. M. and Mathews, R. A. (1997) Anal. Chem., In press.

Collins, J. F. & Richmond, M. H. (1962) Nature, 195, 142.

Cooper, A. (1974) Biochemistry, 13 (14), 2853-2856.

Cooper, A. (1992) J. Amer. Chem. Soc., 114, 9208-9209.

Cooper, A. (1999 - in press) Protein: A Comprehensive Treatise, Series Editor, Geoffrey Allen; Publisher, JAI Press Inc.

Cooper, A., Eyles, S. J., Radford, S. E. & Dobson, C. M. (1992) J. Mol. Biol., 225, 930.

Cooper, A. & Johnson, C. (1992) In Methods in Molecular Biology., Physical Methods of Analysis., Ed Jones C., Mulloy, B. & Thomas, A. H., Human Press, Clifton, N. J.

Cooper, A. & McAuley-Hecht, K. E. (1993) Phil. Trans. R. Soc. Lond. A, 345, 23

Corran, P. H. & Waley, S. G. (1975) Biochem. J., 149, 357.

Creighton, T.E. (1993) Proteins: Structure and Molecular Properties, W.H.Freeman & Co., New York, p.20.

Creighton, T. E. & Goldenberg, D. P. (1984) J. Mol. Biol., 179, 497.

Czarnik, A. W. (1993) ed., Fluorescent Chemosensorsfor ion and molecule Recognition (ACS Symposium Series 538), American Chemical Society.

Danford,R., Krakauer, H. & Sturtevant, J. M. (1967) Rev. Sci. Instrum. 39, 184-187.

Desmet, J, Van, Dael, H., Van, Cauwelaert, F., Nitta, K. & Sugai, S. (1989) J. Inorg. Biochem 37, 185-191.

Dill, K. A. (1990) Biochemistry, 29, 7133.

Dixon, M. & Webb, E. C. (1979), Enzymes, 3rd edn., 322-333

Dobson, C. M. (1992) Curr. Opin. Structr. Biol., 2, 6.

Dobson, C. M., Evans, P. A., & Radford, S. E. (1994); TIBS, 19, 31-37.

Dobson, C. M. & Levine, B. A. (1976) in New Techniques in Biophysics and Cell Biology (Pain, R. H. & Smith, B. J., eds.). vol. 3, pp 19-91, John Wiley and Sons, London.

Dobson, C. M. & Williams, R. J. P. (1977) B. Pullman and N. Goldblum (eds.); Metal-Ligand interactions in organic chemistry and biochemistry, Part 1,D. Reidel Publishing Company, Dordrecht-Hollnd, pp. 255-282.

Donner, J., Caruthers, M. H., Gill, S. J. (1982) J. Biol. Chem. 257, 14826.

Drakenberg, T., Sward, M., Parello, J., & Cave, A. (1985) Biochem. J., 227, 711.

Dwek, R. A. (1973) NMR in Biochemistry, pp 62-75, Oxford University Press, London.

Dwek, R. A., Richards, R. E., Morallee, K. G., Nieboer, E., Williams, R. J. P. & Xavier, A. V. (1971) Eur. J. Biochem. , 21, 204-209.

Edsall, J. T. & Gutfreund, H. (1983) in Biothermodynamics - The Study of Biochemical Processes at Equilibrium, ed. H. Gutfreund, Wiley, New York, p. 170.

Eftink, M. & Biltonen, R. (1980) In Biochemical Microcalorimetry, Ed Beezer, A. E., Academic Press, New York, pp 343-412.

Eftink, M. R. & Ghiron, C. A. (1976a) Biochemistry, 15, 672.

Felsenfeld, H. & Handschumacher, R. E. (1967) Mol. Pharmacol., 3, 153-160.

Fischer, J. J. & Jardetzky, O. (1965) J. Am. Chem. Soc., 87, 3237.

Flynn, E.H. (1972), Cephalosporins and Penicillins, Academic Press.

Fraker, P. J., King, L. E., Lill-Elghanian, D. and Telford, W. G. (1995) Methods Cell Biol., 46, 57-76.

Franks, F. & Eagland, D. (1975) CRC Crit.Rev. Biochem., 3, 165.

Franks, F. & Ives, D. J. G. (1965) Q. Rev. Chem. Soc., 20, 1.

Fukamizo, T., Ikeda, Y., Ohkawa, T., Gotto, S. (1992) Eur. J. Biochem., 210, 351-357.

Gallo, A. A., Swift, T. J., & Sable, H. Z. (1971); Biochem.Biophys.Res.Commun. 43, 1232-1238.

Ganrot, P.O. (1986) Environ.Health Perspect., 86, 363.

Gard, D. L., Cha, B. J. & Schroeder, M. M. (1995) Curr. Top. Dev. Biol., 31, 383-431.

Gill, S. C. & Von Hippel, P. H. (1989) Anal. Biochem., 182, 319.

Glasby, S. J. (1979) Encyclopaedia of Antibiotics, second edition, John Wiley and Sons, 138-139.

Glickson, J. D., Phillips, W. D. & Rupley, J. A. (1971) J. Am. Chem. Soc., 93, 4031.

Goldstein, P.W. & Garau, J. (1997) Lancet 350, 233-234.

Gonzalez, J. E. & Tien, R. Y. (1995) Biophys.J., 69, 1272-80.

Gopal, S. & Ahluwalia, J. C. (1995) Biophysical Chemistry, 54, 119-125.

Griffiths, J. (1976) Colour and constitution of Organic Molecules, Academic Press.

Griko, V. Y; Freire, E; Privalov, G; Van Dael, H. & Privalov, P. L. (1995) J. Mol. Biol; 252, 447-459.

Griko, Y. V; Freire, E. & Privalov, P. L. (1994a) Biochemistry, 33, 1889-1899.

Hanson, M., Unger,K. K., Denoyel, R. & Rouquerol, J. (1994) J. Biochem. Biophys. Methods., 29, 283-294.

Hayashi, K., Imoto, T. & Funatsu, M. (1963) J. Biochem. (Tokyo) 54, 381.

Hayashi, K., Imoto, T. & Funatsu, M. (1964) J. Biochem. (Tokyo) 55, 516.

Harata, K., & Muraki, M. (1992) J. Biol. Chem., 267, 1419.

Hooke, S. D., Radford, S. E. & Dobson, C. M. (1994) Biochemistry, 33, 5867-5876.

Ikeda, K. & Hamaguchi, K. (1973) J. Biochem. 73, 307-322.

Imoto, T., Johnson, L. N., North, A. C. T., Phillips, D. C., & Rupley, J. A. (1972) , in Boyer, P. D. (Ed.), The Enzymes, vol. V11 (3rd ed.), Academic Press, New York, p. 666.

Inuoe, H. & Timasheff, S. N. (1972) Biopolymers, 11, 737.

Izaki, K., Matsuhashi, M. & Strominger, J. L. (1966) Proc. Natl. Acad. Sci. USA., 55, 656.

Jackson, P. (1996) Mol. Biotechnol. , 5, 101-123.

Jardetzky, O. & Wade- Jardetzky,N. G. (1971) Annu. Rev. Biochem. 40, 605-634.

Jimenez-G., Corrales, S., Moreno, F. & Blanco, G. F. (1995) Chem. Pharm. Bull., 43 (11) 1949-1952.

Johnson, C. M., Cooper, A. & Stockley, P. G. (1992) Biochemistry, 31, 9717.

Johnson, L. N. (1967) Proc. R. Soc. London. Ser. B, 167, 439.

Johnson, L. N. & Phillips, D. C. (1965) Nature, 206, 761.

Jones, R., Dwek, R. A. & Forsen, S. (1974) Eur. J. Biochem., 47, 271-283.

Ju, J., Glazer, A. N. & Mathies, R. A. (1996) Nature Medicine; 2, 246-249.

Kataoka, M., Nishii, I., Fujisawa, T., Ueki, T., Tokunaga, F. & Goto, Y. (1995) J. Mol. Biol., 249, 215.

Kauzmann, W. (1959) Adv. Protein Chem., 14, 1,

Khechinashvili, N. N., Privalov, P. L., & Tiktopulo, E. L. (1973) FEBS Lett. 30, 57.

Kishore, N., Tewari, Y. B., Yap, W. T. & Goldberg, R. N. (1994) Biophys. Chem., 49, 163.

Kita, Y., Arakawa, T., Lin, T-Y. & Timasheff, S. N. (1994) Biochemistry, 33, 15178.

Klotz, I. M. & Franzen, J. S. (1962) J. Am. Chem. Soc., 84, 3461.

Klotz, I. M., Urguhart, M. & Weber, W. W. (1950) Arch. Biochem., 26, 420.

Krasovitskii, B. M.& Bolotin, B. M. (1988) Organic Luminescent Materials, VCH Publishers.

Kumagai, I., Maenaka, K., Sunada, F., Takeda, S., Miura, K. (1993) Eur. J. Biochem., 212, 151-156.

Kurachi, K., Sieker, L. C. & Jensen, L. H. (1975) J. Biol.Chem., 250, 7663-7667.

Kuroki, R., Taniyama, Y., Seko, C., Nakamura, H., Kikuchi, M.& Ikehara, M. (1989) Proc. Natl. Acad. Sci. USA; 86, 6903-6907.

Kuroki, R; Nitta, K & Yurani, K. (1992b) Proc. Natl. Acad. Sci. USA, 89, 6803-6807

Kuwajima, K. (1989) Proteins; Struct. Funct. Genes., 6, 87.

Ladbury, J. E., Kishore, N., Hellinga, H. W,, Wynn, R. & Sturtevant, J. M. (1994) Biochemistry, 33, 3688.

Lakowicz, J. R. Ed., Topics in Fluorescence Spectroscopy: Techniques, Vol. 1 (1991); Principles, Vol. 2, (1991); Biochemical Applications, Vol. 3, (1991) Probe Design and Chemical Sensing, Vol. 4, (1994).

Lakowicz, J. R. (1983) Principles of Fluorescence Spectroscopy., Plenum Press, New York.

Lala, A. K. & Kaul, P. (1992) J. Biol. Chem., 267, 19914.

Laskowski, M. Jr. (1966) Federation Proc., 25, 20.

Lee, K. B., Matsuoka, K., Nishimura, S. & Lee, Y. C. (1995) Anal. Biochem., 230, 31-36.

Lehrer, S. S. (1971) Biochemistry, 10, 3254.

Lehrer, S. S. & Fasman, G. D. (1966) Biochem. Biophys. Res. Commun. , 23, 133.

Lin. T-Y. & Timasheff, S. N. (1994) Biochemistry, 33, 12695.

Lumb, K. J., Cheetham, J. C., Dobson, C. M. (1994) J. Mol. Biol., 235, 1072-1089.

Lumry, R., Boyer, in P.D., Lardy, H. & Myrback, K. (Editors), (1959), Enzymes, Vol. 1, Academic Press, New York.

Lyster, R. (1992) J. Dairy Res., 59, 331-338.

MacKay, K.M. and MacKay, R.A. (1981), 3rd. edition, Introduction to Modern Inorganic Chemistry, International Textbook Co., London, p. 274.

Makhatadze, G. I. & Privalov, P. L. (1992) J. Mol. Biol., 226, 491-505.

Martin, E. O. & Drakenberg, T. (1982) Inorganica Chemica Acta, 67, 71-74.

Mathews, B. W., Remington, S. J., Grutter, M. G. & Anderson, W. F. (1981) J. Mol. Biol. 147, 545-558.

Mathews, C.K. and van Holde, K.B. (1990), Biochemistry, Benjamin/Cummings Inc.

McDonald, C. C., & Phillips, W. D. (1969) Biochem. Biophys. Res. Commun. 35, 43-51.

Mckenzie, H. A. & White, F. H. (1991) Adv. In Protein Chem., 41, 124-316.

Mckinnon, J. R., Fall, L., Parody, A., Gill, S. J. (1984) Anal. Biochem. 139, 134.

Melamed, M. R., Lindmo, T. & Mendelsohn, M. L. (1990) eds., Flow Cytometry and Sorting, 2nd Ed, Willey-Liss.

Meot-Nir, M. & Sieck, L. W. (1986) J. Am. Chem. Soc., 108. 7444.

Mitsumori, F., Arati, Y. & Fujiwara, S. (1980) Bull. Chem. Soc. Jpn., 53, 3478-3482

Miura, T., Takenchi, H., Harada, I. (1991) Biochemistry, 30, 6074-6080.

Molyneux, P. & Frank, H. P. (1961) J. Am. Chem. Soc., 83, 3169-3180.

Monk, P. & Wadso, I. (1969) Acta Chem. Scand., 23, 29

Moreau, S., Awade, C.A., Molle, G.Y.L. & Brule, G. (1995) J.Agric.Food Chem., 43, 883-889.

Murakami, K., & Berliner, L. J., (1983) Biochemistry, 22, 3370.

Musci, G., Reed, J. H., & Berliner, L. J. (1986) J. Inorg. Biochem., 26, 229.

Myers, M., Mayorga, O. L., Emtage, J., Freire, E. (1987) Biochemistry, 26, 4309

Nieboer, E. (1975) Struct. Bonding (Berlin) 22, 1-47.

Norton, R. S. & Allerhand, A. (1977) J. Biol. Chem., 252, 1795-1798.

Oliyai, R. & Lindenbaum, S. (1991) Int. J. Pharm., 73, 33-36.

Olmo, R., Socorro, J. M., Garcia, O., Trigo, R. M., & Blanco, M. D. (1996) Journal of Physiology, 493.P, 140S.

Olmo, R., Socorro, J. M., Gomez, C. Agrasal & Teijon, J. M. (1996) Journal of Physiology, 493P., 140S.

Osserman, E. F., Canfield, R. E., & Beychok, S. (Eds.) , (1974), Lysozyme, Academic Press, New York.

Ostroy, F., Gams, R. A., Glickson, J. D. & Lenkinski, R. E. (1978) Biochim. Biophys. Acta 527, 56- 62.

Pace, C. N. & Mcgrath, T. (1980) J. Biol. Chem., 255. 3862.

Palleros, D. R., Katherine, L. S. & Fink, A. L. (1993) Biochemistry, 32, 4314.

Palmeira, C. M., Moreno, A. J.Madeira, V. M.& Wallace, K. B. (1996) J. Pharmacol. Toxicol. Methods., 35, 35-43.

Palmer, T (1995), Understanding Enzymes, 4th edn. , pp 128-152, Prentice Hall/Ellis Harwood, London.

Perkins, S. J., Johnson, L, N., Phillips, D. C., & Dwek, R. A. (1981) Biochem. J., 193, 573-588.

Perkins, S. J., Johnson, L. N., Machin, P. A. & Phillips, D. C. (1979) Biochem. J., 181, 21- 36.

Pfefferle, J. M. (1989) Ph. D. Dissertation, Universite de Lausanne.

Pfeil, W. & Privalov, P. L. (1976a) Biophys. Chem., 4, 23.

Pfeil, W. & Privalov, P. L. (1976b) Biophys. Chem., 4, 41.

Phillips, G. O., Power, D. M., Robinson, C. & Davies, J. V. (1970) Biochem. Biophys. Acta., 215, 491.

Phillips, G. O., Power, D. M. & Richards, J. T. (1973) Isr. J. Chem., 11, 517.

Picker, P., et al., (1971) J. Chem. Thermodynamics, 3, 631-642.

Price, C. Nicholas & Dwek, A. Raymond (1991) Principles and Problems in Physical Chemistry for Biochemists.

Privalov, P. L. (1974) FEBS Lett., 40, supplement, S140.

Privalov, P. L., Filimonov, V. V., Venkstern, T. V., Bayev, A. A. (1975) J. Mol. Biol., 97, 279.

Privalov, P. L. (1979) Adv. Protein Chem., 33, 167.

Privalov, P. L. (1992), in Protein Folding, ed. T. E. Creighton, W. H. Freeman, New York., 83.

Privalov, P. L., Monaselideze, D. R., Mrevlishvili, G. M. & Magaldadze, V. A. (1964) Zh. Eksper. Teoret. Fiz. (U.S.S.R.), 47, 2073-2079.

Privalov, P. L., Plotnikov, V. V. & Filimonov, V. V. (1975) J. Chem. Thermodynamics, 7, 41-47.

Privalov, P. L. & Khechinashvili, N. N. (1974) J. Mol. Biol. 86, 665-684.

Privalov, P. L., (1979) Adv. Protein Chem., 33, 167-241.

Privalov, P. L., (1982) Adv. Protein Chem., 35, 1-104.

Privalov, P. L. & Potekhin, S. A. (1986) Meth. Enzymol., 131, 4.

Rabbany, S. Y., Donner, B. L. & Ligler, F. S. (1994) Crit. Rev. Biomed. Eng., 22, 307-346.

Ramadan, N., Porath, J. (1985) J. Chromatogr., 321, 93-104.

Ramsay, G., Prabhu, R., Freire. E. (1986) Biochemistry, 25, 2265.

Rapson, H. D. C. & Bird, A. E. (1963) J. Pharm. Pharmacol., 15, Suppl. 222T.

Redfield, C., Smith, R. A. G. & Dobson, C. M. (1994) Nature, Struct.Biol., 1, 23.

Relkin, P. (1996) Critical Reviews in Food Science and Nutrition. 36 (6) 565-601.

Reuben, J. (1975) Naturwissenschaften 62, 172-178.

Rizzuto, R., Brini, M., De Giorgi, F., Rossi, R., Heim, R., Tsien, R. Y. & Pozzan, T. (1996) Current Biol., 6, 183-188.

Rose, G. D. & Wolfenden, R. (1993) Annu. Rev. Biophys. Biomol. Struct., 22, 381.

Rossi, G. L., Holler, E., Kumar, S., Rupley, J. A. & Hess, G. P. (1969) Biochem. Biophys. Res. Commun., 37, 757.

Rupley, J. A. (1967) Proc. Roy. Soc., B167, 416.

Rye, H. S. & Glazer, A. N. (1995) Nucleic Acids Res., 23, 1215-1222.

Sabulal, B. & Kishore, N. (1995) J. Chem. Soc., Faraday Trans., 91, 2101.

Sabulal, B.& Kishore, N. (1996) J. Chem. Soc., Faraday Trans., 92 (11), 1905-1912.

Salton, M. R. J. (1964) The Bacterial Cell Wall, Elsevier, Amsterdam.

Schmid, F. X., Mayr, L. M., Mucke, M. & Schonbrunner, E. R. (1993) Adv. Protein Chem., 44, 25-66.

Schomacker, K., Mocker, D., Munze, R., & Beyer, G-J. (1988) Appl. Radiat. Isot., 39 (3), 261-264.

Schon, A. & Freire, E. (1989) B iochemistry, 28, 5019

Secemski, I. I. & LeinhardG. E. (1974) J. Biol. Chem. 249, 2932-2938.

Sharon, N. & Seifter, S. (1964) J. Biol. Chem., 239, PC 2398.

Shelling, J.G., Hofmann, T. & Sykes, B.D. (1985) Biochemistry, 24, 2332-2338.

Shelling, J. G., Sykes, B. D., O'Neil, D. J., & Hofmann, T. (1983) Biochemistry, 22, 2649-2654.

Shiao, D. D. F., Sturtevant, J. M. (1970) Fed. Proc. Fed. Am. Soc. Exp. Biol., 29, 335

Socorro, J. M., Olmo, R., Blanco, M. D. & Teijon, J. M. (1994) Journal of Inorganic Biochemistry, 57, 293-304.

Song, L., Hennink, E. J. & Tanke, H. J. (1995) Biophysical J., 68, 2588-2600.

Song, L., Verma, C. A. G. O., Verhoeven, J. W. & Tanke, H. J. (1996) Biophysical, J., 70, 2959-2968.

Spitzer, N. C., Olson, E. & Gu, X. (1995) J. Neurobiol., 26, 316-324.

Spokane, R. B., Gill, S. J. (1981) Rev. Sci. Instru. 52, 1728.

Stein, R. L. (1993) Adv. Protein Chem., 44, 1-24.

Stöckel, J., Safar, J., Wallace, A.C., Cohen, F.E. & Prusiner, S.B. (1998) Biochemistry, 37, 7185-7193.

Sturtevant, J. M. (1974) Ann. Rev. Biophys. Bioeng., 3, 35.

Sturtevant, J. M. (1987) Ann. Rev. Phys. Chem., 38, 463.

Subramanian, M., Sheshadri, B. S. & Venkatappa, M. P. (1983) J. Biosci., 5 (4), 331-338.

Sun, M. & Song, P. S. (1977) Photochem. Photobiol., 25, 3.

Suurkuusk, J. & Wadso, I. (1982) A Multichannel Microcalorimetry System. Chemica Scripta., 20, 155-163.

Swiger, R. R. & Tucker, J. D. (1996) Environ. Mol. Mutagen., 27, 245-254.

Tanford, C. (1968) Adv. Protein Chem., 23, 121.

Teichberg, V. I., Sharon,N., Moult, J., Smilansky, A., & Yonath, A. (1974) J. Mol. Biol. 87, 357-368.

Thakkar, A. L. & Wilham, W. L. (1971) Chem. Commun., 320.

Timasheff, S. N. (1992) Biochemistry, 31, 9857.

Tipper, D. J. & Strominger, J. L. (1965) Proc. Natl. Acad. Sci. USA., 54, 1133-1141.

Tsien, R. Y. (1992) Am. J. Physiol., 263, C723-728.

Tsien, R. Y. (1989) Methods Cell Biol. 30, 127-156.

Tsong, T. Y. & Baldwin, R. L. (1972) J. Mol. Biol., 69, 145-148.

Tsuge, H., Ago, H.,Noma, M., Nitta, K; Sugai, S & Miyano, M. (1992) J. Biochem. 111, 141-123.

Tyagi, S. & Kramer, F. R. (1996) Nature Biotechnol., 14, 303-308.

Tyutyukov, N. Fabian, J., Mehlhorn, A., Dietz, F. & Tadjer, A. (1991) ; Polymethine Dyes: Structure and Properties, St. Kilment Ohridski University Press, Sofia.

Vallee, B. L., & Williams, . J. P. (1968) Proc. Natl. Acad. Sci., 59, 498.

Van Dael. H., Haezebrouck, P., Morozova, L., Arico-Muendel, C. & Dobson, C. M. (1993); Biochemistry. 32, 11886-11894.

Vredenburgh, J. J., Silva, O., Tyer, C., DeSombre, K., Abou-Ghalia, A., Cook, M., Layfield, L., Peters, W. P. & Bast, R. C., Jr., (1996) J. Hematother. 5, 57-62.

Yang, A.S. & Honig, B. (1993) J. Mol. Biol., 232, 5.

Warshel, A. & Levitt, M. (1976) J.Mol.Biol., 103, 227.

Weiner, S. J., Kollman, P. A., Case, D. A., Singh, U. C., Ghio, C., Alagona, G., Profeta, S. & Weiner. P. (1984) J. Am. Chem. Soc., 106, 765.

Wilson, J. E. & Chin, A. (1991) Anal. Biochem., 193, 16.

Wise, E. R. Jr. & Park, J. T. (1965) Proc. Natl. Acad. Sci. USA., 54. 75.

Wiseman, T., Williston, S., Brandts, J. F., Lin, L-N. (1989) Anal. Biochem. 179, 131

Wrobel, K., Claudio, E., Segade, F., Ramos, S. & Lazo, P. S. (1996) J. Immunol. Methods, 189, 243-249.

Xie, D., Bhakuni, V. & Friere, E. (1991) Biochemistry, 30, 10673.

Yguerabide, J. (1978) Methods in Enzymology, Vol. XXV, 499-507.

Yurov, Y. B., Soloviev, I. V., Vorsanova, S. G., Marcais, B., Roizes, G. & Lewis, R. (1996) Human Genetics; 97, 390-398.

Zeng, Z., Benson, S. C. & Glazer, A. N. (1995) Annal. Biochem., 231, 256-260.